Effect of Processing Parameters on Reliability of VARTM/SCRIMP composites Panels – Phase I

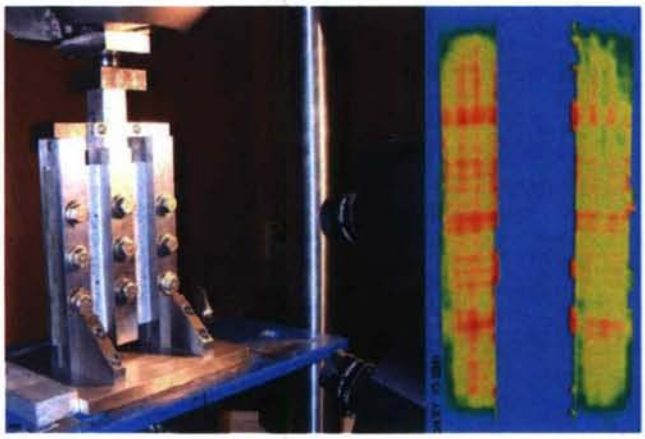

EXPERIMENTAL VARIABILITY OF E-GLASS REINFORCED VINYL ESTER COMPOSITES FABRICATED BY VARTM/SCRIMP

By
Fadi El-Chiti

A Master's Thesis in Mechanical Engineering

August 2005

Advisory Committee:

Habib J. Dagher, Professor of Civil and Environmental Engineering, Co-Advisor

Roberto A. Lopez-Anido, Associate Professor of Civil and Environmental Engineering, Co-Advisor

Michael L. Peterson, Associate Professor of Mechanical Engineering

Lawrence Thompson, Professional Engineer, Applied Thermal Sciences

Prepared for:

Dr. Paul Hess, Office of Naval Research

Mr. Brian Jones, Naval Surface Warfare Center – Carderock Division

EXPERIMENTAL VARIABILITY OF E-GLASS REINFORCED VINYL ESTER COMPOSITES FABRICATED BY VARTM/SCRIMP

By

Fadi El-Chiti

B.E. Notre Dame University, Lebanon, 2002

A THESIS

Submitted in Partial Fulfillment of the

Requirements for the Degree of

Master of Science

(in Mechanical Engineering)

The Graduate School

The University of Maine

August, 2005

Advisory Committee:

Habib J. Dagher, Professor of Civil and Environmental Engineering, Co-Advisor

Roberto A. Lopez-Anido, Associate Professor of Civil and Environmental Engineering, Co-Advisor

Michael L. Peterson, Associate Professor of Mechanical Engineering

Lawrence Thompson, Professional Engineer, Applied Thermal Sciences

LIBRARY RIGHTS STATEMENT

In presenting this thesis in partial fulfillment of the requirements for an advanced degree at The University of Maine, I agree that the Library shall make it freely available for inspection. I further agree that permission for "fair use" copying of this thesis for scholarly purposes may be granted by the Librarian. It is understood that any copying or publication of this thesis for financial gain shall not be allowed without my written permission.

Signature:

Date:

EXPERIMENTAL VARIABILITY OF E-GLASS REINFORCED VINYL ESTER COMPOSITES FABRICATED BY VARTM/SCRIMP

By Fadi El-Chiti

Thesis Co-Advisors: Dr. Habib Dagher
Dr. Roberto Lopez-Anido

An Abstract of the Thesis Presented
in Partial Fulfillment of the Requirements for the
Degree of Master of Science
(in Mechanical Engineering)
August, 2005

It was found that there is significant variability in physical and mechanical properties of marine composites among different manufacturers resulting in inconsistent parameters for structural analysis and design. Experimental variability can be classified in two main groups: 1) variability from experimental preparation and testing techniques and 2) variability from the material constituents and manufacturing process. The objective of the thesis is to resolve the uncertainty surrounding mechanical properties obtained from conventional standard testing by optimizing the testing procedure used in obtaining the material properties of marine FRP composites. A series of ASTM standard test procedures for each material property (tensile, compressive, and shear) are conducted using a 3D digital image correlation system for measuring full-field strains. Glass transition temperature, fiber volume fraction, and density will be measured using ASTM standard tests. The study will lead to drafting material testing specifications to be used in obtaining reliable mechanical and physical properties for FRP composites used in structural applications. Finally, the testing program will be accompanied with a

micromechanics analysis that will be used to characterize the FRP properties using an array of techniques. The micromechanics analysis will be used to explain the results of the material coupon tests and characterize the variability in the tests.

ACKNOWLEDGMENTS

I would like to acknowledge my thesis committee for their guidance and support. Special thanks goes to Roberto and Habib for their confidence in my abilities and for their advice that exceeded the scope of the project. Thanks to Larry for his great technical support and for his management in keeping the project focused on the objective. In addition, I would like to thank Mick for his constant encouragement and help in my academic program, and for his optimistic attitude. The support and guidance of Paul Hess, Brian Jones, and Scott Bartlett from the Office of Naval Research is greatly appreciated. My appreciation extends to my project colleagues: Ghassan Fayad that provided more than technical support and to Keith Berube for his helpful comments. I would like to give credit to the team of undergraduates that helped me finish the testing study. Heading the team was the Oliver brothers, Ronnie and Corey, without them I wouldn't have reached the end. The team included also Adam Greenlaw "Ice" and James Hall whom both put their efforts with great spirit and attitude. My special gratefulness extends to my office mates that were good spirited with my endless distractions and for their great atmosphere that they provided especially outside the office. In addition I extended my thanks to the AEWC family including Doreen Parent and Marcy Smith for their great help in the last minute situations and to the lab manager and operators.

I am forever in grateful to my brother, Imad, who always paves the way for me and prepares me to the different difficulties of life which he learns the hard way. I would like to send my gratitude to my beloved Nadiya that always encouraged me to do my job, especially, when the hours of the days were not enough.

Last but not least, I thank my parents for their patience and their constant encouragements and support.

The research presented in this Thesis was funded by the Office of Naval Research (ONR) through grant N00014-03-1-0542. The support of the program managers Mr. Patrick Potter and Dr. Roshdy Barsoum is greatly appreciated.

TABLE OF CONTENTS

LIST OF TABLES

LIST OF FIGURES

Chapter 1: Introduction

1.1. Motivation and Objective

Variability in material properties obtained from experimental testing has three sources: material variability, fabrication variability, and testing variability. The material variability originates from the constituents of the material. The constituents of polymer matrix composite (PMC) under study in this thesis is the polymer matrix and the reinforcing woven fabric. The material variability is influenced by the resin type that affects the matrix properties; and is influenced by the variation in the number of filaments per tow, fiber areal weight, fiber sizing, and tow spacing that affects the woven fabric properties.

The fabrication variability is influenced by the fabrication method (e.g. hand lay-up, vacuum assistant resin transfer molding, etc.), repeatability of the fabrication method, resin promotion schedule, cure cycle, consolidation method (e.g. vacuum or pressure), thickness variations in the panel, fiber misalignment, fiber volume content, and panel cutting.

The testing variability depends on the experimental technique adopted from specimen configuration and test configuration. The testing variability is also influenced by the test coupon cutting tool, tabbing procedure – if needed, strain measurement system, loading frame including the load measuring device (i.e. load cell), specimen alignment, and operator expertise.

The variability calculated in the experimental results is a combination of all three sources. The equation that defines the relation of the variance of the experimental results to the different sources of variability is depicted in equation (1.1).

$$Var = \sqrt{Var_M^2 + Var_F^2 + Var_T^2} \tag{1.1}$$

where:

Var = variance of the experimental results

Var_M = material variance

Var_F = fabrication variance

Var_T = testing variance

The standard test methods used to calculate the material properties of polymer matrix composites (PMCs) were originally designed for unidirectional laminates, cross ply laminates, and relatively light fabrics. These conventional standards exhibit significant variability in the experimental results when used to test marine grade composites; which are composed of a matrix of rubberized elastomer-modified vinyl ester resin and are reinforced with heavy tow woven fabric. The objective this thesis is characterizing the testing variability of the material properties caused by the adopted experimental methods.

The objective of the thesis was achieved by optimizing the testing procedures used for obtaining mechanical properties: tension, compression, and shear. This objective was achieved by using a 3D-Digital Image Correlation system for measuring full-field strains and displacements. Two standard testing methods were used for calculating each material property. The advantages and disadvantages of each test were used to

recommend modifications in the testing procedure, thus helping reduce the testing variability of marine grade composites. In addition, the physical properties of the material were calculated in accordance with standard methods; the physical properties accompanied the mechanical properties, thereby supporting the modifications suggested by the recommendations.

The fiber dominated material properties were normalized to a nominal thickness and used to obtain the design allowables. Once the material properties were normalized, properties that are the same but are obtained from different test methods and from different panel batches were compared using a statistical tool to signify their difference. In addition, the experimental results were evaluated by comparing these values to a micromechanics model based on the classical lamination theory. A building block approach was followed where the lamina material properties were obtained from PMC specimens reinforced with 8 layers of woven fabric with the warp direction aligned with the laminate principal axis (x-axis). These PMC specimens are referred to as "warps parallel" and are identified with the fiber lay-up sequence: $[0]_{4sf}$, where the subscript f refers to woven fabric. Therefore, the basic composite lamina is reinforced in both warp and fill directions. Then, multidirectional laminate properties were predicted using the model and correlated with experimental results. In addition to $[0]_{4sf}$ the multidirectional laminate fiber lay-up sequences studied were: $[0/90]_{2sf}$ referred to as "warps alternating" and $[0/\pm45/0]_{sf}$ referred to as "pseudo-quasi isotropic". The angle in the laminate lay-up sequence identifies the warp direction of each woven reinforced layer.

A combined experimental and numerical evaluation of the conventional testing standard methods brought about recommendations that helped achieve the thesis's

objective in reducing the variability of the experimental values caused by testing techniques and experimental preparation, testing variability.

1.2. Panel Fabrication

Panels from a commercial manufacturer, *Seemann Composites Inc.*, were obtained for the testing program. The panels were manufactured using vacuum assistant resin transfer molding process (VARTM) with the proprietary Seemann technology, known as Seemann composite resin infusion molding process (SCRIMP). The resin used was Dow Derekane 8084 (now Ashland Derekane 8084 (Ashland, 2004)) and the fabric used was woven with Saint Gobain Vetrotex 324 style (http://www.sgva.com/). Three different fiber lay-ups were adopted: warps parallel, warps alternating, and pseudo-quasi-isotropic. Three different thicknesses were manufactured for each fiber lay-up: 25.4 mm (1 in) and 12.7 mm (0.5 in) used for structural testing, and 5.08 mm (0.2 in) witness panels used for coupon testing.

1.2.1. Fabrication Process

The VARTM/SCRIMP is the fabrication process used to fabricate the panels. The VARTM process uses vacuum to assist the resin to wet out the fabric. The fabric is laid on the mold and is enclosed with a bagging system. The bagging system is sealed around the fabric and vacuum is pulled through the bagging system. The resin then flows through the fabric due to pressure difference suction effect caused by the vacuum.

As for the SCRIMP technology, a flow media is utilized to assist the resin flow through the fabric. The flow media can be any kind of media that helps the resin flow

through the fabric and is not part of the fabric. In our case the flow media was removed after infusion of the part.

1.2.2. Fabric Reinforcement and Polymer Matrix

Marine grade composites are typically fabricated with heavy woven fabric reinforcement and toughened polymer matrices compatible with the VARTM/SCRIMP fabrication process of large structural parts with ambient temperature curing. These PMC composites exhibit enhanced durability in the marine environment and impact resistance in addition to resistance against seawater.

The fiber reinforcement selected for this study was woven fabric with an areal weight of 817.13 g/m^2 (24.1 oz/yd^2) supplied by Saint Gobain. The style of the weave was Vetrotex 324 as defined by the supplier. The fabric was woven from heavy weight E-glass strand rovings and was characterized by having 55% of its weight in the warp direction and 45% in the fill direction. Therefore, the fabric had a tow spacing of 5.1 mm (5 tows per inch) in the warp direction and 6.35 mm (4 tows per inch) in the fill direction. Then, one basic lamina has fiber reinforcement in both the warp and fill directions.

The polymer matrix selected was an elastomer-modified epoxy vinyl ester resin supplied by Derakane. The modified epoxy vinyl ester resin was characterized by its ductility and ability to resist impact.

1.2.3. Laminate Lay-up

Three laminate lay-up sequences were adopted: warps parallel, warps alternating, and pseudo-quasi-isotropic. As explained in a previous section, the angle formed by the warp direction in a layer with respect to the laminate principal axis (x-axis) defines the

layer orientation. For the warps parallel lay-up, each layer of fabric was laid in such a way that the fabric warps were all coincident with the x-axis. The nomenclature of this lay-up is $[0]_{nsf}$, where "[0]" indicates the orientation of each layer's warp direction, "n" stands for the number of fabric layers, "s" indicates the symmetry of the lay-up about the mid plane of the panel, and "f" designates that each layer is reinforced with a woven fabric. The warps alternating lay-up was made with the warps of each layer alternating between zero and ninety degrees from the x-axis, yet keeping symmetry about the panel mid plane. Starting with zero degrees orientation and ending with ninety degrees orientation at the plane of symmetry. The nomenclature of the this lay-up is $[0/90]_{nsf}$, where "[0/90]" corresponds to a set of two layers with alternating warp directions and "n" stands for the number of sets. The pseudo-quasi-isotropic lay-up was made with layers oriented at zero degrees, ninety degrees, and plus-minus forty five degrees orientations. The nomenclature of this lay-up is, $[0/\pm45/0]_{nsf}$, where "[0/±45/0]" corresponds to a set of four layers with different warp directions and "n" stands for the number of sets.

1.2.4. Structural and Witness Panels

Two different batches were used to manufacture the panels. The first batch was used to infuse a 25.4 mm (1 in) thick panel and simultaneously infuse a 5.08 mm (0.2 in) thick panel, which acted as a witness panel for the 25.4 mm (1 in) thick panel. Similarly, the second batch was used to infuse a 12.7 mm (0.5 in) thick panel and simultaneously infuse a 5.08 mm (0.2 in) thick panel which acted as a witness panel for the 12.7 mm (0.5 in) thick panel. The different categories and the lay-up in each category with its estimated thickness based on the rule of thumb (1 oz/yd^2 $\rightarrow$0.001 inches) are described in Table 1.1

Table 1.1: Panel Categories and Fiber Lay-up Architecture

	25.4 mm Structural Panel			12.7 mm Structural Panel			5.08 mm Witness Panel		
Fiber lay-up	$[0]_{20sf}$	$[0/90]_{10sf}$	$[0/\pm45/0]_{5sf}$	$[0]_{10sf}$	$[0/90]_{5sf}$	$[0/\pm45/0]_{2sf}$	$[0]_{4sf}$	$[0/90]_{2sf}$	$[0/\pm45/0]_{sf}$
# of woven layers	40	40	40	20	20	16	8	8	8
Estimated thickness* mm (in)	24.49 (0.964)	24.49 (0.964)	24.49 (0.964)	10.87 (0.428)	10.87 (0.428)	9.80 (0.386)	4.90 (0.193)	4.90 (0.193)	4.90 (0.193)

(*) Based on Rule of Thumb: 1 oz/yd^2 →0.001 inches

Note that the number of layers of the $[0/\pm45/0]_{sf}$ in the 12.7 mm category is sixteen while there are twenty layers in the other lay-ups in the same category. This was required in order to keep symmetry about the mid plane of the panel and keep the same lay-up sequence similar to the other categories.

1.3. Mechanical Properties

The mechanical properties of the marine grade composite were obtained by conducting a series of standardized tests. A pair of test methods was selected for each material property, according to recommendations cited in the literature. The strain measurement tool employed in the study was not a conventional tool recommended in the standards, but rather an innovative non-contact full-field strain measuring technique, 3D digital image correlation system was chosen. The results of each material property test were compared and evaluated to form recommendations on enhancing the testing techniques and reduce material property variabilities originating from the conventional testing methods.

1.3.1. Strain Measurement Using 3-D Digital Image Correlation System

The strain measurement technique implemented in the testing program of the panels under study was 3-D Digital Image Correlation (DIC) system. The 3-D DIC system has the capability of measuring non-contact full-field strains and displacements of specimens under testing. The digital image correlation system determines the displacement and deformation of selected points of a mesh on the surface of the specimen under testing. The mesh is applied to the surface of the specimen prior to testing. The displacement and deformation of the points are determined by comparing successive digital images captured by the DIC system during the specimen loading and these images are correlated. Two cameras are used to cross correlate the distances and obtain out of plane displacements. The specimen surface mesh is recognized by the system as a variable gray intensity pattern. Chapter 2 describes the parameters that control the accuracy and precision of the system and discusses the advantages of capturing full-field strains and displacements in composite testing and pinpointing sources of variability in experimental results.

1.3.2. Tension, Compression, and Shear Properties

Two tension test methods were selected for characterizing the polymer matrix composites (PMC) with woven fabric reinforcement. The first test method was in accordance with ASTM D3039 and is under the jurisdiction of ASTM committee D30 on composite materials (ASTM D3039/D3039M, 2000); while the second test method was in accordance with ASTM D638 and is under the jurisdiction of ASTM committee D20 on plastics (ASTM D638, 2002). The ASTM D3039 tensile specimen was rectangular and contained tabbed grip ends, and the ASTM D638 specimen was dumbbell shaped

with no tabs. Chapter 3 describes the procedures adopted in preparing the specimens, conducting the tests, and calculating the in-plane tensile properties. In addition, Chapter 3 discusses the results of the two test methods and recommends a modified tension test that includes the advantages of the two specimen configurations tested.

Two test methods were selected for characterization of the polymer matrix composites (PMC) with woven fabric reinforcement in compression. The first test method was in accordance to ASTM D6641 and is under the jurisdiction of committee D30 on composite materials; while the second test method selected was in accordance to the Suppliers of Advanced Composite Materials Association (SACMA) SRM 1R recommended test method (SACMA SRM 1R-94, 1994). The method was derived from ASTM D695 which is under the jurisdiction of committee D20 on plastics (ASTM D695, 1996). The ASTM D6641 test specimen was rectangular and un-tabbed with a larger gage section compared to the SACMA SRM 1R test specimen that was rectangular and tabbed. Chapter 4 illustrates the process conducted to prepare and test the specimen. In addition, the chapter describes how the stress-strain curve attained from the tests was modeled with a bi-linear curve. In Chapter 4 the advantages and disadvantages of each test are discussed and the recommendations on modifying the ASTM D6641 specimen configuration are put into practice and its results discussed.

Shear properties of polymer matrix composite (PMC) reinforced with woven fabric were calculated using two ASTM standard tests. The two tests selected were in accordance with ASTM standard test methods. The first was in accordance with ASTM D4255 which is under the jurisdiction of ASTM committee D30 on composite materials (ASTM D4255/D4255M, 2002). The ASTM D4255 test method utilizes a three-rail

fixture and produces a pure shear region in the corresponding specimen. The second test method was in accordance with ASTM D5379 which is also under the jurisdiction of ASTM committee D30 on composite materials (ASTM D5379/D5379M, 1999). The ASTM D5379 test method applies load to a v-notched specimen, which is significantly smaller in size than the three-rail shear specimen; the test method utilizes a fixture commonly know as the Iosipescu shear fixture. The method of calculating the in-plane shear properties is described in Chapter 5. The approach of detecting the failure in the shear specimen is discussed and explained. The advantages and disadvantages of both test methods are addressed and the three-rail shear test is recommended over the v-notch shear test.

The material properties obtained from the tests are summarized in Table 1.2 along with the test conducted and the corresponding standard method followed.

Table 1.2: Material Properties Obtained from Standard Test Methods

Test	**Coupon**	**Standards**	**Properties**
Tension (composites)	Tabbed Rectangular	ASTM D3039	E_1, E_2, ν_{12}, F_{1t}, F_{2t},
Tension (plastics)	Dumbbell	ASTM D638	E_1, E_2, ν_{12}, F_{1t}, F_{2t},
Compression (composites)	Rectangular	ASTM D6641	E_1, E_2, ν_{13} (ν_{12}), F_{1c}, F_{2c},
Compression (plastics)	Tabbed Rectangular	SACMA SRM 1R (ASTM D695)	E_1, E_2, ν_{13}, F_{1c}, F_{2c},
Shear (large – composites)	Three-Rail	ASTM D6641	G_{12}, F_6
Shear (small – composites)	V-Notched	ASTM D5379	G_{12}, F_6

1.4. Physical Properties

As part of characterizing the PMC mechanical property variabilities originating from the test methods used, the physical properties were calculated. Three physical properties were obtained for the panels under study: density, fiber volume fraction, and glass transition temperature. The density test method was in accordance with ASTM D792 which describes the method of determining plastics density by water displacement (ASTM D792, 2000). The fiber volume fraction property was calculated through the burn-out test method which was in accordance with ASTM D 2584. The latter test method describes the procedure of determining ignition loss which is considered to be the PMC resin content (ASTM D2584, 2002). The thickness of one of the panels was measured and a surface plot of the thickness variation across the panel is presented. The thickness variation plot depicted that the measured density and the fiber volume content were dependent on the specimen location extracted from the panel. The glass transition temperature of the PMC was measured by following the test method in accordance with ASTM WK278 which utilized the dynamic mechanical analysis (DMA) method (ASTM WK278, 2003). The physical properties test procedures conducted are presented in Chapter 6 and the experimental results are discussed and correlated.

1.5. Evaluation of the Experimental Results

Once the material and physical properties were determined, a numerical technique was used to evaluate the experimental results. The criterion for selecting the appropriate material properties for design purposes and comparison is stated in Chapter 7. The selected results are then normalized to a nominal thickness value. The method behind the

normalization and the selection of the nominal value is also discussed. The normalized results are then presented and the different issues relating to the inability to normalize some material properties are discussed. Since more than one test was conducted to obtain the same material property, a statistical tool was used to compare the normalized results from different test methods. The statistical tool indicated if the results were significantly the same, come from the same population, or significantly different. A similar method was used to compare similar material properties obtained from different batches. Using the normalized material properties, design allowable values were derived using the sample population standard deviation and its distribution about the mean. The calculation of both A- and B-basis allowables is discussed and the "knock-down" factor for each material property is presented. As part of utilizing the properties obtained from the coupon testing program, a model based on the classical lamination theory (CLT) was used to estimate material property values for different fiber lay-ups: $[0/90]_{2sf}$ and $[0/\pm45/0]_{sf}$; and the estimated values were compared to the experimental values. The model was implemented through a computer model starting with lamina material properties obtained from the experimental results conducted on the $[0]_{4sf}$ fiber lay-up panel. The association between the experimental results and the CLT based model calculated values is stated and discussed in Chapter 7.

1.6. References

ASTM D3039/D3039M, (2000). Standard Test Method for Tensile Properties of Polymer Matrix Composite Materials. Annual Book of ASTM Standards. West Conshohocken, American Society of Testing Materials. **Vol 15.03**.

ASTM D638, (2002). Standard Test Method for Tensile Properties of Plastics. Annual Book of ASTM Standards, American Society of Testing Materials. **Vol 08.01**.

ASTM D695, (1996). Standard Test Method for Compressive Properties of Rigid Plastics. Annual Book of ASTM Standards. West Conshohocken, American Society of Testing Materials. **Vol 08.01**.

SACMA SRM 1R-94, (1994). Recommended Test Method for Compressive Properties of Oriented Fiber-Resin Composites. Washington DC, Suppliers of Advanced Composites Materials Association.

ASTM D4255/D4255M, (2002). Standard Test Method for In-Plane Shear Properties of Polymer Matrix Composite Materials by the Rail Shear Method. Annual Book of ASTM Standards. West Conshohocken, American Society of Testing Materials. **Vol 15.03**.

ASTM D5379/D5379M, (1999). Standard Test Method for Shear Properties of Composite Materials by the V-Notched Beam Method. Annual Book of ASTM Standards. West Conshohocken, American Society of Testing Materials. **Vol 15.03**.

ASTM D792, (2000). Standard Test Methods for Density and Specific Gravity (Relative Density) of Plastics by Displacement. Annual Book of ASTM Standards. West Conshohocken, American Society of Testing Materials. **Vol 08.01**.

ASTM D2584, (2002). Standard Test Method for Ignition Loss of Cured Reinforced Resins. Annual Book of ASTM Standards. West Conshohocken, American Society of Testing Materials. **Vol 08.01**.

ASTM WK278, (2003). Standard Test Method for Glass Transition Temperature (T_g) by DMA of Polymer Matrix Composites. Developed by Subcommittee: D30.04.

West Conshohocken, American Society of Testing Materials. **Status: In Balloting**.

Ashland, (2004). Derekane 8084 Epoxy Vinyl Ester Resins. Composite Polymers. Columbus, OH, Ashland Inc.: 3 pages.

Chapter 2: Strain Measurement Using 3D – Digital Image Correlation System

2.1. Introduction

A 3D-Digital Image Correlation (DIC) strain measurement system was implemented in an experimental program for characterizing polymer matrix composites (PMC) with woven-fabric reinforcement. The 3D-DIC system has the capability of measuring non-contact full field strains and displacements of specimens under testing. The test setup used to conduct the experiment using the 3D-DIC system is presented including specimen preparation and system calibration. The parameters of the system used to measure strain and the technique of strain measurement by the DIC system is explained. In addition, the precision and accuracy of the system is discussed and referenced to a study comparing conventional measuring techniques to DIC system strain measurement.

The experimental program outcome is presented and emphasis on the 3D-DIC strain measurement technique is discussed. Lessons learned from applying the technology in the testing program are discussed and recommendations are stated for adopting the methodology in support of composite material mechanical property measurement.

2.2. Background

Conventional measurement instruments used in composite material testing are surface bonded strain gages, extensometer, and linear variable differential transducers (LVDTs). Usually the conventional tools provide one measurement at a time, either strain

or displacement. Typical problems accompany the use of conventional measurement devices include: 1) adequate bonding of strain gages so they do not de-bond during the loading of the specimen; 2) proper alignment of the strain gages with the fibers; 3) strain gages have to accommodate for transverse sensitivity of the material of the gage; 4) the extensometers have to be removed from the specimen before failure to avoid damage to the instrument; 5) the measurement capacity of LVDTs is limited to linear displacement; 6) all of the conventional measurements require surface contact with the specimen and the measurements are limited to a single spot or an average over the instrument span.

A three-dimensional digital image correlation (DIC) photogrammetry system is capable of non-contact full-field measurements of strains and displacements. The DIC technology was developed in the 1980's and was used to measure deformation and strains under various loading regimes (Ranson, Sutton et al., 1987; Bruck, McNeill et al., 1989). The technology has been applied to determine strains in solid wood, individual wood fibers and papers (Mott, Shaler et al., 1996; Muszyñski, R. Lagana et al., 2002), resin films (Muszyñski, Wang et al., 2002), fiber reinforced polymer composites (Muszyñski, Lopez-Anido et al., 2000; Melrose, Lopez-Anido et al., 2004) and concrete (Choi and Shah, 1997).

Recently a study on fracture mechanics has been done using the DIC system. The system was used to track the crack propagation length and the crack opening displacement between a wood plastic composite and fiber reinforced polymer (Souza, 2005). In addition, the DIC system was used to characterize the creep properties of wood plastic composites (Dura, 2005).

The digital image correlation system determines the displacements of selected reference points of the mesh on the surface of the specimen under testing by comparing and correlating successive images taken during the loading of the specimens. The reference points on the surface of the specimen are recognized by the system as variable gray intensity pattern in their direct neighborhood. In-plane strain values are obtained based on a triangular or rectangular network of points (Muszyñski, Lopez-Anido et al., 2000). Two cameras are used to cross correlate the distances and obtain out of plane displacements. The two cameras, arranged in front of the specimen at an angle and calibrated, can provide stereoscopic information of the specimen surface. The DIC technology is provided by the ARAMIS system by GOM, MbH, and has been successfully applied to a wide range of experimental problems (Schmidt, Tyson et al., 2002; Schmidt, Tyson et al., 2002).

2.3. Composite Specimen Preparation

The only specimen preparation needed for the strain measurement was applying a random black and white speckle pattern to the face of the specimen. The specimen surface was first cleaned with a degreaser to remove any residue of mold release agent remaining from the manufacturing of the panels. The specimen surface facing the cameras during the test was sprayed with a white background as the base color. After the base color dried, a black speckle pattern was sprayed over the white background. The speckle pattern was a random pattern covering 50% of the background. This type of specimen preparation produces a speckle pattern that the DIC cameras recognized and established a unique mesh of gray intensity neighboring unique other meshes. The

randomness of the speckle pattern rendered each mesh and its location on the specimen surface unique.

2.4. Experimental Test Setup

The cameras of the DIC system were placed in front of the specimen when testing the specimen. Two cameras were used to measure out of plane displacement and monitor the specimen for bending, twisting, or buckling. The cameras were placed at the same distance away from the specimen such that the frame of the cameras included the specimen's region of interest (ROI) which was usually the gage section of the specimen. The cameras were facing the specimen at an angle of 25° or 30° which was specified by the manual of the system. A typical setup for testing a shear specimen using the DIC system as strain measurement device is depicted in Figure 2.1.

Figure 2.1: 3D- DIC System Set Up for Testing a Shear Specimen

The system needed calibration for every test setup. Once the cameras were calibrated, the system was able to recognize a pattern and track its changes in a volume in space defined as the calibration volume of cubic shape. Uniform lighting was used to illuminate the specimen surface and remove shadows from the surrounding environment.

During the experiment, the system was capturing pictures at a frequency 1 hertz was selected. The frequency specified the number of data points obtained from the test. The frequency was a compromise between the number of data points and computation time needed. The computation time was the time needed for the system, after the test has been conducted, to correlate the pictures and yield the full-field strain of the specimen

surface during testing. The computation was done separately so that this process did not delay the testing.

2.5. Full-Field Strain Recognition

As mentioned earlier, the DIC system recognized displacements of a mesh of reference patterns on the surface of the specimen. The system recognizes a set of pixels in a square neighborhood or a facet. The facet size can be set by the user in reference to the number of pixels that define the edge of the square, as seen in Figure 2.2. The facet size used in the study was 15 pixels.

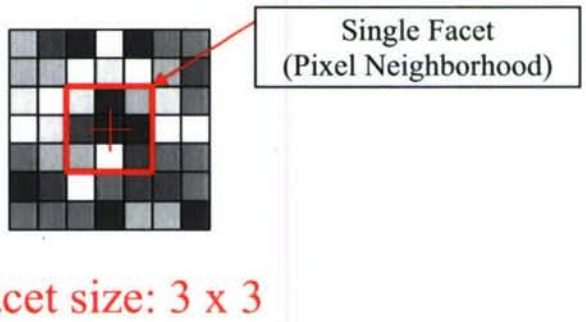

Figure 2.2: Single Facet or Pixel Neighborhood

In addition, the distance between two facets is defined as the facet step, similarly, defined by the number of pixels, as seen in Figure 2.3. For this study, the facet step was taken to be 13 pixels.

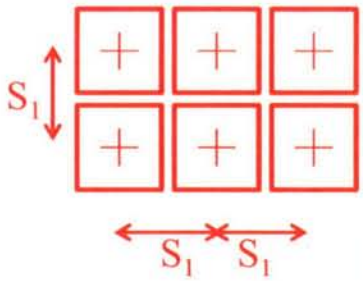

Figure 2.3: Facet Step

2.5.1. Strain Computation

During the test process, the DIC system snapped images at a frequency of 1 Hz. For every snap, the DIC system captured a pair of images, one from the left camera and one from the right camera, which represented a stage of loading. Once the test was completed, the strain computation was initiated by comparing each stage image to the reference image which was usually one taken at the start of the test. The comparison was done by taking each facet from the image and comparing it to the same facet in the reference image and calculating the strains of each facet by measuring the relative change in position of its 8 neighboring facets, for a computation base of 3. A schematic in Figure 2.4 shows the position change in a facet, center dot, and its 8 neighboring facets for a computation base of 3. The strains computed represented the deformation of each facet in the x-direction, ε_x, in the y-direction, ε_y, and in-plane shear, γ_{xy}. In addition, the displacement vectors were calculated by the amount of displacement each facet has moved. The system had the capability of transforming the computed strains to any orthogonal coordinate system. This transformation accounted for any misalignment of the

cameras parallel (or perpendicular) to the line of loading on the specimen. Compared to strain gages, the DIC transformation enabled the operator to reduce errors produced by bonding the strain gage at an angle with the line of loading on the specimen.

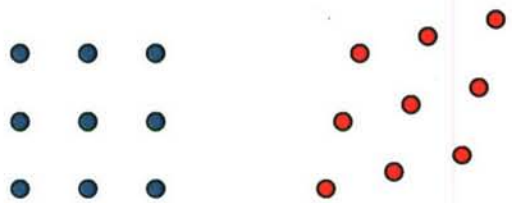

Figure 2.4: Calculation Base Size 3

Once the strain was computed, full field strains were generated for each stage during the loading of the specimen. For the study presented here, an area of the full field strain was selected in the gage section and the average of the strain from each stage was exported to build the stress-strain curve and obtain the elastic properties of the material.

2.5.2. DIC Parameters

The facet size, facet step, and computation base was controlled by the operator. Each parameter affected the computation results and computation time differently. Increasing the facet size improved the precision of point recognition (or determination of an individual facet displacement) without affecting the sensitivity of local strain variations. This was done at the expense of the calculation time; a typical increase in the facet size is shown in Figure 2.5.

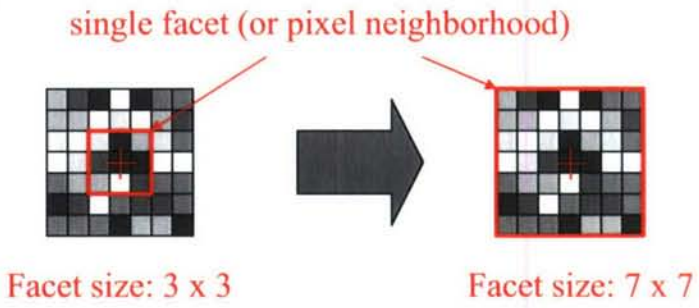

Figure 2.5: Increase in Facet Size

The precision and local accuracy of the calculated strains was improved by increasing the facet step at the expense of losing the sensitivity of local strain variations but with a reduction in the calculation time. An increase in the facet step is shown in Figure 2.6.

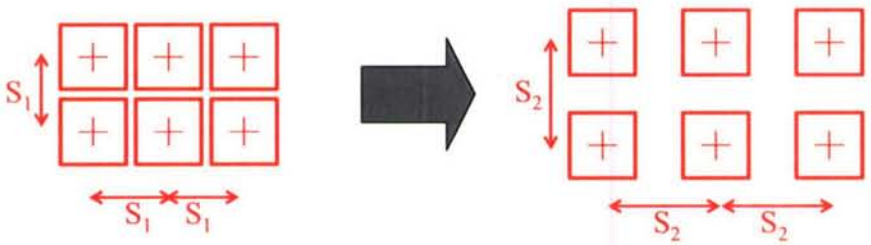

Figure 2.6: Increase in Facet Step

Similarly, the precision and local accuracy of the strains was improved by increasing the calculation base. On the other hand, this was done at the expense of the calculation time and the sensitivity to local strain variation. An increase in the calculation base is shown in Figure 2.7.

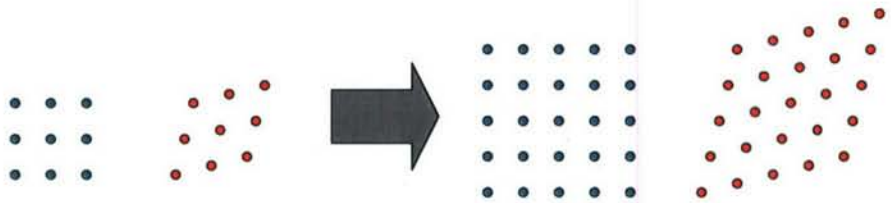

Figure 2.7: Increase in Computation Base

The improvement in the accuracy noticed in changing the DIC parameters was only local and did not seem to improve the global accuracy. In addition, the local strain variation in the full field strain revealed the strain concentrations due to the fabric architecture adopted in the composite. This was seen in the composite under study as wavy strain concentration due to the fabric with heavy tows woven together used in this study (Figure 2.8, Figure 2.9, Figure 2.11, and Figure 2.12).

The best combination of DIC parameters depended on each test's setup. A study was conducted to find the effect of the parameters on a tension test setup. Two areas were used in this study where the average strain was exported from the system to a worksheet for further analysis. The first area was located in the middle of the gage section, not including the edges. The second area included the edges of the specimen. Twenty-four different parameter configurations were implemented and the average strains were exported and compared to each other. The results showed that using the middle area of the gage section to export the average strain was independent of the facet size, facet step, and computation base. Therefore, the average strains exported from the middle area in the gage section (avoiding the edges of the specimen) gave the same values for different

parameter configurations. On the other hand, the average strain exported from the area including the edges of the specimen was slightly sensitive to the computation base and highly sensitive to both the facet size and facet step.

2.5.3. Accuracy and Precision

A study was conducted comparing conventional strain measuring tools to the DIC system (Melrose, 2004). The conventional strain measuring tools in the study were a resistive foil strain gage and a linear extensometer. The study concluded that the DIC system produced lower variation than, or as low as, the conventional strain measuring tools when testing a tensile specimen. The DIC system resulted in measuring the elastic modulus and Poisson's ratio to within 2% of the expected values.

2.6. Composite Materials Evaluated

Marine grade polymer matrix composite reinforced with woven fabric were tested in this study. The PMC panels were reinforced with woven E-glass fabric and manufactured by the VARTM/SCRIMP technique. The fabric had an aerial weight of 817.13 g/m^2 (24.1 oz/yd^2) with 55% of the fabric by weight in the warp direction and 45% of the fabric by weight in the fill direction. The resin used in the composite as a matrix was vinyl ester rubberized resin.

The study was conducted on panels having 3 different fiber lay-ups: $[0]_{4sf}$, $[0/90]_{2sf}$, and $[0/\pm45/0]_{sf}$. The results and the discussion, presented to show the advantages of using the DIC system as a strain measuring technique, address the experimental results obtained from testing the panel with $[0]_{4sf}$ fiber lay-up only.

2.6.1. Test Methods Selected

Two tension tests, two compression tests and two shear tests were used to characterize the PMC. The tests were in accordance to ASTM standards and a SACMA standard, as listed in Table 2.1 (SACMA SRM 1R-94, 1994; ASTM D5379/D5379M, 1999; ASTM D3039/D3039M, 2000; ASTM D6641/D6641M, 2001; ASTM D638, 2002; ASTM D4255/D4255M, 2002).

Table 2.1: Standard Test Methods Selected

Test	Coupon	Standards	Properties
Tension (composites)	Tabbed Rectangular	ASTM D3039	E_1, E_2, ν_{12}, F_{1t}, F_{2t},
Tension (plastics)	Dumbbell	ASTM D638	E_1, E_2, ν_{12}, F_{1t}, F_{2t},
Compression (composites)	Rectangular	ASTM D6641	E_1, E_2, ν_{13} (ν_{12}), F_{1c}, F_{2c},
Compression (plastics)	Tabbed Rectangular	SACMA SRM 1R (ASTM D695)	E_1, E_2, ν_{13}, F_{1c}, F_{2c},
Shear (large – composites)	Three-Rail	ASTM D6641	G_{12}, F_6
Shear (small – composites)	V-Notched	ASTM D5379	G_{12}, F_6

2.6.2. Discussion of Results

The results obtained from the DIC system used with the testing program helped in characterizing possible errors that caused variability in the experimental results obtained from conventional strain measuring techniques. The full field strain produced by the

system revealed a high and low strain variation in accordance to the pattern of the fabric used: high strain values were seen on the relatively heavy tows of the fabric and low strain values were seen in between the tows, on the resin pockets. This strain pattern was depicted clearly on the tension tests which are seen in Figure 2.8 and Figure 2.9.

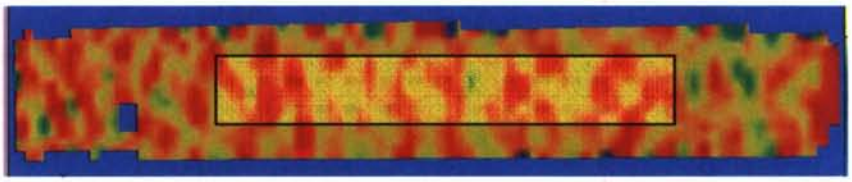

Figure 2.8: Full-Field Strain of a D3039 Tensile Specimen

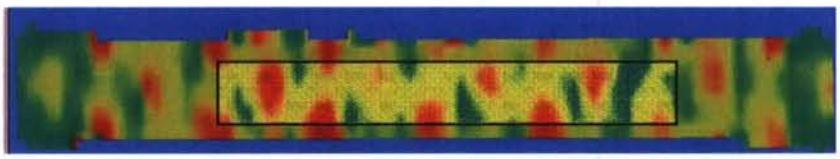

Figure 2.9: Full-Field Strain of a D638 Tensile Specimen

The strain variability pattern seen on the specimen surface was considered to be a source of error in strain measurement when a bonded resistive foil strain gage was used. On the contrary, the DIC system averaged the strain in an area selected in the full-field strain which accounted for the variation of the strain. The white foreground seen in Figure 2.8 and Figure 2.9 represents the area selected to export the average strain.

The DIC system was able to capture twist in the dumbbell shaped tensile specimen. The twist was noticed by measuring the out of plane displacement. A displacement contour image showing the out of plane displacement of a D638 tensile

specimen depicts the twist in Figure 2.10. This type of twist disappeared in the tabbed rectangular D3039 tensile specimen once the load was approximately 5% of the ultimate strength. The D3039 specimen had enough torsional stiffness to initiate the self-aligning mechanism of the testing heads. On the other hand, the D638 specimen had half the width of the D3039 specimen in the gage section and thus did not produce enough torsional stiffness to initiate the self-aligning mechanism of the grips even as the load was increased to more than 50% of the ultimate strength.

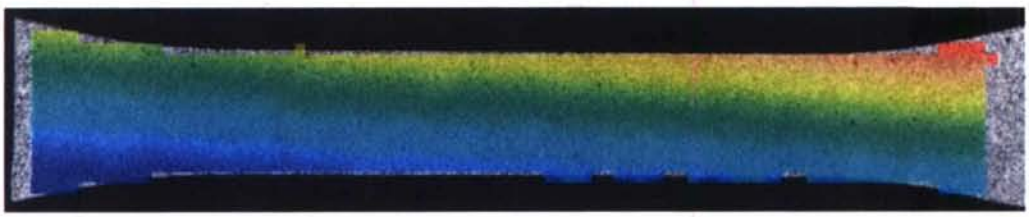

Figure 2.10: Twist Captured on a D638 Tensile Specimen

In the compression specimens, the full-field DIC strain images revealed stress concentrations at the edges of the gage section clamped by the fixture. These stress concentrations are shown in Figure 2.11 and Figure 2.12.

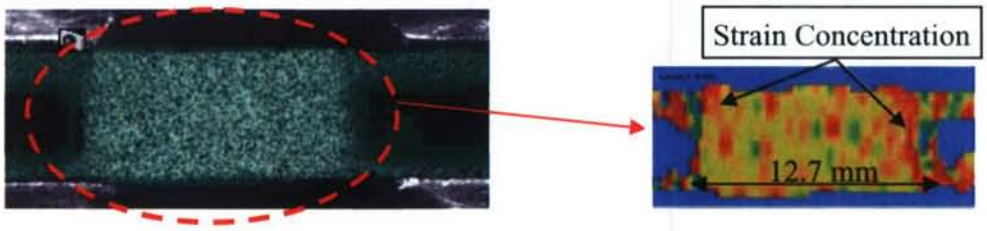

Figure 2.11: Strain Concentration in a D6641 Compression Specimen

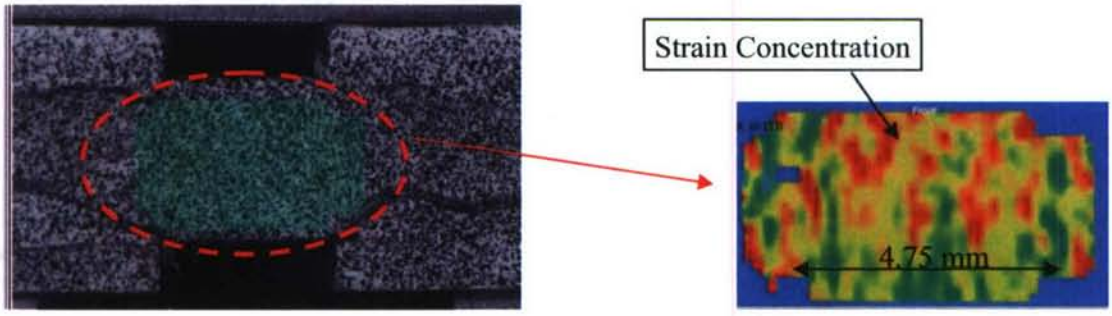

Figure 2.12: Strain Concentration in a SACMA SRM 1R Compression Specimen

The stress concentrations were explained by the sizes of the gage sections used. For compression test ASTM D6641, the length of the gage section was 12.7 mm (0.5 in) as for the compression test SACMA SRM 1R, the length of the gage section was 4.75 mm (0.187 in). Since the woven fabric used to reinforce the PMC material had a tow spacing of 5.1 mm (5 tows per inch) in the warp direction and 6.35 mm (4 tows per inch) in the fill direction, the gage lengths used in the compression tests were not wide enough to include a complete pattern of the fabric. Therefore, the grips of the fixtures confined the specimen to fail properly and caused strain concentrations and non-uniform strain distribution in the areas noted in Figure 2.11 and Figure 2.12.

In addition, the DIC system was used to monitor slipping of the middle rail of the three-rail shear test, ASTM D4255 (Figure 2.13). The problems indicated in the literature when conducting this test were based around the inability for the fixture to hold the specimen without slipping near shear failure of the specimen. To insure the validity of the test, the DIC system was used to monitor the middle rail for slippage on the surface of the specimen.

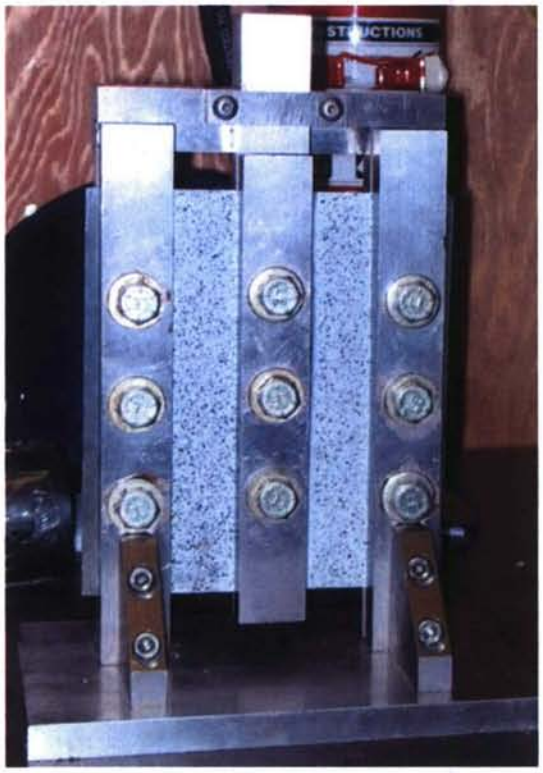

Figure 2.13: Three Rail Shear Fixture with a D4255 Shear Specimen Installed

The experimental results of the v-notch shear test in accordance to ASTM D5379 showed high variability. This variability was explained by the scale of the specimen compared to the coarseness of the fabric used in the composite. As mentioned earlier, the

woven fabric had a tow spacing of 5.1 mm (5 tows per inch) in the warp direction and 6.35 mm (4 tows per inch) in the fill direction. This weave pattern is illustrated in a schematic in Figure 2.14.

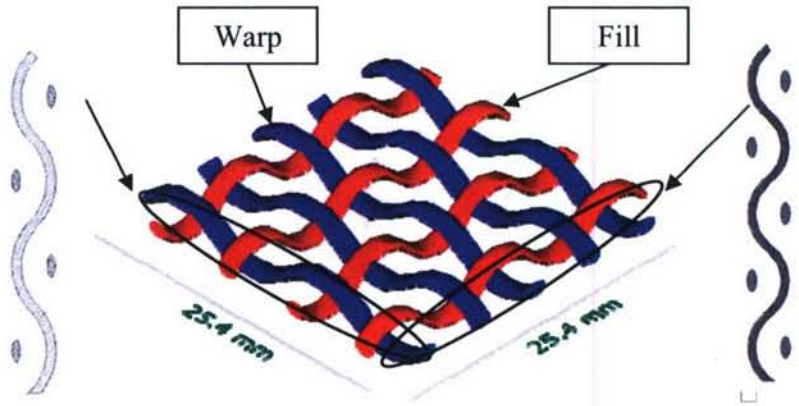

Figure 2.14: Fabric Weave Pattern Schematic

Therefore, comparing the weave to the specimen used in the v-notch shear specimen, it was noticed that in some cases the cross-section between the notches included a tow and in other case it included a gap between two tows. This high randomness of different occurrences of material between the notches explained the high variability in the experimental results. The strain variation from specimen to specimen is depicted in Figure 2.15. In addition, the shaded rectangle in the foreground of each specimen represents the area selected to average the strain and export it. The area size and location were comparable to the size and location of a conventionally bonded cross rosette strain gage.

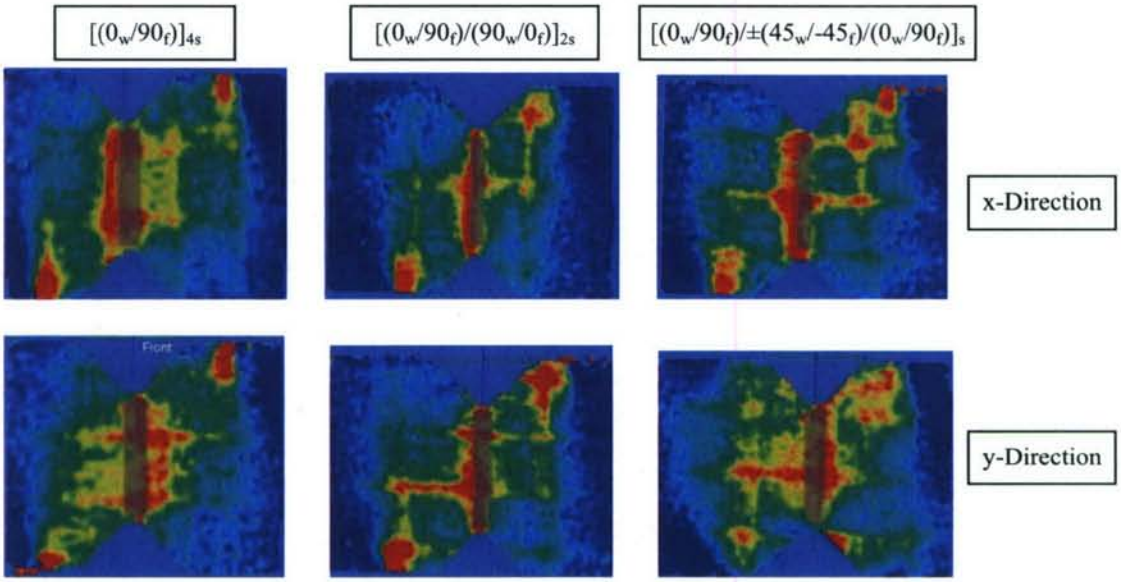

Figure 2.15: Full-Field Strain Concentration in V-Notch Specimens

Due to the fabric architecture used, the strain concentration was seen to deviate from the area between the notches. This resulted in variability of the experimental results since the cross-sectional area between the notches was used to calculate the stress and thus obtain the shear material properties of the PMC.

2.7. Conclusions and Recommendations

The full-field strain produced by the DIC system for the tension, compression, and shear tests demonstrated the benefits of using three-dimensional digital image correlation photogrammetry technology. The advantages of the DIC system over conventional strain measuring tools include producing full strain fields and reducing the experimental variability of the material properties obtained. Orientation of the conventional strain measuring tools parallel to the applied load is one source of testing

variability that is eliminated. The other source of error that is eliminated is due to the point-averaging of strains under conventional strain gages.

The DIC capability to measure full-field strain gave rise to inspecting possible errors caused by accepted testing methods used to derive composite material properties. For example, the compression fixtures used while testing marine grade composites induced non-uniform strain in the gage section introducing errors in the material properties calculated. It is recommended to increase the specimen compression gage region to incorporate at least the full weave pattern of the fabric used. For the material tested in this study, the corresponding gage length described in the ASTM D6641 standard test method was increased from 12.7 mm (0.5 in) to 30.48 mm (1.2 in). The gage length used in this case represents more than 2 weave patterns. A set of specimens were tested with the increased gage length and demonstrated lower variability in mechanical properties and a uniform strain distribution in the gage section. Similarly, an increase in the gage section width of ASTM D638 dumbbell tensile specimen is recommended. The DIC system can also be used to detect and correct small grip misalignments and twisting in a tensile specimen.

The three input parameters of the DIC system were described and a methodology for selecting the appropriate parameter combination for testing marine grade composites was described. The technology of photogrammetry is constantly improving as are computer processing speeds. Advancement in the resolution of digital cameras will continue to enhance the accuracy and precision of 3D-DIC systems leading to further reductions in material testing variabilities and its sources and to more mature, efficient, and higher performance designs.

2.8. References

ASTM D3039/D3039M, (2000). Standard Test Method for Tensile Properties of Polymer Matrix Composite Materials. Annual Book of ASTM Standards. West Conshohocken, American Society of Testing Materials. **Vol 15.03**.

ASTM D638, (2002). Standard Test Method for Tensile Properties of Plastics. Annual Book of ASTM Standards, American Society of Testing Materials. **Vol 08.01**.

ASTM D6641/D6641M, (2001). Standard Test Method for Determining the Compressive Properties of Polymer Matrix Composite Laminates Using a Combined Loading Compression (CLC) Test Fixture. Annual Book of ASTM Standards. West Conshohocken, American Society of Testing Materials. **Vol 15.03**.

SACMA SRM 1R-94, (1994). Recommended Test Method for Compressive Properties of Oriented Fiber-Resin Composites. Washington DC, Suppliers of Advanced Composites Materials Association.

ASTM D4255/D4255M, (2002). Standard Test Method for In-Plane Shear Properties of Polymer Matrix Composite Materials by the Rail Shear Method. Annual Book of ASTM Standards. West Conshohocken, American Society of Testing Materials. **Vol 15.03**.

ASTM D5379/D5379M, (1999). Standard Test Method for Shear Properties of Composite Materials by the V-Notched Beam Method. Annual Book of ASTM Standards. West Conshohocken, American Society of Testing Materials. **Vol 15.03**.

Schmidt, T., J. Tyson, et al. (2002). "Full-Field Dynamic Displacement and Strain Measurement Using Advanced 3-D Image Correlation Photogrammetry. Part II." Experimental Techniques **27** (4): 44-47.

Bruck, H. A., S. R. McNeill, et al. (1989). "Digital Image Correlation Using Newton-Raphson Method of Partial Differential Correction." Experimental Mechanics **28** (3): 261-267.

Choi, S. and S. P. Shah (1997). "Measurement of Deformations on Concrete Subjected to Compression Using Image Correlation." Experimental Mechanics **37** (3): 307-313.

Melrose, P., R. Lopez-Anido, et al. (2004). Elastic Properties of Sandwich Composite Panels using 3-D Digital Image Correlation with the Hydromat Test System. SEM XI International Congress and Exposition on Experimental and Applied Mechanics, Costa Mesa, CA.

Mott, L., S. M. Shaler, et al. (1996). "A novel technique to measure strain distributions in single wood fibers." Wood and Fiber Science **28** (4): 429-437.

Muszyñski, L., R. Lopez-Anido, et al. (2000). Image Correlation Analysis Applied to Measurement of Shear Strains in Laminated Composites. SEM IX International Congress on Experimental Mechanics, Orlando, FL.

Muszyñski, L., R. Lagana, et al. (2002). Optical Measurements of Wood Deformations in Changing Climate. 2002 SEM IX International Congress on Experimental Mechanics, Milwaukee, WI.

Muszyñski, L., F. Wang, et al. (2002). "Short Term Creep Tests on Phenol Resorcinol Formaldehyde (PRF) Resin Undergoing Moisture Content Changes." Wood and Fiber Sience **34** (4): 612-624.

Ranson, W. F., M. A. Sutton, et al. (1987). Holographic and Speckle Interferometry. SEM Handbook of Experimental Mechanics. A. S. Kobayashi. New Jersey, Prentice-Hall, Inc: 388-429.

Chapter 3: Tension Tests for Characterizing Polymer Matrix Composites with Woven Fabric Reinforcement

3.1. Introduction

Two tension test methods were selected for characterizing polymer matrix composites (PMC) with woven fabric reinforcement. The first test was in accordance with ASTM D3039 and is under the jurisdiction of ASTM committee D30 on composite materials (ASTM D3039/D3039M, 2000); while the second test was in accordance with ASTM D638 and is under the jurisdiction of ASTM committee D20 on plastics (ASTM D638, 2002). The test method D638 standard noted that for tensile properties of resin-matrix composites reinforced with fibers of modulus greater than 20 GPa (3 x 10^6 psi) tests should be in accordance with ASTM D3039. Although the reinforcing fiber used is of modulus greater than 20 GPa (3 x 10^6 psi), the literature showed the reliability of conducting tests in accordance with ASTM D638 for such reinforcing fibers. Therefore, both tests were selected for characterizing the PMC with woven fabric reinforcement.

Each test is explained separately and any deviation from the standard is stated. In addition, the chapter describes the method used to cut the samples from the panels, the dimensions of the samples, and the preparation of the samples for testing. The test setup, experimental methods and instrumentation systems are presented, and the different issues that arose during the experimental program discussed. The methods for synthesizing and analyzing the experimental results are explained and the findings are summarized.

The advantages and disadvantages of each test method are described and compared with recommendations from the literature. An experimental mechanics analysis

of the results is presented and a set of recommendations and conclusions are provided in the chapter. A modified tension test method for PMC with woven fabric reinforcement, which combines the benefits of both test methods evaluated, is proposed to obtain better in-plane tensile properties of marine-grade composites.

3.2. Background

A number of issues have been addressed to obtain repeatable and reliable tensile properties of fiber reinforced composites. Among these issues were the preparation of the specimen, the fiber architecture adopted in the composite, and the tabbing procedure needed for some specimens.

A study showed that the edge effects in angle ply composites greatly reduces the stiffness property of the material (Piggott and Wang, 1999). Based on this study, for improved results of modulus of elasticity, the width to length ratio should be about two. In addition, it was shown that the standard test method D3039 was not capable of giving reliable moduli except for [0/90] combinations and the modulus should be calculated from the initial slope of the stress-strain curve of the material rather than the slope of the curve between one quarter and one half of the ultimate strain, as recommended by that standard.

The ASTM D3039 standard test method suggests the use of tabs for gripping highly orthotropic composites to reduce stress concentration around the gripping area and induce acceptable failure in the gage area (ASTM D3039/D3039M, 2000). It was reported that this test has a better performance for cross-ply specimens, since they are less sensitive to imperfection, than for unidirectional specimens (Chaterjee, Adams et al., 1993). In addition, the report discussed the tensile test in accordance with ASTM D638,

Type I, and concluded that stresses peak in the transition region. Furthermore, the report stated that this test cannot be used for unidirectional composites due to failure in the transition region; however, it is more adequate for cross-ply reinforcement.

A detailed study on tabbing specifications of ASTM D3039 tensile specimen was conducted (Adams and Adams, 2002). This study stated that the tabs themselves can result in stress concentrations, particularly at tab terminations adjacent to the specimen gage section. More recently, a finite element analysis of the tensile test in accordance with ASTM D3039 with tabs tapered at an angle of 7^{o} showed that stress concentration is present in the region close to the termination of the tab. The ratio of the stress in the tab termination region to the stress in the gage area was found to be approximately 1.03 (Fayad, 2005).

The study presented in this thesis implements the new experimental technology of digital imaging correlation and explains the different issues indicated previously for tension tests: stress concentration around the tab termination zone, and stress concentration in the transition region in the dumbbell shaped specimen. Based on the experimental findings a specimen configuration is proposed for enhanced experimental characterization of tensile properties of PMC with woven roving reinforcement. Three different fiber lay-up sequences, which are representative of marine-grade composites, were selected for this study: $[0]_{4sf}$, $[0/90]_{2sf}$, and $[0/\pm45/0]_{sf}$. The angle orientation of each layer indicates the angle between the warp direction of the weave and the reference axis, which was the laminate principal axis. The experimental results of the tension test for the different lay-up sequences were analyzed to determine if reliable and repeatable in-plane tensile properties were obtained.

3.3. Tension Test in Accordance with ASTM D3039

The ASTM D3039 standard test method was devised for determining the in-plane tensile properties of polymer matrix composite (PMC) materials reinforced by high-modulus fibers (ASTM D3039/D3039M, 2000). The standard recommends the specimen configuration, the apparatuses needed to measure the width and thickness of the specimen, the testing fixture needed to conduct the test, and the desired strain measuring device. The following sections explain the specimen configuration, the preparation of the specimen and the different apparatuses used to conduct the test. Any deviation from the standard is noted and explained.

3.3.1. Specimen Preparation

Referring to the standard, at least 5 specimens should be tested per testing condition. To account for specimen data that may be lost during the testing process or data analysis, 8 specimens for each direction were tested. Each panel had two orthogonal directions: x-direction and y-direction, where the x-direction was the laminate principal axis. The specimens were cut from the panels with a water-abrasive jet.

The length and width of the specimens were in accordance with Table 1 and Table 2 of the ASTM Standard D3039. The dimensions were 254 mm (10 in) by 25.4 mm (1 in). The witness panels were manufactured with 8 layers of fabric having a total thickness of approximately 5.08 mm (0.2 in), which exceeded the recommended thickness in Table 2 of the standard but abides to the requirements of Table 1 of the standard (ASTM D3039/D3039M, 2000). Since the fabric used is woven with an aerial weight of 817.13 g/m^2 (24.1 oz/yd^2), the surface of the panel that was not on the mold was wavy with a

thickness tolerance of approximately 14%. The thickness tolerance of the specimens did not meet the requirements of the standard. The specimen dimensions are shown in a 2D-ACAD drawing in Figure 3.1.

Figure 3.1: D3039 Specimen Configuration

The specimens were conditioned in accordance with procedure C of test method D5229 (ASTM D5229/D5229M, 2002). The specimens were stored in a conditioning chamber for 3 month at a temperature of 22 ± 3°C (71.6 ± 5°F) and 50 ± 3% relative humidity. While testing the specimens, the testing room was climate controlled at room temperature (22 ± 3°C) and relative humidity of 50 ± 3%.

Although the standard states that testing multidirectional laminates can be successfully tested without tabs, the specimens in this study were tabbed since the findings in the literature recommended the use of tabs in multidirectional laminates. A set of specimens that were similar to the panels under study in this thesis, were tested without tabs and high percentage of grip failure was noticed, which reinforced the idea of tabbing the specimens under consideration in this study. The tabbing material used was a cross-ply E-glass/Epoxy composite known as G11 and used mainly for electric circuit boards. The tabs had a length of 38.1 mm (1.5 in) and the same width of the specimen

with a taper angle of 7° and a thickness of 1.575 mm (0.062 in). The tabs' material and dimensions agreed with the recommendations of the standard.

An 80 grit sand paper was used to roughen the surface where the tabs had to be bonded, and a degreaser was used to remove any residue of mold release from panel manufacturing and any dust particles to improve the bond of the tab to the specimen. The tabs were bonded to the specimen with a structural adhesive, Plio-Grip 7770. The adhesive was mixed and applied in a climate controlled room with a temperature of 20°C and relative humidity of 50% to insure curing of the adhesive. The tabs were clamped and left overnight at the same temperature and relative humidity to cure. A tabbed D3039 tensile specimen is shown in Figure 3.2.

Figure 3.2: Tabbed D3039 Specimen

As recommended in the standard, the specimen thickness and width were measured with a 5 mm (0.19685 in) nominal diameter double-ball-interface micrometer at three random locations along the length of the specimen in the area of interest which had a length of 177.8 mm (7 in). The micrometer had an accuracy of ±2.5 μm (±0.0001 in). The measurements were recorded and the average area was later used in the computation of the tensile properties of the material.

A strain transducer or an extensometer was recommended to be used to measure the strain of the specimen while loading, but, as mentioned in Chapter 2, a 3-D digital

image correlation (DIC) system was used to measure the strains in this study. Therefore, a speckle pattern was applied to the specimen surface that would be facing the digital cameras. The pattern was created by applying a white base first and then a black speckle pattern. The specimens were set aside to dry for a day. The pattern was consistent with the specifications needed for the DIC system to recognize it in the frame of view that covers the region of interest of the specimen.

3.3.2. Test Setup

The two cameras of the DIC system were set in front of the specimen with the speckled pattern facing the cameras. The cameras were then calibrated to measure strain and displacement in the volume of space that the specimen was being tested in.

The specimen was gripped in grip heads that were rotationally self-aligning. The testing machine was a hydraulic machine with the capability of controlling the velocity of the moving head. The testing machine was capable of indicating the total load being carried by the test specimen. The specifications of the testing machine were in conformance with ASTM Practices E4 (ASTM E4, 2002).

The test was conducted with a constant head speed of 1.8 mm/min (0.071 in/min) and each test elapsed between approximately two and a half minutes and three minutes. The load and strain data was collected at a rate of approximately 1 hertz, or one data point every second. The strain data collected was a full-field strain of the area of interest of the specimen. A typical full-field strain captured by the DIC system of a D3039 tensile specimen is depicted in Figure 3.3.

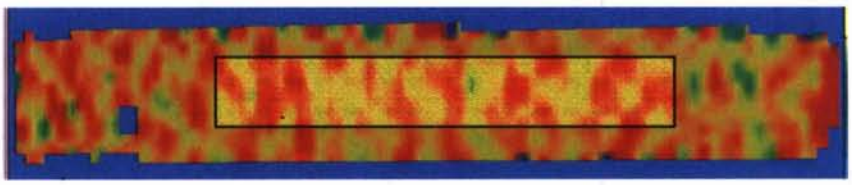

Figure 3.3: Full-Field Strain of a D3039 Specimen

An area in the middle of the specimen was used to extract the strains from the full-field strain. This area represented the gage area which is shown as a faint rectangle in the fore ground in Figure 3.3. The average longitudinal and transverse strains were computed from the full-field strain in the gage area. For every instant the DIC system captured an image from the cameras, the average longitudinal strain, average transverse strain, and the load data were exported.

3.4. Tension Test in Accordance with ASTM D638

The ASTM D638 standard test method was devised for determining the in-plane tensile properties of un-reinforced and reinforced plastics in the form of standard dumbbell-shaped test specimens (ASTM D638, 2002). The standard recommends the specimen configuration, the apparatuses needed to measure the specimen width and thickness, the testing fixture needed to conduct the test, and the desired strain measuring device. The following sections explain the specimen configuration, the specimen preparation and the different apparatuses used to conduct the test. Any deviation from the standard is noted and explained.

3.4.1. Specimen Preparation

Referring to the standard, at least 5 specimens should be tested per testing condition. To account for specimen data that may be lost during the testing process or data analysis, 8 specimens for each direction were tested. Each panel had two orthogonal directions: x-direction and y-direction, where the x-direction is the laminate principal axis. The specimens were cut from the panels with a water-abrasive jet.

The dimensions of the specimens were in accordance with Type I shown in figure 1 of ASTM Standard D638. The dimensions were 165.1 mm (6.5 in) for the overall length, 19.05 mm (0.75 in) for the overall width, 57.15 mm (2.25 in) for the length of the narrow section, 12.7 mm (0.5 in) for the width of the narrow section, and 76.2 mm (3 in) for the radius of the fillet. The witness panels were manufactured with 8 layers of fabric resulting in a total thickness of approximately 5.08 mm (0.2 in), which met the recommended thickness in figure 1 of the standard (ASTM D638, 2002). Since the fabric used is woven with an aerial weight of 817.13 g/m^2 (24.1 oz/yd^2), the surface of the panel that was not on the mold was wavy with a thickness tolerance of approximately 14%. The thickness tolerance of the specimens did not meet the requirements of the standard which was ±4% of the thickness. The specimen dimensions are shown in a 2D-ACAD drawing in Figure 3.1.

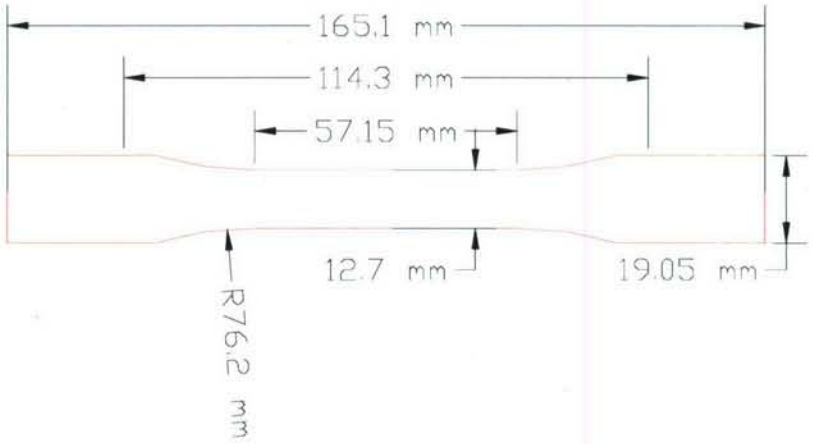

Figure 3.4: D638 Specimen Configuration

The specimens were conditioned in accordance with procedure C of test method D5229 (ASTM D5229/D5229M, 2002). The specimens were stored in a conditioning chamber for 3 month at a temperature of 22 ± 3°C (71.6 ± 5°F) and 50 ± 3% relative humidity. While testing the specimens, the testing room was climate controlled at room temperature (22 ± 3°C) and relative humidity of 50 ± 3%.

As recommended in the standard, the specimen thickness and width were measured with a 5 mm (0.19685 in) nominal diameter double-ball-interface micrometer at three random locations along the length of the specimen in the area of interest which had a length of 57.15 mm (2.25 in). The micrometer had an accuracy of ±2.5 μm (±0.0001 in). The measurements were recorded and the average area was later used in the computation of the material tensile properties.

A strain transducer or an extensometer was recommended to be used to measure the strain of the specimen while loading, but, a 3-D DIC system was used to measure the strains in this study. Therefore, a speckle pattern was applied to the specimen surface that

would be facing the digital cameras. The pattern was created by applying a white base first and then a black speckle pattern. The specimens were set aside to dry for a day. The pattern was consistent with the specifications needed for the DIC system to recognize in the frame of view that covers the region of interest of the specimen.

3.4.2. Test Setup

The two cameras of the DIC system were set in front of the specimen with the speckled pattern facing the cameras. The cameras were then calibrated to measure strain and displacement in the volume of space that the specimen was being tested in.

The specimen was gripped in the testing machine with a distance of 114.3 mm (4.5 in) between the grips and the grip heads were rotationally self-aligning. The testing machine was a servo controlled hydraulic machine with the capability of controlling the velocity of the moving head. The testing machine was capable of indicating the total load being carried by the test specimen with a maximum capacity of 100 kN (22 kip). The specifications of the testing machine were in conformance with ASTM Practices E4 (ASTM E4, 2002).

The test was conducted with a constant head speed of 1.2 mm/min (0.047 in/min) and each test elapsed between approximately two and a half minutes and three minutes. The load and strain data were collected at a rate of approximately 1 hertz, or one data point every second. The strain data collected was a full-field strain of the area of interest of the specimen. A typical full-field strain in the direction of the applied load captured by the DIC system of a D638 tensile specimen is depicted in Figure 3.5.

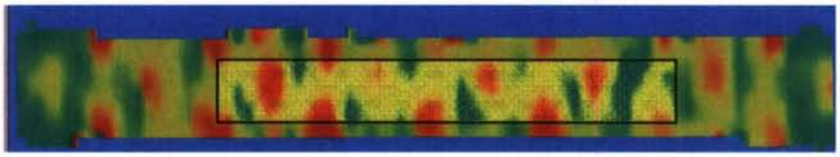

Figure 3.5: Full-Field Strain of a D638 Specimen

An area in the middle of the specimen was used to extract the strains from the full-field strain. This area represented the gage area which is shown as a faint rectangle in the fore ground in Figure 3.5. The average longitudinal and transverse strains were computed from the full-field strain in the gage area. For every instant the DIC system captured an image from the cameras, the average longitudinal strain, average transverse strain, and the load data were exported.

3.5. Stress-Strain Representation

Using the data exported from the DIC system, in addition to the measured average area of the specimen and the calibration factor of the load cell (the load sensing unit of the testing machine), a stress-strain curve was formed for each specimen. Different methods for calculating the modulus of elasticity of a material from the stress-strain curve are described in ASTM E111 standard test method for Young's modulus, tangent modulus, and chord modulus. The Young's modulus is a material property useful in design and is calculated for materials that follow a linear elastic stress-strain behavior. The tangent or chord modulus is calculated for materials that follow a non-linear elastic stress-strain behavior; and is useful to estimate the behavior of the material for a specified range of stress (ASTM E111, 1997). Observing the stress-strain curves for the tensile specimens used in this study, it was observed that the curves were slightly non-linear and

more than one linear range was found. Therefore, a bi-linear representation of the stress-strain curve was adopted. The material was then classified to have an initial modulus of elasticity and a final modulus of elasticity.

The data was accessed by a program code written using Matlab (Mathworks) programming language (Appendix B.1). The code used the load data and strain data to generate the stress-strain curve. Then two regions were selected from the curve: the first region lay between 5% and 20% of the ultimate strain and the second region lay between 60% and 90% of the ultimate strain. For each region, the least square error approach was used to estimate a linear relation of the data. The slope of the linear function was taken to be the modulus of elasticity. The intersection point of the two linear functions was taken to be the transition point from the initial region to the final region. The Poisson's ratio was calculated in accordance with ASTM E132. Two Poisson's ratios were found for each stress-strain curve: initial Poisson's ratio for the initial region and final Poisson's ratio for the final region. The Poisson's ratio was calculated to be the ratio of the modulus of elasticity calculated using the transverse strain to the modulus of elasticity calculated using the longitudinal strain (ASTM E132, 1997).

The stress-strain curve representation and the two regions modeled are shown in Figure 3.6

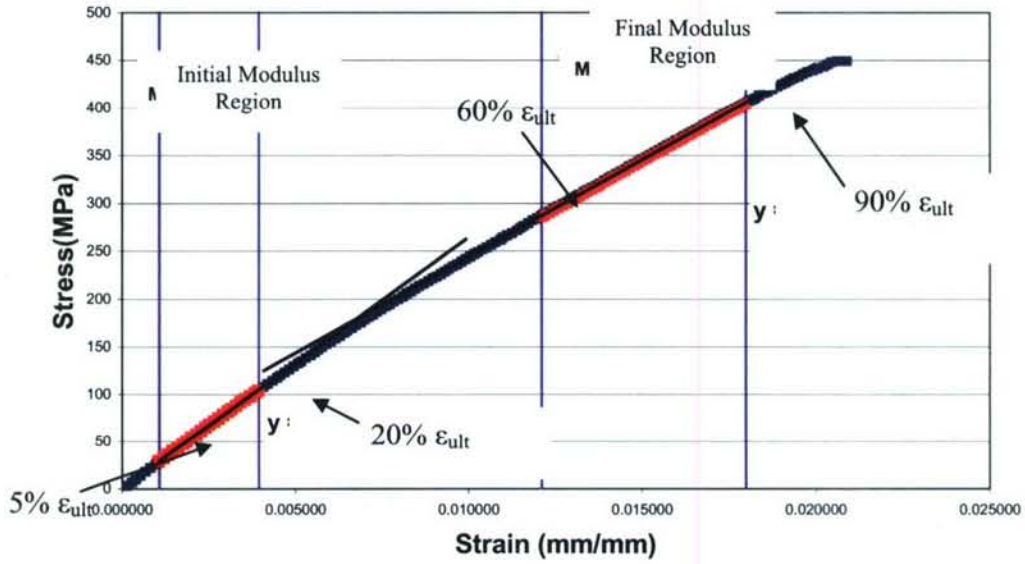

Figure 3.6: Initial and Final Regions in the Stress-Strain Curve

A typical stress-strain curve of a tensile test and its modeled bi-linear curve are shown in Figure 3.7. The values of the initial modulus, final modulus, Poisson's ratio, ultimate point, and transition point are indicated in the figure.

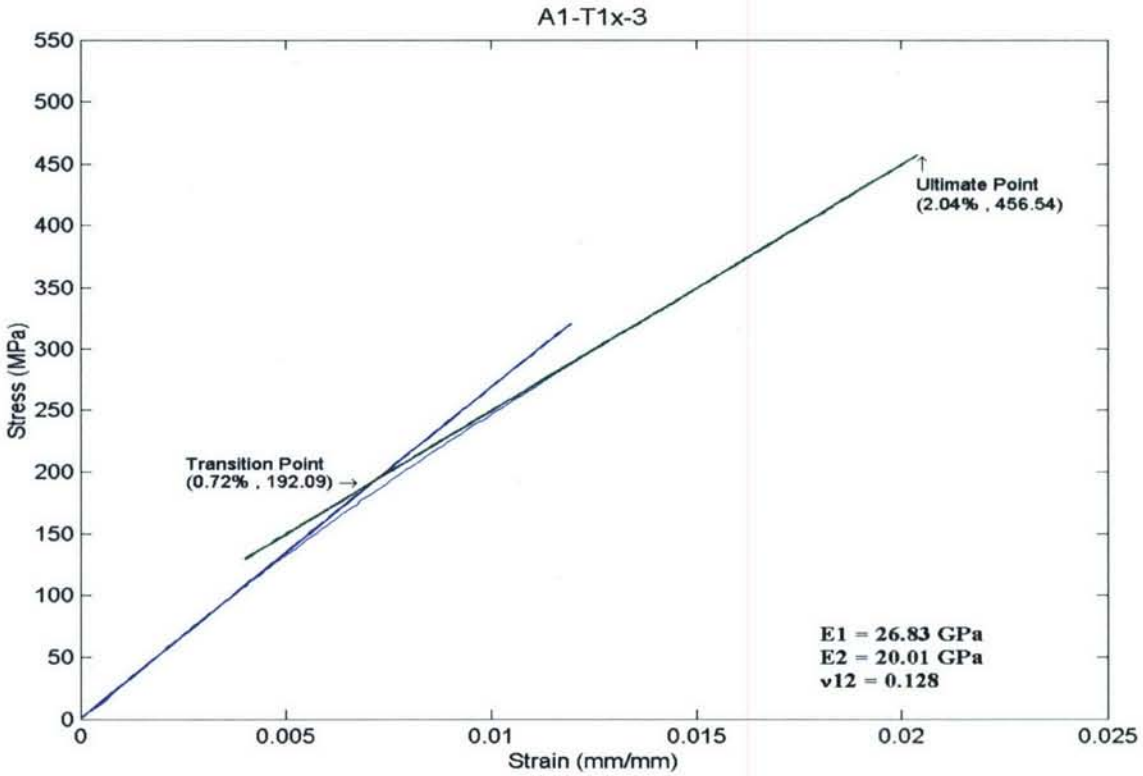

Figure 3.7: Modeled Tensile Stress-Strain Curve

3.6. Discussion of Results

The tension tests were conducted on two sets of panels, manufactured using two different batches. The first batch was used to infuse a 25.4 mm (1 in) thick panel and simultaneously infuse a 5.08 mm (0.2 in) thick panel, which acted as a witness panel for the 25.4 mm (1 in) thick panel. Similarly, the second batch was used to infuse a 12.7 mm (0.5 in) thick panel and simultaneously infuse a 5.08 mm (0.2 in) thick panel which acted as a witness panel for the 12.7 mm (0.5 in) thick panel. For each batch, three fiber lay-ups

were adopted: $[0]_{4sf}$, $[0/90]_{2sf}$, and $[0/\pm45/0]_{sf}$. Therefore, there were two panels for each fiber lay-up that had the same thickness but were infused with a different batch and at different environmental conditions.

A set of 8 specimens was tested for each direction in each panel. Having a total of 6 witness panels, 12 sets of results were computed. The following charts summarize the experimental results obtained from the tension tests conducted on the panels. Each chart has the mean, standard deviation, and coefficient of variation of the material property of the panels. Two material properties are presented: the initial modulus of elasticity and the ultimate strength. The results of each direction are presented on separate charts. The experimental results of the two witness panels with the same lay-up sequence from each batch are represented by two adjacent bars. The complete material properties for all the specimens tested are presented in Appendix C.1.

Each panel had two orthogonal directions: x-direction and y-direction, where the x-direction is the laminate principal axis.

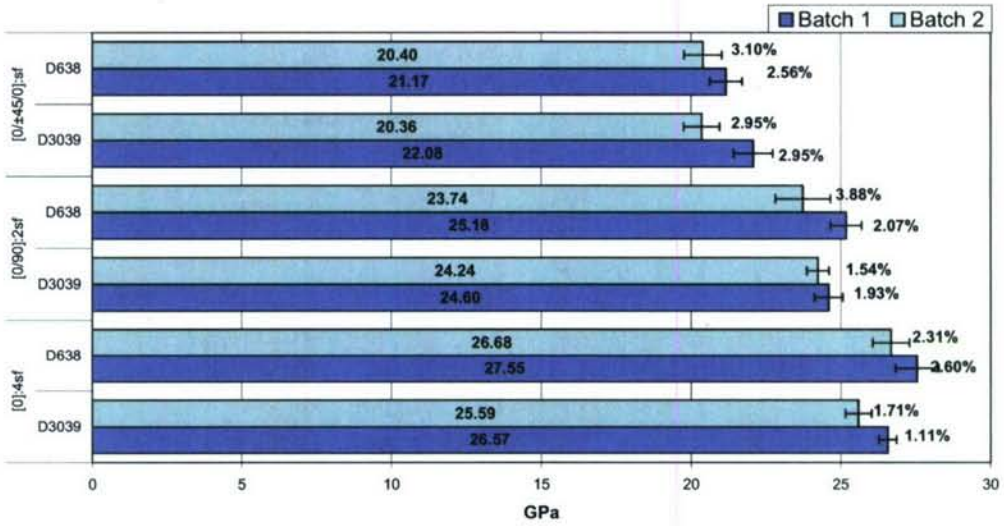

Figure 3.8: Tensile Initial Modulus of Elasticity (x-direction)

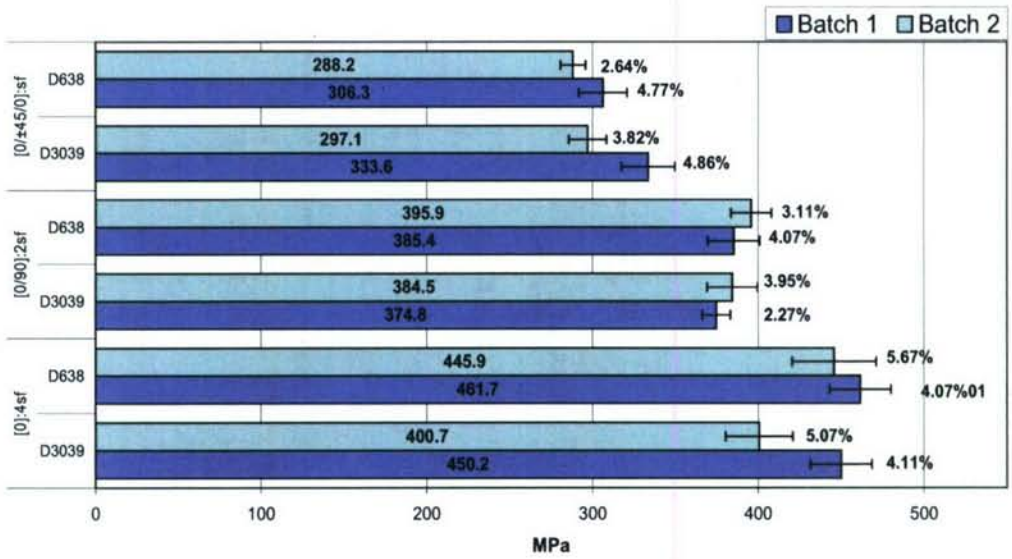

Figure 3.9: Tensile Ultimate Strength (x-direction)

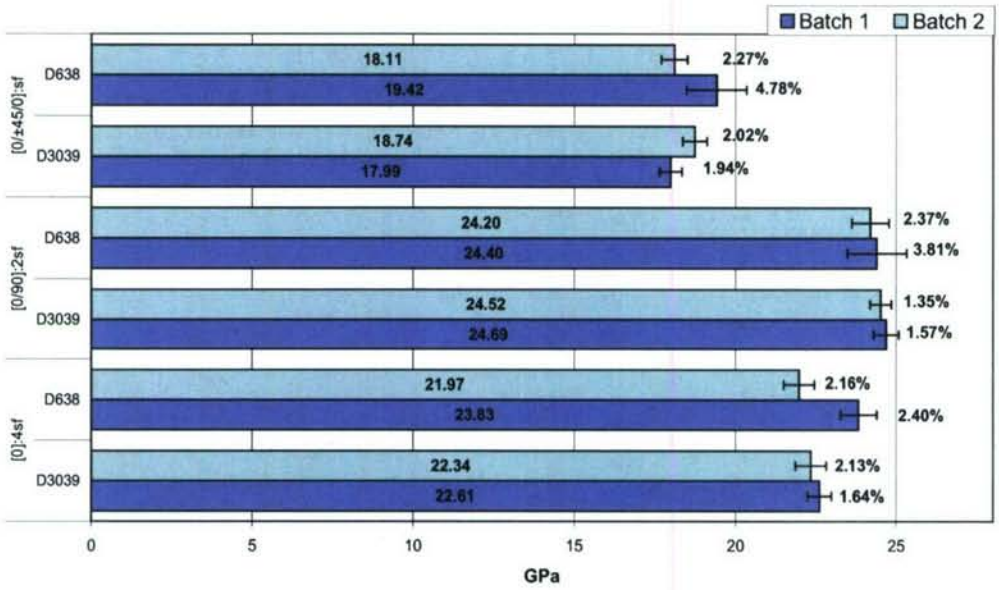

Figure 3.10: Tensile Initial Modulus of Elasticity (y-direction)

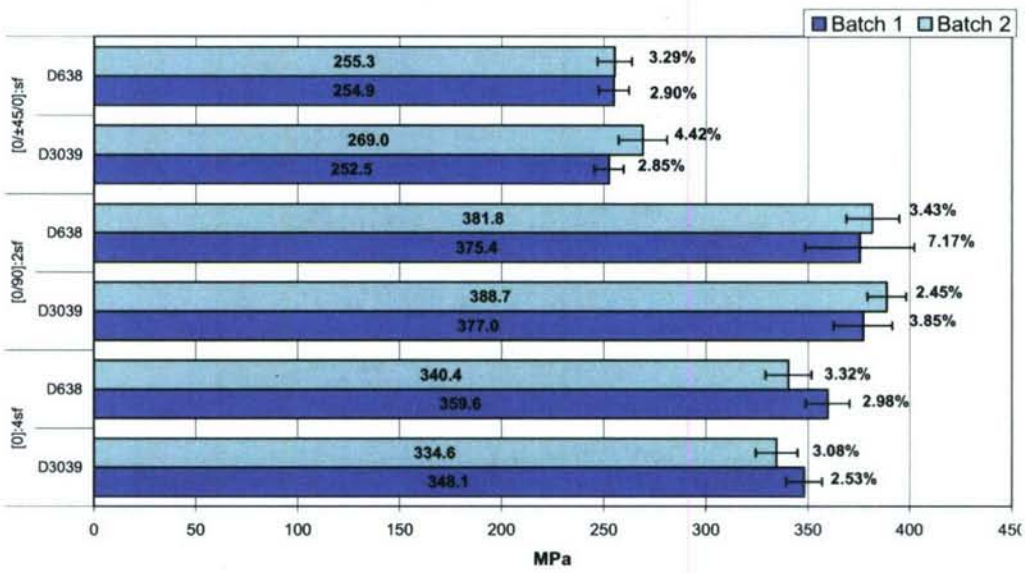

Figure 3.11: Tensile Ultimate Strength (y-direction)

Further analysis of the experimental results was carried on by normalizing the results to one thickness as part of reducing the variability caused by the thickness variation through the panel. The normalization process and the normalized results are presented in section 7.3.1. In addition, the normalized results from both tension test methods were compared using a statistical tool to verify the significance of difference between the two; a similar approach was conducted on normalized results from both batches. The statistical comparison is presented in section 7.3.2.

3.7. Conclusion

While testing the D3039 specimens, failure near the tabs was observed. The tabs were intended to force failure in the gage area but were not effective. The high percentage of failure around the tab region (at least 5 out of 8 specimens) can be justified by the peaking of stresses near the termination of the tab as mentioned in the background section 3.2. Note that the stress concentrations were not captured by the DIC system but were observed in the failure mode.

The self-aligning gripping heads of the testing machine are capable of self-aligning the specimen and removing any twist when the load was applied. But looking at the out-of-plane displacement field of the D638 specimens, it was observed that the specimen remained twisted after the load was applied. The specimen width and material stiffness did not provide enough torsional stiffness to induce the self-aligning mechanism of the gripping heads. The twist in the specimen was depicted in the stress-strain curve of the specimen as a toe region at the start of the curve. The toe region does not represent a property of the material and is an artifact caused by a take-up of slack and alignment of the specimen (ASTM D638, 2002). The twist in the specimen affected the calculation of

the modulus of elasticity of the specimen. The out-of-plane displacement field of a D638 specimen captured by the DIC system shows the twist of the specimen during testing in Figure 3.12. The DIC system is capable of capturing out of plane displacements as well as full-field strains. The D3039 specimens were wide enough to provide enough torsional stiffness for the self-aligning mechanism of the gripping heads. It should be noted that for self-aligning grip heads, the torsional stiffness of the specimen is significant, but when using pre-aligned grip heads, the torsional stiffness of the specimen is not as significant.

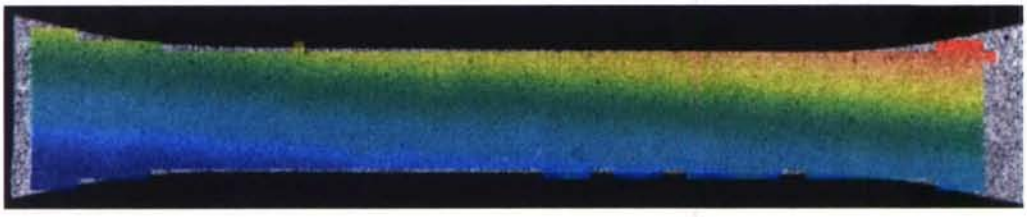

Figure 3.12: Twist captured of a D638 specimen

The woven fabric used in the composite under study had a tow spacing of 5.1 mm (5 tows per inch) in the warp direction and 6.35 mm (4 tows per inch) in the fill direction, producing an unbalanced weave. A schematic representation of the woven fabric used is depicted in Figure 3.13.

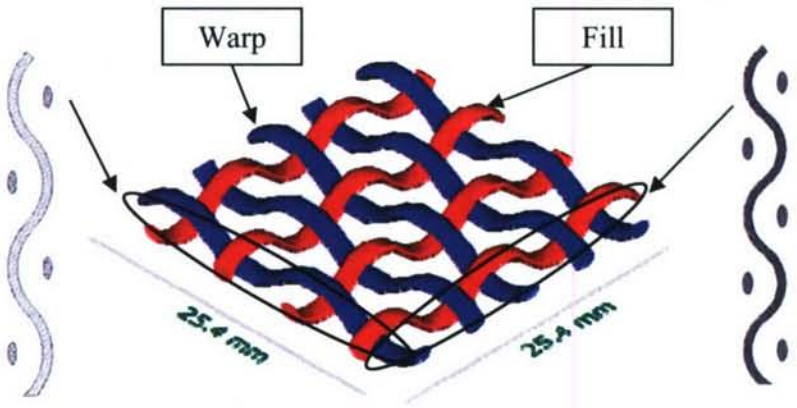

Figure 3.13: Weave Pattern Schematic

The tow pattern of the fabric repeated every 12.7 mm (0.5 in) in the warp direction and every 10.16 mm (0.4 in) in the fill direction. The pattern of the weave is presented in Figure 3.14 for both directions: warp and fill.

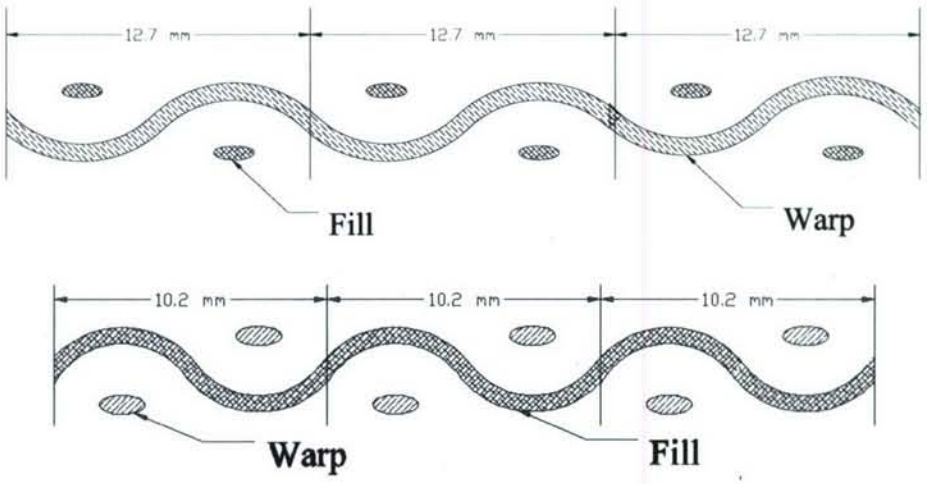

Figure 3.14: Fabric Weave Pattern in the Warp and Fill Direction

The D638 tensile specimen was 12.7 mm (0.5 in) wide in the gage area thus including less than two weave patterns when tested in the warp direction and only one weave pattern when tested in the fill direction. It was observed from the full field strains captured by the DIC system that the strain is larger over the tow compared to the strain over the gap between two tows. The pattern of the woven fabric is perceived when looking at the full field strain in Figure 3.5. When the strains in the gage area were averaged and exported, the value was affected by the presence of a tow in the middle of the specimen or a gap between two tows and thus misrepresenting the average strain needed to obtain in-plane tensile properties of the composite under study.

3.8. Recommendations

3.8.1. Modifications Recommended for the ASTM D3039 Test Method

The tabs in the D3039 specimens were time consuming to bond to the specimens and were ineffective in forcing failure into the gage area. Conversely, the width of the specimen was adequate for the woven fabric used in this study, and produced enough torsional stiffness to align the specimen when loaded. While for the D638 specimens, the dumbbell shape forced the failure into the gage area for more than half the specimens, but the width caused problems in aligning the specimen and in covering a larger number of tows needed to average properly the strain in the gage area.

In conclusion, the width of the specimen should be in accordance with the pattern of the fabric used in the composite under study. The fabric is represented properly when 3 tow patterns are included in the gage section; the edge patterns are affected by the free edge boundary conditions, thus, leaving the middle pattern unaffected by outside

conditions. The tow pattern of the fabric repeated every 12.7 mm (0.5 in) in the warp direction (Figure 3.14) resulting in a recommended specimen width of 30.48 mm (1.2 in); similarly, the tow pattern of the fabric repeated every 10.16 mm (0.4 in) in the fill direction (Figure 3.14) resulting in a recommended specimen width of 38.1 mm (1.5 in). Due to the limitation of most of the testing frames and their load cell, a specimen width of 30.48 mm (1.2 in) was considered for both directions: warp and fill. In addition, it was considered that the free edge effects of the tensile specimen are not large enough to affect the middle tow pattern of the fabric.

To simplify the specimen preparation and remove the tabbing process, a dumbbell shape for the specimen configuration is recommended. Two types of specimen configurations were recommended and are presented in Figure 3.15 and Figure 3.16. The recommended specimen configurations depicts a width of 30.48 mm (1.2 in) in the gage section that is enough to include three weave patterns when obtaining properties in the warp direction and adequate in representing the reinforcing fabric in the fill direction.

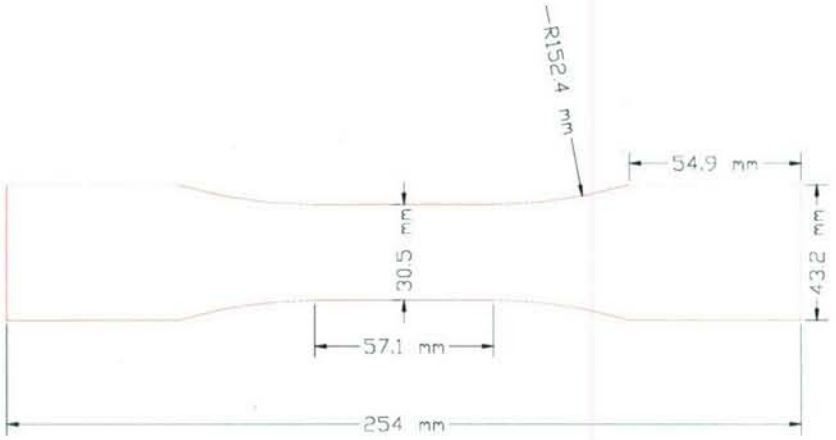

Figure 3.15: Recommended Tensile Specimen (Type One)

Figure 3.16: Recommended Tensile Specimen (Type Two)

3.8.2. Discussion of the Experimental Results of the Recommended Modifications

The recommended test configurations were tested using the same procedure described in section 3.3. Since the cross-sectional area was increased, the loaded needed to fail was the specimen was larger. Due to the significant increase in the failing load

from the ASTM D638 tensile specimen, stress concentration were observed in the transition region, the region that transitions the width of the specimen from the grip width to the gage width. The stress concentrations were captured by the DIC system as strain concentrations and witnessed in the failure mode as failure in the transition region. Both recommended specimen configuration types showed 90% or more of failure in the transition region which rendered the recommendation invalid. The stress concentration in the transition region may cause premature failure thus misrepresenting the materials ultimate strength.

Since both types of the modified specimen configuration did not produce acceptable failures, a finite element analysis, utilizing an optimized procedure, was used to redefine the specimen configuration. The finite element analysis was conducted using ANSYS commercial software with the optimization package. The detailed study is presented in a report by Josh Walls from Applied Thermal Sciences (Walls and Thompson, 2005). The optimized specimen configuration is depicted in Figure 3.17. The main significance of the optimized configuration is the smooth transition from the grip width to the gage width, fillet radius of 365 mm (14.375 in), which caused the specimen to be longer.

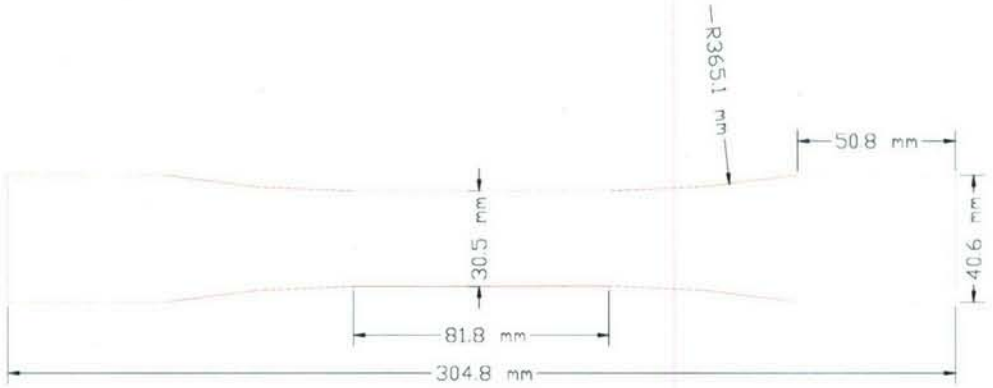

Figure 3.17: FEA Optimized Tensile Specimen

The optimized tensile specimen configuration was cut using the CNC controlled water jet system and tested following the ASTM D3039 test method described in section 3.3. The test was conducted on only one panel in two directions. The panel was from batch 2 and had $[0]_{4sf}$ for fiber lay-up sequence. The percentage of failure in the gage area was ranging between 60% and 50%, with 8 specimens in each direction. The optimized specimen configuration demonstrated a higher percentage of gage failure compared to the rectangular-tabbed ASTM D3039 specimen. The experimental results of the optimized specimens compared with the un-modified specimens, ASTM D3039, are depicted in Figure 3.18 and Figure 3.19. The figures represent the mean value of 8 specimens with the standard error bars and the coefficient of variation.

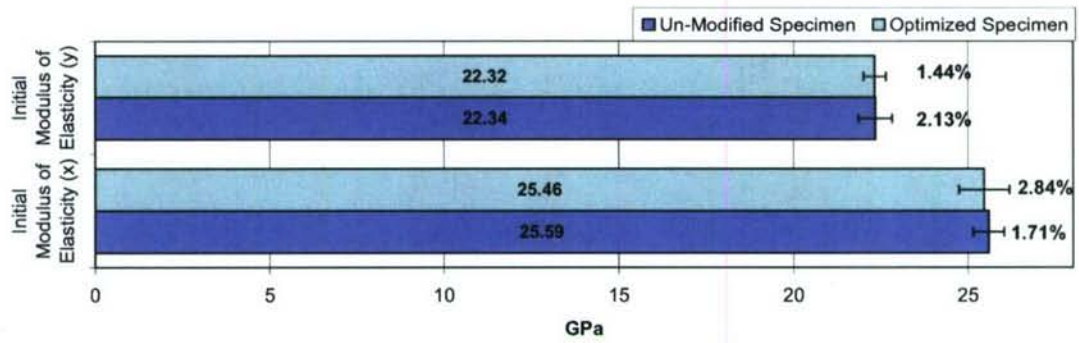

Figure 3.18: Comparison of I-MOE for Optimized and Un-Modified Specimens of ASTM D3039

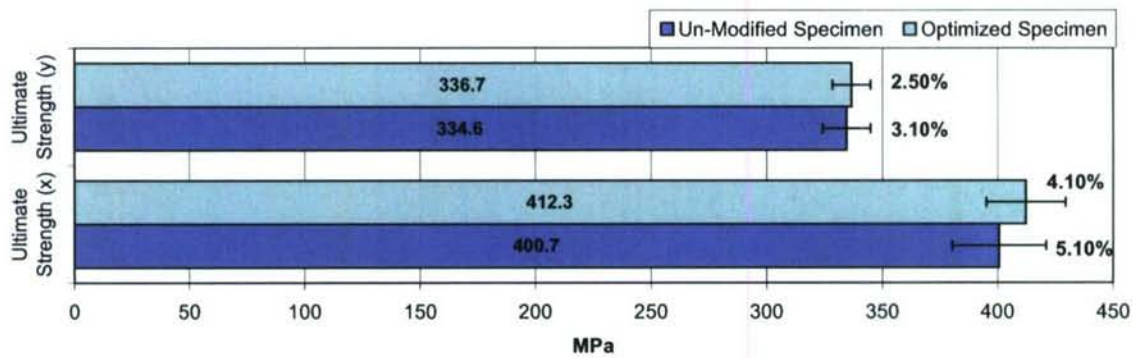

Figure 3.19: Comparison of Ultimate Strength for Optimized and Un-Modified Specimens of ASTM D3039

The results of the optimized specimens showed a high agreement with the rectangular-tabbed specimens. This fact indicated that the ultimate strength was not

highly affected by the failure mode, due to the low factor of stress concentration observed in the tab termination region discussed in section 3.7.

From the total of 5 types of specimen configurations tested to calculate the in-plane tensile properties, it was recommended to use the optimized specimen configuration for the material used in the study, marine grade composites with woven fabric reinforcement. The optimized specimen configuration shown in Figure 3.17 gave repeatable test results and the ratio of failure in the gage area observed was larger than all the other types of specimen configurations tested. In addition, the gage area used in the optimized specimen was large enough to cover at least two weave patterns in the y-direction and three weave patterns in the x-direction, thus giving a good representation of the PMC under study. The dumbbell shape used in the optimized specimen configuration promoted the test to be conducted without the use of tabs in the grip area.

3.9. References

ASTM D3039/D3039M, (2000). Standard Test Method for Tensile Properties of Polymer Matrix Composite Materials. Annual Book of ASTM Standards. West Conshohocken, American Society of Testing Materials. **Vol 15.03**.

ASTM D638, (2002). Standard Test Method for Tensile Properties of Plastics. Annual Book of ASTM Standards, American Society of Testing Materials. **Vol 08.01**.

ASTM D5229/D5229M, (2002). Test Method for Moisture Absorption Properties and Equilibrium Conditioning of Polymer Matrix Composite Materials. Annual Book of ASTM Standards. West Conshohocken, American Society of Testing Materials. **Vol 15.03**.

ASTM E4, (2002). Practices for Force Verification of Testing Machines. Annual Book of ASTM Standards. West Conshohocken, American Society of Testing Materials. **Vol 03.01**.

ASTM E111, (1997). Standard Test Method for Young's Modulus, Tangent Modulus, and Chord Modulus. Annual Book of ASTM Standards. West Conshohocken, American Society of Testing Materials. **Vol 03.01**.

ASTM E132, (1997). Standard Test Method for Poisson's Ratio at Room Temperature. Annual Book of ASTM Standards. West Conshohocken, American Society of Testing Materials. **Vol 03.01**.

Chaterjee, S., D. Adams, et al. 1993. Test Methods for Composites a Status Report Volume I: Tension Test Methods. U.S. Department of Transportation, Washington DC. Report#: DOT/FAA/CT-93/17.

Piggott, M. R. and J. Wang (1999). Basic Errors Appear to be Hampering Composite Aircraft Improvements. 44th International SAMPE Symposium, Long Beach, CA.

Adams, D. O. and D. F. Adams 2002. Tabbing Guide for Composite Test Specimens. U.S. Department of Transportation, Washington DC. Report#: DOT/FAA/AR-02/106.

Fayad, G. (2005). Probabilistic Finite Element Modeling of Marine Grade Composites. Civil and Enviromental Engineering Department. Orono, University of Maine.

Chapter 4: Compression Tests for Characterizing Polymer Matrix Composites with Woven Fabric Reinforcement

4.1. Introduction

For characterizing polymer matrix composites (PMC) with woven fabric reinforcement in compression, two test methods were selected. The first test method was in accordance with ASTM D6641 and is under the jurisdiction of committee D30 on composite materials; while the second test method selected was in accordance with the Suppliers of Advanced Composite Materials Association (SACMA) SRM 1R recommended test method (SACMA SRM 1R-94, 1994). The method was derived from ASTM D695 which is under the jurisdiction of committee D20 on plastics (ASTM D695, 1996). The test method in accordance with SACMA SRM 1R is used for determining the compression properties of reinforced plastics by pure end-loading. Conversely, the test method in accordance with D6641 is used to determining the compression properties of PMC by introducing combined end- and shear loadings (ASTM D6641/D6641M, 2001).

A literature review cites different papers that characterized the compression properties of PMC; the findings of these papers are discussed and compared with the findings of the study presented in the chapter. The test methods used in this study are explained in the following sections and are referenced to the ASTM standard and SACMA recommended method. Any deviation from the standard are explained and justified. The specimen configuration used, the method to cut the specimens, and the specimen preparation before testing, are explained. The test setup and instrumentation

systems are presented; the problems that occurred during the experimental method conducted are stated and discussed.

An experimental mechanical analysis was conducted on the experimental results of the test methods and the advantages and disadvantages of each test are discussed. A set of conclusions and recommendations are presented and the main recommendation is a modified compression test method that combines the advantages of each test method. The modified test method was conducted and the experimental results were analyzed. The results from the test methods in accordance with the standards and the modified test method that were recommended from the study conducted on these tests were compared.

4.2. Background

Various compression tests are used to characterize the material properties of a composite material. These test methods have been modified and changed over the years to improve the results calculated and reduce the uncertainty of the testing method. Recently, the ASTM D30 committee had devised a standard guide for testing PMC materials (ASTM D4762, 2004). For characterizing the composite material compressive properties, the guide recommended four ASTM standards: ASTM D6641, ASTM D695, ASTM D3410, and ASTM D5467 (ASTM D695, 1996; ASTM D6641/D6641M, 2001; ASTM D3410/D3410M, 2003; ASTM D5467/D5467M, 2004). It was commented in the ASTM D4762 standard that the D695 test method is not recommended for continuous fiber composites and a modified version of the D695 test method was released as the SACMA SRM R1 test method (SACMA SRM 1R-94, 1994), but the standard recommended the use of ASTM D6641 instead.

In addition, a report sponsored by the United States Department of Transportation recommended the SACMA SRM R1 for calculating the compressive properties of PMC reinforced with unidirectional tape or woven fabric (Tomblin, Ng et al., 2001). The report presented a qualification plan to help ensure the control of repeatable base material properties.

A more recent conference proceeding compared the various test methods for compression testing (Wolfe and Weiner, 2004). The paper describes the test methods conducted on three types of PMC panels. It was concluded in the study that there was no difference in the compressive material properties between the SACMA SRM 1R test method and ASTM D6641 test method. In addition, the paper stated that ASTM D695 test method produced a lower material compressive strength than the test methods conducted in the study.

An earlier study was made on the effect of the specimen gage length on the material compressive properties (Adams and Lewis, 1990). This study used two test methods: ASTM D3410 and SACMA SRM 1R. It concluded stating that the measured compressive strength of a high-strength, highly orthotropic composite material appeared to be independent of the slenderness ratio, the length ratio of the gage section to the minimum radius of gyration of the cross-sectional area.

Note that the literature reviewed did not illustrate the effect of the fabric used to reinforce the PMC on the type of test conducted. In addition, the scale of the woven fabric used was not related to the specimen configuration.

This chapter addresses two compression test methods that were used to characterize the compression material properties of PMC with woven fabric

reinforcement. The woven fabric was marine grade fabric, which was relatively coarse compared to the studies cited in the background. The compression test methods used are in accordance with ASTM D6641 (ASTM D6641/D6641M, 2001) and in accordance with SACMA SRM 1R (SACMA SRM 1R-94, 1994).

4.3. Compression Test in Accordance with ASTM D6641

The test method is used for determining the compressive strength and stiffness properties of PMC using a combined loading compression (CLC) fixture. The load is introduced into the specimen by combined end- and shear-loading (ASTM D6641/D6641M, 2001). The test method recommended the apparatus needed for measuring the specimen and conducting the experiment. The specimen configuration was also stated by the standard and a limitation for the gage length was specified by the use of the Euler buckling stress for the tested material. The procedure for conducting the test, measuring the strains during loading, and collecting the data needed to obtain the PMC compressive material properties was explained in the ASTM standard.

The following sections explain the specimen configuration, the apparatuses, and procedures used for conducting the compression test in accordance to ASTM D6641 in this study. Any deviation from the standard is stated and justified.

4.3.1. Specimen Preparation

The standard recommended at least 5 specimens to be tested for each testing condition. To account for data loss during testing or during the collection of experiment data, 8 specimens were used in the testing program for each testing condition. Since the fabric in the panels used was woven fabric with an unbalanced weave: 55% of the fabric

volume in the warp direction and 45% of the fabric volume in the fill direction, two sets of specimens were cut from each panel. One set represented the x-direction, the laminate principal axis, and the other set represented the y-direction, orthogonal to the laminate principal axis. The cutting tool used to cut the specimens from the panels was a water-abrasive jet computer numerically controlled (CNC) machine.

The specimen configuration was selected according to the standard recommendations. The specimen length was 139.7 mm (5.5 in) and the specimen width was 19.05 mm (0.75 in). The specimen thickness was confined to be the same as the panel thickness. The witness panels were PMC with woven fabric reinforcement with an aerial weight of 817.13 g/m^2 (24.1 oz/yd^2); the panel thickness was approximately 5.08 mm (0.2 in), which resulted in a specimen thickness of 5.08 mm (0.2 in). A 2D-CAD drawing of the specimen used in this test and the specimen dimensions are depicted in Figure 4.1.

Figure 4.1: D6641 Specimen Configuration

The specimen gage length was 12.7 mm (0.5 in) when placed in the loading fixture. The length of the gage section was checked to be sufficient to rule out the Euler column buckling of the specimen by the use of equation (4.1) that was recommended in the standard (ASTM D6641/D6641M, 2001).

$$h \geq \frac{l_g}{0.9069 \cdot \sqrt{\left(1 - \frac{1.2 \cdot F_c^e}{G_{xz}}\right) \cdot \left(\frac{E^f}{F_c^e}\right)}} \tag{4.1}$$

where:

h = specimen thickness, mm (in),
l_g = length of gage section, mm (in),
F_c^e = expected ultimate compressive strength, MPa (psi),
E^f = expected flexural modulus, MPa (psi),
G_{xz} = through-the-thickness (inter-laminar) shear modulus, MPa (psi).

The expected ultimate compressive strength, expected flexural modulus, and the inter-laminar shear modulus were estimated from the literature on PMC with woven fabric reinforcement.

The specimens were conditioned for 3 months at a temperature of 22 ± 3°C (71.6 ± 5°F) and 50 ± 3% relative humidity in accordance with procedure C of ASTM D5229 (ASTM D5229/D5229M, 2002) prior to testing.

The specimen width and thickness were measured using a 5 mm (0.19685 in) nominal diameter double-ball-interface micrometer at three random locations along the gage length of the specimen which was 12.7 mm (0.5 in). The micrometer had an accuracy of ±2.5 μm (±0.0001 in). The measurements were recorded and the average area was later used in the computation of the compression properties of the material.

Since the cutting tool introduced a taper in the specimen along the thickness, the ends of the specimens were machined square and flat. The taper angle is approximately 2 or 3 degrees. Machining the specimen ends was necessary to prevent end crushing of the specimen while loading was applied.

As recommended by the standard, the loading was introduced to the specimen by using a CLC fixture. The fixture transferred the compression load applied to the specimen into a combined end loading and shear loading. The test fixture was supplied by Wyoming Test Fixtures Inc. and was originally developed at the University of Wyoming. The fixture consisted of two metal blocks that were connected to each other by a pair of rails. The specimen ends were clamped in the metal blocks. The specimen was positioned in the fixture such that the specimen ends were flush with the metal blocks; and the unclamped region of the specimen represented the specimen gage length. A partially disassembled fixture with a specimen clamped in one metal block is represented in Figure 4.1. In addition, an assembled fixture with the specimen installed is also represented in the same figure.

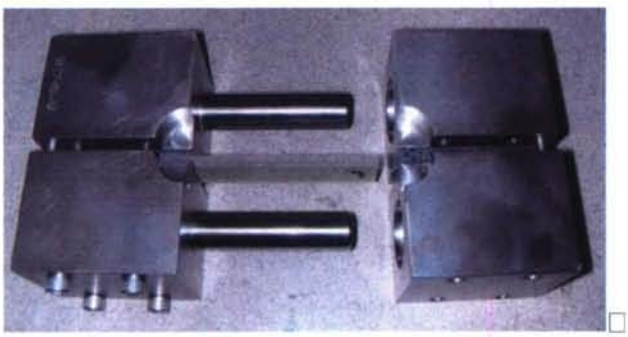

Figure 4.2: D6641 CLC Fixture – Assembled and Disassembled

The circular recess in the center of the fixture is designed for using an extensometer to measure the strain of the specimen as the load is applied. For this study, a 3-D digital image correlation (DIC) system was used to measure the strains. Due to the way the fixture is designed, the cameras of the DIC system were able to view the edge of the specimen gage length when the gage length was 12.7 mm (0.5 in). Therefore, a

speckle pattern was applied to the specimen surface (edge of the specimen) that would be facing the digital cameras. The pattern was applied by applying a white base first and then a black speckle pattern. The pattern was consistent with the specifications needed for the DIC system to recognize the patter in the frame of view that covers the specimen region of interest.

4.3.2. Test Setup

The specimen was installed in the fixture by following the manufacturer's instructions provided. When the specimen was installed, the specimen ends were flush with the metal blocks as seen in Figure 4.2 and the gage length was not supported by the fixture. The four screws of each metal block were torqued in three approximately equal increments. As recommended by the standard, the required torque depends on the thickness of the specimen (ASTM D6641/D6641M, 2001). Several trials were required to reach an acceptable torque that was sufficient to prevent specimen end crushing without inducing stress concentrations that might lead to premature failures. A torque of 3.39 N-m (30 in-lb) was sufficient for the material used in this study with a specimen thickness of approximately 5.08 mm (0.2 in).

The CLC fixture was placed in the testing frame. The testing machine was a servo controlled hydraulic machine with the capability of controlling the velocity of the moving head. The testing machine was capable of indicating the total load being carried by the test specimen with a maximum capacity of 100 kN (22 kip). The testing machine specifications were in conformance with ASTM Practices E4 (ASTM E4, 2002). The load was applied by the testing machine through a ball bearing used to remove any

bending forces on the specimen from imperfections in the frame and fixture. The use of a ball bearing was recommended by ASTM D6641.

The DIC system cameras were placed in front of the fixture with the specimen edge facing the cameras. The cameras were then calibrated to measure strain and displacement in the volume of space that the specimen was being tested in.

The test was conducted at a compressive loading rate of 0.6 mm/min (0.0236 in/min) to failure of the specimen. Each test elapsed between approximately four and a half minutes and five and a half minutes. During the loading process, the data was collected at a rate of approximately 1 hertz, or one data point every second. Every data point collected included the load carried by the specimen as measured by the load cell (the load sensing unit) of the testing machine and the full-field strains on the specimen edge in the gage length as seen by the DIC system. A typical full-field strain in the direction of the load applied as captured by the DIC system of a D6641 compression specimen is shown in Figure 4.3.

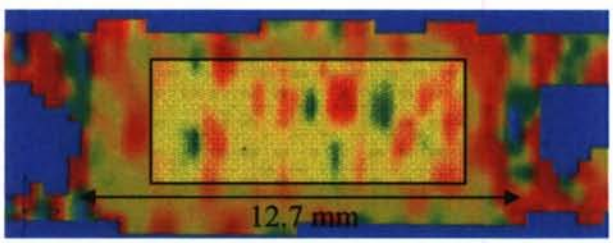

Figure 4.3: Full-Field Strain of a D6641 Specimen

A faint rectangle in the fore ground is depicted in Figure 4.3. This rectangle represented the area that the full-field strains were exported from the DIC system. The

strain in this area was averaged and exported as one data point. The strains exported for each data point were the longitudinal strain, which was in the direction of the applied load, and the transverse strain, which was orthogonal to the longitudinal strain and through the specimen thickness. In addition to the strains, each data point had the value of the load carried by the specimen at that instant.

4.4. Compression Test in Accordance with SACMA SRM R1

The compression test used in this study was in accordance with the SACMA SRM R1 recommended test method. The SACMA recommended test method was derived from ASTM D695 and covered the procedure for the determination of the compressive properties of oriented fiber-resin composites reinforced by continues high modulus fibers (SACMA SRM 1R-94, 1994). The ASTM D695 standard test method for compressive properties of rigid plastics presented the method of determining mechanical properties of reinforced rigid plastics when loaded in compression (ASTM D695, 1996). Referring to the ASTM standard, the SACMA recommended test method described the procedure behind conducting the test and calculating the composite material properties: elastic compressive modulus, ultimate compressive strength, and in-plane Poisson's ratio. Any deviation from the recommendation is noted in the following sections.

4.4.1. Specimen Preparation

Although the standard recommended the use of at least 5 specimens, 8 specimens were used for each testing condition. To accommodate the loss of specimens or data through the testing procedure, 8 specimens were used. From each panel two sets were cut, eight specimens each. Each set represented either the x-direction or the y-direction of

the panel. The x-direction was along the laminate principal axis, and the y-direction was orthogonal to the laminate principal axis. The cutting tool used to cut the specimens from the panels was a (CNC) water-abrasive jet.

The SACMA standard recommended a specimen length of 80.77 mm (30.18 in) and a width of 12.7 mm (0.5 in). The specimen thickness was recommended to be 3.05mm (0.12 in) but the panels were infused with 8 layers of fabric as reinforcement and the total laminate thickness was approximately 5.08 mm (0.2 in). Therefore, the specimen thickness was not in accordance with the recommendation in the standard and was 5.08 mm (0.2 in). The specimen dimensions are shown on a 2D-CAD drawing of the specimen in Figure 4.4

Figure 4.4: SACMA SRM 1R Specimen Configuration

The specimens were stored in a conditioning chamber for 3 months at a temperature of 22 ± 3°C (71.6 ± 5°F) and 50 ± 3% relative humidity. While testing the specimens, the testing room was climate controlled at room temperature (22°C) and relative humidity of 50%.

Two specimen types were recommended by the SACMA standard to measure the modulus of elasticity and the ultimate strength. An un-tabbed specimen used to measure the modulus of elasticity and a tabbed specimen used to measure the ultimate strength.

This procedure was recommended due to the difficulty of using a strain measurement device on the tabbed specimens when loading it to failure since the distance between the tabs is smaller than any conventional strain measuring device, approximately 4.75 mm (0.188 in). On the other hand, the un-tabbed specimen could not be loaded to failure since the ends of the specimen would crush. Since the 3-D DIC system was used to measure the strains as the specimen was loaded, the test was conducted with the use of one specimen to measure both properties: the modulus of elasticity and the ultimate strength.

In order to carry out the test to failure, a tabbed specimen was used. The tabbing material used was a cross-ply E-glass/Epoxy composite known as G11 and used mainly for electric boards. The tabs had a length of 38.1 mm (1.5 in) and the same width as the specimen with a thickness of 1.575 mm (0.062 in). The tabs material and dimensions agreed with the recommendations of the standard.

An 80 grit sand paper was used to roughen the surface where the tabs had to be bonded, and a degreaser was used to remove any residue of mold release from the panel manufacturing process and any dust particles to improve the bond of the tab to the specimen. The tabs were bonded to the specimen with Plio-Grip 7770, a structural adhesive. The adhesive was mixed and applied in a climate controlled room with a temperature of 20°C and relative humidity of 50% to insure curing of the adhesive. The tabs were clamped and left overnight at the same temperature and relative humidity to cure. A 3D-CAD drawing represents a tabbed specimen in Figure 4.5.

Figure 4.5: 3D-CAD Drawing of a SACMA SRM 1R Tabbed Specimen

After the specimens were tabbed, the ends of the specimens were machined parallel and square. In addition, to insure flat faces of the tabbed specimen, the faces of the specimen were also machined parallel and square. The process of preparing the specimen: tabbing and machining, was very time consuming.

The specimens' width and thickness were measured using a 5 mm (0.19685 in) nominal diameter double-ball-interface micrometer at three random locations along the specimen gage length which was 4.75 mm (0.188 in). The micrometer had an accuracy of ±2.5 μm (±0.0001 in). The measurements were recorded and the average area was later used in the computation of the compression properties of the material.

A 3-D DIC system was used to measure the strain on the specimen surface as the load was applied. Similar to the previous compression test, in accordance to ASTM D6641, the cameras of the DIC system were able to view the specimen edge due to the design of the fixture used to hold the specimen during loading. Therefore, a speckle pattern was applied on one edge of the specimen. The pattern was created by applying a white base first and then a black speckle pattern. The pattern was consistent with the

specifications needed for the DIC system to recognize the pattern in the frame of view that covers the specimen region of interest.

4.4.2. Test Setup

The specimen was installed in a test fixture that was supplied by Wyoming Test Fixtures Inc. The test fixture was made of two parallel V-grooved plates. The plates supported the specimen with little friction due to the grooves. The specimen was supported in such a way to resist buckling when the specimen was end loaded in a vertical plane (SACMA SRM 1R-94, 1994). The SACMA standard recommended mounting the specimen in the fixture by torquing the bolts to 0.7 – 0.1 N-m (6 – 10 in-lb), but the bolts were fixed by finger tight torquing which was in accordance with the ASTM D695 standard (ASTM D695, 1996). A disassembled fixture and a fixture with a specimen installed in it are depicted in Figure 4.6.

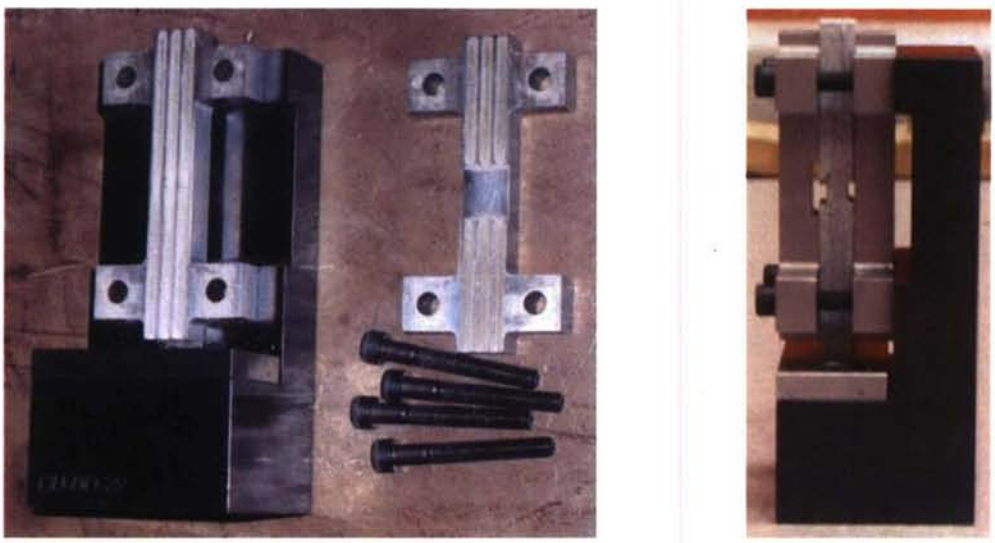

Figure 4.6: SACMA SRM R1 Fixture

The fixture was then placed in the testing machine such that the speckled edge was facing the DIC system cameras. The cameras were then calibrated to measure strain and displacement in the volume of space that the specimen was being tested in.

The testing machine used was a hydraulic machine with the capability of controlling the velocity of the moving head. The testing machine was capable of indicating the total load being carried by the test specimen. The specifications of the testing machine were in conformance with ASTM Practices E4 (ASTM E4, 2002). The load was applied by the testing machine through a ball bearing used to remove any bending forces on the specimen from imperfections in the frame and fixture. The use of a ball bearing was recommended by ASTM D695. The test fixture with the specimen placed in the testing frame and loaded by the ball bearing with the cameras capturing images is shown in Figure 4.7.

Figure 4.7: Testing of a SACMA SRM 1R Specimen

The test was conducted at a compressive loading rate of 0.6 mm/min (0.0236 in/min) to failure of the specimen. Each test lasted between approximately two minutes and three minutes. During the loading process, the data was collected at a rate of approximately 1 hertz, or one data point every second. Every data point collected included the load carried by the specimen as measured by the testing machine load cell (the load sensing unit) and the full-field strains on the specimen edge in the gage length as seen by the DIC system. A typical full-field strain in the direction of the load applied as captured by the DIC system of a SACMA SM R1 compression specimen is shown in Figure 4.8.

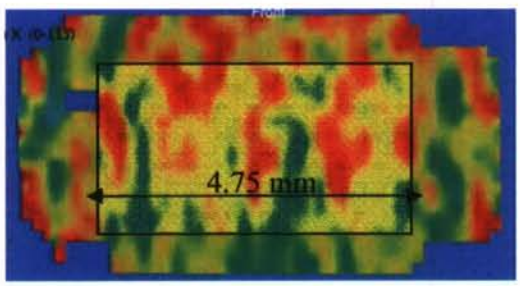

Figure 4.8: Full Field Strain of a SACMA SRM 1R Specimen

A faint rectangle in the fore ground is depicted in Figure 4.8. This rectangle represented the area that the full-field strains were exported from the DIC system. The strain in this area was averaged and exported as one data point. The strains exported for each data point were the longitudinal strain, in the direction of the applied load, and the transverse strain, orthogonal to the longitudinal strain and through the specimen

thickness. In addition to the strains, each data point had the value of the load carried by the specimen at that instant.

4.5. Stress-Strain Representation

Using the data exported from the DIC system, in addition to the measured average area of the specimen and the calibration factor of the load cell (the load sensing unit of the testing machine), a stress-strain curve was formed for each specimen. The standard recommended calculating the compressive modulus of elasticity of the material by considering the stress-strain relation in a specific range. In this range, the chord of the curve was recommended to be used as the laminate compressive modulus. The strain range of 25% and 50% of the ultimate strain was recommended to be used.

Observing the stress-strain curves for the compression specimens used in this study, it was noticed that the curves were slightly non-linear and more than one linear range was found. Therefore, a bi-linear representation of the stress-strain curve was adopted, similar to the tensile stress-strain representation discussed in Chapter 3. The material was then classified to have an initial modulus of elasticity and a final modulus of elasticity.

The data was analyzed by a program code written using Matlab programming language (Appendix B.2). The code used the load data and strain data to generate the stress-strain curve. Then two regions were selected from the curve: the first region lay between 5% and 20% of the ultimate strain and the second region lay between 60% and 90% of the ultimate strain. For each region, the least square error approach was used to estimate a linear relation of the data. The slope of the linear function was taken to be the modulus of elasticity. The intersection point of the two linear functions was considered

the transition point from the initial region to the final region. The Poisson's ratio was calculated in accordance with ASTM E132. Two Poisson's ratios were found for each stress-strain curve: a Poisson's ratio for the initial region and a Poisson's ratio for the final region. The Poisson's ratio was calculated to be the ratio of the modulus of elasticity calculated using the transverse strain to the modulus of elasticity calculated using the longitudinal strain (ASTM E132, 1997). Note that the transverse strain measured was through the specimen thickness.

A typical stress-strain curve of a compression test and its modeled bi-linear curve are shown in Figure 4.9. The values of the initial modulus, final modulus, Poisson's ratio, ultimate point, and transition point are indicated in Figure 4.9.

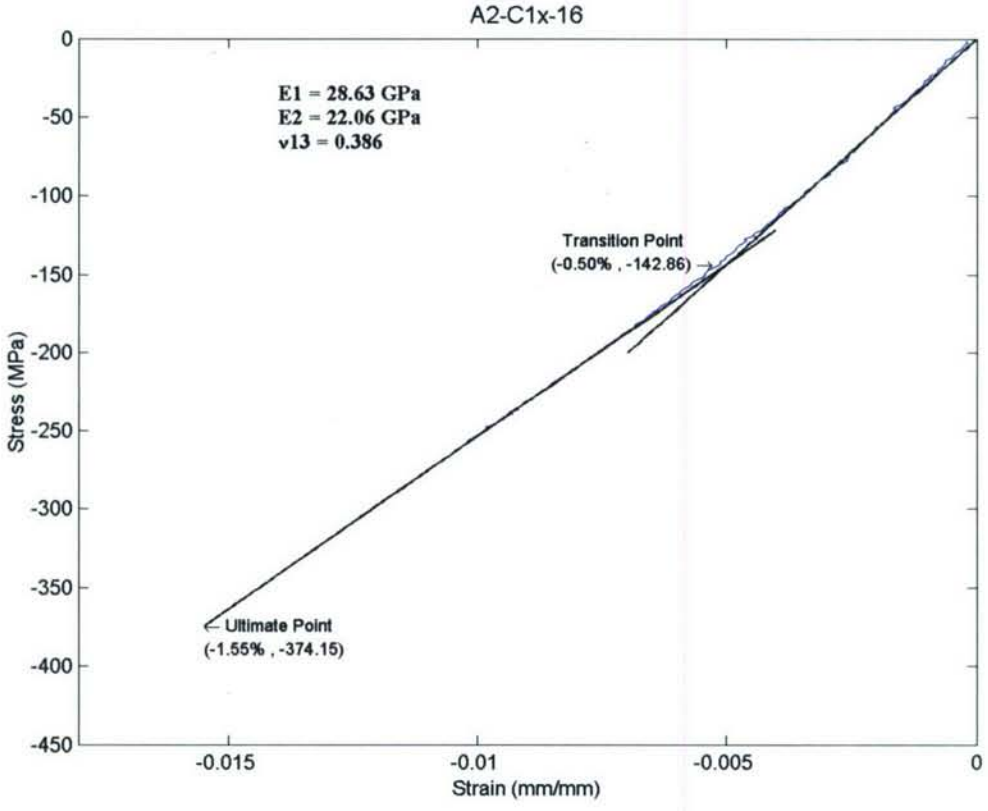

Figure 4.9: Modeled Compression Stress-Strain Curve

4.6. Discussion of the Experimental Results

The compression tests were conducted on two sets of panels, manufactured using two different batches. The first batch was used to infuse a 25.4 mm (1 in) thick panel and simultaneously infuse a 5.08 mm (0.2 in) thick panel, which acted as a witness panel for the 25.4 mm (1 in) thick panel. Similarly, the second batch was used to infuse a 12.7 mm (0.5 in) thick panel and simultaneously infuse a 5.08 mm (0.2 in) thick panel which acted as a witness panel for the 12.7 mm (0.5 in) thick panel. For each batch, three fiber lay-ups

were adopted: $[0]_{4sf}$, $[0/90]_{2sf}$, and $[0/\pm45/0]_{sf}$. Therefore, there were two panels for each fiber lay-up that had the same thickness but were infused with a different batch and at different environmental conditions.

A set of 8 specimens was tested for each direction in each panel. Having a total of 6 witness panels, 12 sets of results were computed. The following charts summarize the experimental results obtained from the compression tests conducted on the panels. Each chart has the mean, standard deviation, and coefficient of variation of the material property of the panels. Two material properties are only presented: the initial modulus of elasticity and the ultimate strength. The results of each direction are presented on separate charts. The experimental results of every two witness panels with the same lay-up sequence are presented by two adjacent bars. The complete material properties calculated for all the specimens tested are presented in Appendix C.2.

Each panel had two orthogonal directions: x-direction and y-direction, where the x-direction is the laminate principal axis.

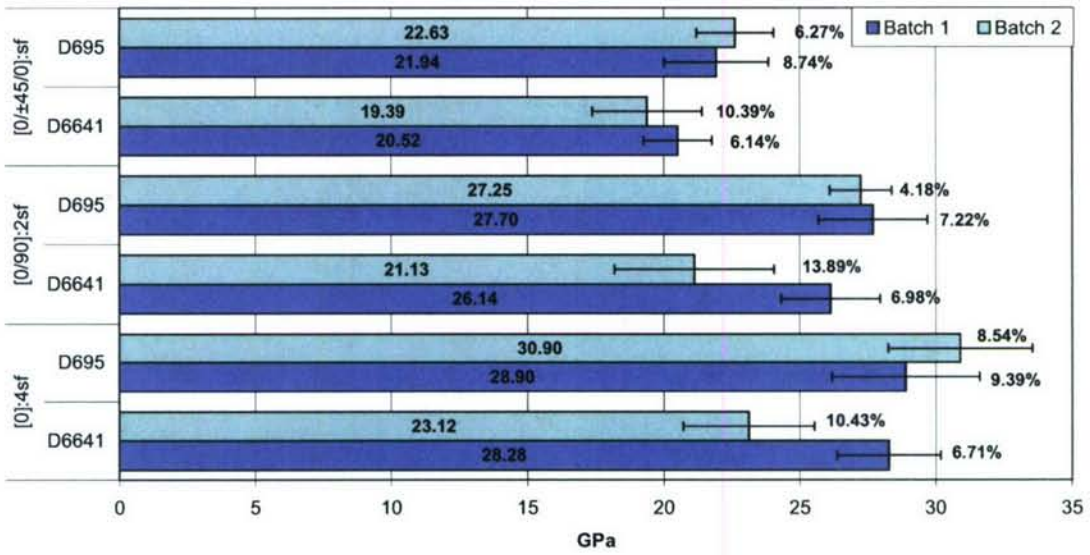

Figure 4.10: Compressive Initial Modulus of Elasticity (x-Direction)

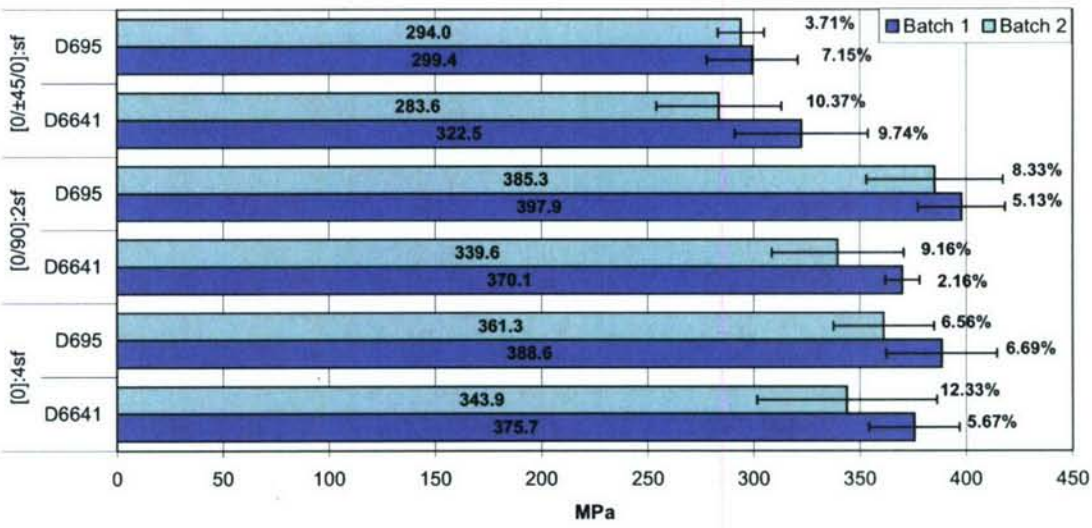

Figure 4.11: Compressive Ultimate Strength (x-Direction)

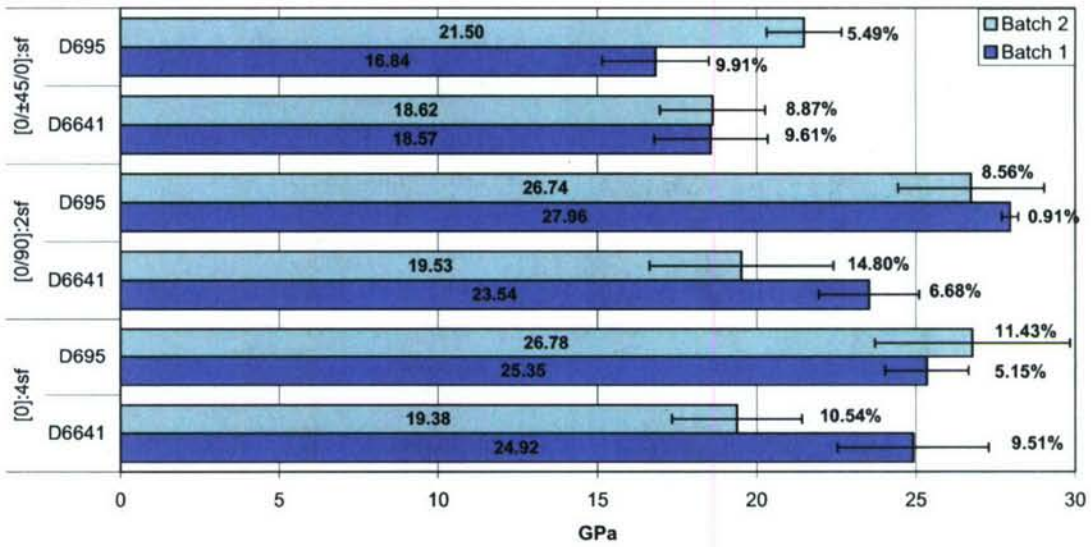

Figure 4.12: Compressive Initial Modulus of Elasticity (y-Direction)

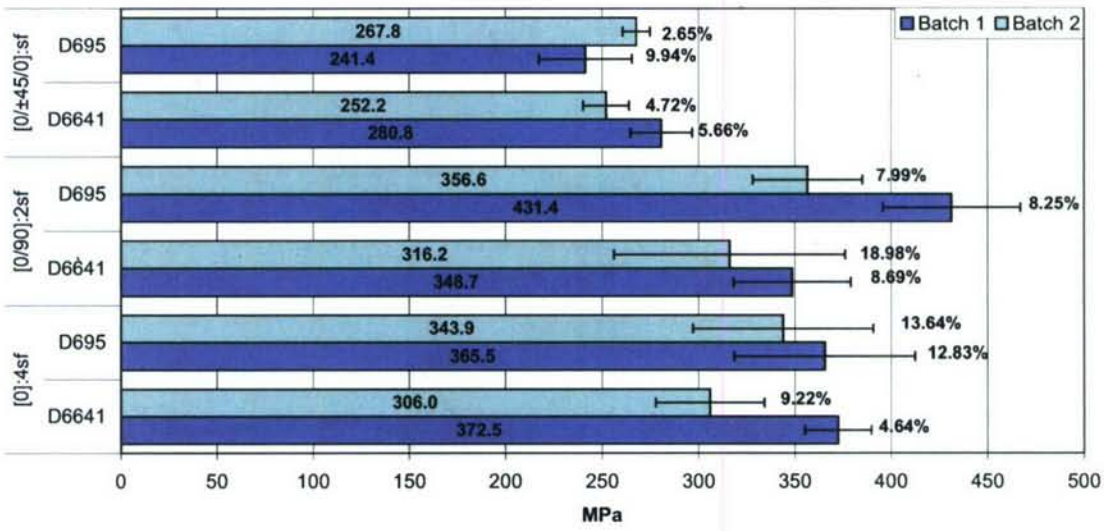

Figure 4.13: Compressive Ultimate Strength (y-Direction)

Further analysis of the experimental results was carried on by normalizing the results to one thickness as part of reducing the variability caused by the thickness variation through the panel. The normalization process and the normalized results are presented in section 7.3.1. In addition, the normalized results from both compression test methods were compared using a statistical tool to verify the significance of difference between the two; a similar approach was conducted on normalized results from both batches. The statistical comparison is presented in section 7.3.2.

4.7. Conclusion

One of the common disadvantages for both the test methods, was the strain field viewed by the DIC cameras. As mentioned in the test setup of each test method, the cameras were able to view the edge of the specimen due to the configuration of the fixtures. Therefore, the full-field strain captured by the DIC system was through the specimen thickness and the area of the strain was confined to 5.08 mm by the specimen width and to the length of the specimen gage section. In addition, when exporting the strains from the DIC system, the areas selected did not include the whole area of the strain field. As a result, the area used to compute the material compression properties did not have a sufficient representation of the material under study.

The DIC system captured strain concentrations in the specimens of both test methods. These strain concentrations can be translated to stress concentrations. The stress concentration in a D6641 specimen is depicted in Figure 4.14, and the stress concentration in a SRM 1R specimen is depicted in Figure 4.15.

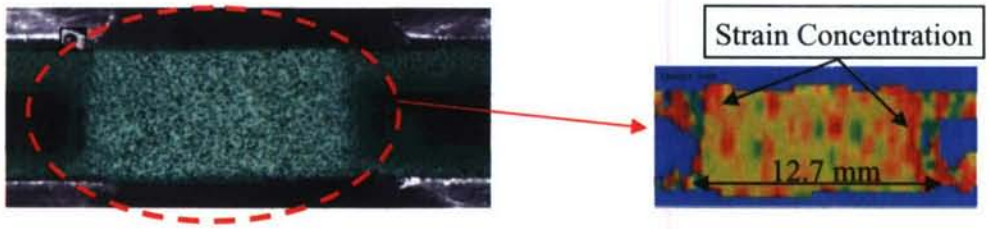

Figure 4.14: Strain Concentration in a D6641 Specimen

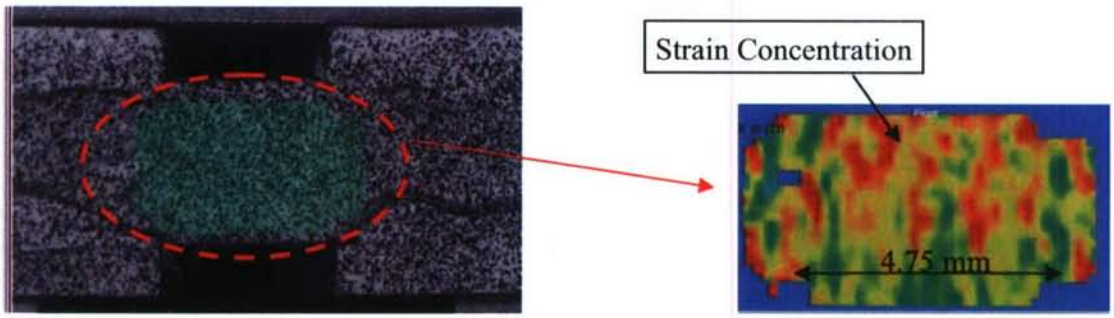

Figure 4.15: Strain Concentration in a SACMA SRM 1R Specimen

The strain concentrations are justified by the small length of the gage sections. The gage length of the D6641 specimen was 12.7 mm (0.5 in) and the gage length of the SRM 1R specimen was 4.75mm (0.188 in). The woven fabric used in the composite under study had a tow spacing of 5.1 mm (5 tows per inch) in the warp direction and 6.35 mm (4 tows per inch) in the fill direction, producing an unbalanced weave. A schematic representation of the woven fabric used is depicted in Figure 4.16.

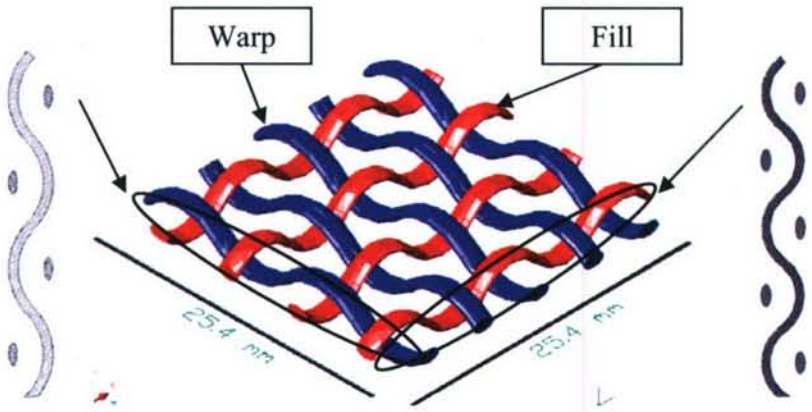

Figure 4.16: Weave Pattern Schematic

The tow pattern of the fabric repeated every 12.7 mm (0.5 in) in the warp direction and every 10.16 mm (0.4 in) in the fill direction. The patterns of the weave are presented in Figure 4.17 for both the warp and fill directions.

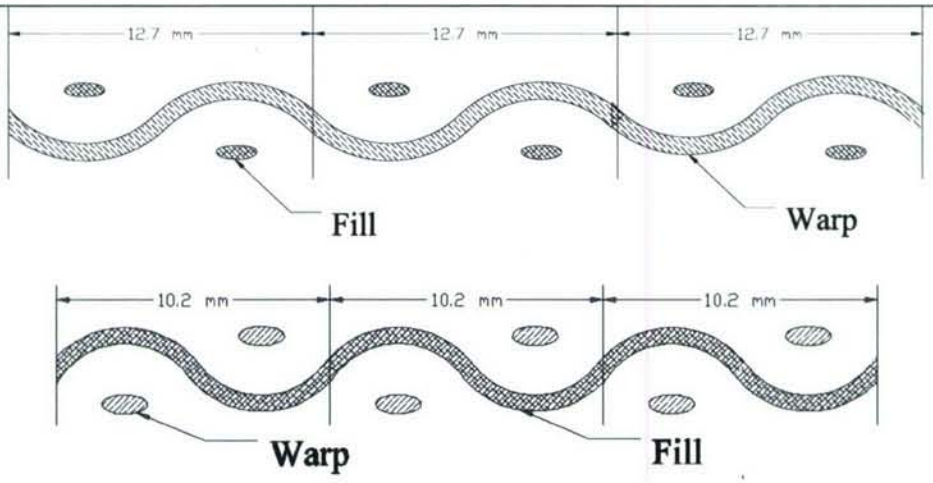

Figure 4.17: Fabric Weave Pattern in the Warp and Fill Direction

Therefore, with a gage length of 12.7 mm (0.5 in), for the D6641 specimen, the gage section contained approximately 2 or 2½ tows and in some cases the tow was under the clamping edge of the specimen, barely covering one weave pattern. More severely were the strain concentrations in the SRM 1R specimens. Since the gage length of that specimen was 4.75mm (0.188 in), the gage length contained approximately one tow or part of a tow and in some cases it contained a gap between two tows. Such small gage lengths did not properly represent the composite under study. Consequently, the small gage section could have confined the specimen from failing properly, especially with such a small number of tows in the gage section. Such a failing process over estimated the ultimate strength value as discussed in section 4.8.2.

Since the SRM 1R specimen was very time consuming to prepare prior to testing, a modification for the D6641 specimen was recommended. In addition, since the fixture of the SACMA SRM 1R test method did not allow for the possibility of increasing the length of the specimen, the D6641 test method was selected for modification.

4.8. Recommendations

4.8.1. Modifications Recommended for the ASTM D6641 Test Method

One of the major set backs in both the test methods conducted was the specimen surface that the DIC cameras were unable to view. In both tests, the cameras viewed the specimen edge, which was relatively small to represent the PMC with woven fabric reinforcement under study. Therefore, in the modified test method of ASTM D6641 the cameras were placed in such a way to view the front specimen surface.

The specimen width was increased from 19.05 mm (0.75 in) to 25.4 mm (1 in) to increase the area viewed by the DIC cameras and to include more of the fabric weave pattern. The increased width was the maximum possible width that can be incorporated in the D6641 CLC fixture. After increasing the specimen width, the need to increase the gage length was desired. Increasing the gage length was desired to obtain a good representation of the material under study. A proper representation of the PMC with woven fabric reinforcement is to include at lease three weave patterns in the gage section; the edge patterns are affected by the boundary conditions, thus, leaving the middle pattern unaffected by outside conditions. In order to increase the gage length, an Euler buckling check was conducted on the material for all three fiber lay-ups to prevent buckling induced failure in the specimen while testing. Two equations were used to check for buckling (Adams and Lewis, 1990). One equation governed by the material ultimate stress and is shown in equation (4.2). Another equation governed by the material ultimate strain and is shown in equation (4.3).

$$L_g = t \cdot \sqrt{\left(\frac{E_{11}}{F_{1C}} - 1.2\frac{E_{11}}{G_{13}}\right) \cdot \frac{\pi^2}{12 \cdot K^2}} \tag{4.2}$$

where:

L_g = length of gage section, mm (in),
t = specimen thickness, mm (in),
E_{11} = compressive modulus of elasticity, MPa (psi),
F_{1C} = ultimate compressive strength, MPa (psi),
G_{13} = inter-laminar shear modulus, MPa (psi),
K = constant depending on the degree of constraint of the column
K = 1 when the column ends are pinned (free to rotate)
K = ½ when the column ends are clamped (restrained against rotation)

$$L_g = t \cdot \sqrt{\left(\frac{1}{\varepsilon_{1C}} - 1.2\frac{E_{11}}{G_{13}}\right) \cdot \frac{\pi^2}{12 \cdot K^2}} \tag{4.3}$$

where:

L_g = length of gage section, mm (in),
t = specimen thickness, mm (in),
E_{11} = compressive modulus of elasticity, MPa (psi),
ε_{1C} = ultimate compressive strain, mm/mm (in/in),
G_{13} = inter-laminar shear modulus, MPa (psi),
K = constant depending on the degree of constraint of the column
K = 1 when the column ends are pinned (free to rotate)
K = ½ when the column ends are clamped (restrained against rotation)

Using equation (4.2), equation (4.3), and the material properties obtained previously from the testing program, the gage lengths were calculated for each fiber lay-up. Two assumptions were made for calculating the gage lengths. The inter-laminar shear modulus, G_{13}, was assumed to be equal to the in-plane shear modulus, G_{12}. This assumption was made since the inter-laminar shear modulus of the material under study was not available; and assuming the latter equal to the in-plane shear modulus gave conservative results for the gage section length. In addition, the column constraints were assumed to be pinned. Such an assumption was also conservative and gave smaller values of the gage length than assuming the ends of the column clamped. The calculated lengths for the different fiber lay-ups and direction of loadings are presented in Table 4.1.

Table 4.1: Length of Gage Section of Modified D6641 Specimen

Fiber Lay-up	$[(0_w/90_f)]_{4s}$		$[(0_w/90_f)/(0_f/90_w)]_{2s}$		$[(0_w/90_f)/\pm(45_w/-45_f)/(0_w/90_f)]_s$	
Direction of Loading	x-Direction	y-Direction	x-Direction	y-Direction	x-Direction	y-Direction
Gage Length (Ultimate Stress)	36.182 mm (1.424 in)	35.292 mm (1.389 in)	34.828 mm (1.371 in)	34.806 mm (1.370 in)	37.276 mm (1.468 in)	38.857 mm (1.530 in)
Gage Length (Ultimate Strain)	34.936 mm (1.375 in)	34.094 mm (1.342 in)	33.455 mm (1.317 in)	34.006 mm (1.339 in)	35.162 mm (1.384 in)	35.899 mm (1.413 in)

Since the two assumptions used for the calculation of the gage section length were conservative, the latter was chosen to be 30.48 mm (1.2 in).

Therefore, the modification to the ASTM D6641 specimen was increasing the gage section length from 12.7 mm (0.5 in) to 30.48 mm (1.2 in) and the gage section width from 19.05 mm (0.75 in) to 25.4 mm (1 in), thus incorporating as much of fabric weave patterns as possible. The modified D6641 specimen configuration is depicted in Figure 4.18.

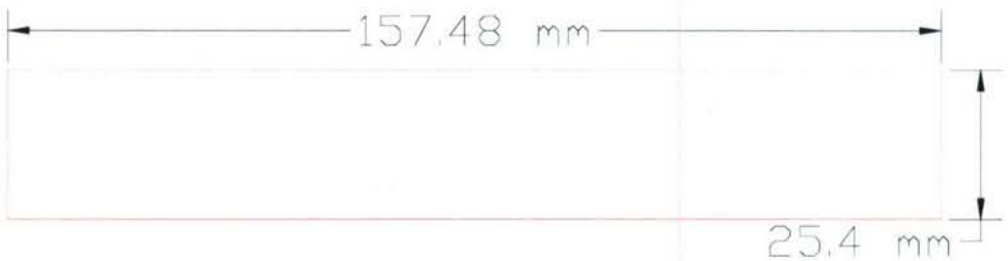

Figure 4.18: Modified D6641 Specimen Configuration

4.8.2. Discussion of the Experimental Results of the Recommended Modifications

The test was conducted similar to the ASTM D6641 test method described in section 4.3.2, except that the DIC cameras were facing the specimen front face as discussed in the previous section. The test was conducted on only one panel in two directions. The panel was from batch 1 and had $[0]_{4sf}$ for the fiber lay-up sequence.

A comparison of the experimental results between the specimens tested in accordance with ASTM D6641, described in section 4.3, and the modified specimens of the same test method is shown in Figure 4.19 and Figure 4.20. The charts compare the initial modulus of elasticity and ultimate strength of the two tests and present the means and coefficient of variations. In addition, the standard deviation error bars are depicted in the charts.

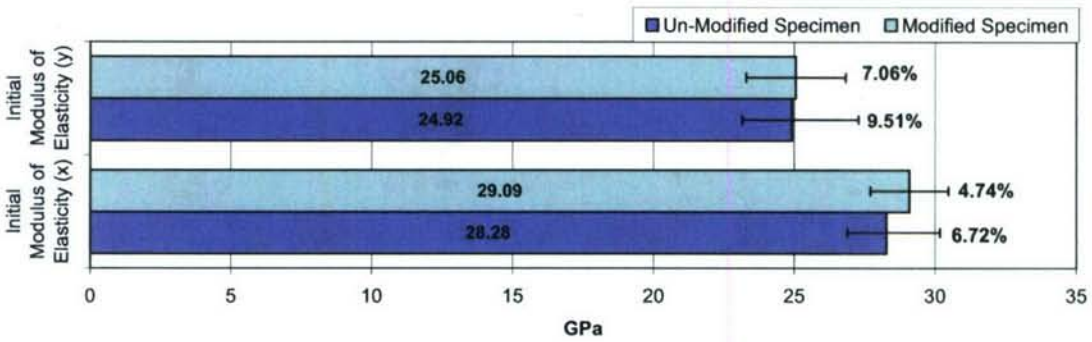

Figure 4.19: Comparison of Results for Modified and Un-Modified Specimens of ASTM D6641 (I-MOE)

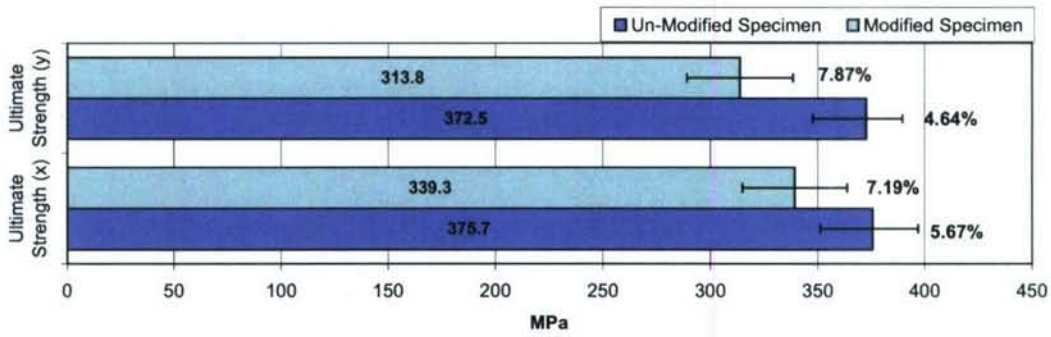

Figure 4.20: Comparison of Results for Modified and Un-Modified Specimens of ASTM D6641 (U. Strength)

As observed in the charts, the coefficient of variation has improved in the calculated results of the initial modulus of elasticity when testing the modified specimen. The improvements in the results of the initial modulus of elasticity were contributed to the change in the surface viewed by the DIC cameras. Instead of viewing the edge of the specimen, the cameras viewed the front surface of the specimen which was larger and better represents the material.

Conversely, the coefficient of variation of the ultimate strength did not improve. This can be explained by the fact that the fixture was constraining the specimen from failing normally; the fixture introduced more consistency in the ultimate strength calculated compared to having the specimen failing normally. In addition, the ultimate strength calculated for the modified specimen had lower values than the un-modified specimen. Similarly, this can be explained by the constraint the fixture introduced on the gage delaying the failure of the specimen and causing the over estimation of the ultimate strength of the material.

The modifications recommended for the compression test improved the experimental results. With the help of the DIC system these recommendation were suggested and proven to enhance the testing method for obtaining the compressive material properties of PMC with woven fabric reinforcement. Further testing can be conducted on other lay-ups to prove the validity of the recommendations based on these lay-ups.

4.9. References

ASTM D5229/D5229M, (2002). Test Method for Moisture Absorption Properties and Equilibrium Conditioning of Polymer Matrix Composite Materials. Annual Book of ASTM Standards. West Conshohocken, American Society of Testing Materials. **Vol 15.03**.

ASTM E4, (2002). Practices for Force Verification of Testing Machines. Annual Book of ASTM Standards. West Conshohocken, American Society of Testing Materials. **Vol 03.01**.

ASTM E132, (1997). Standard Test Method for Poisson's Ratio at Room Temperature. Annual Book of ASTM Standards. West Conshohocken, American Society of Testing Materials. **Vol 03.01**.

ASTM D6641/D6641M, (2001). Standard Test Method for Determining the Compressive Properties of Polymer Matrix Composite Laminates Using a Combined Loading Compression (CLC) Test Fixture. Annual Book of ASTM Standards. West Conshohocken, American Society of Testing Materials. **Vol 15.03**.

ASTM D695, (1996). Standard Test Method for Compressive Properties of Rigid Plastics. Annual Book of ASTM Standards. West Conshohocken, American Society of Testing Materials. **Vol 08.01**.

SACMA SRM 1R-94, (1994). Recommended Test Method for Compressive Properties of Oriented Fiber-Resin Composites. Washington DC, Suppliers of Advanced Composites Materials Association.

Adams, D. F. and E. Q. Lewis (1991). "Influence of Specimen Gage Length and Loading Method on the Axial Compressive Strength of a Unidirectional Composite Material." Experimental Mechanics **31** (2): 14-20.

Adams, D. F. and E. Q. Lewis (1990). "Influence of Specimen Gage Length and Loading Method on the Axial Compressive Strength of a Unidirectional Composite Material." Experimental Mechanics (March 1991).

ASTM D4762, (2004). Standard Guide for Testing Polymer Matrix Composite Materials. Annual Book of ASTM Standards. West Conshohocken, American Society of Testing Materials. **Vol 08.04**.

Tomblin, J. S., Y. C. Ng, et al. 2001. Material Qualification and Equivalency for Polymer Matrix Composite Material Systems. U.S. Department of Transportation, Washington DC. Report#: DOT/FAA/AR-00/47.

Wolfe, A. R. and M. Weiner (2004). Compression Testing - Comparison of Various Test Methods. Composites 2004 Convention and Trade Show, Florida, American Composites Manufacturers Association.

ASTM D3410/D3410M, (2003). Standard Test Method for Compressive Properties of Polymer Matrix Composite Materials with Unsupported Gage Section by Shear Loading. Annual Book of ASTM Standards. West Conshohocken, American Society of Testing Materials. **Vol 15.03**.

ASTM D5467/D5467M, (2004). Standard Test Method for Compressive Properties of Unidirectional Polymer Matrix Composites Using a Sandwich Beam. Annual

Book of ASTM Standards. West Conshohocken, American Society of Testing Materials. **Vol 15.03**.

Chapter 5: Shear Tests for Characterizing Polymer Matrix Composites with Woven Fabric Reinforcement

5.1. Introduction

Shear properties of polymer matrix composite (PMC) reinforced with woven fabric were calculated using two American Society for Testing and Materials (ASTM) standard tests. This chapter introduces the literature behind the different studies conducted on obtaining the shear properties of PMC materials and the issues related to the testing process and specimen configuration.

The two tests selected are in accordance with ASTM standard test methods. The first was in accordance with ASTM D4255 which is under the jurisdiction of ASTM committee D30 on composite materials (ASTM D4255/D4255M, 2002).The second test method was in accordance with ASTM D5379 which is also under the jurisdiction of ASTM committee D30 on composite materials (ASTM D5379/D5379M, 1999). The main difference between the two test standards is the size of the specimen and the size of the gage section.

The different techniques used to conduct the test are explained in the following sections. The specimen configuration used for each test, the specimen preparation, the process of collecting the data, and the analyzing techniques are all explained and compared to the recommendations of the standards. Any deviation from the standard is noted and justified.

Once the results from each test standard were collected, they were compared to one another. An experimental mechanical analysis was employed to make the

comparison between the two sets of experimental results. Recommendations conclude the chapter and the advantages and disadvantages of each test method used in this study are stated.

5.2. Background

Several test methods have been used to obtain the shear properties of a fiber reinforced PMC. One of the main obstacles faced when these test methods were conducted was the inability to induce a uniform shear state. A standard guide for testing PMC materials supplied by ASTM recommended three test methods for calculating the in-plane shear properties of the composite material (ASTM D4762, 2004). The tests were: the v-notch specimen method ASTM D5379, the rail shear method ASTM D4255, and the tensile test of [±45] lay-up ASTM D3518 (ASTM D5379/D5379M, 1999; ASTM D3518/D3518M, 2001; ASTM D4255/D4255M, 2002). It was noted in the ASTM D4762 standard that the tensile test of [±45] laminate was limited to panels with [±45] fiber lay-up. As for the two standards selected for this study, it was noted that the v-notch specimen method was recommended where stress-strain data is required and that it gave accurate modulus measurements for laminates of the [0/90] family; while, it was noted that the three-rail method was a difficult test to run.

A theoretical and experimental analysis of the rail shear test method, presented in a journal paper (Whitney, Stansbarger et al., 1971), stated that the most idealized means of measuring the in-plane shear properties of a material was by torquing a tubular specimen. But due to the difficulties that accompanied preparing tubular specimen, a flat specimen was preferred. The paper concluded that a uniform shear stress state was produced in the gage section at a short distance away from the free edges, for rail

specimens having the ratio of the specimen length to the gage section width less than or equal to ten.

A study was conducted to improve the measurement of strain between the notches of a v-notch shear specimen (Ifju, 1994). The study presented a new type of strain gage that covers the entire section between the notches and averages the shear strain across this section. The article concluded that a benefit of the strain gage was that it accounts for non-uniform and impure shear distributions. In addition, since the strain gage covers a large area, it made it an effective method to measure shear strains for laminated and textile composite materials.

The short beam shear method ASTM D2344, the v-notch shear method ASTM D5379, the axial tension of a [±45] laminate method ASTM D3518, and the two-rail shear test method ASTM D4255, were selected for a study to assess the different shear test methods (Adams and Lewis, 1997). The paper concluded that of the four ASTM shear test methods evaluated, the v-notch shear test method appeared to have the best results. It was also observed in the paper that the rail shear test offered the possibility of a pure shear stress state similar to the v-notch shear test method.

Both the v-notch shear test method ASTM D5379 and the short beam shear test method ASTM D2344 were recommended as part of a testing program for material qualification of PMC material systems (Tomblin, Ng et al., 2001).

The v-notch shear test method ASTM D5379 was used to evaluate the shear material properties of a unidirectional hybrid composite. The study showed that the v-notch test method exhibits a limited region having a reasonable pure and uniform strain state between the notches. The paper stated that the v-notch test was effective for the

evaluation of the shear modulus, but not for the shear strength of the hybrid composite (He, Chiang et al., 2002).

5.3. Shear Test in Accordance with ASTM D4255

Two procedures were recommended in the standard: two-rail shear test and three-rail shear test. The three-rail shear test procedure was selected for the study and is addressed in the chapter. The three-rail shear test was selected over the two-rail shear test due to the balance that the three-rail test fixture provides on the specimen and since the off axis load of the two-rail method introduces small tensile load in the specimen while during loading (ASTM D4255/D4255M, 2002).

The three-rail shear method utilized a three-rail fixture that was made from three rails parallel to each other. The rails secure the specimen, a flat panel. The edge rails were supported by the fixture base and the load was applied on the center rail. The applied loading to he three-rail fixture produced almost pure shear in the two gage sections of the specimen. Note that a perfectly pure shear stress condition was hard to achieve to failure on the specimen's gage section. The three-rail shear fixture is shown in Figure 5.1, in addition, the specimen used for the test is depicted next to the fixture in Figure 5.1.

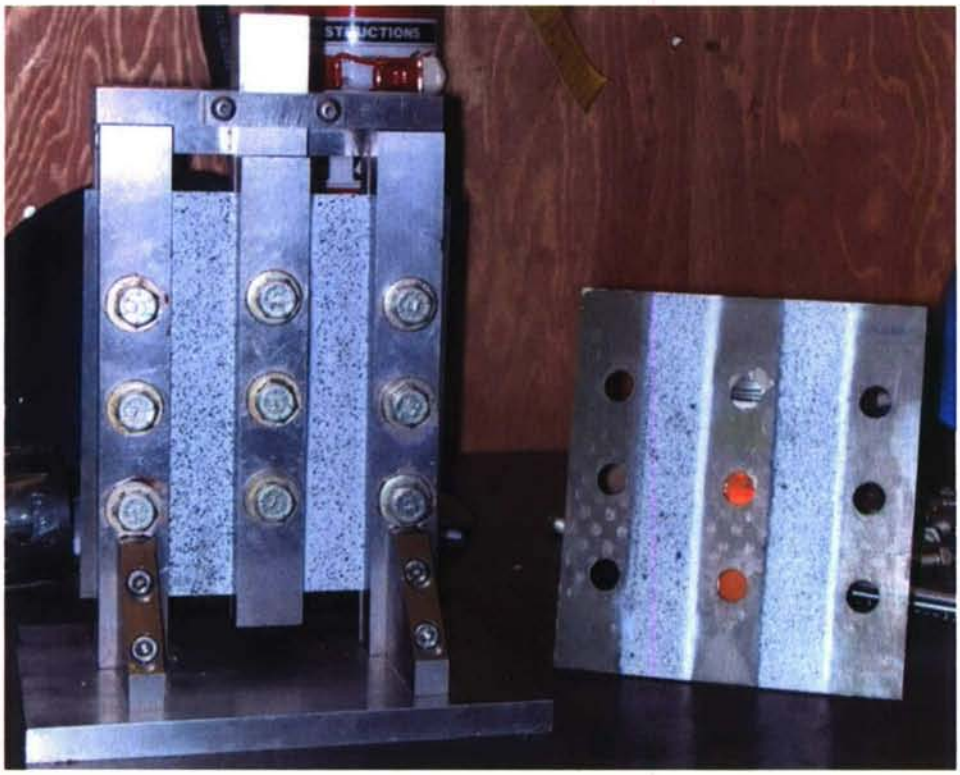

Figure 5.1: Three-Rail Shear Fixture with D4255 Specimen

The ASTM D4255 standard recommended the procedure to cut the specimens and prepare the specimens for testing. In addition, the procedure used for conducting the test and collecting the data was explained in the standard. The following sections state the procedure used to conduct the test in this study; the tools used to measure the specimen dimension, the strain measuring devices and the procedure to collect the data are explained in the following sections.

5.3.1. Specimen Preparation

The ASTM D4255 standard recommended that at least 5 specimens per test condition be tested (ASTM D4255/D4255M, 2002). For this study 8 specimens were

tested per test condition. Extra specimens were needed to account for lose of data while testing or during data collection. The fabric used to reinforce the PMC was E-glass woven fabric having 55% by weight of fiber in the warp direction and 45% in the fill direction. Therefore, two sets of specimens were cut from each panel. One set in the x-direction, the laminate principal axis, and another set in the y-direction, orthogonal to the laminate principal axis. Although, ideally, there should be no difference in the shear properties of the PMC in these two directions, the two sets were selected to verify that fact. The specimens were cut using a computer numerical control (CNC) water-abrasive jet machine.

The specimen configuration was in accordance with the recommendation in the standard. The specimen length was 152.4 mm (6 in) and the width was 136.53 mm (5.375 in). The specimen contained 9 holes with a diameter of 12.7 mm (0.5 in) each as depicted in the 2D-CAD drawing in Figure 5.2.

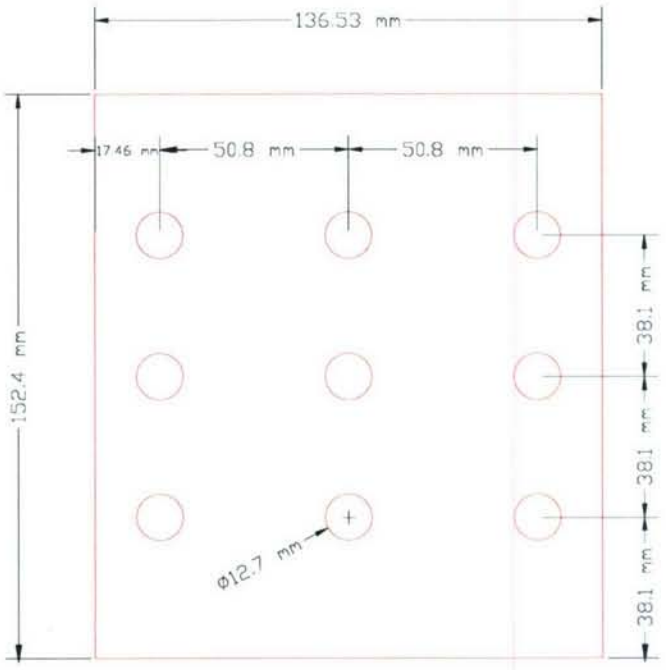

Figure 5.2: D4255 Specimen Configuration

The specimens were conditioned for 3 months at a temperature of 22 ± 3°C (71.6 ± 5°F) and 50 ± 3% relative humidity in accordance with procedure C of ASTM D5229 (ASTM D5229/D5229M, 2002) prior to testing.

The specimen thickness was measured using a 5 mm (0.19685 in) nominal diameter double-ball-interface micrometer at two random locations on each specimen gage length, since each specimen contained two gage sections. The micrometer had an accuracy of ±2.5 μm (±0.0001 in), while the specimen length was measured at the same locations using a double-flat-anvil caliper with an accuracy of ±12.7 μm (±0.0005 in). The measurements were recorded and the average area was later used in the computation of the material shear properties.

The specimen configuration provided two gage sections to be used to measure shear strain while loading. Each gage section was considered to be approximately 140 mm (5.51 in) by length and 25.4 mm (1 in) by width. The gage section was not of the same specimen length due to impure stresses present on the specimen edges. The gage section was chosen were almost pure shear stresses were found.

The standard recommended the use of four three-element strain gage rosettes for measuring the shear strain while the specimen was loaded. In stead of using strain gages, a 3-D digital image correlation (DIC) system was used to measure full-field strains of the gage section. The DIC system measured strains by recognizing a pattern in the specimen and follow it while the load was applied. Therefore, a speckle pattern was applied to the specimen surface that would be facing the digital cameras of the DIC system. The pattern was made by applying a white base first and then a black speckle pattern. The specimens were set aside to dry for a day. The pattern was consistent with the specifications needed for the DIC system to recognize the pattern in the frame of view that covers the specimen region of interest, gage section.

When the specimen was installed in the fixture, 9 grade eight steel bolts were used to clamp the specimen. The torquing force recommended by the standard was 94.9 N-m (70 lbf-ft). To simplify the torquing process a thread lubricant was used and the torque applied was 54.2 N-m (40 lbf-ft), which was the limiting torque before the bolts material yielded. To insure good clamping with every specimen, the bolts and nuts were replaced for every specimen.

5.3.2. Test Setup

After the specimen was installed in the fixture, the fixture was placed in the testing machine. The testing machine was a servo controlled hydraulic machine capable of controlling the velocity of the moving head. The testing machine was capable of indicating the total load being carried by the test specimen with a maximum capacity of 100 kN (22 kip). The testing machine specifications were in conformance with ASTM Practices E4 (ASTM E4, 2002). The load applied by the testing machine through a ball bearing was used to remove any bending forces on the specimen from imperfections in the frame and fixture. The three-rail fixture with a specimen installed in it is shown in Figure 5.3 as it is being tested and the DIC cameras capturing images.

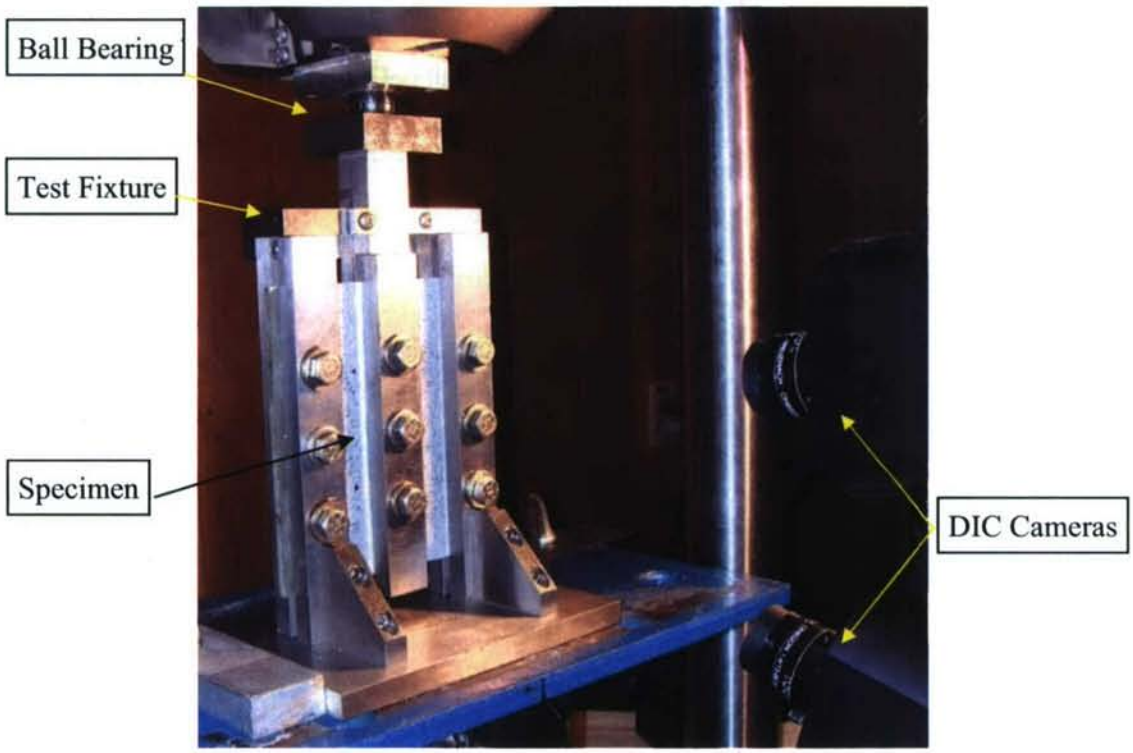

Figure 5.3: Testing of D4255, Three-Rail Shear, Specimen

Since the DIC system was used to measure strains, the cameras of the DIC system were placed in front of the specimen surface. The distance and the setup of the cameras were in accordance with the manual of the system. Once the cameras were calibrated, the system was able to measure strains in a volume space that contained the specimen.

The test was conducted at a grip head speed of 1.2 mm/min (0.047 in/min). At this rate, the test lasted approximately 5 minutes to 6 minutes. The load and strain data were collected at a rate of 1 hertz, one data point per second. The DIC system collected the data as a series of digital images that were later computed to obtain full-field strains of the specimen during loading; in addition, the load data was collected with every pair of pictures captured by the cameras of the DIC system to indicate the load carried by the

specimen at that instant. The load data was collected as analog signals that were later converted to load values using an appropriate calibration factor. A typical full-field shear strain of a D4255 specimen is depicted in Figure 5.4.

Figure 5.4: Full-Field Shear Strain of a D4255 Specimen

The strains were exported from the DIC system by selecting two areas over the specimen gage lengths. The average shear strain from each area was exported. The areas represented the specimen gage length and are shown in Figure 5.4 as two faint rectangles in the fore ground. The data exported had two strain values for each data point. The average of these values was used to represent the stress strain curve, which is explained in details in section 5.5. The load data was exported simultaneously for each data point with the accompanied shear strain.

5.4. Shear Test in Accordance with ASTM D5379

The second test conducted in this study to obtain the material in-plane shear properties was the v-notched beam method described in ASTM D5379 (ASTM D5379/D5379M, 1999). In this method, the specimen was a rectangular flat strip with a centrally located v-notch; and a special fixture, referred to as Iosipescu shear test fixture, was utilized to transfer the loading to the specimen. The intent of the fixture and the specimen configuration was to produce pure shear strain in the material along the area between the notches of the specimen. A picture of a specimen installed in the fixture is shown in Figure 5.5.

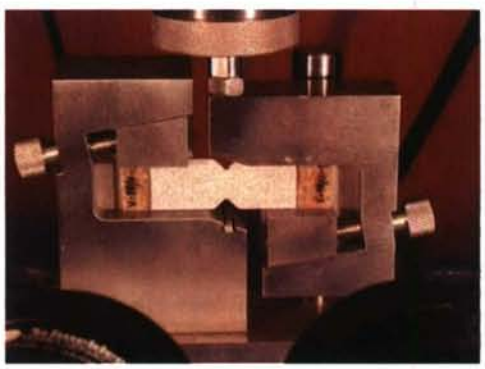

Figure 5.5: D5379 Specimen installed in the V-Notch Fixture

The standard describes the method to prepare the specimen and conduct the test. Specimen configuration and the fixture used for the test were described in the standard. In addition, the standard explained the procedure to conduct the test and measure the

strains needed to calculate the material in-plane shear properties. In accordance with the standard recommendations, the procedure conducted in this study is presented in the following sections and any deviation from the ASTM standard is stated and justified.

5.4.1. Specimen Preparation

Referring to the standard, it is stated that at least 5 specimens should be tested per testing condition. To account for specimen data that may be lost during the testing process or during the data analysis, 8 specimens for each direction were tested. The fabric used in reinforcing the PMC was E-glass woven fabric with 55% of the fiber weight in the warp direction and 45% in the fill direction. Therefore, each panel had two orthogonal directions: x-direction and y-direction, where the x-direction was the laminate principal axis. Although the in-plane shear properties of the panels were ideally independent of the principal in-plane direction the test was conducted, the specimens were cut from the panels in two directions, x-direction and y-direction, and tested to verify this fact. The specimens were cut from the panels with a CNC water-abrasive jet machine.

The standard recommended a specimen configuration that was used with the Iosipescu test fixture. The standard recommendations were adhered to and the specimen configuration and dimensions used in this study are shown in Figure 5.6.

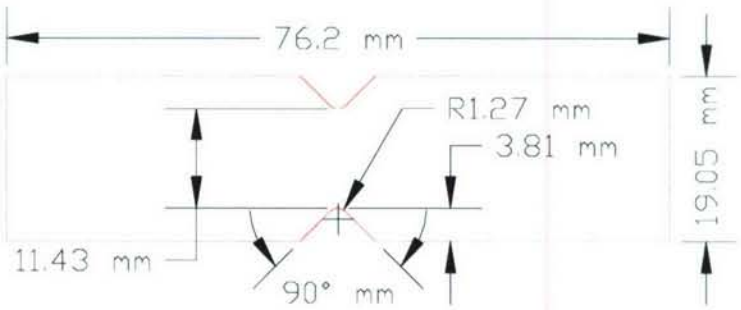

Figure 5.6: D5379 Specimen Configuration

The specimens were conditioned in accordance to procedure C of test method D5229 (ASTM D5229/D5229M, 2002). The specimens were stored in a conditioning chamber for 3 months at a temperature of 22 ± 3°C (71.6 ± 5°F) and 50 ± 3% relative humidity. While testing the specimens, the testing room was climate controlled at room temperature (22°C) and relative humidity of 50%.

As recommended in the standard, the specimen thickness was measured with a 5 mm (0.19685 in) nominal diameter double-ball-interface micrometer at three random locations between the notches of the specimen which had a length of 11.43 mm (0.45 in). The micrometer had an accuracy of ±2.5 μm (±0.0001 in). The length of the notched section was measured using an edge-end caliper with an accuracy of ±12.7 μm (±0.0005 in). The measurements were recorded and the calculated average area was later used in the computation of the material in-plane shear properties.

The ASTM D5379 standard recommended the use of strain gages to measure the shear strain in the gage section. Two strain gages were recommended to be bonded between the notches at an angle of +45° and -45° to the loading axis. Instead of using strain gages, a 3-D DIC system was used which measures full-field strains compared to a

point value shear strain measured by the strain gages. The DIC system recognized a speckle pattern on the specimen surface through capturing digital images and tracked the pattern as load was applied. Through correlating the images captured by the cameras, the DIC system calculated full-field strains on the specimen surface. The specimen surface was sprayed with a speckle pattern for the DIC system to track. The speckle pattern was applied by spraying a white base first and then a black random speckle pattern. The pattern was consistent with the specifications needed for the DIC system to recognize the pattern in the frame of view that covers the specimen gage section.

5.4.2. Test Setup

The specimen was installed in the fixture and placed in the testing frame which was a hydraulic machine capable of controlling the velocity of the moving head. The testing machine was capable of indicating the total load being carried by the test specimen. The specifications of the testing machine were in conformance with ASTM Practices E4 (ASTM E4, 2002).

The cameras of the DIC system were placed in front of the fixture and calibrated. The distance of the cameras from the specimen and the setup were in accordance with the manual of the system. The calibrated cameras were able to recognize a pattern in a volume of space where the specimen was placed. The DIC cameras, the fixture, and specimen installed in the fixture are shown in Figure 5.7 as the test was in progress.

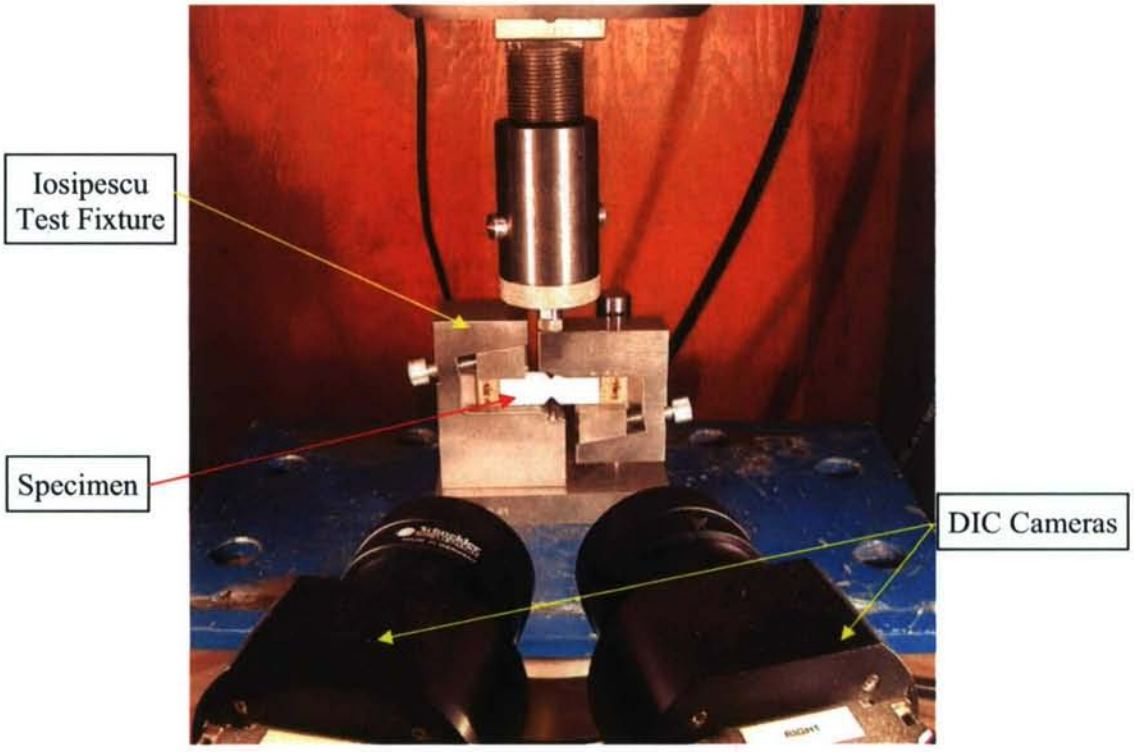

Figure 5.7: Testing of D5379, V-Notched Shear Specimen

The speed of the grip heads was judged by the time elapsed during the test. The standard recommended the test speed to cause failure within one to ten minutes. The grip head speed selected was 1.2 mm/min (0.047 in/min) that caused a failure after approximately three minutes of the test start. During the loading process, the data was collected at a rate of approximately one hertz, or one data point every second. Every data point collected included the load carried by the specimen as measured by the load cell, the load sensing unit, of the testing machine, and the full-field strains on the face of the specimen in the gage section as seen by the DIC system. A typical full-field shear strain captured by the DIC system for an ASTM D5379 v-notch shear specimen under load is shown in Figure 5.8.

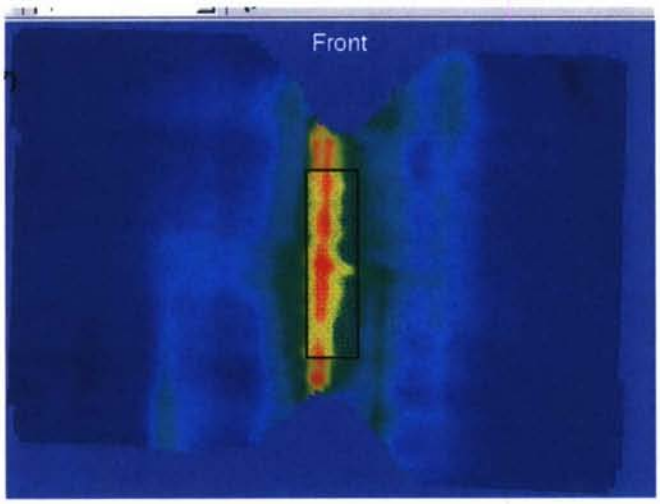

Figure 5.8: Full-Field Shear Strain of a D5379 Specimen

A faint rectangle in the fore ground is depicted in Figure 5.8. This rectangle represented the area of full-field shear strain that was exported from the DIC system. The strain in this area was averaged and exported as one data point. In addition to the shear strain, each data point was accompanied with the value of the load carried by the specimen at that instant.

5.5. Stress-Strain Representation

The data exported from the DIC system was imported into a Matlab program (Appendix B.3). The Matlab code used the imported data and the measurement data of the gage section thickness and width to build the stress-strain curve for each specimen tested. The load was converted from an analog signal (as received from the load cell) to a load value using the appropriate calibration factor. The stress-strain curve generated by the code depicted an elastic nonlinear behavior of the material.

The standard recommended calculating the material shear modulus of elasticity by taking the chord of the curve over a range of 4000 micro-strain at the start of the curve, beginning in the range of approximately 2000 micro-strain. The shear strength was recommended to be calculated by taking the intersection of the curve with the 0.2% offset of the chord modulus calculated. The standard recommendations were not followed to calculate the material properties of the material tested in this study. Instead a hyperbolic tangent curve fit was used. The hyperbolic tangent curve fit is given in equation (5.1) (Barbero, 1998).

$$\tau_{12} = a \cdot \tanh\left(\gamma \cdot {}^{b}\!/_{a}\right) \tag{5.1}$$

where:

τ_{12} = shear stress, MPa (psi),
γ = shear angle, radians
a = asymptote of the curve, MPa (psi),
b = slope of the tangent of the curve at the base, MPa (psi).

Using equation (5.1) the elastic shear modulus was considered to be the value of b. The value of the asymptote of the curve was recommended in the reference to be used as the ultimate shear strength of the material. For this study, the stress-strain curve of the material exhibited an asymptote for the curve fit that had a large value. The failure of the material was detected in the curve by a flat region were the strain increased at a constant load. Therefore, the ultimate shear strength of the material was considered to be the point at which the strain increased and the load was constant or decreased. A typical stress-strain curve of a shear specimen with the hyperbolic tangent curve fit is depicted in

Figure 5.9. The calculated value of the shear modulus of elasticity and shear ultimate strength of the stress-strain curve are presented in Figure 5.9.

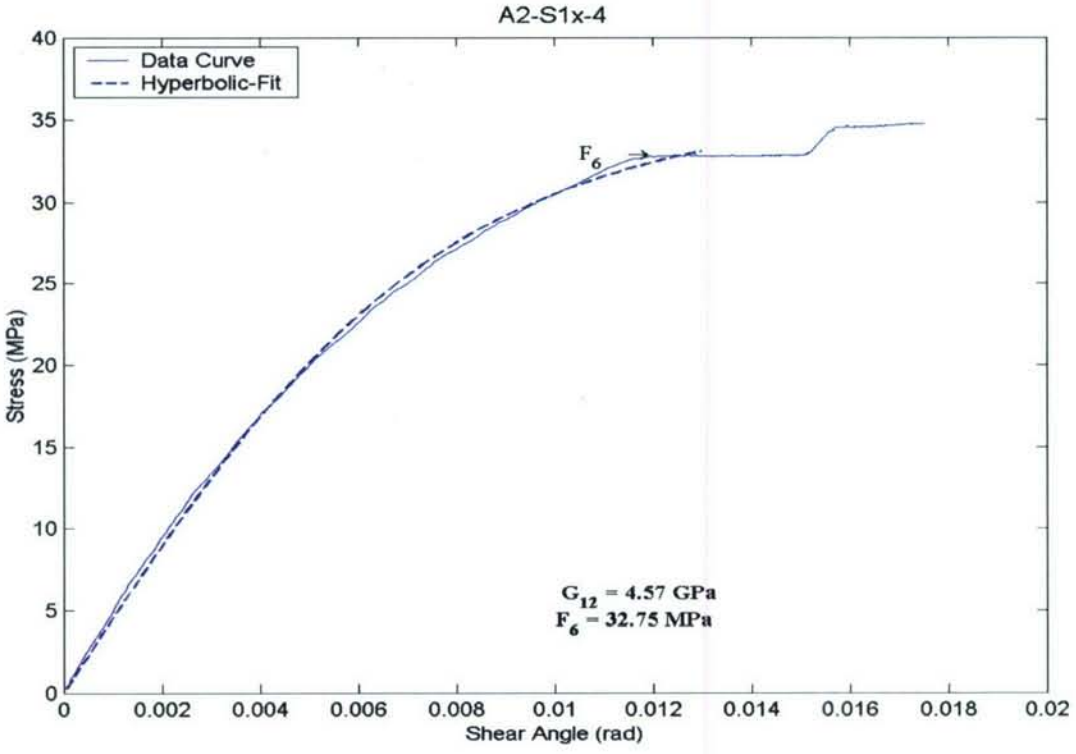

Figure 5.9: Typical Stress-Strain Shear Curve with Hyperbolic Tangent Curve Fit

5.6. Discussion of the Experimental Results

The shear tests were conducted on two sets of panels, manufactured using two different batches. The first batch was used to infuse a 25.4 mm (1 in) thick panel and simultaneously infuse a 5.08 mm (0.2 in) thick panel, which acted as a witness panel for the 25.4 mm (1 in) thick panel. Similarly, the second batch was used to infuse a 12.7 mm (0.5 in) thick panel and simultaneously infuse a 5.08 mm (0.2 in) thick panel which acted

as a witness panel for the 12.7 mm (0.5 in) thick panel. For each batch, three fiber lay-ups were adopted: $[0]_{4sf}$, $[0/90]_{2sf}$, and $[0/\pm45/0]_{sf}$. Therefore, there were two panels for each fiber lay-up that had the same thickness but were infused with a different batch and at different environmental conditions. A set of 8 specimens was tested for each direction in each panel. Having a total of 6 witness panels, 12 sets of results were computed.

5.6.1. Shear Properties in Accordance with ASTM D4255

The shear modulus of elasticity was calculated by using the hyperbolic tangent fit curve given in equation (5.1) to model the stress-strain curve. The mean values of each set of specimens are presented in Figure 5.10. The chart has the standard deviation error bars and the coefficient of variation for each set. The chart was organized in such a way to compare the shear modulus values between the two batches tested for each fiber lay-up. As noted earlier, each panel had two orthogonal directions: x-direction and y-direction, where the x-direction is the laminate principal axis. Both directions are plotted in one chart to verify that the shear modulus was independent of the in-plane principal material axes.

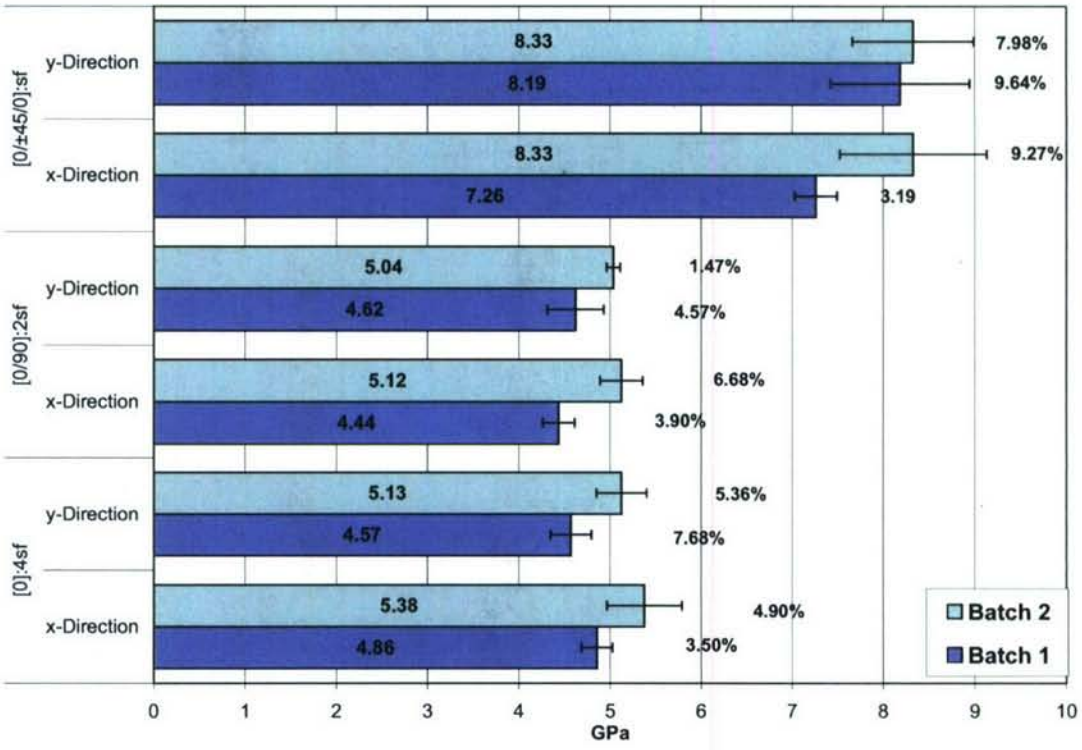

Figure 5.10: Shear Modulus of Elasticity (D4255)

Since the in-plane shear properties of the material are not fiber dominated propertied, normalization of the results was not carried on the results. The details of normalization and the conditions for it to be applied are explained in section 7.3.1. This constraint hindered the results to be compared between two different shear test methods and two different batches.

The ultimate shear strength of the composite was measured by observing the stress strain curve for a flat region. The flat region illustrated an increase in the strain with a constant load or, in some cases, a drop in the load. This behavior was explained by the reorientation of the reinforcing fabric after the matrix fails. And in some cases, an

increase in the load and strain continued after the flat region and then produced another flat region. This is a result of the fabric holding the load for a given amount until it started to reorient again. This behavior is seen in Figure 5.9, which is a typical stress-strain curve of an ASTM D4255 three-rail shear specimen from batch 1.

The shear ultimate strengths of the PMC under study for batch 1 and for two fiber lay-ups only are shown in Figure 5.11.

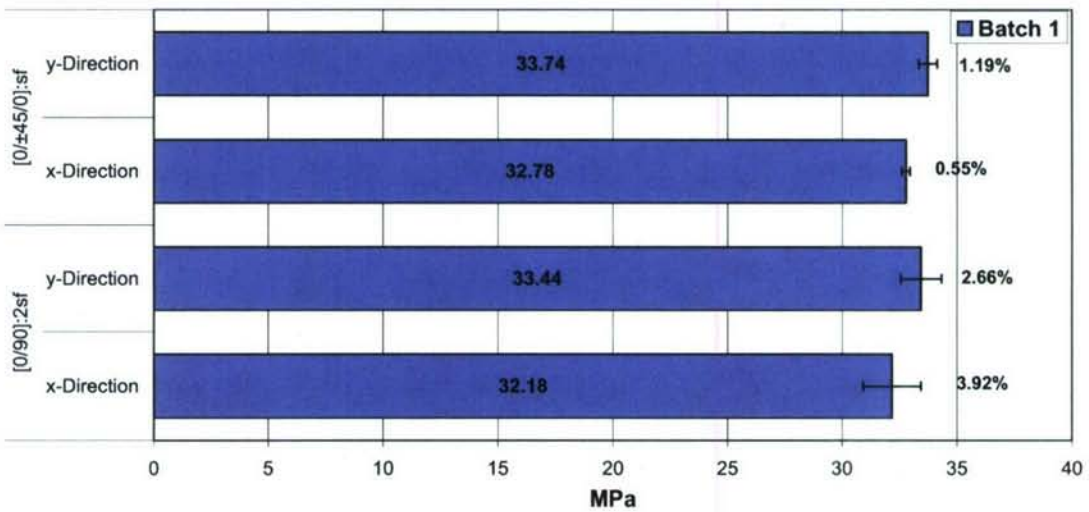

Figure 5.11: Shear Ultimate Strength (D4255 – Batch 1)

The shear ultimate strength for the $[0]_{4sf}$ fiber lay-up for batch 1 was not calculated due to some small glitches while testing the specimens. As for the shear ultimate strength for batch 2, the data was calculated but a premature failure was noticed in the specimens. The premature failure was detected in the stress-strain curve that depicted a small drop in the load at the early stages of loading. A stress strain curve for an ASTM D4255 specimen from batch 2 is represented in Figure 5.12. The shear ultimate

strength for $[0]_{4sf}$ and $[0/90]_{2sf}$ fiber lay-ups ranged between approximately 19 GPa (2755.7 ksi) and 17.8 GPa (2581.7 ksi); while, the ultimate shear strength for $[0/\pm45/0]_{sf}$ fiber lay-up was approximately 45 GPa (6526.7 ksi).

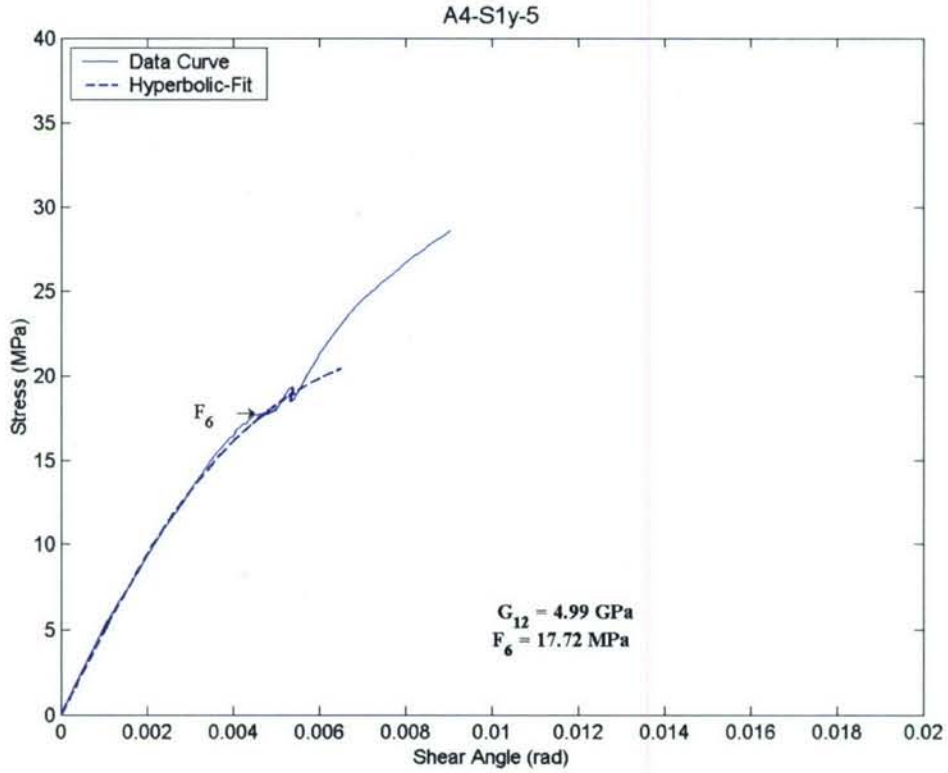

Figure 5.12: Premature Failure in an ASTM D4255 Batch 2 Specimen

5.6.2. Shear Properties in Accordance with ASTM D5379

The stress-strain curve for the v-notch specimens was obtained by considering the shear strain between the notches. An area between the notches was selected and the shear strain in that area was averaged and used with the cross-sectional area and the load

carried by the specimen to build the stress-strain curve. It was noticed that the shear strain was not solely concentrated between the notches as was intended by the design of the test. A set of full-field shear strains are depicted in Figure 5.13, they represent the strain of all three lay-ups in the two directions tested: x-direction and y-direction.

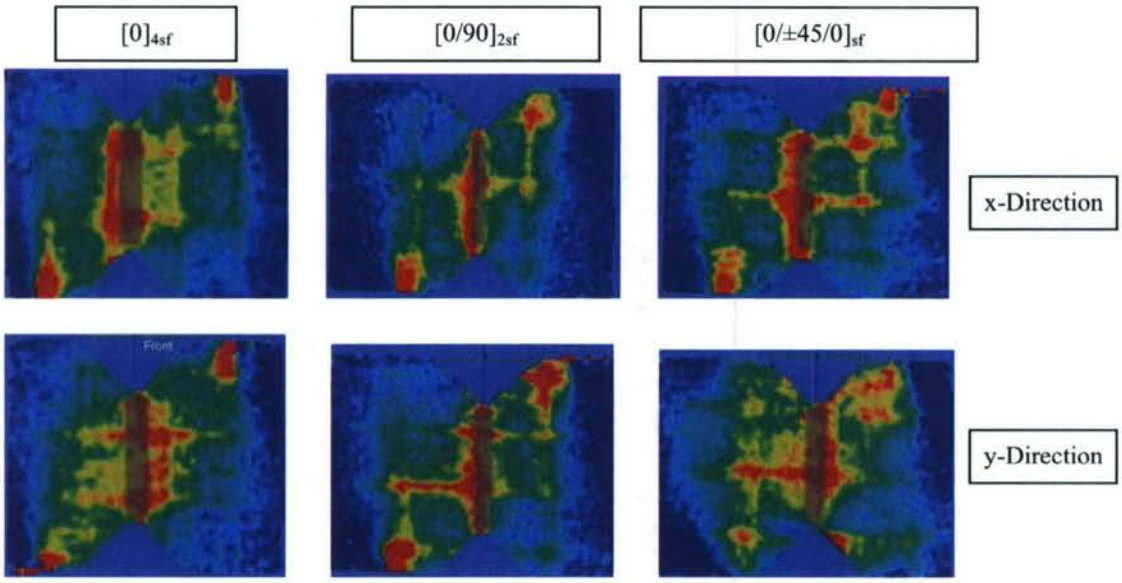

Figure 5.13: Full-Field Shear Strain Distribution in V-Notch Specimens

Due to the inconsistent strain concentrations observed in the full-field shear strain distributions captured by the DIC system (Figure 5.13), large variability was observed in the experimental results. The variability was a result of the distribution of the shear strain across the surface specimen. The material shear properties were calculated by considering the cross-sectional area and shear strain located between the notches as recommended by the ASTM standard. The results ranged between 2 GPa (290 ksi) to 3 GPa (435 ksi) for the specimens cut from batch 1 with a coefficient of variation of up to 30%.

Another factor that caused the variability in the experimental results was the coarseness of the fabric used. As mentioned earlier, the fabric used to reinforce the PMC was woven fabric with an aerial weight of 817.13 gm/m^2 (24.1 oz/yd^2) having 55% by weight of the fabric in the warp direction and 45% by weight of the fabric in the fill direction. A schematic of the weave is shown in Figure 5.14. In addition, two cross-sections of the weave, along the warp and along the fill, are shown in Figure 5.14.

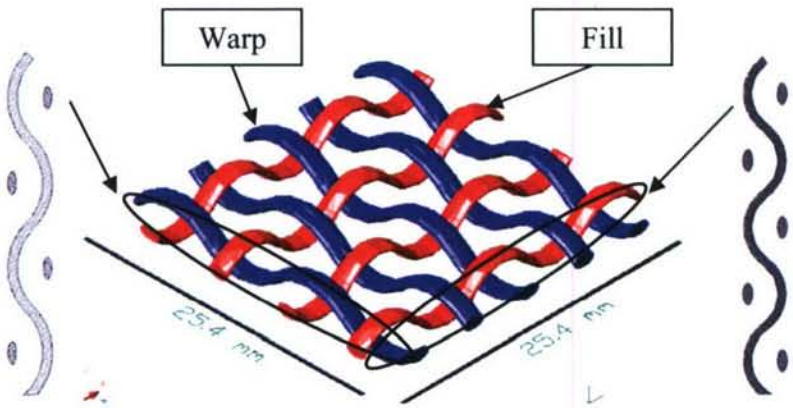

Figure 5.14: Weave Pattern Schematic

This type of fabric used had a tow spacing of 5.1 mm (5 tows per inch) in the warp direction and 6.35 mm (4 tows per inch) in the fill direction. This added to the variability of the results. The notch in the ASTM D5379 specimen in some cases was over a tow and in other instances was over a gap between two tows. The randomness of the notch placement with respect to the weave pattern caused large difference in the experimental results which was observed in the comparison of the values calculated from batch 1 and batch 2. The shear modulus of elasticity of the second batch ranged between

0.3 GPa (43.5 ksi) and 0.4 GPa (58 ksi), which was approximately one order of magnitude smaller than the values calculated from the specimens in the first batch. Similarly, the coefficient of variation of the results was up to 30% in some cases.

The ultimate shear strength was unable to be calculated for the ASTM D5379 test method. The stress-strain curve had no flat region or a drop in the load. A 0.2% offset value could have been used to obtain the ultimate shear strength as recommended in the standard (ASTM D5379/D5379M, 1999);but, since there was large variability in the experimental results of the shear modulus of elasticity, the shear ultimate strength was not calculated.

5.7. Recommendations and Conclusion

The experimental results obtained were very dependent on the type of fabric used. The fabric used in this study was coarse and woven with relatively large tows. The ASTM test methods conducted did not relate the specimen configuration or gage section to the type of fabric used. When the ASTM D4255 test method was conducted, the results were comparable to test results found in the literature and the variability was less than 10%. On the other hand, when the ASTM D5379 test method was conducted the results had coefficients of variability of up to 30% with very different results between batch 1 and batch 2 of the specimens. The gage section in the three rail shear test method was approximately 140 mm x 25.4 mm (5.51 in x 1 in), which was enough to cover a large area of the fabric reinforcing the PMC.

The fabric is represented properly when 3 tow patterns are included in the gage section; the edge patterns are affected by the boundary conditions, thus, leaving the middle pattern unaffected by outside conditions. The tow pattern of the fabric used

repeated every 12.7 mm (0.5 in) in the warp direction and every 10.16 mm (0.4 in) in the fill direction. The pattern of the weave is presented in Figure 5.15 for both directions: warp and fill.

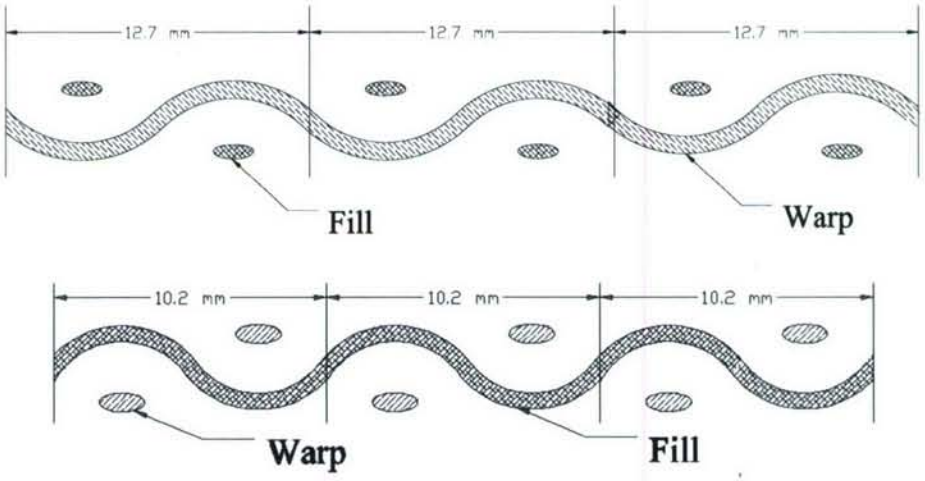

Figure 5.15: Fabric Weave Pattern in the Warp and Fill Direction

In conclusion, the three rail shear test (ASTM D4255) performed better than the v-notch shear test (ASTM D5279). The main reason was the specimen configuration and the scale of the specimen compared to the fabric used. The specimen configuration and the gage section of the specimen should be correlated to the reinforcing fabric of the PMC. In the case were the PMC is reinforced with fibrous fibers (not tows) small gage sections would give acceptable results. In addition, failure was detected in the stress-strain curve of the three rail shear test by a flat region in the curve or by a drop in the load, which was not found in the v-notch shear test.

5.8. References

ASTM D5229/D5229M, (2002). Test Method for Moisture Absorption Properties and Equilibrium Conditioning of Polymer Matrix Composite Materials. Annual Book of ASTM Standards. West Conshohocken, American Society of Testing Materials. **Vol 15.03**.

ASTM E4, (2002). Practices for Force Verification of Testing Machines. Annual Book of ASTM Standards. West Conshohocken, American Society of Testing Materials. **Vol 03.01**.

ASTM D4762, (2004). Standard Guide for Testing Polymer Matrix Composite Materials. Annual Book of ASTM Standards. West Conshohocken, American Society of Testing Materials. **Vol 08.04**.

Tomblin, J. S., Y. C. Ng, et al. 2001. Material Qualification and Equivalency for Polymer Matrix Composite Material Systems. U.S. Department of Transportation, Washington DC. Report#: DOT/FAA/AR-00/47.

ASTM D4255/D4255M, (2002). Standard Test Method for In-Plane Shear Properties of Polymer Matrix Composite Materials by the Rail Shear Method. Annual Book of ASTM Standards. West Conshohocken, American Society of Testing Materials. **Vol 15.03**.

ASTM D5379/D5379M, (1999). Standard Test Method for Shear Properties of Composite Materials by the V-Notched Beam Method. Annual Book of ASTM Standards. West Conshohocken, American Society of Testing Materials. **Vol 15.03**.

Barbero, E. J. (1998). Introduction to Composite Materials Design. Philadelphia, Taylor & Francis, Inc.

ASTM D3518/D3518M, (2001). Standard Test Method for In-Plane Shear Response of Polymer Matrix Composite Materials by a Tensile Test of a ±45 laminate. Annual Book of ASTM Standards. West Conshohocken, American Society of Testing Materials. **Vol 15.03**.

Whitney, J. M., D. L. Stansbarger, et al. (1971). "Analysis of the Rail Shear Test-Applications and Limitations." Composite Materials **5**: 24-34.

Ifju, P. G. (1994). "The Shear Gage: For Reliable Shear Modulus Measurements of Composite Materials." Experimental Mechanics **34**: 369-378.

Adams, D. F. and E. Q. Lewis (1997). "Experimental Assessment of Four Composite Material Shear Test Methods." Journal of Testing and Evaluation **Vol. 25** (March 1997).

He, J., M. Y. M. Chiang, et al. (2002). "Application of the V-Notch Shear Test for Unidirectional Hybrid Composites." Composite Materials **36** (23): 2653-2666.

Chapter 6: Density, Fiber Volume Fraction, and Glass Transition Temperature of Polymer Matrix Composites with Woven Fiber Reinforcement

6.1. Introduction

As part of characterizing the polymer matrix composite (PMC), three physical properties were obtained for the panels under study: density, fiber volume fraction, and glass transition temperature. The density test method was in accordance with ASTM D792 which describes the method of determining the density of plastics by the displacement of water (ASTM D792, 2000). The test procedure conducted is presented in the chapter and a discussion of the experimental results follows the procedure. As for the fiber volume fraction property, it was calculated by the use of the burn-out test which was in accordance with ASTM D 2584 which describes the method of determining the ignition loss that was considered to be the resin content in the PMC (ASTM D2584, 2002). The test procedure used to calculate the fiber volume fraction of the composite is explained in the chapter and is followed by a discussion of the experimental results. The thickness of one of the panels was measured and a surface plot of the thickness variation across the panel is presented. The thickness variation illustrated that the density and the fiber volume content measured, were depending on the location each specimen was cut from.

The glass transition temperature of the PMC was measured by following the test method in accordance to ASTM WK278 which utilized the dynamic mechanical analysis

(DMA) method (ASTM WK278, 2003). The test procedure conducted is presented and the method behind the DMA process is explained. This section is followed by the discussion of the experimental results obtained from the test method.

The physical property tests were conducted on two sets of panels, manufactured using two different batches. The first batch was used to infuse a 25.4 mm (1 in) thick panel and simultaneously infuse a 5.08 mm (0.2 in) thick panel, which acted as a witness panel for the 25.4 mm (1 in) thick panel. Similarly, the second batch was used to infuse a 12.7 mm (0.5 in) thick panel and simultaneously infuse a 5.08 mm (0.2 in) thick panel which acted as a witness panel for the 12.7 mm (0.5 in) thick panel. For each batch, three fiber lay-ups were adapted: $[0]_{4sf}$, $[0/90]_{2sf}$, and $[0/\pm45/0]_{sf}$. Therefore, there were two panels for each fiber lay-up that had the same thickness but were infused with a different batch and at different environmental conditions.

6.2. Background

The physical properties of a PMC are used to characterize the material and identify the manufacturing quality of the panels. The fiber volume fraction and density are directly related by the degree of compaction during infusion. In this study, the fiber volume fraction of the PMC under study was measured and related to the density. The higher the fiber volume fraction achieved in infusing a PMC panel, the higher the quality of the resulting composite. The process used to manufacture the panels under study was vacuum assistant resin transfer molding (VARTM) with Seemann Composites resin infusion molding process (SCRIMP) technology. The test used to obtain the fiber volume fraction of the panels was the ignition loss test recommended by the American Society for Testing and Materials (ASTM D4762, 2004). In this test method, the void content was

assumed negligible and the fiber volume fraction was measured from the resin content in the specimen. A study was conducted to measure the occurrence of voids in VARTM/SCRIMP infused panels and concluded that micro voids were present in the PMC due to out gassing and solvent ablation in the resin (Herzog, Goodell et al., 2004).

The glass transition temperature (T_g) of composites is a significant parameter for characterizing the material and defining its upper temperature limit. Problems are often present in defining the transition temperature of the matrix in the PMC which are known as highly cross-linked polymers. The high cross-link density in the polymer affected the relaxation in the transition region which produced difficulty in measuring the glass transition temperature. This effect caused a very broad transition region (Chartoff, Weissman et al., 1994). In addition, since the PMC are used for structural applications, the most appropriate assignment of T_g was the point where the storage modulus curve begins to drop. This point was specified by the onset point, defined by the intersection of the tangents to the storage modulus glassy state curve and transition region curve.

The glass transition temperature is used to set the post cure temperature needed for the composite to reach complete cure. Often a post cure temperature higher than the maximum glass transition temperature of the polymer insured a complete cure of the system (Valea, Martinez et al., 1998). Conversely, an incomplete cure schedule led to variations when the cured materials had to be in contact with solvents.

During the curing process, the polymer changes from a liquid rubbery state to a glassy state. A cure temperature, as high as the glass transition temperature, induces vitrification, the transition from rubbery state to a glassy state, and the reaction of cross-linking starts. The degree of cure of a polymer is defined as the density of cross-linking

and network free volume. A fully cured polymer theoretically has optimum properties (Dumant, 2000).

It was seen that the Dynamic Mechanical Thermal Analysis (DMTA) techniques provided an insight into the structure and viscoelastic response of the PMC material. The glass transition temperature measured using the DMTA tool was affected by the frequency used and the rate of heating. An increase in the frequency shifted the T_g to a higher temperature; similarly, an increase in the heating rate shifted the T_g to higher temperature (Karbhari and Wang, 2004). The DMTA technique provided three curves for calculating the glass transition temperature: the storage modulus curve, the loss modulus curve, and the tan-delta curve. The peak of the tan-delta fell at the end of the transition region and the peak of the loss modulus fell in the middle of the transition region. On the other hand, the onset of the storage modulus fell at the beginning of the curve drop, the transition from glassy state to rubbery state.

6.3. Density Test in Accordance with ASTM D792

The density of the PMC with woven fabric reinforcement was measured in accordance with ASTM D792 standard test method. The standard contained two methods to follow depending on the material under study. Since the panels in this study are PMC, method A was chosen which was specified for testing solid plastics in water. The other method, method B, was for testing solid plastics in liquids other than water (ASTM D792, 2000).

Five specimens were cut out of each panel for density measurement. The specimen configuration was selected to meet the requirements of the apparatus used for conducting the test. The specimens were cut to a size as large as the immersion vessel

could hold. A large specimen was selected to increase the accuracy of the test and reduce the variability arising from errors while conducting the test. A 2d-CAD drawing of the specimen configuration is shown in Figure 6.1.

Figure 6.1: D792 Specimen Configuration

The specimens were conditioned in accordance to procedure C of test method D5229 (ASTM D5229/D5229M, 2002). The specimens were stored in a conditioning chamber for 3 months at a temperature of 22 ± 3°C (71.6 ± 5°F) and 50 ± 3% relative humidity. While testing the specimens, the testing room was climate controlled at room temperature (22°C) and relative humidity of 50%.

6.3.1. Test Procedure

The room's temperature and relative humidity were recorded; similarly, the temperature of the distilled water was measured and recorded. The weight of each specimen in air was measured and recorded using a digital balance with a precision of 0.1 mg (3.5×10^{-6} oz) according to the recommendation of the standard. A plastic beaker was used as the immersion vessel. It was partially filled with distilled water to a height of at least the specimen submersion depth. The weight of the filled beaker was zeroed out prior to starting. A rigid wire was used to carry the specimen in water; in order to correct for the buoyant force of the submergible portion of the wire, it was measured separately and

recorded. The buoyant force was considered to be the weight of the item fully submerged in water. The latter was achieved by submerging the item into the beaker and reading the scale display. The buoyant force of the specimen with the metal wire was measured by holding the specimen with the metal wire and lowering both, the specimen and wire, into the water. The reading on the scale was recorded and used with the previous indicated reading to calculate the density of the specimen. The density of the specimen was calculated by the use of equation (6.1).

$$D = w \Big/ \left(\frac{a-b}{c} \right) \tag{6.1}$$

where:

D = density of the specimen, g/cm^3 (lb/in^3),
w = mass of the specimen in air, g (lb),
a = mass of the specimen and portion of the metal wire completely immersed in water, g (lb),
b = mass of the portion of the metal wire immersed in water, g (lb),
c = density of the distilled water at the temperature measured, g/cm^3 (lb/in^3).

6.3.2. Discussion of Experimental Results

The experimental results were collected for each specimen and the mean, standard deviation, and coefficient of variation were calculated for each set. The means of each batch for each lay-up are plotted together to demonstrate the difference between the density of the panels from batch 1 and from batch 2. A chart illustrating the means, standard deviation error bars, and coefficient of variations are presented in Figure 6.2.

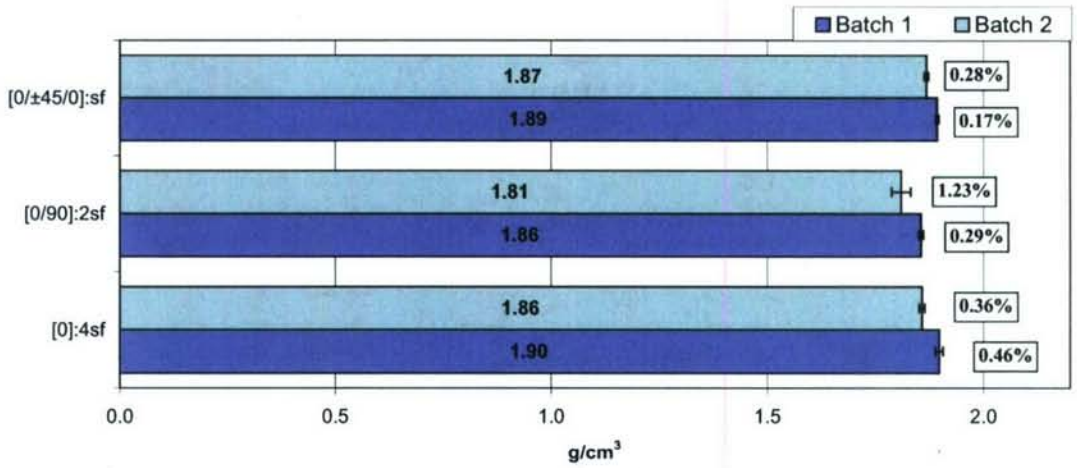

Figure 6.2: Density Experimental Results (ASTM D792)

It was noticed that the density of the panels from batch 2, for all the lay-ups, were slightly smaller than the density of the panels from batch 1. This can be interpreted as panels from batch 1 had a higher fiber volume fraction than panels from batch 2, because the density of the E-glass reinforcing the PMC was 2.54 g/cm^3 (158.57 lb/ft^3) while the density of the resin was 1.13 g/cm^3 (70.54 lb/ft^3). This was also supported by the experimental results of the fiber volume fraction test which is discussed in the following section.

6.4. Fiber Volume Fraction in Accordance with ASTM D2584

The standard test method for ignition loss of cured reinforced resins, ASTM D2584, was designed for the determination of the resin content of a composite. Assuming the void content of the PMC under study as negligible, the resin content was used to determine the fiber volume fraction of the composite using the densities of the fabric and resin.

The standard recommended that the specimen weigh approximately 5 g (0.176 oz) with a maximum size of 25.4 mm by 25.4 mm (1 in by 1 in) (ASTM D2584, 2002). Therefore, the specimen configuration selected for this study was a circular specimen with a diameter of 25.4 mm (1 in). The weight of the specimen was approximately 4.8 g (0.169 oz). The size fit in the crucibles used for conducting the test. Six specimens were tested from each panel.

The specimens were conditioned in accordance to procedure C of test method D5229 (ASTM D5229/D5229M, 2002). The specimens were stored in a conditioning chamber for 3 months at a temperature of 22 ± 3°C (71.6 ± 5°F) and 50 ± 3% relative humidity. While testing the specimens, the testing room was climate controlled at room temperature (22°C) and relative humidity of 50%.

6.4.1. Test Procedure

The crucible weight was measured (W) using a digital balance with a precision of 0.1 mg ($3.5x10^{-6}$ oz) according to the recommendation of the standard. Each specimen was placed in a crucible and the combined mass of the crucible and the specimen were measured (W_1) using the same digital balance. The crucibles containing the specimens were then placed into an electric furnace and heated to a temperature of 400° C (752° F) for five to ten minutes. The specimens were then ignited using a butane torch. Once all the specimens had self-extinguished, the temperature of the furnace was increased to 565° C (1049° F) and the specimens were left for a period of five hours at that temperature. This process burned the resin and removed any carbonaceous material on the fabric of the composite. When the specimens were removed, the crucibles only contained clean layers of woven fabric that was reinforcing the PMC. When the specimens had cooled to room

temperature the mass of the residue plus the crucible was measured (W_2). The weight fraction of the resin that was present in the specimen was obtained using equation (6.2).

$$W_R = \frac{W_1 - W_2}{W_1 - W} \tag{6.2}$$

where:

W_R = weight fraction of the resin,
W_1 = weight of specimen and crucible, g (oz),
W_2 = weight of residue and crucible, g (oz),
W = weight of crucible, g (oz).

The fiber volume fraction of the composite was obtained by the use of equation (6.3). The density of the fabric according to the supplier's technical sheet was 2.54 g/cm^3 (158.57 lb/ft^3). Similarly, the density of the resin was taken to be according the supplier's technical information, which was 1.13 g/cm^3 (70.54 lb/ft^3).

$$V_f = \frac{1}{1 + \frac{\rho_f}{\rho_R \cdot W_R \cdot (1 - W_R)}} \tag{6.3}$$

where:

V_f = volume fraction of the fiber,
W_R = weight fraction of the resin,
ρ_f = density of the fiber, gm/cm^3 (lb/ft^3),
ρ_R = density of the resin, gm/cm^3 (lb/ft^3).

6.4.2. Discussion of Experimental Results

The experimental results of each panel were collected and statistical analysis was conducted on each set. The mean, standard deviation, and coefficient of variation were

obtained for each set and are displayed in Figure 6.3. The values from batch 1 and batch 2 with the same fiber lay-up are displayed adjacent to each other, in order to signify the difference in the experimental results between the two batches.

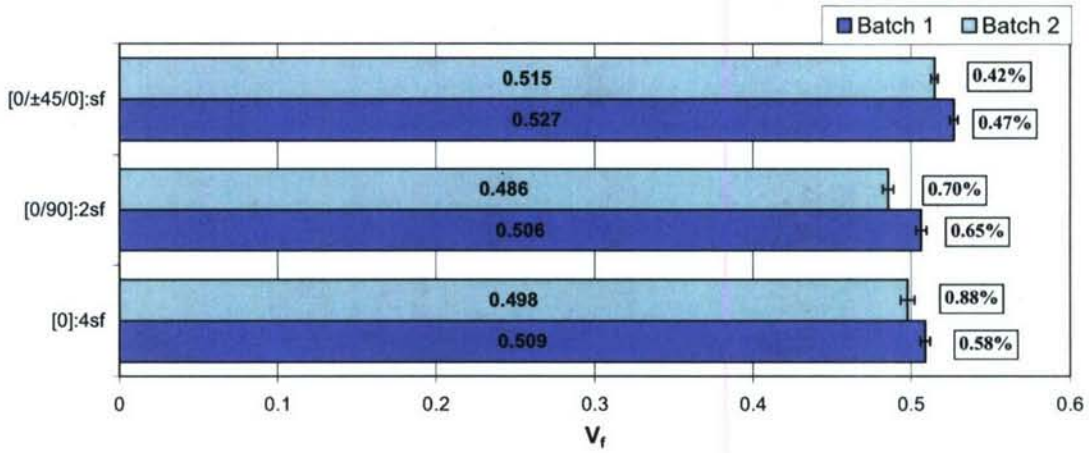

Figure 6.3: Fiber Volume Fraction Experimental Results (ASTM D2584)

Similar to the discussion of section 6.3.2, it was noted that the fiber volume fraction experimental results showed a slight difference between the results from batch 1 and batch 2. The difference was consistent and indicated that the panels from batch 2 had a lower fiber volume fraction than the panels from batch 1. This agrees with the experimental results of the density test that showed that panels from batch 2 had a slightly lower density than the panels from batch 1. Comparing a panel from batch 1 with a panel from batch 2 with the same fiber lay-up, the panel from batch 1 with a higher fiber volume fraction indicated that the panel had more fibers than matrix compared to the panel from batch 2. This fact gave the panel from batch 1 a larger density than the

panel from batch 2 since the fabric's density was more significant than the resin's density.

In addition, examination of the experimental results shown in Figure 6.3, revealed that the pseudo quasi-isotropic lay-up $[0/\pm45/0]_{sf}$ had the highest value of fiber volume fraction. This indicated that while infusing the panel, the fabric pattern compacted best compared to the other types of lay-ups.

6.5. Thickness Variation of the Panels under Study

One of the panels under study was selected for measuring the thickness variation of the surface. The panels were infused on a flat mold which produced a flat surface referred to as the mold face; while, the opposite surface was in contact with the vacuum bag during the infusion process and was referred to as the vacuum bag face. Two thickness variations were measured, the local thickness variation and the total thickness variation.

The local thickness variation was caused by the fabric pattern that was perceived on the vacuum bag face, and consisted of waviness across the surface. The local variation of the thickness was measured using a 5 mm (0.19685 in) nominal diameter double-ball-interface micrometer having an accuracy of ±2.5 μm (±0.0001 in). The panel selected was from batch 2 and had $[0/90]_{2sf}$ as the fiber lay-up sequence. The panel showed a local thickness variation of approximately 0.48 mm (0.0189 in), which accounted for 10% of the total thickness.

The variation in the total thickness was caused by the infusion process or by the mold's surface used to infuse the panel on. The total thickness variation was measured using a double-anvil-interface micrometer having an accuracy of ±2.5 μm (±0.0001 in).

The double-anvil-interface was used to exclude the local thickness variation from the total thickness variation, knowing that the anvil interface was larger than the local waviness. The total thickness variation measured on the panel selected was approximately 0.68 mm (0.0268 in), which accounted for 13% of the total thickness of the panel. A surface contour plot of the thickness variation of the panel selected is depicted in Figure 6.4. Note that the panel was 1.22 m (4 ft) in width and 1.83 m (6 ft) in length.

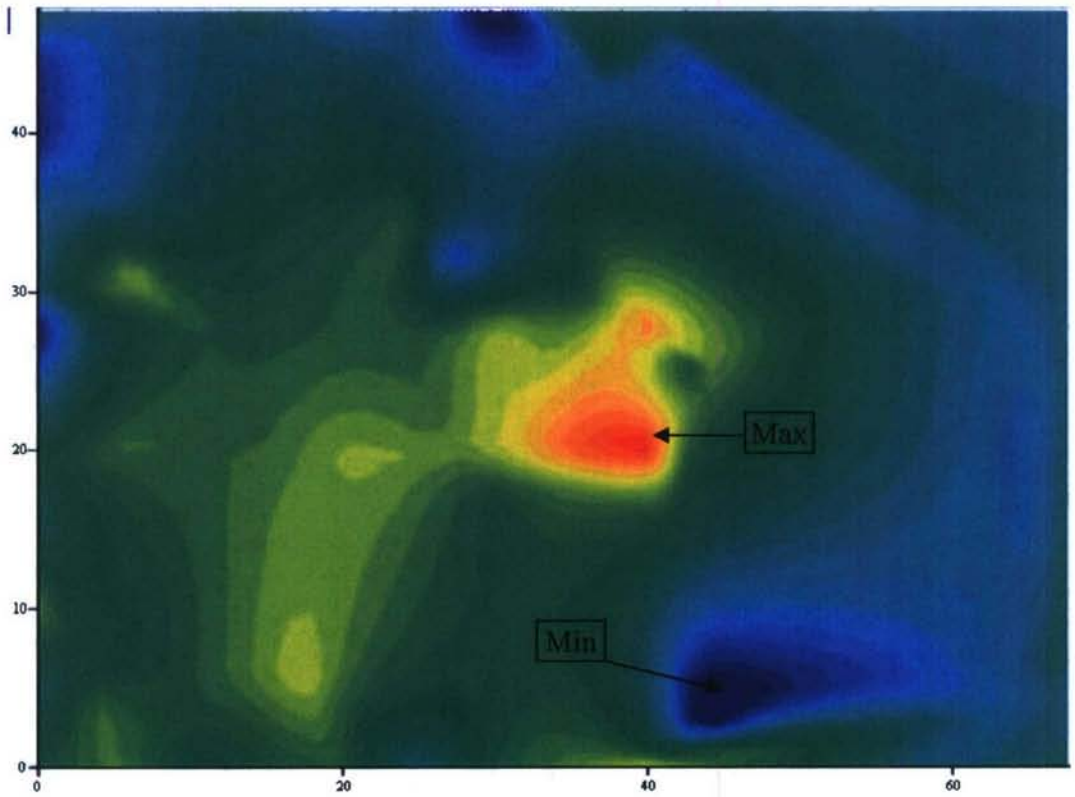

Figure 6.4: Contour Plot of the Total Thickness Variation

Due to the thickness variation across the panel, the density and the fiber volume content measured for each panel were local properties of the panel. In other words, the experimental results of these two tests were function of the thickness and as the thickness varied the density varied and similarly the fiber volume fraction varied.

6.6. Glass Transition Temperature in Accordance with ASTM WK278

The glass transition temperature (T_g) of a PMC represents the temperature range the glass transition of the matrix in the PMC takes place. The glass transition of the matrix is the state at which the polymer changes from the glassy state to the rubbery state. The T_g of a PMC is used to define the upper use temperature of the composite. In addition, the T_g is used to define the degree of cure of the composite and for quality control of the composite.

The T_g was measured by following the procedure stated in the standard test method ASTM WK278. The procedure defined the determination of the T_g by the use of the DMTA tool (ASTM WK278, 2003). The DMTA was designed to load a specimen with a cyclic loading of a controlled frequency in a controlled temperature environment. The oven of the DMTA was capable of heating the specimen above the glass transition temperature of the composite with controlled heating rate. The DMTA tool had the ability to monitor the structural and viscoelastic response of the composite while simultaneously detecting changes in the internal molecular mobility.

The specimens were conditioned in accordance to procedure C of test method D5229 (ASTM D5229/D5229M, 2002). The specimens were stored in a conditioning chamber for 3 month at a temperature of $22 \pm 3^{\circ}C$ ($71.6 \pm 5^{\circ}F$) and $50 \pm 3\%$ relative humidity.

6.6.1. Test Procedure

The DMTA tool supported different loading configurations. The 3 point bending loading configuration was selected for this study. The specimens were cut approximately 46.0 mm (1.81 in) long with a width of 5.0 mm (0.197 in) and a thickness of 3.0 mm (0.118 in). The width of the specimen was the thickness of the panel. Due to the waviness of the vacuum bag face, the width of the T_g specimens were wavy as mentioned in section 6.5.

The specimen was installed into the fixture and then placed into the DMTA furnace. The fixture with the specimen installed is presented in Figure 6.5.

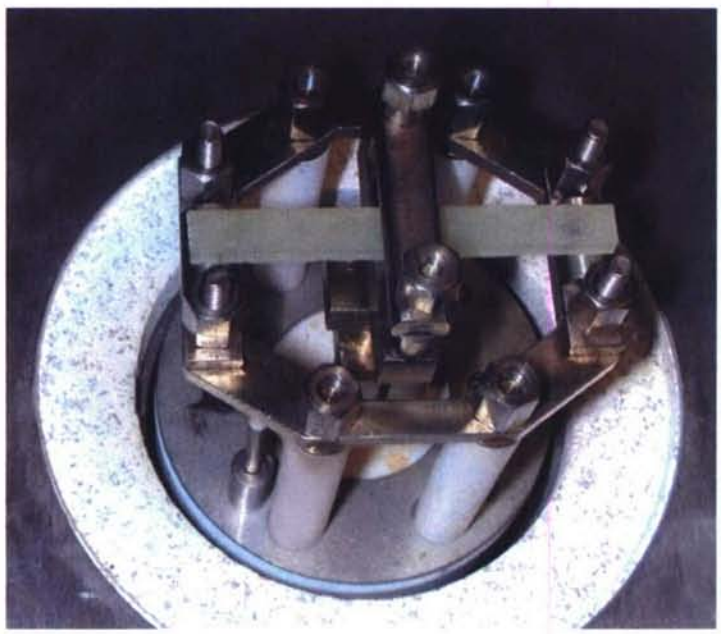

Figure 6.5: DMTA Fixture and an Installed Specimen in a 3-pt Bending Configuration

The test was conducted at a cycling load frequency of 1 hertz and a temperature ramp of 5°C/min (41°F/min). The maximum temperature the test reached was up to approximately 150°C (302°F).

The DMTA machine applied cycling loading on the specimen. The cyclic loading was modeled as forced vibration with hysteresis damping having a governing equation given in equation (6.4). Two forms of the same equation are presented in equation (6.4).

$$m \cdot \ddot{x} + \frac{\beta k}{\varpi} \cdot \dot{x} + k \cdot x = F_o \cdot \sin(\varpi \cdot t)$$

$$m \cdot \ddot{x} + k(1 + i \cdot \beta)x = F_o \cdot \sin(\varpi \cdot t) \qquad (6.4)$$

where:

x = deflection of the beam, m (in),
$\dot{x}$ = velocity of the deflection of the beam, m/sec (in/sec),
$\ddot{x}$ = acceleration of the deflection of the beam, m/sec^2 (in/sec^2),
m = mass of the beam, kg (slug),
$\frac{\beta k}{\varpi}$ = damping constant, kg/sec (slug/sec),
k = stiffness constant, kg/sec^2 (slug/sec^2).
F_o = amplitude of applied cyclic loading, N (lb).
ϖ = angular velocity, radians/sec,
t = time, sec,
i = imaginary symbol $\left(\sqrt{-1}\right)$.

The displacement coefficient had two terms: imaginary and real. The real term was related to the storage modulus and the imaginary term related to the loss modulus. The ratio of the loss modulus to the storage modulus was considered to be the tan-delta.

The DMTA produced three curves as the output of testing the specimen. The curves were used to calculate the storage modulus, loss modulus, and tan-delta. The curves of a typical T_g specimen are depicted in Figure 6.6.

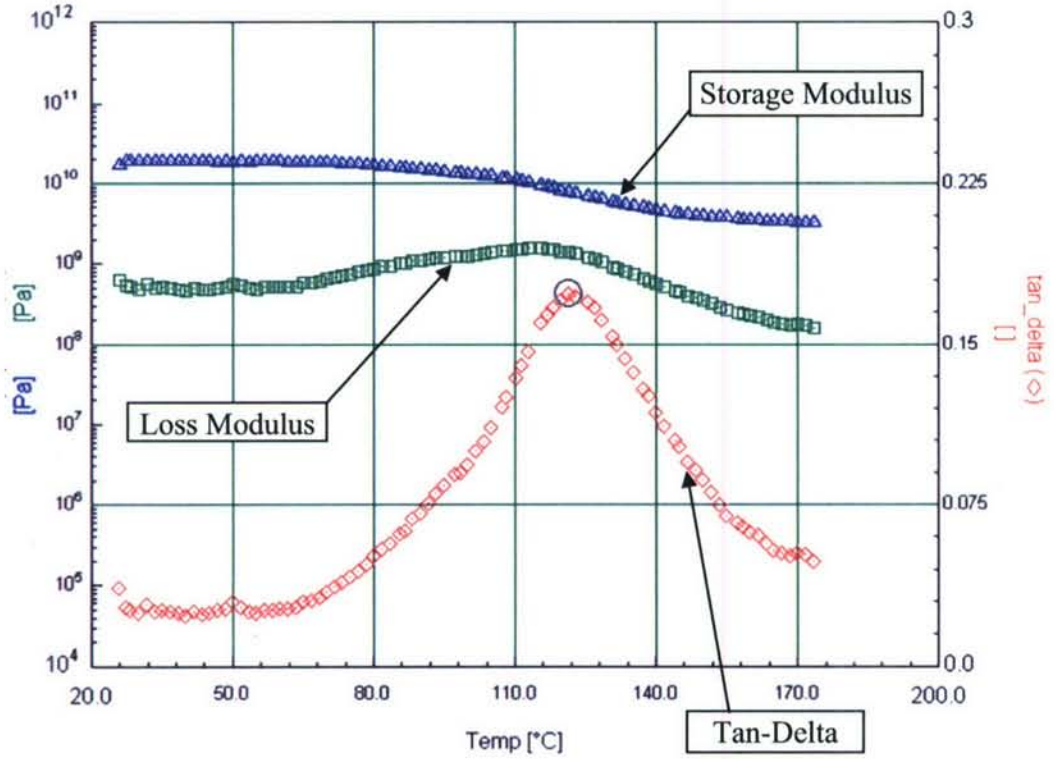

Figure 6.6: Typical T_g Output-Curves from DMTA

According to ASTM WK278, the peak of the loss modulus curve was considered to be the loss modulus glass transition temperature. Similarly, the peak of the tan-delta curve was considered to be the tan-delta glass transition temperature. As for the storage modulus curve, the plot of the logarithm of the curve was needed. A plot of the logarithm of the curve is shown in Figure 6.7. Two tangent lines were drawn before and after the transition, the drop in the curve. The intersection of the two lines was taken to be the

storage modulus glass transition temperature. The tangent lines are also depicted in Figure 6.7.

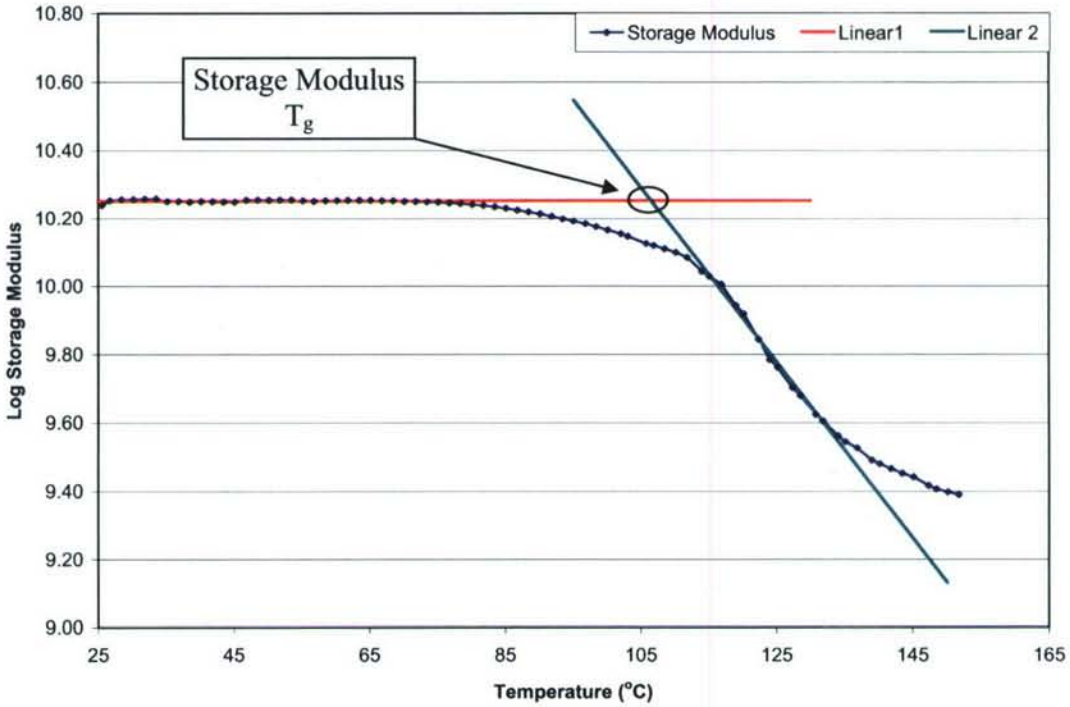

Figure 6.7: Storage Modulus Logarithmic Curve

6.6.2. Discussion of Experimental Results

As mentioned in the previous section, three values of T_g were calculated for each set of specimens tested, containing 5 to 6 specimens each. Two sets were taken from each panel. The first set represented the x-direction, the principal laminate axis, and the second set represented the y-direction, orthogonal to the principal laminate axis. The results were computed and collected for statistical analysis: mean, standard deviation, and coefficient

of variation. The storage modulus T_g had the smallest value thus being the most conservative result as a design value. In addition, the peak of the tan-delta curve occurred at the end of the transition region and the peak of the loss modulus occurred at the middle of the transition region (Karbhari and Wang, 2004). Therefore, the data presented in Figure 6.8 is only for the storage modulus T_g.

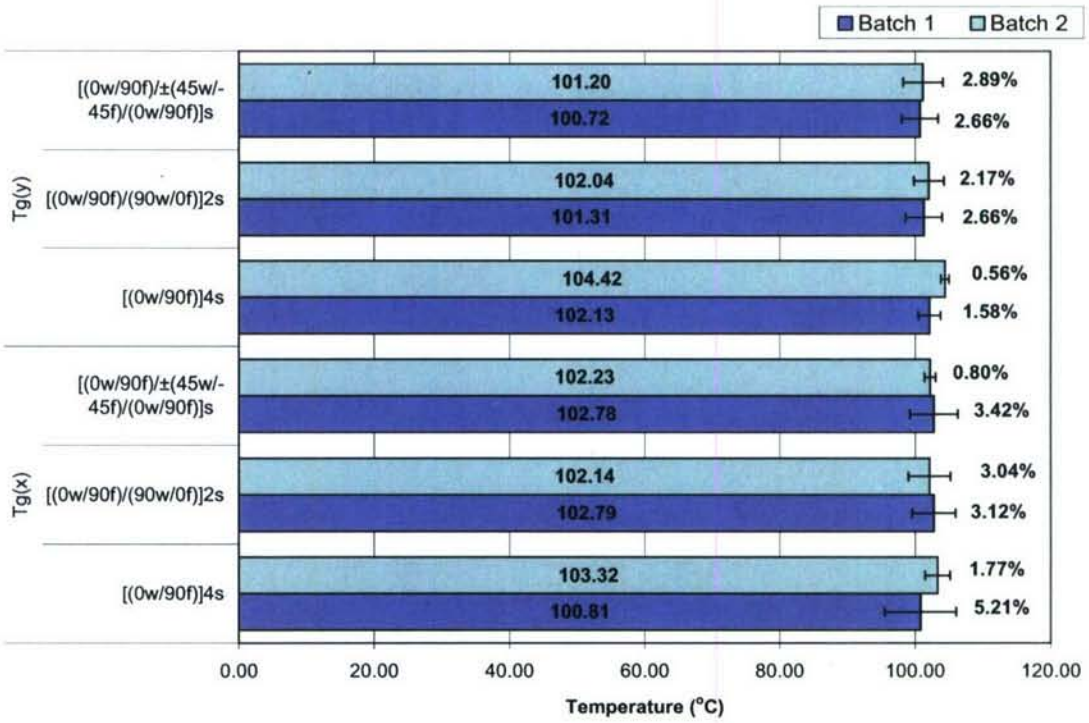

Figure 6.8: Storage Modulus Glass Transition Temperature DMTA Results (ASTM WK278)

The experimental results depicted in Figure 6.8 revealed that the result is independent of the direction of the test, the fiber lay-up, and the batch. Therefore, it was concluded that the glass transition temperature was solely dependent on the matrix.

It was perceived that the experiment was unable to specify the degree of cure of the panels. The panels were infused and post-cured for 6 hours at a temperature of approximately 71°C (160°F). Since the DMTA method utilized high temperature to measure the degree of cure, it affected the degree of cure during the experiment. In other words, the specimen was post cured again as the degree of post cure was attempted to be measured. Therefore, the DMTA method was not a successful tool to indicate the degree of cure of the composite. On the other hand, the DMTA method provided a glass transition temperature that defined the upper use temperature limit of the composite.

6.7. Recommendations and Conclusion

The density and fiber volume fraction experimental results were dependent on the thickness variation of the panels. The thickness variation of the specimen was caused by either the mold used or the infusion process, or both. The thickness variation was depicted as the degree of compaction of the fabric. Thinner panels were a result of higher compaction, and thus resulting in higher fiber volume fraction. The two batches showed a difference in fiber volume fraction and density, which both were correlated together. Both batches were laid and infused at the same manufacturing laboratory and with the same procedure, but at different times and using different fiber and resin batches. Therefore, the difference in the fiber volume fraction resulted in a difference in the material properties: tension, compression, and shear as seen in the previous chapters.

The degree of cure of the panels was not established. The DMTA method proved to be unsuccessful in defining the degree of cure of PMC. The cause was the use of high temperature to measure the degree of cure. The high temperatures caused the material to change its degree of cure as the latter was being measured. The DMTA method was a

successful quality control tool and a comparative tool for defining different PMCs. In addition, the DMTA method measured the glass transition temperature of the composite; thus defining the upper temperature limit the composite can be used at.

6.8. References

ASTM D5229/D5229M, (2002). Test Method for Moisture Absorption Properties and Equilibrium Conditioning of Polymer Matrix Composite Materials. Annual Book of ASTM Standards. West Conshohocken, American Society of Testing Materials. **Vol 15.03**.

ASTM D4762, (2004). Standard Guide for Testing Polymer Matrix Composite Materials. Annual Book of ASTM Standards. West Conshohocken, American Society of Testing Materials. **Vol 08.04**.

ASTM D792, (2000). Standard Test Methods for Density and Specific Gravity (Relative Density) of Plastics by Displacement. Annual Book of ASTM Standards. West Conshohocken, American Society of Testing Materials. **Vol 08.01**.

ASTM D2584, (2002). Standard Test Method for Ignition Loss of Cured Reinforced Resins. Annual Book of ASTM Standards. West Conshohocken, American Society of Testing Materials. **Vol 08.01**.

ASTM WK278, (2003). Standard Test Method for Glass Transition Temperature (T_g) by DMA of Polymer Matrix Composites. Developed by Subcommittee: D30.04. West Conshohocken, American Society of Testing Materials. **Status: In Balloting**.

Karbhari, V. M. and Q. Wang (2004). "Multi-Frequency Dynamic Mechanical Thermal Analysis of Moisture Uptake in E-Glass/Vinylester Composites." Composites Part B: Engineering **35**.

Herzog, B., B. Goodell, et al. (2004). "Electron Microprobe Imaging for the Characterization of Polymer Matrix Composites." Composites Part A: Applied Science and Manufacturing **35**.

Chartoff, R. P., P. T. Weissman, et al., (1994). The Application of Dynamic Mechanical Methods to T_g Determination in Polymers: An Overview. ASTM STP 1294. R. J. Seyler. Philadelphia, American Society for Testing and Materials: pp. 88 - 107.

Valea, A., I. Martinez, et al. (1998). "Influence of Cure Schedule and Solvent Exposure on the Dynamic Mechanical Behavior of a Vinyl Ester Resin Containing Glass Fibers." Journal of Applied Polymer Science **70** (13): 2595 - 2602.

Dumant, N. (2000). Effects of Curing on Vinyl Ester-Derakrane 8084 Properties. Department of Materials and Manufacturing Engineering, Lulea University of Technology.

Chapter 7: Evaluation of the Experimental Results and Implementation of the Classical Lamination Theory

7.1. Introduction

Material properties of composites were obtained from several different standard tests. The tests conducted were tension, compression, and shear. The density and fiber volume fraction of the material was obtained in accordance with ASTM standard methods. The experimental test results were used to obtain the material properties. The criterion for selecting the appropriate material properties for design purposes and comparison is stated. The selected results were then normalized to a nominal thickness value. The method behind the normalization and the selection of the nominal value is discussed. The normalized results were then presented and the different issues related to the inability to normalize some material properties are discussed. Since more than one test was conducted to obtain the same material property, a statistical tool was used to compare the normalized results from different test methods. The statistical tool indicated if the results were significantly the same, come from the same population, or significantly different. A similar method was used to compare similar material properties obtained from different batches. Using the normalized material properties, design allowable values were derived using the standard deviation of the sample population and its distribution about the mean. The calculation of both A- and B-basis allowables is discussed and the "knockdown" factor for each material property is represented.

As part of utilizing the properties obtained from the coupon testing program, the classical lamination theory (CLT) was used to estimate material property values for

different fiber lay-up: $[0/90]_{2sf}$ and $[0/\pm45/0]_{sf}$; the estimated values were compared to the experimental values. The CLT was implemented through a computer model starting with lamina material properties obtained from the experimental results conducted on the $[0]_{4sf}$ fiber lay-up panel. The association between the experimental results and the CLT calculated values is stated and discussed.

7.2. Background

Developing design allowables for composite materials requires extensive testing to accommodate the orthotropic nature of the material. Therefore, obtaining the design allowables for composites is more complex when compared to metallic materials (Wang, Banbury et al., 1998). Variability of the material properties of composites commonly originate from the nature of the material. To account for this variability, the assignment of the design allowables for the material should acknowledge the variability through the statistical procedure (Tomblin, Ng et al., 2001).

As part of reducing the variability in the experimental results originating from the fiber volume content of the material, the experimental data were normalized to a nominal fiber volume content value (Tomblin, Ng et al., 2001). This process reduced the variability of fiber dominated properties and was justified on the basis that most of the load was carried by the fibers, whether under tension or compression.

Design allowables are produced from the statistical distribution of the data. A "knock-down" factor was a calculated value that was multiplied by the mean of the data to give the design allowable. More data points for a material property result in a higher confidence level in the data, consequently, resulting in a higher "knock-down" factor. One material property might have more than one design allowable. Each design

allowable has a different confidence level (About.com, 2005). Two common confidence levels used in the aerospace industry is the A-basis and the B-basis. The A-basis offers 95% confidence that 99% of the samples will exceed the allowable. The B-basis offers 95% confidence that 90% of the samples will exceed the allowable.

7.3. Evaluating the Experimental Results

The material properties of the polymer matrix composite (PMC) reinforced with woven fabric was evaluated by conducting a series of experimental tests in accordance with ASTM standard methods shown in Table 7.1. The tensile properties were calculated by conducting two tests in accordance with ASTM standard methods: ASTM D3039 and ASTM D638 (ASTM D3039/D3039M, 2000; ASTM D638, 2002). The compression properties were calculated by conducting two tests, one in accordance with ASTM D6641 (ASTM D6641/D6641M, 2001) and the other in accordance with SACMA SRM 1R (SACMA SRM 1R-94, 1994). The properties calculated from the experimental results from the ASTM D6641 test were considered, due to problems involved in conducting the SACMA SRM 1R test method; Chapter 4 discusses in detail the difference between the two test methods and the advantages and disadvantages of each test. As for the shear properties, similarly, two test methods were conducted. The first test in accordance with ASTM D4255 (ASTM D4255/D4255M, 2002), and the second test in accordance with ASTM D5379 (ASTM D5379/D5379M, 1999). The shear properties for ASTM D5379 were not considered due to the high variability in the results that were due to non-uniform strain in the region of interest, the gage section. Chapter 5 confirms the high variability in the results and explicates the different issues related in conducting each test method and the advantages and disadvantages of each test.

For both, the tension and compression tests, a bi-linear curve was implemented to model the stress strain curve of each specimen. This procedure resulted in obtaining an initial modulus of elasticity and a final modulus of elasticity for the material. In addition, a transition point was obtained to indicate the transition between the initial region and final region. For design purposes, the initial modulus was considered, and this chapter will tackle the evaluation of the experimental results through use of the initial modulus of elasticity. The material properties obtained from each test are summarized in Table 7.1, the properties presented are from the initial range.

Table 7.1: Material Properties Obtained from Standard Test Methods

Test	Coupon	Standards	Properties
Tension (composites)	Tabbed Rectangular	ASTM D3039	E_1, E_2, ν_{12}, F_{1t}, F_{2t}
Tension (plastics)	Dumbbell	ASTM D638	E_1, E_2, ν_{12}, F_{1t}, F_{2t}
Compression (composites)	Rectangular	ASTM D6641	E_1, E_2, ν_{13} (ν_{12}), F_{1c}, F_{2c}
Compression (plastics)	Tabbed Rectangular	SACMA SRM 1R (ASTM D695)	E_1, E_2, ν_{13}, F_{1c}, F_{2c}
Shear (large – composites)	Three-Rail	ASTM D6641	G_{12}, F_6
Shear (small – composites)	V-Notched	ASTM D5379	G_{12}, F_6

7.3.1. Normalizing the Material Properties

Two sets of panels were tested; each set was manufactured at a different time and is referred to as a different batch. Three fiber lay-up architectures constituted each set of

panels: $[0]_{4sf}$, $[0/90]_{2sf}$, and $[0/\pm45/0]_{sf}$ – a total of 8 layers for each lay-up. Due to the fact that each batch was manufactured, infused, at a different time, the physical properties of the batches differed. The difference was mainly in the thickness of the panel and the resin properties. The thickness of the batches differed depending on the vacuum pressure applied during infusion of the resin; in addition, each panel had thickness variations across the surface. The thickness variation was characterized by either total thickness variation or local thickness variation. The local thickness variation was measured to be approximately 0.48 mm (0.0189 in); while, the total thickness variation was measured to be approximately 0.68 mm (0.0268 in). A surface contour plot presented in Figure 7.1 shows the thickness variation of one of the panels under study; the panels were manufactured with a length of 1.83 m (6 ft) and a width of 1.22 m (4 ft).

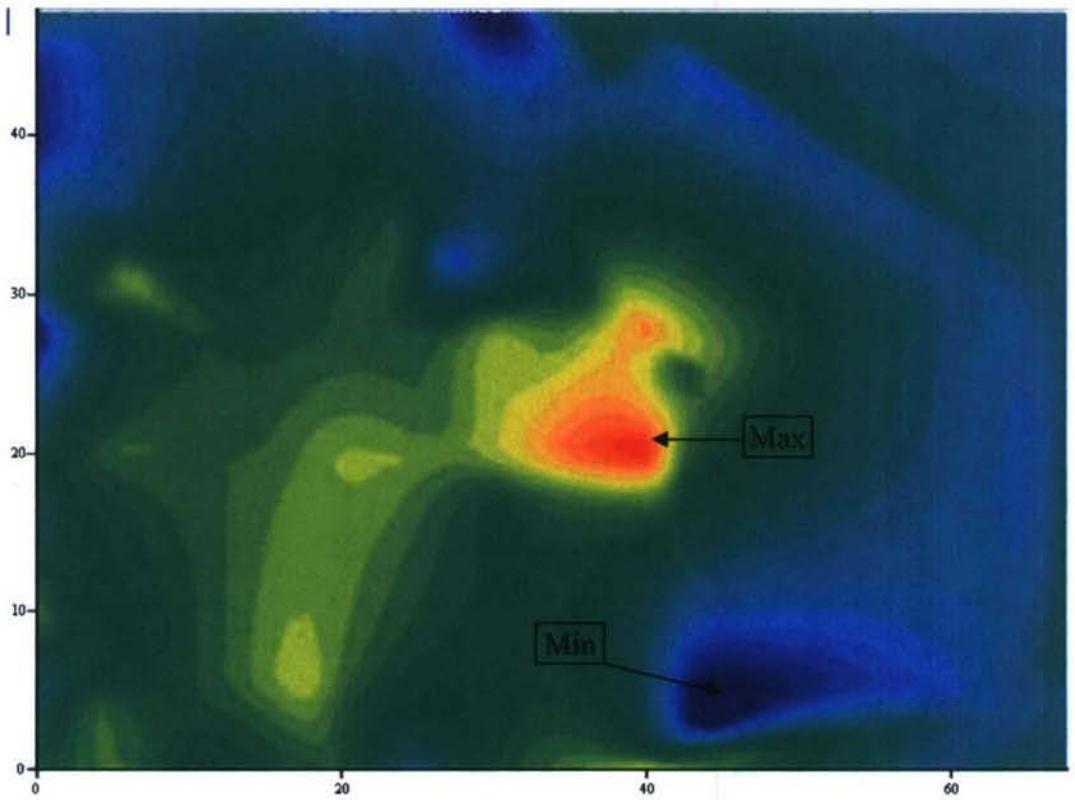

Figure 7.1: Contour Plot of the Total Thickness Variation

The thickness of the panels varied locally and across the surface of the panel, which necessitated the material properties to be normalized to a nominal thickness. The thickness variation affected fiber dominated material properties: E_1, E_2, F_{1t}, F_{1c}, F_{2t}, and F_{2c}. These properties were normalized to a nominal thickness of 5.08 mm (0.2 in). The properties were normalized based on the fiber areal weight, as given by the fabric supplier: 817.13 g/m^2 (24.1 oz/yd^2), and the E-glass fiber density: 2.54 g/cm^3 (158.57 lb/ft^3). Using these two properties, it was found that the product of the material thickness and the fiber volume fraction is constant. The constant value and the equation are given in equation (4.1).

$$V_f \cdot t = N \cdot \frac{A_w}{D_f} = 2.574\,mm \tag{7.1}$$

where:

V_f = volume fraction of the fiber,
t = thickness of the material, mm (in),
N = number of layers of the fabric, 8 layers,
A_w = aerial density weight, 817.13 g/m^2 (24.1 oz/yd^2),
D_f = density of the fiber, 2.54 g/cm^3 (158.57 lb/ft^3).

The fiber dominated properties were normalized by multiplying the experimental value by the ratio of the nominal thickness and the average thickness of the coupon. This process was carried out for every specimen tested in tension or compression from each batch and for both standard tests.

The matrix dominated properties: G_{12}, ν_{13}, and F_6, were not normalized due to the complexity of the different parameters that control the matrix. The matrix was made of vinyl ester rubberized resin. Some of the parameters that control the properties of the matrix are: temperature and relative humidity of infusion, additives used, gel time, and vacuum applied during infusion. Such parameters are not measurable after the panels are manufactured and thus making it difficult to normalize to a nominal value.

A summary of the normalized experimental values are presented in Table 7.2. The table presents the results from batch 1 separate from batch 2 for emphasis on the difference in the results.

Table 7.2: Summary of Normalized Experimental Results

		$[0]_{4sf}$	$[0/90]_{2sf}$	$[0/\pm45/0]_{sf}$
		Experimental	Experimetal	Experimetal
Batch 1	E1t (GPa)	25.82	24.56	20.19
	E2t (GPa)	22.41	24.33	17.37
	v12	0.14	0.128	0.334
	F1t (MPa)	435	374.9	298.6
	F2t (MPa)	342.2	372.8	235.5
	E1c (GPa)	27.84	26.05	18.97
	E2c (GPa)	24.24	23.81	17.05
	v13c	0.369	0.408	0.436
	F1c (MPa)	369.88	368.7	298.15
	F2c (MPa)	362.4	352.15	257.5
	G12 (GPa)	4.71	4.53	7.72
	F6 (MPa)	35.53	32.81	33.26
Batch 2	E1t (GPa)	26.22	24.32	19.48
	E2t (GPa)	22.58	24.17	18.03
	v12	0.146	0.127	0.331
	F1t (MPa)	424.3	395.5	279.6
	F2t (MPa)	344	382.4	256.4
	E1c (GPa)	23.27	21.04	18.6
	E2c (GPa)	19.49	19.87	17.92
	v13c	0.432	0.439	0.423
	F1c (MPa)	346.42	338.31	271.7
	F2c (MPa)	307.78	321.7	242.9
	G12 (GPa)	5.25	5.08	8.33
	F6 (MPa)	19.03	17.81	43.485

The tensile properties represented in the table are the average of the normalized results of the two tensile tests conducted: ASTM D3039 and ASTM D638. The compression properties are the normalized values of the ASTM D6641 test and the shear properties are the normalized values of the ASTM D4255 test. The values in the shaded area shown in Table 7.2 were obtained from un-normalized properties.

7.3.2. Statistical Comparison of Normalized Material Properties

Since two standard test methods were conducted to obtain the same material property, it was substantial to check if the results were from the same sample population.

The comparison was conducted on all pair of combinations of four different experimental results obtained from two test standards and from two batches. In addition, all four results were compared simultaneously. Both the student t-test and the ANOVA statistical tool were used to identify the significance of difference between each pair of results. The level of confidence was set to 95% (alpha = 0.05). Both tools gave the same results. As for the comparison of all four experimental results, the ANOVA statistical tool was used. The statistical comparison was conducted on normalized material properties to eliminate the effect of the thickness variation in the panel. Therefore, the statistical study was conducted on tension and compression material properties but not on shear properties. It was conducted on the modulus of elasticity obtained from the initial range and the ultimate strength, in both principal material directions. The results of the comparison are represented in Table 7.3 for tension and Table 7.4 for compression and are summarized in a matrix format in which all three lay-ups are presented. The color of the material property indicates if the statistical comparison showed that the experimental results of the compared pair come from the same population sample; the green color indicate that the experimental results come from the same population sample while the red color indicate that they are significantly different.

Table 7.3: Statistical Comparison of Tension Normalized Material Properties

Tension		Batch One								Batch Two					
		D3039				D638				D3039				D638	
Batch One	D3039														
	D638	E1	E2	F1	F2	$[0]_{4sf}$									
		E1	E2	F1	F2	$[0/90]_{2sf}$									
		E1	E2	F1	F2	$[0/\pm45/0]_{4sf}$									
Batch Two	D3039	E1	E2	F1	F2	E1	E2	F1	F2	$[0]_{4sf}$					
		E1	E2	F1	F2	E1	E2	F1	F2	$[0/90]_{2sf}$					
		E1	E2	F1	F2	E1	E2	F1	F2	$[0/\pm45/0]_{4sf}$					
	D638	E1	E2	F1	F2	E1	E2	F1	F2	E1	E2	F1	F2	$[0]_{4sf}$	
		E1	E2	F1	F2	E1	E2	F1	F2	E1	E2	F1	F2	$[0/90]_{2sf}$	
		E1	E2	F1	F2	E1	E2	F1	F2	E1	E2	F1	F2	$[0/\pm45/0]_{4sf}$	

ALL		E1	E2	F1	F2	$[0]_{4sf}$
		E1	E2	F1	F2	$[0/90]_{2sf}$
		E1	E2	F1	F2	$[0/\pm45/0]_{4sf}$

Table 7.4: Statistical Comparison of Compression Normalized Material Properties

Compression		Batch One								Batch Two					
		D6641				D695				D6641				D695	
Batch One	D6641														
	D695	E1	E2	F1	F2	$[0]_{4sf}$									
		E1	E2	F1	F2	$[0/90]_{2sf}$									
		E1	E2	F1	F2	$[0/\pm45/0]_{4sf}$									
Batch Two	D6641	E1	E2	F1	F2	E1	E2	F1	F2	$[0]_{4sf}$					
		E1	E2	F1	F2	E1	E2	F1	F2	$[0/90]_{2sf}$					
		E1	E2	F1	F2	E1	E2	F1	F2	$[0/\pm45/0]_{4sf}$					
	D695	E1	E2	F1	F2	E1	E2	F1	F2	E1	E2	F1	F2	$[0]_{4sf}$	
		E1	E2	F1	F2	E1	E2	F1	F2	E1	E2	F1	F2	$[0/90]_{2sf}$	
		E1	E2	F1	F2	E1	E2	F1	F2	E1	E2	F1	F2	$[0/\pm45/0]_{4sf}$	

ALL		E1	E2	F1	F2	$[0]_{4sf}$
		E1	E2	F1	F2	$[0/90]_{2sf}$
		E1	E2	F1	F2	$[0/\pm45/0]_{4sf}$

The latter tables were inconclusive and a definite pattern was not found in the agreement of the compared results. Therefore, the experimental results were not concluded to come from the same population sample when tested using different test methods or different panel batches.

7.3.3. Selecting the Relevant Material Properties

The results of the tests conducted showed higher variability in the compression values than in the tension values. In addition, as part of obtaining design values from the properties, the relevant material properties were selected. Therefore, the moduli of elasticity calculated by the tension tests were considered to be the moduli of the material and Table 7.5 displays the material properties selected for further evaluation. The tension properties from batch 1 and batch 2 were averaged due to the small differences between the values. The tension properties were fiber dominated properties that did not change significantly between batch 1 and batch 2. Therefore, the compression and shear properties for each batch were not averaged due to the large difference in the values; note that the compression properties were not considered to be fiber dominated properties due to the nature of the fabric used which was woven fabric with relatively heavy tows with an areal weight of 817.13 g/m^2 (24.1 oz/yd^2). The compression ultimate strength, F_{1c} and F_{2c}, were not considered to be fiber dominated properties since the compression failure was controlled by the local buckling of the fabric in the matrix which was governed by the resin's properties.

Table 7.5: Selected Relevant Material Properties

		$[0]_{4sf}$	$[0/90]_{2sf}$	$[0/\pm45/0]_{sf}$
		Experimental	Experimetal	Experimetal
	E1 (GPa)	26.01	24.44	19.83
	E2 (GPa)	22.51	24.25	17.7
	v12	0.143	0.127	0.332
	F1t (MPa)	429.1	385.2	289.1
	F2t (MPa)	343.2	377.6	245.96
Batch 1	F1c (MPa)	369.9	368.7	298.15
Batch 1	F2c (MPa)	362.4	352.15	257.5
Batch 1	G12 (GPa)	4.71	4.53	7.72
Batch 1	F6 (MPa)	35.5	32.81	33.26
Batch 2	F1c (MPa)	346.4	338.31	271.7
Batch 2	F2c (MPa)	307.8	321.7	242.9
Batch 2	G12 (GPa)	5.25	5.08	8.33
Batch 2	F6 (MPa)	19.0	17.81	43.485

7.3.4. Obtaining the Design Allowable Values

The experimental results obtained from the tests were useful for comparison purposes with other composite data or for preliminary design. As part of using the material properties obtained for the PMC with woven fabric reinforcement, statistical analysis was implemented to calculate the design allowables for the material. The design allowables were generated for A-basis and B-basis statistical analysis. The A-basis allowable provided 95% confidence that 99% of the material sample would exceed the allowable. This type of design allowable is typically used for critical structures. On the other hand, the B-basis allowable provided 95% confidence that 90% of the material sample would exceed the allowable and is typically used for non-critical structures.

The methodology for obtaining design allowables for composite materials is explained in the Military Hand Book 17-1E (MIL-HDBK-17-1E) section 2.4.3. The procedure is summarized in the following reference (Tomblin, Ng et al., 2001). The data

for each material property was grouped together. Each testing environment group was pooled together; in the testing program presented in this study, one testing environment was used which was standard conditions of 22°C (71.6°F) and 50% relative humidity. The pool of sample values for one material property was normalized to a nominal thickness of 5.08 mm (0.2 in). Outliers were checked from each group by calculating the Maximum Normed Residual (MNR) according to equation (7.2). The MNR value for each sample was compared to the critical value of the sample size of the pool. The critical value was provided by the MIL-HDBK-17-1E for a wide number of sample sizes. For every sample that had its MNR greater than the critical value, it was considered to be an outlier and thus removed from the pool which was carried on for statistical analysis.

$$MNR_i = \frac{|x_i - \bar{x}|}{s} \tag{7.2}$$

where:

MNR_i = Maximum Normed Residual of sample i,
x_i = the data value of sample i, Pa (psi),
$\bar{x}$ = the mean of the pooled samples, Pa (psi),
s = the standard deviation of the pooled samples, Pa (psi).

The pooled data was then checked for normality. In other words, the data was checked if it had a normal distribution. This process was conducted by visual comparison of the data distribution with the best-fit normal curve. The probability of survival of each sample from the pool was calculated according to equation (7.3) and plotted against its corresponding data value.

$$\text{Probability of Survival of } x_i = 1 - \frac{i}{n+1} \tag{7.3}$$

where:

i = rank of the x_i data value in the sorted list, ascending order,
n = the total number of samples in the pool.

The generated curve was visually compared to the best-fit normal curve which was generated from the mean and standard deviation of the pooled data. A typical graph of such a comparison is depicted in Figure 7.2. The graph presented in Figure 7.2 was generated from the pooled data of F_{1t} experimental values.

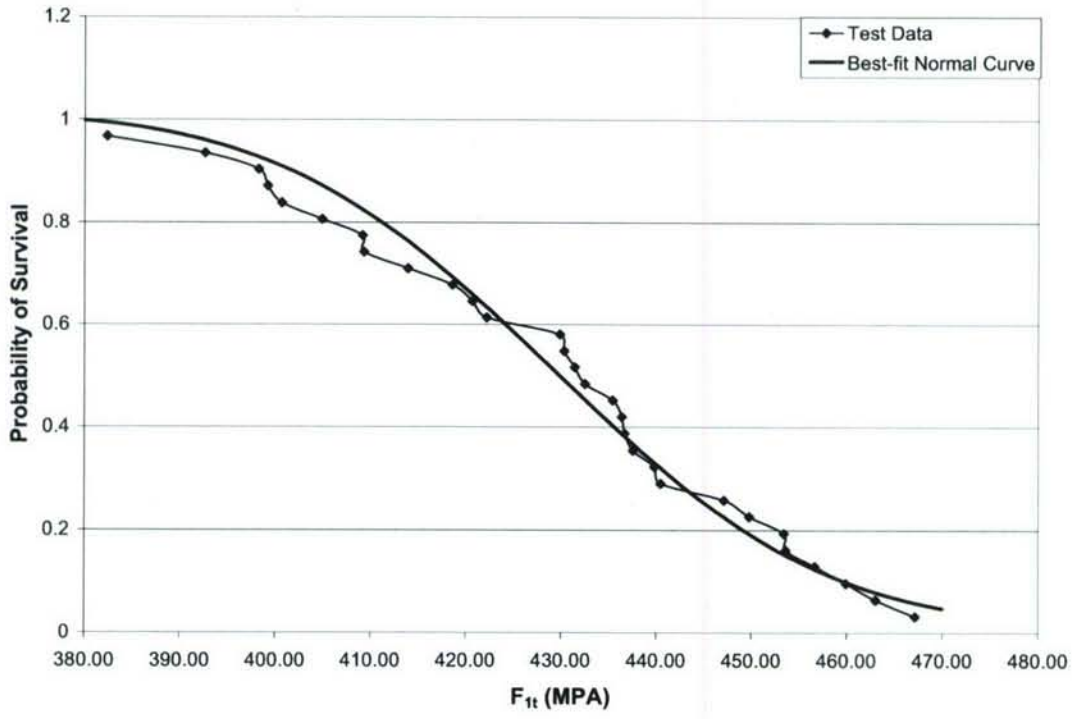

Figure 7.2: Typical Normality Check

If the assumption for normality was violated, the Weibull distribution would have been chosen for data fitting. After the normality distribution of the data was verified, the A- and B- basis "knock-down" factors were calculated. The tolerance factor was first calculated according to equations (7.4) and (7.5).

$$k_A = z_A\sqrt{\frac{f}{Q}} + \sqrt{\frac{1}{c_A \cdot n} + \left(\frac{b_A}{2c_A}\right)^2} - \frac{b_A}{2c_A} \tag{7.4}$$

where:

k_A = A-basis tolerance factor
z_A = 2.32635
f = $n-2$
n = the number of pooled samples
Q = $f - 2.327\sqrt{f} + 1.138 + 0.6057\frac{1}{\sqrt{f}} - 0.3287\frac{1}{f}$
c_A = $0.36961 + 0.0026958\frac{1}{\sqrt{f}} - 0.65201\frac{1}{f} + 0.011320\frac{1}{f\sqrt{f}}$
b_A = $2.0643\frac{1}{\sqrt{f}} - 0.95145\frac{1}{f} + 0.51251\frac{1}{f\sqrt{f}}$

$$k_B = z_B\sqrt{\frac{f}{Q}} + \sqrt{\frac{1}{c_B \cdot n} + \left(\frac{b_B}{2c_B}\right)^2} - \frac{b_B}{2c_B} \tag{7.5}$$

where:

k_B = B-basis tolerance factor
z_B = 1.28115
f = $n-2$
n = the number of pooled samples
Q = $f - 2.327\sqrt{f} + 1.138 + 0.6057\frac{1}{\sqrt{f}} - 0.3287\frac{1}{f}$
c_B = $0.36961 + 0.0040342\frac{1}{\sqrt{f}} - 0.71750\frac{1}{f} + 0.19693\frac{1}{f\sqrt{f}}$

$$b_B = 1.1372\frac{1}{\sqrt{f}} - 0.49162\frac{1}{f} + 0.18612\frac{1}{f\sqrt{f}}$$

Once the tolerance factors were determined, the normal distribution allowables were calculated according to the equations presented in (7.6). These values are considered as "knock-down" factors less than 1.

$$A = \bar{x} - k_A \cdot s$$
$$B = \bar{x} - k_B \cdot s \tag{7.6}$$

where:

A = normal distribution A-basis allowable
B = normal distribution B-basis allowable
k_A = A-basis tolerance factor
k_B = B-basis tolerance factor
$\bar{x}$ = the mean of the pooled samples, Pa (psi)
s = the standard deviation of the pooled samples, Pa (psi).

The basis values are calculated by multiplying the mean of each pooled set by the "knock-down" factors. The design allowables were calculated for one set of fiber lay-up panels, $[0]_{4sf}$. A summary of the values obtained are presented in Table 7.6, which depicts the average normalized values, the "knock-down" factors, and the basis values for both the A- and B- basis design.

Table 7.6: A- and B-basis Design Allowable Values

	$[0]_{4sf}$				
	Average Normalized Experimental	"knockdown" factor		Statistic Basis Value	
		A-basis	B-basis	A-basis	B-basis
E1 (GPa)	26.01	0.9291	0.9589	24.17	24.94
E2 (GPa)	22.51	0.9337	0.9616	21.02	21.65
F1t (MPa)	429.1	0.8383	0.9063	359.7	388.9
F2t (MPa)	343.2	0.9111	0.9485	312.7	325.5
F1c (MPa)	360.1	0.6311	0.7831	227.3	282.0
F2c (MPa)	336.9	0.6236	0.7794	210.1	262.6

Note that the values of batch 1 and batch 2 were combined to calculate the design allowables. Since there was a large variability in the ultimate compression strength values, the "knock-down" factors are relatively small compared to the "knock-down" factors of the other properties, thus, reducing the design allowables calculated.

7.4. Classical Lamination Theory Based Modeling Approach

A Classical Lamination Theory (CLT) based model was implemented to verify, through modeling techniques, the experimental results. The model predicts the behavior of multidirectional laminate as a function of the properties of the individual layers and the stacking sequence of the layers. The CLT takes into account basic assumptions as part of predicting the behavior of the laminate. The assumptions are the following (Daniel and Ishai, 1994):

1. Each layer of the laminate is quasi-homogenous and orthotropic.
2. The laminate and its layers are in a state of plane stress.
3. All displacements are small compared with the thickness of the laminate.
4. Displacements are continuous throughout the laminate.

5. In-plane displacements vary linearly through the thickness of the laminate.
6. Transverse shear strains γ_{xz} and γ_{yz} are negligible.
7. Strain-displacement and stress-strain relations are linear.
8. The transverse normal strain ε_z is negligible.

The properties of the lamina were obtained from the experimental results of testing the $[0]_{4sf}$ lay-up laminate. In this type of fabric lay-up sequence, the laminate properties are the same as the individual layer properties as long as all the layers are composed of the same material. By this approach, the lamina properties of the PMC reinforced with woven E-glass fabric under study was calculated experimentally. Using the properties of the lamina, the properties of the different fabric lay-up sequence was predicted using the CLT based model approach. Since two other fabric lay-up sequences were tested, $[0/90]_{2sf}$ and $[0/\pm45/0]_{sf}$, the properties of these lay-up sequences were predicted using the model and compared with the experimental results.

7.4.1. Method of Implementing the CLT Based Model

As mentioned earlier, the model starts with the properties of one lamina. The properties of each lamina were supplied from the experimental results and they consist of the thickness of the layer, the orientation of the layer with respect to a reference axis, elastic constants, and strength parameters. Once these properties were supplied, the reduced stiffness matrix or the principal stiffness matrix was calculated for each layer. With the help of the transformation matrix, the principal stiffness matrix of each layer is used to build the extensional stiffness matrix [A], coupling stiffness matrix [B], and the bending stiffness matrix [D] of the laminate. Combining all three matrices, the laminate stiffness matrix was obtained [ABD]. The inverse of the latter matrix gave the laminate

compliance matrix. Using the component of the laminate compliance matrix, the elastic constants of the laminate were calculated. The elastic constants were the elastic moduli, E_{xx} and E_{yy}, the Poisson's Ratios, ν_{xy} and ν_{yx}, and the shear modulus, G_{xy}.

A stress of one unit was assumed to be applied to the material. Depending on what strength parameter was needed to be calculated, the load was applied. In other words, if the ultimate tensile strength was needed in the principal direction, F_{xt}, a unit tensile stress was applied in the principal direction, N_x. Once the stress was applied, the strains and curvatures on the reference plane were calculated using the laminate compliance matrix. Since both lay-up sequences under study were balanced and symmetrical, the curvatures were zero. The strains of each lamina in the laminate were obtained from the reference strains and curvatures. Using each lamina's stiffness matrix, the stresses in each layer were calculated in the global coordinate system, x-y-z coordinate system. Using the transformation matrix, the principal material stresses were calculated (1-2-6 coordinate system).

For this study, the interactive tensor polynomial failure theory (Tsai-Wu Failure Theory) was implemented. The safety factor of each lamina was calculated and the minimum was considered to be the laminate safety factor. The latter safety factor was the laminate strength for the first ply failure approach, when damage was detected in one of the laminas either matrix failure or fiber failure.

To predict ultimate failure of the PMC, a damage factor was applied to the material properties. A typical damage factor is 0.25, applied to material properties governed by the matrix. Since the material's stress-strain curve of the following study was modeled with a bi-linear model, the ratio of the elastic modulus of the final region to

the elastic modulus of the initial region was taken to be the degradation factor that was applied to the material's property in the CLT based model. The degradation factors calculated for both principal material directions were as following: $r_1 = 0.83$ and $r_2 = 0.76$. As for the degradation factor in the shear direction, r_{12}, a different method was implemented since the shear stress strain curve was not represented by a bi-linear model but rather by a hyperbolic tangent curve fit. Therefore, an optimization technique was implemented to calculate the r_{12} degradation factor such that the $[0/\pm45/0]_{sf}$ experimental results agree with the CLT based model predictions; and the calculated value was 0.51.

Once the degradation factors were applied to the material's elastic properties, the same process of calculating the first ply failure was repeated but matrix failure was ignored and fiber failure only detected. This approach focused on detecting fiber failure in the material which was considered the ultimate failure of the material. The safety factor calculated in this approach was considered the material ultimate failure in the direction and state of loading assumed at the beginning, tension, compression, or shear. In some cases, the first ply failure was the same as the ultimate failure and occurs when the first ply failure detected is fiber failure. The procedure of implementing the CLT based model was taken from the following reference (Daniel and Ishai, 1994).

A computer program was used to carry out the calculation of the model procedure. The program was written on MATCAD software. MATCAD was chosen due to it's clarity in carrying calculation steps, especially matrix calculations, and its ease in monitoring the procedure. In addition, the same program was used to calculate all the material properties needed for comparison with the experimental results by a simple change of the layers' orientation and the applied loading.

7.4.2. Discussion of the Comparison of Results

As mentioned earlier, the material properties used in the model were the experimental values of the $[0]_{4sf}$ fiber lay-up panel. Since two batches were tested, two sets of material properties were obtained from each fabric lay-up sequence. The material properties were normalized to a nominal thickness of 0.508 mm (0.2 in). As discussed in section 7.3.3, the tensile properties obtained from both batches showed relatively similar values while the compression and shear properties showed large difference between the two batches. This was explained by the difference in the matrix between the two batches which introduced significant effects on the compression and shear properties obtained from the experiments and did not affect the tensile experimental values, since they were solely fiber dominated properties. The lamina properties were taken form the $[0]_{4sf}$ experimental results after normalizing the values and selecting the relevant properties; the values are presented in Table 7.5.

The lamina properties used as an input were different for batch 1 and batch 2. The values of the predicted properties compared to the experimental properties are presented in Table 7.7. The presented comparison in Table 7.7 show a high agreement between the experimental and CLT based model predictions. This was due to the use of degradation factors obtained from experimental results. It was observed that the Poisson's ratio and the shear ultimate strength of the $[0/\pm45/0]_{sf}$ showed large errors in the comparison. It was explained by the inability to normalize the results and thus rendering them universal for comparison with the CLT based model. The shaded properties in Table 7.7 are un-normalized values.

Table 7.7: CLT Predictions and Experimental Results Comparison

		Lamina Data Input $[0]_{4sf}$	$[0/90]_{2sf}$			$[0/\pm45/0]_{sf}$			
			CLT	U Maine		CLT		U Maine	
		Experimental	Pred.	Exp.	%Error	(FPF)	(FF)	Exp.	%Error
Batch 1	E1 (GPa)	25.82	24.12	24.56	1.82%	20.58		20.19	1.90%
	E2 (GPa)	22.41	24.12	24.33	0.87%	18.99		17.37	8.53%
	v12	0.140	0.13	0.128	1.54%	0.298		0.334	12.08%
	F1t (MPa)	435.0	366.9	374.9	2.19%	119.2	306.6	298.6	2.62%
	F2t (MPa)	342.2	366.9	372.8	1.62%	118.8	253.4	235.5	7.05%
	F1c (MPa)	369.9	346.8	368.7	6.33%	117.3	262.1	298.2	13.75%
	F2c (MPa)	362.4	346.8	352.2	1.56%	110.0	275.2	257.5	6.43%
	G12 (GPa)	4.71	4.71	4.53	3.82%	7.69		7.72	0.39%
	F6 (MPa)	35.53	35.53	32.81	7.66%	58.01	140.4	33.26	42.67%
Batch 2	E1 (GPa)	26.22	24.4	24.32	0.33%	21.27		19.48	8.42%
	E2 (GPa)	22.58	24.4	24.17	0.94%	19.56		18.03	7.82%
	v12	0.146	0.135	0.127	5.93%	0.288		0.331	14.93%
	F1t (MPa)	424.3	370.1	395.5	6.87%	60.41	298.3	279.6	6.28%
	F2t (MPa)	344.0	370.1	382.4	3.33%	56.58	258.0	256.4	0.63%
	F1c (MPa)	346.4	323.4	338.3	4.62%	58.92	252.1	271.7	7.77%
	F2c (MPa)	307.8	323.4	321.7	0.51%	55.12	242.3	242.9	0.26%
	G12 (GPa)	5.25	5.25	5.08	3.24%	8.00		8.33	4.13%
	F6 (MPa)	19.03	19.03	17.81	6.41%	29	139.1	43.49	49.95%

= un-normalized data

7.5. Conclusion and Recommendations

It was essential to normalize the composite material properties, obtained from experiments, for comparison of different panels. This was achieved by using a nominal thickness chosen according to the needs of the comparison. The normalization was possible only for fiber dominated properties. Therefore, the matrix dominated properties were not normalized and were not comparable between different panels. A statistical analysis was conducted on the normalized properties to measure the degree of significance of two set of results that should ideally give the same values. The statistical analysis compared results from different test methods and different material batches.

Normalized properties were used to obtain the corresponding design allowables. The "knock-down" factor obtained through calculating the design allowables was based

on the variation of the results and their distribution. In other words, the "knock-down" factor revealed the repeatability and reliability of properties obtained through the testing program. Due to the difficulties faced during the compression testing, the design allowables were significantly smaller than the mean of the experimental results. Normalization of the matrix dominated properties is necessary for future work, and further understanding and improving with composite materials designs.

The CLT based model showed accurate predictions of experimental results when the properties were normalized. The pseudo-quasi isotropic lay-up experimental results were used to calculate the degradation factor needed to predict the failure of the material in the CLT based model. Since the matrix dominated properties were not normalized, the comparison of the CLT based model and the experimental results did not show good agreement with the in-plane shear properties. As part of verifying the model, different fiber lay-ups can be tested and used in comparison with the CLT based model predictions. Such further study is recommended for future work.

7.6. References

ASTM D3039/D3039M, (2000). Standard Test Method for Tensile Properties of Polymer Matrix Composite Materials. Annual Book of ASTM Standards. West Conshohocken, American Society of Testing Materials. **Vol 15.03**.

ASTM D638, (2002). Standard Test Method for Tensile Properties of Plastics. Annual Book of ASTM Standards, American Society of Testing Materials. **Vol 08.01**.

ASTM D6641/D6641M, (2001). Standard Test Method for Determining the Compressive Properties of Polymer Matrix Composite Laminates Using a Combined Loading Compression (CLC) Test Fixture. Annual Book of ASTM Standards. West Conshohocken, American Society of Testing Materials. **Vol 15.03**.

SACMA SRM 1R-94, (1994). Recommended Test Method for Compressive Properties of Oriented Fiber-Resin Composites. Washington DC, Suppliers of Advanced Composites Materials Association.

Tomblin, J. S., Y. C. Ng, et al. 2001. Material Qualification and Equivalency for Polymer Matrix Composite Material Systems. U.S. Department of Transportation, Washington DC. Report#: DOT/FAA/AR-00/47.

ASTM D4255/D4255M, (2002). Standard Test Method for In-Plane Shear Properties of Polymer Matrix Composite Materials by the Rail Shear Method. Annual Book of ASTM Standards. West Conshohocken, American Society of Testing Materials. **Vol 15.03**.

ASTM D5379/D5379M, (1999). Standard Test Method for Shear Properties of Composite Materials by the V-Notched Beam Method. Annual Book of ASTM Standards. West Conshohocken, American Society of Testing Materials. **Vol 15.03**.

Daniel, I. M. and O. Ishai (1994). Engineering Mechanics of Composite Materials. New York, Oxford University Press.

Wang, J., A. Banbury, et al. (1998). "Evaluation of Approaches for Determining Design Allowables for Bolted Joints in Laminated Composites." Elsevier Science - Composite Structures **41**: 167 - 176.

About.com (2005). Statistics and the Strength of Composite Materials, http://composite.about.com/library/weekly/aa060997. **February 16, 2005**.

Chapter 8: Conclusions and Recommendations

8.1. Strain Measurement Using 3-D Digital Image Correlation System

The full-field strain captured by the three-dimensional digital image correlation (DIC) system for the tension, compression, and shear tests demonstrated the benefits of using 3-D digital image correlation photogrammetry technology. The advantages of the DIC system over conventional strain measuring tools include producing full-field strains and reducing the experimental variability of the obtained material properties. Orientation of the conventional strain measuring tools parallel to the applied load is one source of testing variability that is eliminated. The other source of error that is eliminated is due to the point-averaging of strains under conventional strain gages.

The DIC capability to measure full-field strain gave rise to inspecting possible errors caused by accepted testing methods, used to derive composite material properties. For example, the compression fixtures used to test marine grade composites induced non-uniform strain in the gage section, thereby, introducing errors in the material properties calculated. It is recommended that the specimen compression gage region be increased to incorporate at least the full weave pattern of the fabric used. For the material tested in this study, the corresponding gage length described in the ASTM D6641 standard test method was increased from 12.7 mm (0.5 in) to 30.48 mm (1.2 in). The gage length used in this case represents more than two weave patterns. A set of specimens were tested with the increased gage length and demonstrated lower variability in mechanical properties and a uniform strain distribution in the gage section. Similarly, an increase in the gage section width of the ASTM D638 dumbbell tensile specimen is recommended. The DIC

system can also be used to detect and correct small grip misalignments and twisting in a tensile specimen.

The technology of photogrammetry is constantly improving as are computer processing speeds. Advancement in the resolution of digital cameras will continue to enhance the accuracy and precision of 3D-DIC systems leading to further reductions in material testing variabilities and its sources, and to more mature, efficient, and higher performance designs.

8.2. Tension Tests for Characterizing Polymer Matrix Composites with Woven Fabric Reinforcement

Each test conducted, in accordance with ASTM D3039 and ASTM D638, had advantages and disadvantages. The tabs in the D3039 specimens were time consuming to bond to the specimens and were not effective in forcing the failure in the gage area. Conversely, the specimen width was adequate for the woven fabric used in this study, and produced enough torsional stiffness to align the specimen while loading. As for the D638 specimens, the dumbbell shape forced the failure into the gage area without causing stress concentration in the transition region, but the width caused problems in specimen alignment and in covering a larger number of tows needed to properly average the gage area strains.

In conclusion, the width of the specimen should be in accordance with the pattern of the fabric used in the composite under study. The fabric is represented properly when 3 tow patterns are included in the gage section; the edge patterns are affected by the boundary conditions, thus, leaving the middle pattern unaffected by outside conditions. The tow pattern of the fabric repeated every 12.7 mm (0.5 in) in the warp direction

resulting in a recommended specimen width of 30.48 mm (1.2 in), which was also used for the fill direction. To simplify the specimen preparation and remove the tabbing process, a dumbbell shape for the specimen configuration is recommended. The latter configuration was analyzed using a finite element analysis with an optimization package that modified the transition region, from grip width to gage width, by reducing the stress concentration typically found in that region.

8.3. Compression Tests for Characterizing Polymer Matrix Composites with Woven Fabric Reinforcement

One of the common disadvantages for both test methods, in accordance with ASTM D6641 and in accordance with SACMA SRM 1R, was the strain field viewed by the DIC cameras. The full-field strain captured by the DIC system was through the specimen thickness and the strain area was confined to a width of 5.08 mm. Therefore, when exporting the strains from the DIC system, the areas selected to compute the material compression properties did not have a sufficient representation of the material under study. In addition, the DIC system captured strain concentrations in the specimens of both test methods. These strain concentrations can be translated to stress concentrations. The strain concentrations are justified by the small length of the gage sections. The tow pattern of the fabric repeated every 12.7 mm (0.5 in) in the warp direction and every 10.16 mm (0.4 in) in the fill direction. Therefore, with a gage length of 12.7 mm (0.5 in), for the D6641 specimen, the gage section contained approximately two or two and a half tows and in some cases the tow was under the clamping edge of the specimen, barely covering one weave pattern. The strain concentrations in the SRM 1R specimens were observed to be greater compared to the ASTM D6641 specimens. Since

the gage length of the SRM 1R specimen was 4.75mm (0.188 in), the gage length contained approximately one tow or part of a tow and in some cases it contained a gap between two tows. Such small gage lengths did not properly represent the composite under study. Consequently, the small gage section could have confined the specimen from failing properly, especially with such a small number of tows in the gage section. Such failing process over estimated the value of the ultimate strength.

Since the SRM 1R specimen was very time consuming to prepare prior to testing, a modification to the D6641 specimen was recommended. In addition, since the fixture of the SACMA SRM 1R test method did not incorporate the possibility of increasing the specimen length, the D6641 test method was selected for modification. The modification to the ASTM D6641 specimen was increasing the gage section length from 12.7 mm (0.5 in) to 30.48 mm (1.2 in) and the gage section width from 19.05 mm (0.75 in) to 25.4 mm (1 in), thus incorporating as much of fabric weave patterns as possible. The modifications recommended for the compression test improved the experimental results. With the help of the DIC system these recommendations were suggested and proven to enhance the testing method for calculating the compressive material properties of polymer matrix composite (PMC) with woven fabric reinforcement.

8.4. Shear Tests for Characterizing Polymer Matrix Composites with Woven Fabric Reinforcement

The experimental results obtained were very dependent on the type of fabric used. The fabric used in this study was coarse and woven with relatively large tows. The ASTM test methods conducted did not relate the specimen configuration or gage section to the type of fabric used. When ASTM D4255 test method was conducted the results

were comparable to test results found in the literature and the variability was less than 10%. Conversely, when ASTM D5379 test method was conducted the results had coefficients of variation of up to 30% with very different results between batch 1 and batch 2 of the specimens. The gage section in the three-rail shear test method was approximately 140 mm x 25.4 mm (5.51 in x 1 in), which was large enough to cover a large area of the fabric reinforcing the PMC. The fabric used was represented properly when three tow patterns were included in the gage section; the edge patterns are affected by the boundary conditions, thus leaving the middle pattern unaffected by outside conditions. The tow pattern of the fabric used repeated every 12.7 mm (0.5 in) in the warp direction and every 10.16 mm (0.4 in) in the fill direction.

In conclusion, the three-rail shear test (ASTM D4255) performed better than the v-notch shear test (ASTM D5279). The main reason was the specimen configuration and the specimen scale compared to the fabric used. In addition, failure was detected in the stress strain curve by a flat region in the curve or by a drop in the load.

8.5. Density, Fiber Volume Fraction, and Glass Transition Temperature of Polymer Matrix Composites with Woven Fiber Reinforcement

The density and fiber volume fraction experimental results were dependent on the panel thickness variations. The specimen thickness variation was caused by either the mold used, the infusion process, or a combination of both. The panel thickness variation was related to the degree of compaction of the fabric during infusion. Thinner panels were a result of higher compaction, thus resulting in higher fiber volume fraction. The two batches showed a difference in fiber volume fraction and density, which were

correlated together. Both batches were laid and infused at the same manufacturing laboratory and with the same procedure, but at different times and using different fiber and resin batches. The difference in the fiber volume fraction resulted in a difference in the material properties: tension, compression, and shear as shown in the previous chapters.

The degree of cure of the panels was not established. The DMTA method proved to be unsuccessful in defining the degree of cure of PMC. The cause was the use of high temperature to measure the degree of cure. The high temperatures caused the material to change its degree of cure as the latter was being measured. The DMTA method was a successful quality control tool and a comparative tool for defining different PMCs. In addition, the DMTA method measured the glass transition temperature of the composite; thus defining the composites upper temperature limit.

8.6. Evaluation of the Experimental Results and Implementation of the Classical Lamination Theory

It was essential to normalize the composite material properties, obtained from experiments, for comparison of different panels. This was achieved by using a nominal thickness chosen according to the needs of the comparison. The normalization was possible only for fiber dominated properties. Therefore, the matrix dominated properties were not normalized and were not comparable between different panels. A statistical analysis was conducted on the normalized properties to measure the degree of significance of two set of results that should ideally give the same values. The statistical analysis compared results from different test methods and different material batches.

Normalized properties were used to obtain the corresponding design allowables. The "knock-down" factor obtained through calculating the design allowables was based on the variation of the results and their distribution. In other words, the "knock-down" factor revealed the repeatability and reliability of properties obtained through the testing program. Due to the difficulties faced during the compression testing, the design allowables were significantly smaller than the mean of the experimental results. Normalization of the matrix dominated properties is necessary for future work, further understanding, and improving with composite materials design.

The CLT based model showed accurate predictions of experimental results when the properties were normalized. The pseudo-quasi isotropic lay-up experimental results were used to calculate the degradation factor needed to predict the failure of the material in the CLT based made. Since the matrix dominated properties were not normalized, the comparison of the CLT based model and the experimental results did not show good agreement with the in-plane shear properties.

8.7. Conclusion and Recommendations

The experimental techniques presented in this study and adopted in the test program, focused on reducing the material property variabilities of marine grade composites originating from the experimental methods by using a 3-D Digital Image Correlation (DIC) system for measuring full-field strains. The full-field strains captured by the 3-D DIC system helped enhance the experimental techniques by eliminating the sources of variability caused by conventional strain measuring tools.

One source of variability captured by the DIC system was the presence of high and low strain variation as a result of the reinforcing fabric weave pattern of the PMC.

Therefore, the fabric type was the controlling aspect in the recommended modifications for the mechanical material testing. The modifications were according to the fabric's coarseness and weave pattern. The gage section of the modified coupon specimens were recommended to include three weaves of the fabric to properly represent the material under study. Three weaves were chosen because the edge weaves would be affected by the boundary conditions, whether fixture clamping or edge effects, which leaves the middle weave unaffected by boundary conditions.

Another source of error was the thickness variation in the panel. Therefore, the experimental results were normalized to a nominal thickness which enabled comparison of the test results from different panel batches. The normalization was only performed on fiber dominated properties. Design allowables were calculated from the normalized data and the latter showed test result repeatability and distribution. The experimental results were compared to a micro mechanics based approach for laminated composite: Classical Lamination Theory (CLT). The CLT based model predictions agreed with the fiber dominated properties of the test results.

Future research works that can be conducted related to the findings of the study addressed in this Thesis are as follows:

- Conduct experimental tests employing recommended modifications of testing methods to verify the modifications validity.
- Conduct a similar test program on panels manufactured by different suppliers to identify the material variability in relation to the panel manufacturing process.

- Apply a cyclic loading on the composite material studied in this program to identify a physical meaning to the transition point calculated in the bi-linear approach adopted for modeling the stress-strain curve.
- Devise a method to normalize the matrix dominated properties.
- Conduct experimental tests on panels with different fiber lay-up to compare and verify the validity of the CLT based model.

BIBLIOGRAPHY

About.com (2005). Statistics and the Strength of Composite Materials, http://composite.about.com/library/weekly/aa060997. **February 16, 2005**.

Adams, D. F. and E. Q. Lewis (1991). "Influence of Specimen Gage Length and Loading Method on the Axial Compressive Strength of a Unidirectional Composite Material." Experimental Mechanics **31** (2): 14-20.

Adams, D. F. and E. Q. Lewis (1997). "Experimental Assessment of Four Composite Material Shear Test Methods." Journal of Testing and Evaluation **Vol. 25** (March 1997).

Adams, D. O. and D. F. Adams 2002. Tabbing Guide for Composite Test Specimens. U.S. Department of Transportation, Washington DC. Report#: DOT/FAA/AR-02/106.

Ashland, (2004). Derekane 8084 Epoxy Vinyl Ester Resins. Composite Polymers. Columbus, OH, Ashland Inc.: 3 pages.

ASTM D695, (1996). Standard Test Method for Compressive Properties of Rigid Plastics. Annual Book of ASTM Standards. West Conshohocken, American Society of Testing Materials. **Vol 08.01**.

ASTM E111, (1997). Standard Test Method for Young's Modulus, Tangent Modulus, and Chord Modulus. Annual Book of ASTM Standards. West Conshohocken, American Society of Testing Materials. **Vol 03.01**.

ASTM E132, (1997). Standard Test Method for Poisson's Ratio at Room Temperature. Annual Book of ASTM Standards. West Conshohocken, American Society of Testing Materials. **Vol 03.01**.

ASTM D5379/D5379M, (1999). Standard Test Method for Shear Properties of Composite Materials by the V-Notched Beam Method. Annual Book of ASTM Standards. West Conshohocken, American Society of Testing Materials. **Vol 15.03**.

ASTM D3039/D3039M, (2000). Standard Test Method for Tensile Properties of Polymer Matrix Composite Materials. Annual Book of ASTM Standards. West Conshohocken, American Society of Testing Materials. **Vol 15.03**.

ASTM D792, (2000). Standard Test Methods for Density and Specific Gravity (Relative Density) of Plastics by Displacement. Annual Book of ASTM Standards. West Conshohocken, American Society of Testing Materials. **Vol 08.01**.

ASTM D6641/D6641M, (2001). Standard Test Method for Determining the Compressive Properties of Polymer Matrix Composite Laminates Using a Combined Loading Compression (CLC) Test Fixture. Annual Book of ASTM Standards. West Conshohocken, American Society of Testing Materials. **Vol 15.03**.

ASTM D3518/D3518M, (2001). Standard Test Method for In-Plane Shear Response of Polymer Matrix Composite Materials by a Tensile Test of a ±45 laminate. Annual Book of ASTM Standards. West Conshohocken, American Society of Testing Materials. **Vol 15.03**.

ASTM D638, (2002). Standard Test Method for Tensile Properties of Plastics. Annual Book of ASTM Standards, American Society of Testing Materials. **Vol 08.01**.

ASTM D5229/D5229M, (2002). Test Method for Moisture Absorption Properties and Equilibrium Conditioning of Polymer Matrix Composite Materials. Annual Book of ASTM Standards. West Conshohocken, American Society of Testing Materials. **Vol 15.03**.

ASTM E4, (2002). Practices for Force Verification of Testing Machines. Annual Book of ASTM Standards. West Conshohocken, American Society of Testing Materials. **Vol 03.01**.

ASTM D4255/D4255M, (2002). Standard Test Method for In-Plane Shear Properties of Polymer Matrix Composite Materials by the Rail Shear Method. Annual Book of ASTM Standards. West Conshohocken, American Society of Testing Materials. **Vol 15.03**.

ASTM D2584, (2002). Standard Test Method for Ignition Loss of Cured Reinforced Resins. Annual Book of ASTM Standards. West Conshohocken, American Society of Testing Materials. **Vol 08.01**.

ASTM D3410/D3410M, (2003). Standard Test Method for Compressive Properties of Polymer Matrix Composite Materials with Unsupported Gage Section by Shear Loading. Annual Book of ASTM Standards. West Conshohocken, American Society of Testing Materials. **Vol 15.03**.

ASTM WK278, (2003). Standard Test Method for Glass Transition Temperature (T_g) by DMA of Polymer Matrix Composites. Developed by Subcommittee: D30.04. West Conshohocken, American Society of Testing Materials. **Status: In Balloting**.

ASTM D4762, (2004). Standard Guide for Testing Polymer Matrix Composite Materials. Annual Book of ASTM Standards. West Conshohocken, American Society of Testing Materials. **Vol 08.04**.

ASTM D5467/D5467M, (2004). Standard Test Method for Compressive Properties of Unidirectional Polymer Matrix Composites Using a Sandwich Beam. Annual Book of ASTM Standards. West Conshohocken, American Society of Testing Materials. **Vol 15.03**.

Barbero, E. J. (1998). Introduction to Composite Materials Design. Philadelphia, Taylor & Francis, Inc.

Beckwith, S. W. and C. R. Hyland (1998). "Resin Transfer Molding: A Decade of Technology Advances." SAMPE Journal **34** (6): 7-19.

Bruck, H. A., S. R. McNeill, et al. (1989). "Digital Image Correlation Using Newton-Raphson Method of Partial Differential Correction." Experimental Mechanics **28** (3): 261-267.

Chartoff, R. P., P. T. Weissman, et al. (1994). The Application of Dynamic Mechanical Methods to T_g Determination in Polymers: An Overview. ASTM STP 1294. R. J. Seyler. Philadelphia, American Society for Testing and Materials: pp. 88 - 107.

Chaterjee, S., D. Adams, et al. 1993. Test Methods for Composites a Status Report Volume I: Tension Test Methods. U.S. Department of Transportation, Washington DC. Report#: DOT/FAA/CT-93/17.

Choi, S. and S. P. Shah (1997). "Measurement of Deformations on Concrete Subjected to Compression Using Image Correlation." Experimental Mechanics **37** (3): 307-313.

Daniel, I. M. and O. Ishai (1994). Engineering Mechanics of Composite Materials. New York, Oxford University Press.

Dumant, N. (2000). Effects of Curing on Vinyl Ester-Derakrane 8084 Properties. Department of Materials and Manufacturing Engineering, Lulea University of Technology.

Dura, M. (2005). Behavior and Design of Reinforced Wood-Plastic Composite Sections for Use in Sustained Loading Structural Applications. Civil and Enviromental Engineering Department. Orono, University of Maine.

Fayad, G. (2005). Probabilistic Finite Element Modeling of Marine Grade Composites. Civil and Enviromental Engineering Department. Orono, University of Maine.

He, J., M. Y. M. Chiang, et al. (2002). "Application of the V-Notch Shear Test for Unidirectional Hybrid Composites." Composite Materials **36** (23): 2653-2666.

Herzog, B., B. Goodell, et al. (2004). "Electron Microprobe Imaging for the Characterization of Polymer Matrix Composites." Composites Part A: Applied Science and Manufacturing **35**.

Hess, P. E., B. J. Jones, et al. (2004). A Virtual Testing Methodology for Marine Composites to Develop Design Allowables. Composites 2004, Tampa, FL.

Ifju, P. G. (1994). "The Shear Gage: For Reliable Shear Modulus Measurements of Composite Materials." Experimental Mechanics **34**: 369-378.

Karbhari, V. M. and Q. Wang (2004). "Multi-Frequency Dynamic Mechanical Thermal Analysis of Moisture Uptake in E-Glass/Vinylester Composites." Composites Part B: Engineering **35**.

Melrose, P., R. Lopez-Anido, et al. (2004). Elastic Properties of Sandwich Composite Panels using 3-D Digital Image Correlation with the Hydromat Test System. SEM XI International Congress and Exposition on Experimental and Applied Mechanics, Costa Mesa, CA.

Melrose, P. T. (2004). Elastic Properties of Sandwich Composite Panels Using 3-D Digital Image Correlation with the Hydromat Test System. Mechanical Engineering Department. Orono, University of Maine.

Mott, L., S. M. Shaler, et al. (1996). "A novel technique to measure strain distributions in single wood fibers." Wood and Fiber Science **28** (4): 429-437.

Muszyñski, L., R. Lopez-Anido, et al. (2000). Image Correlation Analysis Applied to Measurement of Shear Strains in Laminated Composites. SEM IX International Congress on Experimental Mechanics, Orlando, FL.

Muszyñski, L., R. Lagana, et al. (2002). Optical Measurements of Wood Deformations in Changing Climate. 2002 SEM IX International Congress on Experimental Mechanics, Milwaukee, WI.

Muszyñski, L., F. Wang, et al. (2002). "Short Term Creep Tests on Phenol Resorcinol Formaldehyde (PRF) Resin Undergoing Moisture Content Changes." Wood and Fiber Sience **34** (4): 612-624.

Piggott, M. R. and J. Wang (1999). Basic Errors Appear to be Hampering Composite Aircraft Improvements. 44th International SAMPE Symposium, Long Beach, CA.

Ranson, W. F., M. A. Sutton, et al., (1987). Holographic and Speckle Interferometry. SEM Handbook of Experimental Mechanics. A. S. Kobayashi. New Jersey, Prentice-Hall, Inc: 388-429.

SACMA SRM 1R-94, (1994). Recommended Test Method for Compressive Properties of Oriented Fiber-Resin Composites. Washington DC, Suppliers of Advanced Composites Materials Association.

Schmidt, T., J. Tyson, et al. (2002). "Full-Field Dynamic Displacement and Strain Measurement Using Advanced 3-D Image Correlation Photogrammetry. Part II." Experimental Techniques **27** (4): 44-47.

Schmidt, T., J. Tyson, et al. (2002). Advanced Photogrammetry For Robust Deformation and Strain Measurement. the SEM XI International Congress on Experimental Mechanics, Milwaukee, WI.

Souza, B. (2005). Fracture Mechanics Characterization of WPC-FRP Composite Materials Fabricated by the Composites Pressure Resin Infusion System (ComPRIS) Process. Civil Engineering Department. Orono, University of Maine.

Tomblin, J. S., Y. C. Ng, et al. 2001. Material Qualification and Equivalency for Polymer Matrix Composite Material Systems. U.S. Department of Transportation, Washington DC. Report#: DOT/FAA/AR-00/47.

Valea, A., I. Martinez, et al. (1998). "Influence of Cure Schedule and Solvent Exposure on the Dynamic Mechanical Behavior of a Vinyl Ester Resin Containing Glass Fibers." Journal of Applied Polymer Science **70** (13): 2595 - 2602.

Vendroux, G. and W. G. Knauss (1998). "Submicron Deformation Field Measurements: Part 2. Improved Digital Image Correlation." Experimental Mechanics **38** (2): 86-92.

Walls, J. and L. Thompson 2005. Parametric Shape Optimization of Tensile Coupons for Marine Grade Glass Fiber Reinforced Plastics. Applied Thermal Sciences, Orono, Maine. Report#: ATS-RELY/2-2005-02.

Wang, J., A. Banbury, et al. (1998). "Evaluation of Approaches for Determining Design Allowables for Bolted Joints in Laminated Composites." Elsevier Science - Composite Structures **41**: 167 - 176.

Whitney, J. M., D. L. Stansbarger, et al. (1971). "Analysis of the Rail Shear Test-Applications and Limitations." Composite Materials **5**: 24-34.

Wolfe, A. R. and M. Weiner (2004). Compression Testing - Comparison of Various Test Methods. Composites 2004 Convention and Trade Show, Florida, American Composites Manufacturers Association.

APPENDICIES

APPENDIX A. NOMENCLATURE FOR SPECIMEN LABELING

The specimen label included 5 terms that define the specimen:

1. The supplier/fabrication reference
2. The panel number
3. The test type
4. The orientation of the specimen
5. The specimen number

The supplier/fabrication reference is one character (i.e. "A").

"A" Seemann Composites Inc

The 5.08 mm (0.2 in) thick panels were labeled from 1 through 6:

"1" panel from batch one with $[0]_{4sf}$ fiber lay-up
"2" panel from batch one with $[0/90]_{2sf}$ fiber lay-up
"3" panel from batch one with $[0/\pm45/0]_{sf}$ fiber lay-up
"4" panel from batch two with $[0]_{4sf}$ fiber lay-up
"5" panel from batch two with $[0/90]_{2sf}$ fiber lay-up
"6" panel from batch two with $[0/\pm45/0]_{sf}$ fiber lay-up

The tests were referenced as follows:

"T1" tensile test in accordance with ASTM D3039 (rectangular)
"T2" tensile test in accordance with ASTM D638 (dumbbell)
"C1" compressive test in accordance with ASTM D6641
"C2" compressive test in accordance with SACMA SRM R1 (ASTM D695)
"S1" shear test in accordance with ASTM D4255 (three-rail)
"S1" shear test in accordance with ASTM D5379 (v-notch)

Two specimen orientations were tested:

"x" load applied on the specimen was parallel to the principal laminate axis
"y" load applied on the specimen was orthogonal to the principal laminate axis

The specimens numbers were relative to the set the specimens were cut from.

Examples of some specimen labels are: A1-T1x-1
A5-S2y-7
A2-C2x-4

APPENDIX B. DATA ANALYSIS (MATLAB CODE)

Appendix B.1. Tension Code

Appendix B.2. Compression Code

Appendix B.3. Shear Code

B.1 Tension Code

Main program code for analyzing the tensile raw data:

```
function Tensile

clear

%-----------------------------------User Input---------------------------------

Label = 'A1-T1x-';          %Label of each specimen
Filename = 'Data';
SummaryTitle = ['Tensile D3039 (Panel One x-direction)'];

Area = [125.319
    122.943
    122.768
    123.26
    124.187
    124.537
    123.435
    124.259];   %Areas of the specimens (in mm)

CalF = 10.078;     %Calibration Factor (in kN/V)

N=8;      %specifies the number of specimens

PI1=5;     %choosing the percent of ultimate strain to define the lower bound of the initial linear range
PI2=20;    %choosing the percent of ultimate strain to define the upper bound of the initial linear range

PF1=60;    %choosing the percent of ultimate strain to define the lower bound of the final linear range
PF2=90;    %choosing the percent of ultimate strain to define the upper bound of the final linear range

%-------------------------------------------------------------------------------

NN=N;

for i = 1:N

  %-------------------------- Loading Raw Data Through a Loop ----------------

  specimen = int2str(i);
  File = [Filename,specimen];

  fid = fopen(File);

  if fid~=-1;

  fclose(fid);

  [Ex_R,Ey_R,V_R] =
textread(File,'%f%f%f%f%*f','delimiter',',','headerlines',4,'expchars','eEdD','emptyvalue',0);

  Ex{i} = Ex_R/100;
  Ey{i} = Ey_R/100;
```

```
Str{i}=V_R*CalF/Area(i);

%----------Calculating the Ultimate Strength and Strain----------

M_Stress = max(Str{i});
for j=1:size(Str{i},1)
   if Str{i}(j)== M_Stress
      M_Strain = Ex{i}(j);
      break
   end
end

%----------Calculating the lower and upper bound for initial and final -----

I1 = PI1*M_Strain/100;
I2 = PI2*M_Strain/100;
F1 = PF1*M_Strain/100;
F2 = PF2*M_Strain/100;

%----------Collecting the Data into Separate Matrices----------

h=1;
h_=1;
k=1;
r=1;
l=1;
l_=1;
l__=1;

while Ex{i}(h)<I2
   Ex_I{i}(h) = Ex{i}(h);
   Ey_I{i}(h) = Ey{i}(h);
   Str_I{i}(h) = Str{i}(h);
   h = h+1;
end

for j=1:size(Ex_I{i},2)
   if Ex_I{i}(j)>I1
      Ixstrain{i}(k) = Ex_I{i}(j);
      Iystrain{i}(k) = Ey_I{i}(j);
      Istress{i}(k) = Str_I{i}(j);
      k=k+1;
   end
end

while Ex{i}(r)<F2
   Ex_F{i}(r) = Ex{i}(r);
   Ey_F{i}(r) = Ey{i}(r);
   Str_F{i}(r) = Str{i}(r);
   r = r+1;
end

for j=1:size(Ex_F{i},2)
   if Ex_F{i}(j)>F1
      Fxstrain{i}(l) = Ex_F{i}(j);
      Fystrain{i}(l) = Ey_F{i}(j);
```

```
      Fstress{i}(l) = Str_F{i}(j);
      l=l+1;
   end
end

%---------- Generating a Linear Regression for the Initial Fit --------

EI=polyfit(Ixstrain{i},Istress{i},1);

%---------- Generating a Linear Regression for the Final Fit ----------

EF=polyfit(Fxstrain{i},Fstress{i},1);

%--------- Forcing the curve and fit to pass through the Origin -------

Ex_F_t{i}=Ex_F{i}+EI(2)/EI(1);
EI_t(1)=EI(1);
EI_t(2)=0;
EF_t(1)=EF(1);
EF_t(2)=EF(2)-EI(2)/EI(1)*EF(1);

%--------------------Defining the Transition Point----------------------

TP_x=EF_t(2)/(EI_t(1)-EF_t(1));
TP_y=EI_t(1)*TP_x;

%----------Recalculating the Ultimate Strain----------------------

M_Strain = (M_Stress-EF_t(2))/EF_t(1);

%-------------------Calculating the Poisson's Ratio--------------------

PR_L_I=polyfit(Istress{i},Ixstrain{i},1);
PR_T_I=polyfit(Istress{i},Iystrain{i},1);
PR_L_F=polyfit(Fstress{i},Fxstrain{i},1);
PR_T_F=polyfit(Fstress{i},Fystrain{i},1);

PR_I=-PR_T_I(1)/PR_L_I(1);
PR_F=-PR_T_F(1)/PR_L_F(1);

%-------------Collecting the Results for Statistical Analysis----------

A(i,1)=Area(i);
A(i,2)=EI_t(1);
A(i,3)=EF_t(1);
A(i,4)=TP_x*100;
A(i,5)=TP_y*1000;
A(i,6)=M_Strain*100;
A(i,7)=M_Stress*1000;
A(i,8)=PR_I;
A(i,9)=PR_F;

%-------------------------- Used for Plotting Only --------------------

while Ex{i}(h_)<F1
   Plotx_I{i}(h_) = Ex{i}(h_);
```

```
        h_ = h_+1;
    end

    while Str{i}(l_) <= M_Stress
        Plotx_F{i}(l_) = (Str{i}(l_)-EF_t(2))/EF_t(1);
        if Str{i}(l_) == M_Stress
            break
        end
        l_ = l_+1;
    end

    for j=1:size(Plotx_F{i},2)
        if Plotx_F{i}(j)>I2
            Plotx_F_{i}(l__) = Plotx_F{i}(j);
            l__=l__+1;
        end
    end

    %----------Generating a Linear Data Set for Plotting----------

    fEI_t=polyval(EI_t,Plotx_I{i});
    fEF_t=polyval(EF_t,Plotx_F_{i});

    %----------Creating Plots for Each Specimen----------

figures(i,Label,Ex_F_t{i},Str_F{i},Plotx_I{i},fEI_t,Plotx_F_{i},fEF_t,TP_x,TP_y,M_Strain,M_Stress,EI_
t(1),EF_t(1),PR_I);

    %----------Screening Out the Missing Specimens----------

    else

        NN=NN-1;

    end

end

%----------Statistical Analysis----------

Means = sum(A)/NN;
Stdev = sqrt((NN*sum(A.^2)-sum(A).^2)/(NN*(NN-1)));
COV = Stdev./Means*100;

%----------Creating a Summary Table in Excel Worksheet----------

Table(A,Label,SummaryTitle,Means,Stdev,COV,N);
```

Subroutine for creating plots for each specimen:

```
function
figures(i,Label,Ex_F_t,Str_F,Plotx_I,fEI_t,Plotx_F_,fEF_t,TP_x,TP_y,M_Strain,M_Stress,EI_t,EF_t,PR_I
)

  figure
  plot(Ex_F_t,Str_F*1000)
  hold on
  plot(Plotx_I,fEI_t*1000,Plotx_F_,fEF_t*1000,'LineWidth',1)

  axis([0 0.025 0 550])
  number = num2str(i);
  filename = [Label,number];
  title(filename,'fontsize',12)
  xlabel('Strain (mm/mm)')
  ylabel('Stress (MPa)')

  str1 = {'Transition Point       '};
  str2 = {['(',num2str(TP_x*100,'%1.2f%%'),' , ',num2str(TP_y*1000,'%3.2f'),') \rightarrow  ']};
  str3(1) = {'\uparrow'};
  str3(2) = {'Ultimate Point'};
  str3(3) = {['(',num2str(M_Strain*100,'%1.2f%%'),' , ',num2str(M_Stress*1000,'%3.2f'),')']};
  str4(1) = {['\fontname{times}\bfE1 = ',num2str(EI_t,'%2.2f'),' GPa']};
  str4(2) = {['\fontname{times}\bfE2 = ',num2str(EF_t,'%2.2f'),' GPa']};
  str4(3) = {['\fontname{times}\bf\nu12 = ',num2str(PR_I,'%1.3f')]};

  text(TP_x,TP_y*1000,str2,'HorizontalAlignment','right','fontsize',8)
  text(TP_x,(TP_y+0.015)*1000,str1,'HorizontalAlignment','right','fontsize',8)
  text(M_Strain,M_Stress*1000,str3,'HorizontalAlignment','left','verticalalignment','top','fontsize',8)
  text(0.018,50,str4,'HorizontalAlignment','left','fontsize',10)

  saveas(gcf,filename,'tif')

  hold off
```

Subroutine for creating summary table in Excel worksheet for a set of specimens:

```
function Table(A,Label,SummaryTitle,Means,Stdev,COV,N)

Filename = ['Summary_',Label,'.xls'];
fid = fopen(Filename,'w');
str = [SummaryTitle,'\nSpecimen\tArea (mm^2)\tInital (GPa)\tFinal(GPa)\tTP Strain%%\tTP Stress
(MPa)\tU Strain%%\tU Stress (MPa)\tPR Initial\tPR Final\n'];
fprintf(fid,str);

for i = 1:N;

   a = A(i,:);
   number = num2str(i);
   filename = [Label,number];
   fprintf(fid,filename);
   fprintf(fid,'\t%3.3f\t%2.2f\t%2.2f\t%1.3f\t%3.1f\t%1.3f\t%3.1f\t%1.3f\t%1.3f\n',a);

end

fprintf(fid,'\nMean');
fprintf(fid,'\t%3.3f\t%2.2f\t%2.2f\t%1.3f\t%3.1f\t%1.3f\t%3.1f\t%1.3f\t%1.3f\n',Means);
fprintf(fid,'St Dev');
fprintf(fid,'\t%3.3f\t%2.2f\t%2.2f\t%1.3f\t%3.1f\t%1.3f\t%3.1f\t%1.3f\t%1.3f\n',Stdev);
fprintf(fid,'COV%%');
fprintf(fid,'\t%3.3f\t%2.2f\t%2.2f\t%1.3f\t%3.1f\t%1.3f\t%3.1f\t%1.3f\t%1.3f\n',COV);

fclose(fid);
```

B.2 Compression Code

Main program code for analyzing the compression raw data:

```
function Compression

clear

%-----------------------------------User Input----------------------------------

Label = 'A1-C1x-';          %Label of each specimen
Filename = 'Data';
SummaryTitle = ['Compression D6641 (Panel One x-direction)'];

Area = [123.709
   124.330
   121.645
   121.550
   124.022
   126.203
   123.919
   124.505
   121.834];    %Areas of the specimens (in mm)

CalF = 9.99;      %Caliberation Factor (in kN/V)


N=9;      %specifies the number of specimens

PI1=5;     %choosing the percent of ultimate strain to define the lower bound of the initial linear range
PI2=20;    %choosing the percent of ultimate strain to define the upper bound of the initial linear range

PF1=60;    %choosing the percent of ultimate strain to define the lower bound of the final linear range
PF2=90;    %choosing the percent of ultimate strain to define the upper bound of the final linear range

%-------------------------------------------------------------------------------

NN=N;

for i = 1:N

   %---------------------------- Loading Raw Data Through a Loop ------------------

   specimen = int2str(i);
   File = [Filename,specimen];

   fid = fopen(File);

   if fid~=-1;

   fclose(fid);

   [Ey_R,Ex_R,V_R] =
textread(File,'%f%f%f%f%*f','delimiter',',','headerlines',4,'expchars','eEdD','emptyvalue',0);
```

```
Ex{i} = Ex_R/100;
Ey{i} = Ey_R/100;
Str{i}=V_R*CalF/Area(i);

%----------Calculating the Ultimate Strength and Strain----------

M_Stress = min(Str{i});
for j=1:size(Str{i},1)
   if Str{i}(j)== M_Stress
      M_Strain = Ex{i}(j);
      break
   end
end

%----------Calculating the lower and upper bound for initial and final -----

I1 = PI1*M_Strain/100;
I2 = PI2*M_Strain/100;
F1 = PF1*M_Strain/100;
F2 = PF2*M_Strain/100;

%--------------------Collecting the Data into Separate Matrices----------

h=1;
h_=1;
k=1;
r=1;
l=1;
l_=1;
l__=1;

while Ex{i}(h)>I2
   Ex_I{i}(h) = Ex{i}(h);
   Ey_I{i}(h) = Ey{i}(h);
   Str_I{i}(h) = Str{i}(h);
   h = h+1;
end

for j=1:size(Ex_I{i},2)
   if Ex_I{i}(j)<I1
      Ixstrain{i}(k) = Ex_I{i}(j);
      Iystrain{i}(k) = Ey_I{i}(j);
      Istress{i}(k) = Str_I{i}(j);
      k=k+1;
   end
end

while Ex{i}(r)>F2
   Ex_F{i}(r) = Ex{i}(r);
   Ey_F{i}(r) = Ey{i}(r);
   Str_F{i}(r) = Str{i}(r);
   r = r+1;
end

for j=1:size(Ex_F{i},2)
   if Ex_F{i}(j)<F1
```

```
      Fxstrain{i}(l) = Ex_F{i}(j);
      Fystrain{i}(l) = Ey_F{i}(j);
      Fstress{i}(l) = Str_F{i}(j);
      l=l+1;
    end
end

%---------- Generating a Linear Regression for the Initial Fit --------

EI=polyfit(Ixstrain{i},Istress{i},1);

%---------- Generating a Linear Regression for the Final Fit ----------

EF=polyfit(Fxstrain{i},Fstress{i},1);

%--------- Forcing the curve and fit to pass through the Origin -------

Ex_F_t{i}=Ex_F{i}+EI(2)/EI(1);
EI_t(1)=EI(1);
EI_t(2)=0;
EF_t(1)=EF(1);
EF_t(2)=EF(2)-EI(2)/EI(1)*EF(1);

%--------------------Defining the Transition Point----------------------

TP_x=EF_t(2)/(EI_t(1)-EF_t(1));
TP_y=EI_t(1)*TP_x;

%----------Recalculating the Ultimate Strain----------------------

M_Strain = (M_Stress-EF_t(2))/EF_t(1);

%--------------------Calculating the Poisson's Ratio--------------------

PR_L_I=polyfit(Istress{i},Ixstrain{i},1);
PR_T_I=polyfit(Istress{i},Iystrain{i},1);
PR_L_F=polyfit(Fstress{i},Fxstrain{i},1);
PR_T_F=polyfit(Fstress{i},Fystrain{i},1);

PR_I=-PR_T_I(1)/PR_L_I(1);
PR_F=-PR_T_F(1)/PR_L_F(1);

%-------------Collecting the Results for Statistical Analysis----------

A(i,1)=Area(i);
A(i,2)=EI_t(1);
A(i,3)=EF_t(1);
A(i,4)=TP_x*100;
A(i,5)=TP_y*1000;
A(i,6)=M_Strain*100;
A(i,7)=M_Stress*1000;
A(i,8)=PR_I;
A(i,9)=PR_F;

%-------------------------- Used for Plotting Only --------------------
```

```
        while Ex{i}(h_)>F1
          Plotx_I{i}(h_) = Ex{i}(h_);
          h_ = h_+1;
        end

        while Str{i}(l_) >= M_Stress
          Plotx_F{i}(l_) = (Str{i}(l_)-EF_t(2))/EF_t(1);
          if Str{i}(l_) == M_Stress
            break
          end
          l_ = l_+1;
        end

        for j=1:size(Plotx_F{i},2)
          if Plotx_F{i}(j)<I2
            Plotx_F_{i}(l__) = Plotx_F{i}(j);
            l__=l__+1;
          end
        end

        %--------------Generating a Linear Data Set for Plotting---------------

        fEI_t=polyval(EI_t,Plotx_I{i});
        fEF_t=polyval(EF_t,Plotx_F_{i});

        %---------------------Creating Plots for Each Specimen-----------------

figures(i,Label,Ex_F_t{i},Str_F{i},Plotx_I{i},fEI_t,Plotx_F_{i},fEF_t,TP_x,TP_y,M_Strain,M_Stress,EI_
t(1),EF_t(1),PR_I);

        %------------------Screening Out the Missing Specimens----------------

        else

          NN=NN-1;

        end

      end

      %-------------------------------Statistical Analysis-----------------------

      Means = sum(A)/NN;
      Stdev = sqrt((NN*sum(A.^2)-sum(A).^2)/(NN*(NN-1)));
      COV = Stdev./Means*100;

      %-----------------Creating a Summary Table in Excel Worksheet--------------

      Table(A,Label,SummaryTitle,Means,Stdev,COV,N);
```

Subroutine for creating plots for each specimen:

```
function
figures(i,Label,Ex_F_t,Str_F,Plotx_I,fEI_t,Plotx_F_,fEF_t,TP_x,TP_y,M_Strain,M_Stress,EI_t,EF_t,PR_I
)

  figure
  plot(Ex_F_t,Str_F*1000)
  hold on
  plot(Plotx_I,fEI_t*1000,'k',Plotx_F_,fEF_t*1000,'k','LineWidth',1)

  axis([-0.016 0 -450 0])
  number = num2str(i);
  filename = [Label,number];
  title(filename,'fontsize',12)
  xlabel('Strain (mm/mm)')
  ylabel('Stress (MPa)')

  str1 = {'Transition Point        '};
  str2 = {['(',num2str(TP_x*100,'%1.2f%%'),' , ',num2str(TP_y*1000,'%3.2f'),') \rightarrow   ']};
  str3(1) = {'\leftarrow Ultimate Point'};
  str3(2) = {['(',num2str(M_Strain*100,'%1.2f%%'),' , ',num2str(M_Stress*1000,'%3.2f'),')']};
  str4(1) = {['\fontname{times}\bfE1 = ',num2str(EI_t,'%2.2f'),' GPa']};
  str4(2) = {['\fontname{times}\bfE2 = ',num2str(EF_t,'%2.2f'),' GPa']};
  str4(3) = {['\fontname{times}\bf\nu12 = ',num2str(PR_I,'%1.3f')]};

  text(TP_x,(TP_y+0.015)*1000,str1,'HorizontalAlignment','right','fontsize',8)
  text(TP_x,TP_y*1000,str2,'HorizontalAlignment','right','fontsize',8)
  text(M_Strain,M_Stress*1000,str3(1),'HorizontalAlignment','left','fontsize',8)
  text(M_Strain,(M_Stress-0.015)*1000,str3(2),'HorizontalAlignment','left','fontsize',8)
  text(-0.014,-50,str4,'HorizontalAlignment','left','fontsize',10)

  saveas(gcf,filename,'tif')

  hold off
```

Subroutine for creating summary table in Excel worksheet for a set of specimens:

```
function Table(A,Label,SummaryTitle,Means,Stdev,COV,N)

Filename = ['Summary_',Label,'.xls'];
fid = fopen(Filename,'w');
str = [SummaryTitle,'\nSpecimen\tArea (mm^2)\tInital (GPa)\tFinal(GPa)\tTP Strain%%\tTP Stress
(MPa)\tU Strain%%\tU Stress (MPa)\tPR Initial\tPR Final\n'];
fprintf(fid,str);

for i = 1:N;

   a = A(i,:);
   number = num2str(i);
   filename = [Label,number];
   fprintf(fid,filename);
   fprintf(fid,'\t%3.3f\t%2.2f\t%2.2f\t%1.3f\t%3.1f\t%1.3f\t%3.1f\t%1.3f\t%1.3f\n',a);

end

fprintf(fid,'\nMean');
fprintf(fid,'\t%3.3f\t%2.2f\t%2.2f\t%1.3f\t%3.1f\t%1.3f\t%3.1f\t%1.3f\t%1.3f\n',Means);
fprintf(fid,'St Dev');
fprintf(fid,'\t%3.3f\t%2.2f\t%2.2f\t%1.3f\t%3.1f\t%1.3f\t%3.1f\t%1.3f\t%1.3f\n',Stdev);
fprintf(fid,'COV%%');
fprintf(fid,'\t%3.3f\t%2.2f\t%2.2f\t%1.3f\t%3.1f\t%1.3f\t%3.1f\t%1.3f\t%1.3f\n',COV);

fclose(fid);
```

B.3 Shear Code

Main program code for analyzing the shear raw data:

```
function Shear1

clear

%-----------------------------------User Input----------------------------------

Label = 'A1-S1x-';            %Label of each specimen
Filename = 'Data';
SummaryTitle = ['Shear D4255 (Panel One x-direction)'];

Area = [749.901
   743.973
   728.384
   735.543
   728.338
   724.568
   746.374
   731.699];    %Areas of the specimens (in mm)

CalF = 9.99;      %Calibration Factor (in kN/V)


N=8;       %specifies the number of specimens

H1=0;    %choosing the lower bound shear angle for the hyperbolic fit
H2=0.013;    %choosing the upper bound shear angle for the hyperbolic fit

%-------------------------------------------------------------------------------

NN=N;

for i = 1:N

   %-------------------------- Loading Raw Data Through a Loop -----------------

   specimen = int2str(i);
   File = [Filename,specimen,'.txt'];

   fid = fopen(File);

   if fid~=-1;

   fclose(fid);

   [SA_1,SA_2,V_R] =
textread(File,'%f%f%f%f*f','delimiter',',','headerlines',4,'expchars','eEdD','emptyvalue',0);

   SA = (abs(SA_1)+abs(SA_2))/2;
   Str=abs(V_R)*1000*CalF/Area(i)/2;

   %-------------------Collecting the Data into Seperate Matrices---------------
```

```
h=1;
h_=1;
k=1;
r=1;
l=1;
l_=1;
l__=1;

while SA(r)<H2
   SA_H(r) = SA(r);
   Str_H(r) = Str(r);
   r = r+1;
end

for j=1:size(SA_H,2)
   if SA_H(j)>H1
      HSh_A(l) = SA_H(j);
      Hstress(l) = Str_H(j);
      l=l+1;
   end
end

%------------------ Generating a Tangent Hyperbolic Fit ----------------

x_guess = [20,500];

fun = inline ('x(2)*tanh(HSh_A*x(1)/x(2))','x','HSh_A');
x_fit = lsqcurvefit(fun, x_guess, HSh_A, Hstress);

%-------------Collecting the Results for Statistical Analysis----------

A(i,1)=Area(i);
A(i,2)=x_fit(1)/1000;
A(i,3)=abs(x_fit(2));

%--------------Generating a Data Set for Plotting---------------

for j=1:size(HSh_A,2)
   H_fit(j) = x_fit(2)*tanh(HSh_A(j)*x_fit(1)/x_fit(2));
end

%---------------------Creating Plots for Each Specimen-----------------

figures(i,Label,SA,Str,HSh_A,H_fit,x_fit(1),abs(x_fit(2)));

%-------------------------Emptying the Matrices-----------------------

SA(:,:)=[];
Str(:,:)=[];
SA_H(:,:)=[];
Str_H(:,:)=[];
HSh_A(:,:)=[];
Hstress(:,:)=[];
H_fit(:,:)=[];
```

```
    %------------------Screening Out the Missing Specimens-----------------

    else

       NN=NN-1;

    end


end

%------------------------------Statistical Analysis-----------------------

Means = sum(A)/NN;
Stdev = sqrt((NN*sum(A.^2)-sum(A).^2)/(NN*(NN-1)));
COV = Stdev./Means*100;

%-----------------Creating a Summary Table in Excel Worksheet---------------

Table(A,Label,SummaryTitle,Means,Stdev,COV,N);
```

Subroutine for creating plots for each specimen:

```
function figures(i,Label,SA,Str,HSh_A,H_fit,x_fit1,x_fit2)

   figure
   plot(SA,Str)
   hold on
   plot(HSh_A,H_fit,'--','LineWidth',1)
   legend('Data Curve','H-Fit',2);

   axis([0 0.03 0 50])
   number = num2str(i);
   filename = [Label,number];
   title(filename,'fontsize',12)
   xlabel('Shear Angle (rad)')
   ylabel('Stress (MPa)')


   str1(1) = {['\fontname{times}\bfH G_1_2 = ',num2str(x_fit1/1000,'%2.2f'),' GPa']};
   str1(2) = {['\fontname{times}\bfF_6 = ',num2str(x_fit2,'%2.2f'),' MPa']};

   text(0.02,5,str1,'HorizontalAlignment','left','fontsize',10)

   saveas(gcf,filename,'tif')

   hold off
```

Subroutine for creating summary table in Excel worksheet for a set of specimens:

```
function Table(A,Label,SummaryTitle,Means,Stdev,COV,N)

Filename = ['Summary_',Label,'.xls'];
fid = fopen(Filename,'w');
str = [SummaryTitle,'\nSpecimen\tArea (mm^2)\tG12 H_fit (GPa)\tF6 (MPa)\n'];
fprintf(fid,str);

for i = 1:N;

   a = A(i,:);
   number = num2str(i);
   filename = [Label,number];
   fprintf(fid,filename);
   fprintf(fid,'\t%3.3f\t%1.3f\t%2.2f\n',a);

end

fprintf(fid,'\nMean');
fprintf(fid,'\t%3.3f\t%1.3f\t%2.2f\n',Means);
fprintf(fid,'St Dev');
fprintf(fid,'\t%3.3f\t%1.3f\t%2.2f\n',Stdev);
fprintf(fid,'COV%%');
fprintf(fid,'\t%3.3f\t%1.3f\t%2.2f\n',COV);

fclose(fid);
```

APPENDIX C. SUMMARY TABLES

Table C.1: Tensile D3039 Panel One through Panel Six (x and y directions)

Tensile D3039 (Panel One x-direction)									
Specimen	**Area (mm^2)**	**Inital (GPa)**	**Final(GPa)**	**TP Strain%**	**TP Stress (MPa)**	**U Strain%**	**U Stress (MPa)**	**PR Initial**	**PR Final**
A1-T1x-1	0	0	0	0	0	0	0	0	0
A1-T1x-2	122.943	26.35	20.22	0.679	178.9	2.015	449.1	0.143	0.053
A1-T1x-3	122.768	26.83	20.01	0.716	192.1	2.037	456.5	0.128	0.037
A1-T1x-4	123.26	27	20.24	0.647	174.8	2.119	472.7	0.13	0.042
A1-T1x-5	124.187	26.62	20.21	0.629	167.4	2.091	462.8	0.143	0.047
A1-T1x-6	124.537	26.34	19.81	0.718	189	1.854	414.1	0.114	0.047
A1-T1x-7	123.435	26.67	19.91	0.675	180.1	2.039	451.7	0.145	0.048
A1-T1x-8	124.259	26.18	19.59	0.661	173	2.046	444.3	0.146	0.064
Mean	123.627	26.57	20	0.675	179.3	2.029	450.2	0.136	0.048
St Dev	0.697	0.29	0.25	0.033	8.8	0.085	18.5	0.012	0.008
COV%	0.564	1.11	1.24	4.912	4.9	4.181	4.1	8.779	17.261

Tensile D3039 (Panel One y-direction)									
Specimen	**Area (mm^2)**	**Inital (GPa)**	**Final(GPa)**	**TP Strain%**	**TP Stress (MPa)**	**U Strain%**	**U Stress (MPa)**	**PR Initial**	**PR Final**
A1-T1y-1	125.103	22.61	15.22	0.607	137.3	2.065	359.1	0.127	0.038
A1-T1y-2	125.306	21.87	14.78	0.652	142.6	1.962	336.2	0.125	0.04
A1-T1y-3	0	0	0	0	0	0	0	0	0
A1-T1y-4	123.961	22.92	15.12	0.652	149.4	1.898	337.8	0.105	0.038
A1-T1y-5	124.257	22.41	15.05	0.611	136.9	2.035	351.3	0.129	0.032
A1-T1y-6	123.117	22.7	15.28	0.64	145.3	2.007	354.1	0.116	0.029
A1-T1y-7	125.272	22.82	15.05	0.645	147.1	1.954	344.1	0.115	0.036
A1-T1y-8	124.399	22.92	15.63	0.596	136.7	1.987	354	0.125	0.037
Mean	124.488	22.61	15.16	0.629	142.2	1.987	348.1	0.12	0.036
St Dev	0.804	0.37	0.26	0.023	5.3	0.055	8.8	0.009	0.004
COV%	0.646	1.64	1.73	3.715	3.7	2.79	2.5	7.078	10.809

Table C.1 continued

Tensile D3039 (Panel Two x-direction)									
Specimen	**Area (mm^2)**	**Inital (GPa)**	**Final(GPa)**	**TP Strain%**	**TP Stress (MPa)**	**U Strain%**	**U Stress (MPa)**	**PR Initial**	**PR Final**
A2-T1x-1	130.745	24.63	16.87	0.639	157.3	1.881	367	0.074	0.024
A2-T1x-2	129.661	24.16	17.59	0.61	147.4	1.957	384.5	0.112	0.035
A2-T1x-3	0	0	0	0	0	0	0	0	0
A2-T1x-4	131.043	23.92	17.1	0.609	145.6	1.913	368.8	0.159	0.047
A2-T1x-5	127.786	25.14	17.75	0.611	153.5	1.928	387.4	0.083	0.062
A2-T1x-6	130.021	24.59	16.95	0.652	160.3	1.888	369.8	0.138	0.054
A2-T1x-7	128.869	24.5	16.83	0.628	153.9	1.901	368.1	0.161	0.038
A2-T1x-8	128.34	25.23	17.08	0.607	153.2	1.924	378.1	0.145	0.035
Mean	129.495	24.6	17.17	0.622	153	1.913	374.8	0.125	0.042
St Dev	1.219	0.48	0.36	0.018	5.1	0.026	8.5	0.035	0.013
COV%	0.941	1.93	2.11	2.838	3.4	1.366	2.3	28.498	30.519

Tensile D3039 (Panel Two y-direction)									
Specimen	**Area (mm^2)**	**Inital (GPa)**	**Final(GPa)**	**TP Strain%**	**TP Stress (MPa)**	**U Strain%**	**U Stress (MPa)**	**PR Initial**	**PR Final**
A2-T1y-1	127.549	25.05	17.78	0.598	149.9	2.001	399.3	0.141	0.043
A2-T1y-2	0	0	0	0	0	0	0	0	0
A2-T1y-3	128.9	24.81	17.65	0.585	145.1	1.906	378.3	0.151	0.034
A2-T1y-4	128.473	25.1	17.47	0.59	148.1	1.863	370.4	0.162	0.058
A2-T1y-5	130.056	24.07	17.27	0.572	137.6	1.832	355.3	0.141	0.039
A2-T1y-6	128.449	24.93	17.48	0.549	137	1.872	368.2	0.118	0.044
A2-T1y-7	129.31	24.58	17.17	0.582	143.1	1.949	377.9	0.122	0.034
A2-T1y-8	129.004	24.32	17.25	0.615	149.6	2.008	389.8	0.141	0.034
Mean	128.82	24.69	17.44	0.585	144.3	1.919	377	0.139	0.041
St Dev	0.783	0.39	0.22	0.021	5.4	0.069	14.5	0.015	0.009
COV%	0.608	1.57	1.28	3.554	3.7	3.602	3.8	10.996	21.409

Table C.1 continued

Tensile D3039 (Panel Three x-direction)									
Specimen	**Area (mm^2)**	**Inital (GPa)**	**Final(GPa)**	**TP Strain%**	**TP Stress (MPa)**	**U Strain%**	**U Stress (MPa)**	**PR Initial**	**PR Final**
A3-T1x-1	118.63	20.96	14.16	0.55	115.2	1.862	301.2	0.34	0.39
A3-T1x-2	110.829	22.67	14.6	0.619	140.2	2.033	346.8	0.367	0.383
A3-T1x-3	111.467	22.36	15.2	0.524	117.1	1.937	332	0.353	0.418
A3-T1x-4	110.658	22.2	14.22	0.636	141.3	1.938	326.4	0.339	0.327
A3-T1x-5	113.291	22.08	13.95	0.65	143.4	2.013	333.6	0.348	0.342
A3-T1x-6	109.472	22.59	15.07	0.569	128.6	2.024	347.9	0.315	0.384
A3-T1x-7	111.202	22.58	14.43	0.627	141.7	2.084	351.8	0.326	0.346
A3-T1x-8	119.803	21.21	13.42	0.61	129.4	2.101	329.4	0.335	0.327
Mean	113.169	22.08	14.38	0.598	132.1	1.999	333.6	0.34	0.365
St Dev	3.893	0.65	0.58	0.045	11.3	0.081	16.2	0.016	0.034
COV%	3.44	2.95	4.06	7.539	8.6	4.038	4.9	4.698	9.199

Tensile D3039 (Panel Three y-direction)									
Specimen	**Area (mm^2)**	**Inital (GPa)**	**Final(GPa)**	**TP Strain%**	**TP Stress (MPa)**	**U Strain%**	**U Stress (MPa)**	**PR Initial**	**PR Final**
A3-T1y-1	120.841	18.52	10.43	0.609	112.9	2.034	261.4	0.315	0.288
A3-T1y-2	117.661	17.75	9.7	0.612	108.6	1.997	243	0.336	0.277
A3-T1y-3	119.258	17.76	9.97	0.594	105.5	1.999	245.5	0.315	0.311
A3-T1y-4	115.321	18.2	9.92	0.635	115.5	2.052	256	0.312	0.287
A3-T1y-5	119.075	17.49	9.86	0.585	102.4	2.062	248	0.29	0.31
A3-T1y-6	118.814	17.91	10.13	0.595	106.5	2.008	249.7	0.304	0.268
A3-T1y-7	118.75	17.89	9.92	0.631	112.8	2.058	254.4	0.313	0.329
A3-T1y-8	120.088	18.38	10.55	0.641	117.8	2.011	262.3	0.318	0.283
Mean	118.726	17.99	10.06	0.613	110.3	2.028	252.5	0.313	0.294
St Dev	1.668	0.35	0.29	0.021	5.3	0.027	7.2	0.013	0.02
COV%	1.405	1.94	2.89	3.4	4.8	1.331	2.8	4.126	6.936

Table C.1 continued

Tensile D3039 (Panel Four x-direction)									
Specimen	**Area (mm^2)**	**Inital (GPa)**	**Final(GPa)**	**TP Strain%**	**TP Stress (MPa)**	**U Strain%**	**U Stress (MPa)**	**PR Initial**	**PR Final**
A4-T1x-1	127.728	25.84	19.77	0.684	176.6	1.914	419.9	0.136	0.038
A4-T1x-2	127.63	25.63	19.07	0.724	185.7	1.867	403.7	0.136	0.039
A4-T1x-3	132.994	25.54	18.86	0.685	174.9	1.731	372.2	0.144	0.055
A4-T1x-4	132.801	25.39	18.84	0.697	176.9	1.825	389.4	0.136	0.041
A4-T1x-5	132.606	26.02	19.41	0.65	169.1	1.755	383.7	0.164	0.047
A4-T1x-6	133.218	24.82	19.11	0.681	169.1	1.861	394.5	0.148	0.042
A4-T1x-7	133.243	25.27	18.78	0.628	158.8	1.952	407.4	0.137	0.046
A4-T1x-8	129.152	26.18	19.8	0.646	169	1.99	435.1	0.135	0.039
Mean	131.172	25.59	19.2	0.674	172.5	1.862	400.7	0.142	0.043
St Dev	2.535	0.44	0.41	0.031	7.9	0.09	20.3	0.01	0.006
COV%	1.933	1.71	2.14	4.622	4.6	4.844	5.1	7.215	13.104

Tensile D3039 (Panel Four y-direction)									
Specimen	**Area (mm^2)**	**Inital (GPa)**	**Final(GPa)**	**TP Strain%**	**TP Stress (MPa)**	**U Strain%**	**U Stress (MPa)**	**PR Initial**	**PR Final**
A4-T1y-1	130.05	22.58	14.92	0.558	126.1	1.978	337.9	0.135	0.024
A4-T1y-2	132.277	22.06	14.88	0.562	124	1.856	316.6	0.099	0.047
A4-T1y-3	130.942	22.05	14.96	0.574	126.5	1.944	331.5	0.103	0.028
A4-T1y-4	134.102	22.02	14.57	0.562	123.8	1.984	331	0.142	0.02
A4-T1y-5	133.206	21.69	14.9	0.537	116.5	2.036	339.9	0.087	0.037
A4-T1y-6	128.469	22.71	15.39	0.518	117.6	2.033	350.9	0.124	0.036
A4-T1y-7	130.449	22.41	15.05	0.552	123.6	1.998	341.4	0.113	0.054
A4-T1y-8	127.891	23.18	15.46	0.515	119.4	1.863	327.8	0.124	0.032
Mean	130.923	22.34	15.02	0.547	122.2	1.962	334.6	0.116	0.035
St Dev	2.183	0.48	0.29	0.022	3.8	0.07	10.3	0.019	0.012
COV%	1.667	2.13	1.92	3.969	3.1	3.544	3.1	16.142	33.555

Table C.1 continued

Tensile D3039 (Panel Five x-direction)									
Specimen	**Area (mm^2)**	**Inital (GPa)**	**Final(GPa)**	**TP Strain%**	**TP Stress (MPa)**	**U Strain%**	**U Stress (MPa)**	**PR Initial**	**PR Final**
A5-T1x-1	131.054	23.82	17.1	0.621	147.9	2.07	395.8	0.134	0.041
A5-T1x-2	128.987	24.13	17.28	0.642	154.9	1.991	388	0.129	0.034
A5-T1x-3	130.366	23.88	16.94	0.643	153.5	1.987	381.2	0.125	0.028
A5-T1x-4	133.054	24.11	16.91	0.598	144.2	2.029	386.1	0.119	0.038
A5-T1x-5	131.292	24.61	17.39	0.592	145.7	1.905	374.1	0.117	0.041
A5-T1x-6	129.36	24.59	17.44	0.587	144.3	2.105	408.9	0.136	0.029
A5-T1x-7	131.352	24.8	17.21	0.568	140.8	1.825	357	0.129	0.034
A5-T1x-8	133.124	23.97	17.15	0.619	148.3	2	385.2	0.159	0.025
Mean	131.074	24.24	17.18	0.609	147.4	1.989	384.5	0.131	0.034
St Dev	1.514	0.37	0.19	0.027	4.8	0.089	15.2	0.013	0.006
COV%	1.155	1.54	1.11	4.424	3.3	4.483	3.9	10.08	17.922

Tensile D3039 (Panel Five y-direction)									
Specimen	**Area (mm^2)**	**Inital (GPa)**	**Final(GPa)**	**TP Strain%**	**TP Stress (MPa)**	**U Strain%**	**U Stress (MPa)**	**PR Initial**	**PR Final**
A5-T1y-1	121.113	24.2					376.2	0.124	
A5-T1y-2	129.582	24.8					397.9	0.14	
A5-T1y-3	127.205	24.77					390.6	0.123	
A5-T1y-4	131.353	24.02					398.0	0.113	
A5-T1y-5	127.88	24.76					393.7	0.104	
A5-T1y-6	128.688	24.69					381.5	0.116	
A5-T1y-7	130.339	24.14					396.2	0.108	
A5-T1y-8	129.964	24.74					375.6	0.133	
Mean	128.266	24.52					388.7	0.12	
St Dev	3.186	0.33					9.53	0.012	
COV%	2.484	1.35					2.45	10.244	

Table C.1 continued

Tensile D3039 (Panel Six x-direction)									
Specimen	**Area (mm^2)**	**Inital (GPa)**	**Final(GPa)**	**TP Strain%**	**TP Stress (MPa)**	**U Strain%**	**U Stress (MPa)**	**PR Initial**	**PR Final**
A6-T1x-1	119.319	21.14					290.9	0.313	
A6-T1x-2	110.847	21.25					319.9	0.339	
A6-T1x-3	113.586	20.13					298.4	0.309	
A6-T1x-4	112.795	20.49					305.0	0.322	
A6-T1x-9	125.546	20.45					296.3	0.331	
A6-T1x-10	125.159	20.15					293.6	0.33	
A6-T1x-11	128.967	19.59					282.3	0.33	
A6-T1x-12	128.471	19.71					290.2	0.319	
Mean	120.586	20.36					297.1	0.324	
St Dev	7.407	0.6					11.36	0.01	
COV%	6.143	2.95					3.823	3.118	

Tensile D3039 (Panel Six y-direction)									
Specimen	**Area (mm^2)**	**Inital (GPa)**	**Final(GPa)**	**TP Strain%**	**TP Stress (MPa)**	**U Strain%**	**U Stress (MPa)**	**PR Initial**	**PR Final**
A6-T1y-1	123.038	18.95					268.9	0.303	
A6-T1y-2	124.989	18.48					262.2	0.308	
A6-T1y-3	125	18.76					262.4	0.306	
A6-T1y-4	123.093	18.37					275.7	0.306	
A6-T1y-5	123.952	18.23					273.1	0.299	
A6-T1y-6	123.935	18.69					247.4	0.306	
A6-T1y-7	126.391	19.12					275.4	0.314	
A6-T1y-8	122.208	19.33					287.2	0.322	
Mean	124.076	18.74					269.0	0.308	
St Dev	1.342	0.38					11.9	0.007	
COV%	1.082	2.02					4.42	2.299	

Table C.2: Tensile D638 Panel One through Panel Six (x and y directions)

Tensile D638 (Panel One x-direction)									
Specimen	**Area (mm^2)**	**Inital (GPa)**	**Final(GPa)**	**TP Strain%**	**TP Stress (MPa)**	**U Strain%**	**U Stress (MPa)**	**PR Initial**	**PR Final**
A1-T2x-1	60.779	27.78	20.81	0.565	157	2.017	459.1	0.173	0.033
A1-T2x-2	59.425	27.52	20.52	0.639	175.8	2.054	466.2	0.128	0.028
A1-T2x-3	60.479	26.13	20.37	0.666	174	2.013	448.3	0.174	0.068
A1-T2x-4	60.137	27.64	20.98	0.531	146.7	2.136	483.6	0.142	0.038
A1-T2x-5	59.112	28.57	20.3	0.577	164.9	1.91	435.4	0.129	0.066
A1-T2x-6	58.661	27.48	20.64	0.651	178.9	1.967	450.5	0.132	0.068
A1-T2x-7	59.864	28.11	20.57	0.554	155.7	2.027	458.7	0.135	0.08
A1-T2x-8	59.858	27.17	20.17	0.557	151.3	2.244	491.6	0.133	0.052
Mean	59.789	27.55	20.55	0.592	163	2.046	461.7	0.143	0.054
St Dev	0.702	0.72	0.27	0.051	12.1	0.103	18.5	0.019	0.019
COV%	1.174	2.6	1.3	8.683	7.4	5.048	4	13.274	35.328

Tensile D638 (Panel One y-direction)									
Specimen	**Area (mm^2)**	**Inital (GPa)**	**Final(GPa)**	**TP Strain%**	**TP Stress (MPa)**	**U Strain%**	**U Stress (MPa)**	**PR Initial**	**PR Final**
A1-T2y-1	60.786	23.33	15.47	0.572	133.5	2.023	357.8	0.114	0.028
A1-T2y-2	61.975	23.49	15.7	0.507	119	1.963	347.8	0.125	0.031
A1-T2y-3	61.821	23.77	15.82	0.522	124	2.017	360.6	0.081	0.04
A1-T2y-4	0	0	0	0	0	0	0	0	0
A1-T2y-5	61.466	24.58	15.24	0.543	133.5	1.963	349.9	0.137	0.034
A1-T2y-6	61.249	23.12	15.47	0.517	119.6	2.029	353.5	0.095	0.025
A1-T2y-7	60.358	24.55	15.86	0.507	124.6	2.076	373.4	0.118	0.024
A1-T2y-8	59.933	23.97	16.19	0.535	128.2	2.056	374.4	0.058	0.032
Mean	61.084	23.83	15.68	0.529	126.1	2.018	359.6	0.104	0.031
St Dev	0.758	0.57	0.31	0.023	5.9	0.043	10.7	0.027	0.005
COV%	1.242	2.4	2.01	4.397	4.7	2.116	3	26.258	17.203

Table C.2 continued

Tensile D638 (Panel Two x-direction)									
Specimen	**Area (mm^2)**	**Inital (GPa)**	**Final(GPa)**	**TP Strain%**	**TP Stress (MPa)**	**U Strain%**	**U Stress (MPa)**	**PR Initial**	**PR Final**
A2-T2x-1	62.917	24.38	18.1	0.641	156.4	1.968	396.5	0.115	0.045
A2-T2x-2	64.411	25.97	17.25	0.654	169.9	1.915	387.3	0.157	0.062
A2-T2x-3	61.624	24.78	17.91	0.603	149.3	1.949	390.5	0.121	0.052
A2-T2x-4	64.955	25.06	16.76	0.617	154.6	1.896	368.9	0.108	0.075
A2-T2x-5	62.06	25.64	18.43	0.625	160.3	2.001	413.9	0.157	0.074
A2-T2x-6	64.207	25.11	16.87	0.595	149.5	1.999	386.3	0.111	0.059
A2-T2x-7	62.112	25.61	17.76	0.531	135.9	1.849	370	0.143	0.07
A2-T2x-8	63.996	24.93	16.9	0.635	158.3	1.887	369.9	0.137	0.122
Mean	63.285	25.18	17.5	0.613	154.3	1.933	385.4	0.131	0.07
St Dev	1.264	0.52	0.64	0.039	9.9	0.055	15.7	0.02	0.023
COV%	1.997	2.07	3.64	6.285	6.4	2.862	4.1	15.081	33.452

Tensile D638 (Panel Two y-direction)									
Specimen	**Area (mm^2)**	**Inital (GPa)**	**Final(GPa)**	**TP Strain%**	**TP Stress (MPa)**	**U Strain%**	**U Stress (MPa)**	**PR Initial**	**PR Final**
A2-T2y-1	64.522	24.83	16.99	0.659	163.7	2.003	392	0.144	0.04
A2-T2y-2	65.397	24.31	16.31	0.688	167.3	1.905	365.7	0.102	0.05
A2-T2y-3	64.143	24.08	16.51	0.634	152.6	1.843	352.1	0.109	0.018
A2-T2y-4	64.519	25.1	16.5	0.586	147.1	1.863	357.7	0.156	0.049
A2-T2y-5	60.692	22.43	14.87	0.661	148.4	2.014	349.5	0.102	0.045
A2-T2y-6	64.65	24.64	17.18	0.613	151.1	1.829	360	0.111	0.038
A2-T2y-7	63.595	24.27	17.33	0.64	155.3	2.101	408.6	0.139	0.036
A2-T2y-8	64.985	25.55	17.62	0.613	156.6	2.096	418	0.124	0.059
Mean	64.063	24.4	16.66	0.637	155.2	1.957	375.4	0.123	0.042
St Dev	1.463	0.93	0.86	0.033	7.1	0.111	26.9	0.021	0.012
COV%	2.284	3.81	5.15	5.138	4.6	5.683	7.2	16.89	29.377

Table C.2 continued

Tensile D638 (Panel Three x-direction)									
Specimen	**Area (mm^2)**	**Inital (GPa)**	**Final(GPa)**	**TP Strain%**	**TP Stress (MPa)**	**U Strain%**	**U Stress (MPa)**	**PR Initial**	**PR Final**
A3-T2x-1	58.725	20.85	12.57	0.662	137.9	2.078	315.9	0.334	0.303
A3-T2x-2	59.581	21.49	13.09	0.626	134.5	1.908	302.3	0.332	0.346
A3-T2x-3	59.477	21.25	13.37	0.644	136.9	1.972	314.4	0.314	0.324
A3-T2x-4	60.289	22.19	12.07	0.729	161.7	2.121	329.8	0.352	0.367
A3-T2x-5	59.737	21.42	13.08	0.627	134.3	1.943	306.4	0.32	0.313
A3-T2x-6	60.883	20.52	11.84	0.712	146.2	1.84	279.7	0.31	0.359
A3-T2x-7	59.652	21.05	11.83	0.697	146.7	2.002	301.1	0.319	0.323
A3-T2x-8	60.23	20.61	12.54	0.617	127.2	2	300.7	0.338	0.335
Mean	59.822	21.17	12.55	0.664	140.7	1.983	306.3	0.327	0.334
St Dev	0.647	0.54	0.6	0.043	10.6	0.09	14.6	0.014	0.022
COV%	1.081	2.56	4.75	6.489	7.5	4.533	4.8	4.269	6.68

Tensile D638 (Panel Three y-direction)									
Specimen	**Area (mm^2)**	**Inital (GPa)**	**Final(GPa)**	**TP Strain%**	**TP Stress (MPa)**	**U Strain%**	**U Stress (MPa)**	**PR Initial**	**PR Final**
A3-T2y-1	58.534	19.69	9.8	0.626	123.3	1.934	251.4	0.298	0.272
A3-T2y-2	58.816	19.56	9.86	0.631	123.5	2.044	262.7	0.336	0.3
A3-T2y-3	58.351	19.98	10.22	0.585	116.8	1.991	260.6	0.267	0.291
A3-T2y-4	0	0	0	0	0	0	0	0	0
A3-T2y-5	59.863	18.8	9.86	0.64	120.3	2.063	260.6	0.286	0.276
A3-T2y-6	0	0	0	0	0	0	0	0	0
A3-T2y-7	60.612	20.58	10.04	0.545	112.1	1.911	249.2	0.29	0.287
A3-T2y-8	61.488	17.94	9.59	0.636	114.1	2	244.9	0.31	0.275
Mean	59.611	19.42	9.89	0.61	118.3	1.99	254.9	0.298	0.283
St Dev	1.262	0.93	0.22	0.038	4.8	0.06	7.4	0.024	0.011
COV%	2.118	4.78	2.19	6.218	4	3	2.9	7.921	3.874

Table C.2 continued

Tensile D638 (Panel Four x-direction)									
Specimen	**Area (mm^2)**	**Inital (GPa)**	**Final(GPa)**	**TP Strain%**	**TP Stress (MPa)**	**U Strain%**	**U Stress (MPa)**	**PR Initial**	**PR Final**
A4-T2x-1	66.093	26.32	19.44	0.624	164.2	1.92	416.2	0.164	0.06
A4-T2x-2	0	0	0	0	0	0	0	0	0
A4-T2x-3	65.31	25.59	19.36	0.643	164.4	1.895	406.9	0.133	0.069
A4-T2x-4	65.804	26.51	20.09	0.602	159.5	2.048	450.2	0.144	0.086
A4-T2x-5	65.107	27.26	20.26	0.59	160.8	2.019	450.5	0.143	0.065
A4-T2x-6	63.534	27.01	20.65	0.624	168.6	2.118	477.1	0.155	0.057
A4-T2x-7	64.06	27.38	20.72	0.561	153.7	2.044	460.9	0.176	0.083
A4-T2x-8	62.303	26.67	20.49	0.564	150.5	2.073	459.7	0.136	0.066
Mean	64.602	26.68	20.14	0.601	160.2	2.017	445.9	0.15	0.07
St Dev	1.363	0.62	0.55	0.031	6.4	0.081	25.3	0.016	0.011
COV%	2.11	2.31	2.74	5.187	4	4.021	5.7	10.428	15.678

Tensile D638 (Panel Four y-direction)									
Specimen	**Area (mm^2)**	**Inital (GPa)**	**Final(GPa)**	**TP Strain%**	**TP Stress (MPa)**	**U Strain%**	**U Stress (MPa)**	**PR Initial**	**PR Final**
A4-T2y-1	66.947	21.64	15.48	0.567	122.7	1.911	330.8	0.115	0.028
A4-T2y-2	65.368	22.51	14.35	0.563	126.7	2.135	352.3	0.117	-0.018
A4-T2y-3	67.262	20.97	14.55	0.549	115.2	1.965	321.2	0.135	0.016
A4-T2y-4	66.748	21.96	15.05	0.489	107.4	2.004	335.4	0.132	0.046
A4-T2y-5	67.267	22.31	14.56	0.525	117.1	2.127	350.4	0.109	-0.024
A4-T2y-6	66.103	22.08	15.91	0.469	103.5	2.017	349.9	0.101	0.066
A4-T2y-7	67.249	22.12	15.24	0.48	106.2	1.987	335.9	0.119	0.057
A4-T2y-8	66.539	22.14	15.28	0.466	103.2	2.066	347.6	0.114	0.059
Mean	66.685	21.97	15.05	0.514	112.8	2.026	340.4	0.118	0.029
St Dev	0.672	0.47	0.53	0.043	9	0.078	11.3	0.011	0.035
COV%	1.007	2.16	3.54	8.299	8	3.851	3.3	9.463	121.044

Table C.2 continued

Tensile D638 (Panel Five x-direction)									
Specimen	**Area (mm^2)**	**Inital (GPa)**	**Final(GPa)**	**TP Strain%**	**TP Stress (MPa)**	**U Strain%**	**U Stress (MPa)**	**PR Initial**	**PR Final**
A5-T2x-1	65.516	24.07	17.22	0.553	133	2.109	401.1	0.118	0.031
A5-T2x-2	66.974	24.43	17.17	0.606	148	2.021	390.9	0.157	0.051
A5-T2x-3	66.798	23.69	17.32	0.607	143.8	2.082	399.3	0.094	0.025
A5-T2x-4	65.778	24.09	17.01	0.606	145.9	2.109	401.7	0.126	0.095
A5-T2x-5	65.422	24.24	17.22	0.61	148	2.101	404.7	0.12	0.033
A5-T2x-6	65.769	21.53	16.86	0.953	205.1	1.924	368.9	0.112	0.046
A5-T2x-7	66.041	23.99	17.17	0.603	144.6	2.047	392.7	0.126	0.035
A5-T2x-8	64.881	23.89	16.89	0.612	146.2	2.163	408	0.119	0.037
Mean	65.897	23.74	17.11	0.644	151.8	2.07	395.9	0.122	0.044
St Dev	0.7	0.92	0.17	0.126	22.1	0.073	12.3	0.018	0.022
COV%	1.062	3.88	0.98	19.635	14.5	3.511	3.1	14.606	49.946

Tensile D638 (Panel Five y-direction)									
Specimen	**Area (mm^2)**	**Inital (GPa)**	**Final(GPa)**	**TP Strain%**	**TP Stress (MPa)**	**U Strain%**	**U Stress (MPa)**	**PR Initial**	**PR Final**
A5-T2y-1	64.963	24.32	17.03	0.592	144.1	2.024	387.8	0.114	0.035
A5-T2y-2	64.523	24.39	17.05	0.614	149.8	2.039	392.8	0.079	0.026
A5-T2y-3	66.094	24.01	17.09	0.591	141.9	2.117	402.8	0.13	0.014
A5-T2y-4	65.474	24.19	17.23	0.604	146.2	1.932	375	0.133	0.042
A5-T2y-5	62.735	22.96	15.95	0.63	144.6	2.024	367.1	0.129	0.031
A5-T2y-6	62.131	24.91	17.19	0.577	143.7	1.975	384.1	0.131	0.043
A5-T2y-7	65.43	24.62	17.8	0.58	142.9	1.819	363.3	0.135	0.029
A5-T2y-8	65.989	24.18	17.16	0.604	145.9	1.978	381.8	0.112	0.035
Mean	64.667	24.2	17.06	0.599	144.9	1.989	381.8	0.12	0.032
St Dev	1.478	0.57	0.51	0.018	2.5	0.088	13.1	0.019	0.009
COV%	2.285	2.37	3	2.94	1.7	4.417	3.4	15.661	29.56

Table C.2 continued

Tensile D638 (Panel Six x-direction)									
Specimen	**Area (mm^2)**	**Inital (GPa)**	**Final(GPa)**	**TP Strain%**	**TP Stress (MPa)**	**U Strain%**	**U Stress (MPa)**	**PR Initial**	**PR Final**
A6-T2x-1	61.917	20.78	11.92	0.718	149.2	1.907	290.9	0.345	0.311
A6-T2x-2	60.791	21.1	12.43	0.683	144.2	1.887	293.8	0.336	0.33
A6-T2x-3	61.897	19.74	11.34	0.758	149.7	1.885	277.5	0.324	0.312
A6-T2x-4	63.155	19.53	12.06	0.668	130.5	1.906	279.7	0.357	0.343
A6-T2x-5	62.747	20.22	11.89	0.701	141.8	1.87	280.8	0.343	0.322
A6-T2x-6	62.274	19.94	12.78	0.707	141	1.922	296.3	0.336	0.334
A6-T2x-7	62.018	20.71	12.53	0.68	140.8	1.88	291.2	0.343	0.336
A6-T2x-8	61.88	21.21	12.52	0.633	134.2	1.918	295	0.322	0.351
Mean	62.085	20.4	12.18	0.694	141.4	1.897	288.2	0.338	0.33
St Dev	0.697	0.63	0.47	0.037	6.6	0.019	7.6	0.011	0.014
COV%	1.123	3.1	3.84	5.36	4.7	0.992	2.6	3.375	4.353

Tensile D638 (Panel Six y-direction)									
Specimen	**Area (mm^2)**	**Inital (GPa)**	**Final(GPa)**	**TP Strain%**	**TP Stress (MPa)**	**U Strain%**	**U Stress (MPa)**	**PR Initial**	**PR Final**
A6-T2y-1	64.189	18.05	9.75	0.65	117.2	2.104	259.1	0.296	0.268
A6-T2y-2	63.923	17.48	9.85	0.656	114.7	2.024	249.4	0.312	0.275
A6-T2y-3	65.776	17.54	9.27	0.682	119.6	1.999	241.6	0.304	0.287
A6-T2y-4	62.897	18.4	9.93	0.638	117.4	2.157	268.4	0.294	0.275
A6-T2y-5	63.012	18.3	10.15	0.643	117.8	2.046	260.1	0.292	0.314
A6-T2y-6	62.684	18.17	9.68	0.626	113.8	2.094	255.9	0.318	0.267
A6-T2y-7	63.214	18.22	9.86	0.638	116.3	1.977	248.3	0.319	0.272
A6-T2y-8	62.242	18.67	9.84	0.622	116.1	2.078	259.3	0.305	0.299
Mean	63.492	18.11	9.79	0.644	116.6	2.06	255.3	0.305	0.282
St Dev	1.119	0.41	0.25	0.019	1.8	0.06	8.4	0.011	0.017
COV%	1.762	2.27	2.57	2.915	1.6	2.905	3.3	3.487	5.966

Table C.3: Optimized Tension D3039 Panel Four (x and y directions)

Tension D3039 -optimized- (Panel Four x-direction)									
Specimen	**Area (mm^2)**	**Inital (GPa)**	**Final(GPa)**	**TP Strain%**	**TP Stress (MPa)**	**U Strain%**	**U Stress (MPa)**	**PR Initial**	**PR Final**
A4-oT1x-1	157.32	26.24	19.93	0.614	161.1	1.773	392.2	0.16	0.068
A4-oT1x-2	159.94	25.82	19.46	0.682	176.1	1.995	431.7	0.117	0.059
A4-oT1x-3	164.36	25.52	19.41	0.618	157.7	1.896	405.7	0.162	0.063
A4-oT1x-4	164.81	24.4	18.5	0.675	164.7	1.968	404	0.132	0.07
A4-oT1x-5	163.51	24.69	18.99	0.703	173.6	2.125	443.6	0.149	0.062
A4-oT1x-6	163.78	25.77	19.38	0.613	158.1	1.92	411.3	0.139	0.053
A4-oT1x-7	152.83	26.35	20.26	0.627	165.2	1.838	410.5	0.119	0.055
A4-oT1x-8	162.07	24.91	17.89	0.737	183.6	1.945	399.6	0.148	0.105
Mean	161.077	25.46	19.23	0.659	167.5	1.933	412.3	0.141	0.067
St Dev	4.181	0.72	0.76	0.047	9.3	0.106	17.1	0.017	0.017
COV%	2.595	2.84	3.96	7.184	5.6	5.472	4.1	12.113	24.598

Tension D3039 -optimized- (Panel Four y-direction)									
Specimen	**Area (mm^2)**	**Inital (GPa)**	**Final(GPa)**	**TP Strain%**	**TP Stress (MPa)**	**U Strain%**	**U Stress (MPa)**	**PR Initial**	**PR Final**
A4-oT1y-1	157.16	22.45	15.01	0.583	131	1.974	339.7	0.13	0.017
A4-oT1y-2	160.73	22.23	14.72	0.577	128.2	1.907	323.9	0.116	0.028
A4-oT1y-3	155.41	22.52	15.02	0.585	131.8	2.035	349.6	0.107	0.025
A4-oT1y-4	160.19	21.92	14.6	0.574	125.7	2.002	334.2	0.141	0.031
A4-oT1y-5	156.05	22.04	14.7	0.583	128.6	2.054	344.7	0.121	0.018
A4-oT1y-6	156.93	22.22	14.76	0.562	125	1.938	328	0.108	0.032
A4-oT1y-7	154.1	22.21	14.73	0.584	129.8	1.984	335.9	0.128	0.017
A4-oT1y-8	152.37	22.95	15.2	0.594	136.4	1.915	337.2	0.128	0.012
Mean	156.618	22.32	14.84	0.58	129.6	1.976	336.7	0.122	0.023
St Dev	2.834	0.32	0.21	0.01	3.6	0.054	8.3	0.012	0.007
COV%	1.81	1.44	1.39	1.639	2.8	2.717	2.5	9.513	32.621

Table C.4: Compression D6641 Panel One through Panel Six (x and y directions)

Compression D6641 (Panel One x-direction)									
Specimen	**Area (mm^2)**	**Inital (GPa)**	**Final(GPa)**	**TP Strain%**	**TP Stress (MPa)**	**U Strain%**	**U Stress (MPa)**	**PR Initial**	**PR Final**
A1-C1x-1	93.692	31.48	26.95	-0.566	-178.1	-1.157	-337.4	0.432	0.522
A1-C1x-2	0	0	0	0	0	0	0	0	0
A1-C1x-3	92.173	28.38	25.97	-0.404	-114.7	-1.371	-365.7	0.293	0.315
A1-C1x-4	91.694	26.53	25.96	-0.407	-108.1	-1.507	-393.7	0.339	0.448
A1-C1x-5	93.977	29.14	24.06	-0.58	-169.1	-1.435	-374.8	0.377	0.53
A1-C1x-6	98.795	26.72	23.46	-0.541	-144.5	-1.514	-372.8	0.432	0.537
A1-C1x-7	95.391	26.32	23.19	-0.676	-177.8	-1.556	-382	0.369	0.526
A1-C1x-8	93.342	29.41	26.9	-0.822	-241.6	-1.423	-403.4	0.342	0.478
Mean	94.152	28.28	25.21	-0.571	-162	-1.423	-375.7	0.369	0.479
St Dev	2.379	1.9	1.61	0.147	45.4	0.133	21.3	0.051	0.08
COV%	2.526	6.71	6.37	-25.73	-28	-9.373	-5.7	13.719	16.587

Compression D6641 (Panel One y-direction)									
Specimen	**Area (mm^2)**	**Inital (GPa)**	**Final(GPa)**	**TP Strain%**	**TP Stress (MPa)**	**U Strain%**	**U Stress (MPa)**	**PR Initial**	**PR Final**
A1-C1y-1	93.131	24.95	20.64	-0.653	-163	-1.772	-393.9	0.381	0.454
A1-C1y-2	93.608	23.26	21.41	-0.635	-147.7	-1.758	-388.2	0.451	0.517
A1-C1y-3	93.378	22	20.76	-0.794	-174.6	-1.82	-387.6	0.407	0.555
A1-C1y-4	94.62	23.1	20.42	-0.657	-151.7	-1.722	-369.1	0.44	0.577
A1-C1y-5	92.223	23.58	21.82	-0.946	-223.1	-1.66	-378.7	0.367	0.489
A1-C1y-6	93.988	26.03	21.99	-0.575	-149.6	-1.494	-351.9	0.405	0.489
A1-C1y-7	93.12	28.32	22.43	-0.61	-172.9	-1.395	-348.9	0.436	0.652
A1-C1y-8	92.433	28.09	22.23	-0.568	-159.7	-1.476	-361.5	0.374	0.421
Mean	93.313	24.92	21.46	-0.68	-167.8	-1.637	-372.5	0.408	0.519
St Dev	0.783	2.37	0.77	0.128	24.5	0.16	17.3	0.032	0.074
COV%	0.839	9.51	3.61	-18.898	-14.6	-9.762	-4.6	7.883	14.195

Table C.4 continued

Compression D6641 (Panel Two x-direction)									
Specimen	**Area (mm^2)**	**Inital (GPa)**	**Final(GPa)**	**TP Strain%**	**TP Stress (MPa)**	**U Strain%**	**U Stress (MPa)**	**PR Initial**	**PR Final**
A2-C1x-7	95.679	25.42	22.52	-0.6	-152.5	-1.589	-375.2	0.435	0.601
A2-C1x-8	99.997	26.2	22.17	-0.606	-158.9	-1.571	-372.7	0.366	0.493
A2-C1x-15	95.341	24.33	20.52	-0.545	-132.7	-1.644	-358.1	0.445	0.52
A2-C1x-16	94.261	28.63	22.06	-0.499	-142.9	-1.547	-374.1	0.386	0.53
Mean	96.32	26.14	21.82	-0.563	-146.7	-1.588	-370.1	0.408	0.536
St Dev	2.525	1.82	0.89	0.05	11.4	0.041	8	0.038	0.046
COV%	2.622	6.98	4.07	-8.963	-7.8	-2.601	-2.2	9.358	8.583

Compression D6641 (Panel Two y-direction)									
Specimen	**Area (mm^2)**	**Inital (GPa)**	**Final(GPa)**	**TP Strain%**	**TP Stress (MPa)**	**U Strain%**	**U Stress (MPa)**	**PR Initial**	**PR Final**
A2-C1y-1	94.8	23.71	20.69	-0.766	-181.7	-1.773	-390	0.415	0.517
A2-C1y-2	0	0	0	0	0	0	0	0	0
A2-C1y-3	0	0	0	0	0	0	0	0	0
A2-C1y-4	100.37	24.46	20.62	-0.729	-178.2	-1.559	-349.4	0.435	0.567
A2-C1y-5	97.337	21.82	19.75	-0.954	-208.2	-1.785	-372.3	0.424	0.558
A2-C1y-6	97.459	23.33	20.92	-0.784	-182.9	-1.568	-346.9	0.474	0.647
A2-C1y-7	99.988	25.96	20.27	-0.765	-198.7	-1.29	-304.9	0.432	0.523
A2-C1y-8	99.152	21.92	18.47	-0.672	-147.3	-1.654	-328.6	0.415	0.521
Mean	98.184	23.54	20.12	-0.778	-182.8	-1.605	-348.7	0.432	0.556
St Dev	2.082	1.57	0.9	0.095	20.9	0.182	30.3	0.022	0.049
COV%	2.12	6.68	4.49	-12.196	-11.4	-11.364	-8.7	5.128	8.901

Table C.4 continued

Compression D6641 (Panel Three x-direction)									
Specimen	**Area (mm^2)**	**Inital (GPa)**	**Final(GPa)**	**TP Strain%**	**TP Stress (MPa)**	**U Strain%**	**U Stress (MPa)**	**PR Initial**	**PR Final**
A3-C1x-1	88.706	22.07	16.59	-0.677	-149.4	-1.649	-310.7	0.46	0.563
A3-C1x-2	87.603	21.2	16.41	-0.758	-160.8	-1.94	-354.7	0.473	0.583
A3-C1x-3	89.45	19.47	16.66	-0.985	-191.9	-1.938	-350.6	0.408	0.588
A3-C1x-4	89.607	20.08	16.05	-0.739	-148.4	-1.585	-284.2	0.434	0.564
A3-C1x-5	89.647	21.5	17.31	-0.639	-137.3	-1.691	-319.4	0.443	0.6
A3-C1x-6	88.076	18.45	15.87	-0.816	-150.5	-1.658	-284.1	0.415	0.546
A3-C1x-7	0	0	0	0	0	0	0	0	0
A3-C1x-8	88.766	20.86	17.25	-0.702	-146.5	-1.905	-353.9	0.42	0.538
Mean	88.836	20.52	16.59	-0.759	-155	-1.767	-322.5	0.436	0.569
St Dev	0.79	1.26	0.55	0.115	17.7	0.154	31.4	0.024	0.023
COV%	0.89	6.14	3.3	-15.138	-11.4	-8.744	-9.7	5.587	4.005

Compression D6641 (Panel Three y-direction)									
Specimen	**Area (mm^2)**	**Inital (GPa)**	**Final(GPa)**	**TP Strain%**	**TP Stress (MPa)**	**U Strain%**	**U Stress (MPa)**	**PR Initial**	**PR Final**
A3-C1y-1	86.194	19.87	15.05	-0.789	-156.7	-1.752	-301.6	0.482	0.836
A3-C1y-2	86.935	19.76	15.07	-0.8	-158.1	-1.676	-290.1	0.4	0.604
A3-C1y-3	88.944	15.84	12.83	-0.983	-155.7	-1.855	-267.6	0.448	0.66
A3-C1y-4	88.984	20.16	14.4	-0.726	-146.3	-1.579	-269.2	0.442	0.664
A3-C1y-5	89.273	16.05	13	-0.879	-141	-1.841	-266.1	0.487	0.728
A3-C1y-6	89.245	19.76	14.7	-0.775	-153.1	-1.588	-272.7	0.423	0.587
A3-C1y-7	88.539	19.44	14.67	-0.798	-155.1	-1.603	-273.3	0.435	0.597
A3-C1y-8	86.407	17.73	15.76	-0.707	-125.3	-1.849	-305.4	0.432	0.607
Mean	88.065	18.57	14.44	-0.807	-148.9	-1.718	-280.8	0.444	0.66
St Dev	1.321	1.78	1.02	0.088	11.2	0.121	15.9	0.029	0.085
COV%	1.5	9.61	7.07	-10.902	-7.5	-7.072	-5.7	6.566	12.916

Table C.4 continued

Compression D6641 (Panel Four x-direction)									
Specimen	**Area (mm^2)**	**Inital (GPa)**	**Final(GPa)**	**TP Strain%**	**TP Stress (MPa)**	**U Strain%**	**U Stress (MPa)**	**PR Initial**	**PR Final**
A4-C1x-1	0	0	0	0	0	0	0	0	0
A4-C1x-2	98.234	20.78	19.47	-0.728	-151.4	-1.767	-353.6	0.45	0.542
A4-C1x-3	99.287	24.43	21.47	-0.587	-143.5	-1.271	-290.4	0.377	0.546
A4-C1x-4	0	0	0	0	0	0	0	0	0
A4-C1x-5	99.894	21.06	20.13	-0.939	-197.8	-1.718	-354.5	0.421	0.514
A4-C1x-6	0	0	0	0	0	0	0	0	0
A4-C1x-7	88.425	26.54	24.2	-0.593	-157.3	-1.607	-402.7	0.379	0.492
A4-C1x-8	93.296	22.76	18.73	-0.612	-139.3	-1.568	-318.4	0.481	0.591
Mean	95.827	23.12	20.8	-0.692	-157.9	-1.586	-343.9	0.422	0.537
St Dev	4.886	2.41	2.15	0.15	23.4	0.194	42.4	0.045	0.037
COV%	5.099	10.43	10.35	-21.626	-14.8	-12.2	-12.3	10.738	6.951

Compression D6641 (Panel Four y-direction)									
Specimen	**Area (mm^2)**	**Inital (GPa)**	**Final(GPa)**	**TP Strain%**	**TP Stress (MPa)**	**U Strain%**	**U Stress (MPa)**	**PR Initial**	**PR Final**
A4-C1y-1	96.487	17.19	16.07	-0.647	-111.2	-1.745	-287.7	0.41	0.544
A4-C1y-2	97.318	21.7	19.41	-0.527	-114.3	-1.627	-327.8	0.408	0.532
A4-C1y-3	100.286	16.18	16.44	-0.679	-109.8	-1.887	-308.4	0.441	0.568
A4-C1y-4	99.591	20.29	16.59	-0.59	-119.7	-1.41	-255.7	0.415	0.595
A4-C1y-5	97.575	19.16	17.67	-0.782	-149.8	-1.827	-334.4	0.47	0.609
A4-C1y-6	0	0	0	0	0	0	0	0	0
A4-C1y-7	96.198	21.24	18.64	-0.548	-116.3	-1.692	-329.6	0.435	0.571
A4-C1y-8	96.523	19.91	18.01	-0.589	-117.2	-1.596	-298.7	0.442	0.569
Mean	97.711	19.38	17.54	-0.623	-119.8	-1.683	-306	0.431	0.57
St Dev	1.609	2.04	1.24	0.088	13.7	0.159	28.2	0.022	0.027
COV%	1.647	10.54	7.08	-14.073	-11.4	-9.445	-9.2	5.153	4.68

Table C.4 continued

Compression D6641 (Panel Five x-direction)									
Specimen	**Area (mm^2)**	**Inital (GPa)**	**Final(GPa)**	**TP Strain%**	**TP Stress (MPa)**	**U Strain%**	**U Stress (MPa)**	**PR Initial**	**PR Final**
A5-C1x-1	97.905	22.46	19.84	-0.589	-132.2	-1.73	-358.7	0.411	0.504
A5-C1x-2	97.668	17.52	16.98	-0.854	-149.7	-1.611	-278.2	0.451	0.54
A5-C1x-3	97.33	20.48	18.42	-0.714	-146.2	-1.765	-339.8	0.394	0.529
A5-C1x-4	96.8	21.92	19.21	-0.572	-125.3	-1.753	-352.2	0.422	0.521
A5-C1x-5	96.076	18.66	17.12	-0.552	-103	-1.976	-346.8	0.549	0.607
A5-C1x-6	0	0	0	0	0	0	0	0	0
A5-C1x-7	94.887	25.73	22.33	-0.493	-126.7	-1.546	-361.9	0.409	0.506
Mean	96.778	21.13	18.98	-0.629	-130.5	-1.73	-339.6	0.439	0.535
St Dev	1.135	2.93	1.99	0.132	16.8	0.148	31.1	0.057	0.038
COV%	1.172	13.89	10.48	-21.031	-12.9	-8.576	-9.2	12.995	7.116

Compression D6641 (Panel Five y-direction)									
Specimen	**Area (mm^2)**	**Inital (GPa)**	**Final(GPa)**	**TP Strain%**	**TP Stress (MPa)**	**U Strain%**	**U Stress (MPa)**	**PR Initial**	**PR Final**
A5-C1y-1	98.062	20.1	18.53	-0.567	-114.1	-1.882	-357.7	0.454	0.563
A5-C1y-2	93.118	14.85	15.72	-0.27	-40.1	-1.655	-257.7	0.398	0.566
A5-C1y-3	99.718	23.29	20.13	-0.696	-162.1	-1.655	-355.1	0.44	0.548
A5-C1y-4	98.848	17.21	16.75	-0.47	-80.9	-1.269	-214.7	0.374	0.517
A5-C1y-5	100.009	22.42	20.07	-0.607	-136.2	-1.795	-374.6	0.376	0.528
A5-C1y-6	99.707	19.4	17.86	-0.438	-85.1	-1.669	-304.8	0.39	0.498
A5-C1y-7	99.215	19.41	17.81	-0.629	-122	-1.903	-349.1	0.39	0.537
Mean	98.382	19.53	18.12	-0.525	-105.8	-1.69	-316.2	0.403	0.537
St Dev	2.412	2.89	1.62	0.144	40.4	0.214	60	0.031	0.024
COV%	2.452	14.8	8.96	-27.368	-38.2	-12.645	-19	7.79	4.556

Table C.4 continued

Compression D6641 (Panel Six x-direction)									
Specimen	**Area (mm^2)**	**Inital (GPa)**	**Final(GPa)**	**TP Strain%**	**TP Stress (MPa)**	**U Strain%**	**U Stress (MPa)**	**PR Initial**	**PR Final**
A6-C1x-1	87.325	19.83	17.07	-0.64	-126.9	-1.804	-325.7	0.402	0.528
A6-C1x-3	89.833	19.94	16.81	-0.577	-115.1	-1.624	-291	0.39	0.519
A6-C1x-5	88.824	19.4	16.2	-0.589	-114.2	-1.487	-259.8	0.477	0.691
A6-C1x-6	90.601	20.51	17.26	-0.574	-117.8	-1.745	-319.8	0.368	0.498
A6-C1x-9	95.104	22.91	16.61	-0.517	-118.4	-1.571	-293.4	0.44	0.576
A6-C1x-10	95.205	17.37	15.21	-0.601	-104.5	-1.535	-246.4	0.434	0.541
A6-C1x-11	94.407	16.23	14.61	-0.524	-85.1	-1.685	-254.7	0.419	0.541
A6-C1x-12	93.696	18.93	15.74	-0.561	-106.1	-1.653	-278	0.457	0.583
Mean	91.874	19.39	16.19	-0.573	-111	-1.638	-283.6	0.423	0.56
St Dev	3.095	2.01	0.93	0.04	12.6	0.107	29.4	0.036	0.06
COV%	3.369	10.39	5.77	-6.988	-11.4	-6.515	-10.4	8.51	10.691

Compression D6641 (Panel Six y-direction)									
Specimen	**Area (mm^2)**	**Inital (GPa)**	**Final(GPa)**	**TP Strain%**	**TP Stress (MPa)**	**U Strain%**	**U Stress (MPa)**	**PR Initial**	**PR Final**
A6-C1y-1	93.087	18.76	15.24	-0.567	-106.3	-1.441	-239.5	0.421	0.64
A6-C1y-2	91.567	17.91	14.75	-0.518	-92.8	-1.579	-249.3	0.405	0.568
A6-C1y-3	93.239	16.33	14.57	-0.555	-90.7	-1.66	-251.6	0.443	0.614
A6-C1y-4	92.899	18.93	14.72	-0.581	-109.9	-1.603	-260.4	0.456	0.618
A6-C1y-5	90.716	22.08	15.09	-0.527	-116.3	-1.541	-269.4	0.436	0.714
A6-C1y-6	93.601	18.98	14.62	-0.558	-105.9	-1.601	-258.5	0.512	0.648
A6-C1y-7	91.534	17.59	13.79	-0.52	-91.6	-1.542	-232.3	0.442	0.595
A6-C1y-8	92.518	18.35	13.95	-0.613	-112.5	-1.647	-256.8	0.443	0.636
Mean	92.395	18.62	14.59	-0.555	-103.3	-1.577	-252.2	0.445	0.629
St Dev	1.011	1.65	0.5	0.033	10.1	0.07	11.9	0.031	0.043
COV%	1.095	8.87	3.46	-5.899	-9.8	-4.442	-4.7	7.02	6.857

Table C.5: Compression D695 Panel One through Panel Six (x and y directions)

Compression D695 (Panel One x-direction)									
Specimen	**Area (mm^2)**	**Inital (GPa)**	**Final(GPa)**	**TP Strain%**	**TP Stress (MPa)**	**U Strain%**	**U Stress (MPa)**	**PR Initial**	**PR Final**
A1-C2x-1	0	0	0	0	0	0	0	0	0
A1-C2x-2	59.951	26.59	22.1	-0.81	-215.3	-1.404	-346.6	0.389	0.709
A1-C2x-3	60.848	27.75	23.29	-0.797	-221.2	-1.63	-415.3	0.402	0.622
A1-C2x-4	59.754	26.84	22.65	-0.729	-195.6	-1.667	-408.2	0.406	0.586
A1-C2x-5	59.535	29.34	21.62	-0.784	-229.9	-1.46	-376.1	0.372	0.596
A1-C2x-6	60.012	28.93	22.22	-0.787	-227.7	-1.471	-379.6	0.402	0.607
A1-C2x-7	59.266	33.97	24.49	-0.779	-264.5	-1.355	-405.8	0.394	0.77
Mean	59.894	28.9	22.73	-0.781	-225.7	-1.498	-388.6	0.394	0.648
St Dev	0.542	2.71	1.03	0.028	22.7	0.125	26	0.012	0.074
COV%	0.905	9.39	4.53	-3.56	-10	-8.315	-6.7	3.152	11.445

Compression D695 (Panel One y-direction)									
Specimen	**Area (mm^2)**	**Inital (GPa)**	**Final(GPa)**	**TP Strain%**	**TP Stress (MPa)**	**U Strain%**	**U Stress (MPa)**	**PR Initial**	**PR Final**
A1-C2y-1	60.331	26.86	23.01	-0.661	-177.6	-1.295	-323.4	0.442	0.751
A1-C2y-2	59.951	25.86	17.7	-0.67	-173.3	-1.589	-336	0.348	0.465
A1-C2y-3	60.848	27.21	22.46	-0.618	-168.3	-1.479	-361.5	0.358	0.541
A1-C2y-4	0	0	0	0	0	0	0	0	0
A1-C2y-5	59.535	24.39	18.21	-0.718	-175.1	-1.628	-340.8	0.376	0.594
A1-C2y-6	60.012	23.96	17.61	-0.74	-177.3	-1.782	-360.9	0.388	0.603
A1-C2y-7	59.266	24.84	18.46	-0.767	-190.6	-2.254	-465	0.425	0.68
A1-C2y-8	59.522	24.29	17.65	-0.734	-178.3	-1.823	-370.4	0.399	0.704
Mean	59.924	25.35	19.3	-0.701	-177.2	-1.693	-365.5	0.391	0.62
St Dev	0.544	1.31	2.37	0.053	6.8	0.305	46.9	0.034	0.099
COV%	0.907	5.15	12.29	-7.503	-3.9	-18.018	-12.8	8.729	16.007

Table C.5 continued

Compression D695 (Panel Two x-direction)									
Specimen	**Area (mm^2)**	**Inital (GPa)**	**Final(GPa)**	**TP Strain%**	**TP Stress (MPa)**	**U Strain%**	**U Stress (MPa)**	**PR Initial**	**PR Final**
A2-C2x-1	65.142	27.21	21.06	-0.808	-219.9	-1.656	-398.4	0.338	0.637
A2-C2x-2	64.483	24.44	17.41	-0.724	-177	-1.88	-378.2	0.396	0.677
A2-C2x-3	64.601	29.42	21.35	-0.719	-211.6	-1.592	-397.9	0.378	0.67
A2-C2x-4	65.65	25.02	20.37	-0.802	-200.5	-1.973	-439.1	0.416	0.605
A2-C2x-5	64.612	28.72	20.91	-0.788	-226.2	-1.576	-391.1	0.334	0.693
A2-C2x-6	65.428	29.39	20.55	-0.592	-174	-1.552	-371.3	0.347	0.654
A2-C2x-7	62.832	29.43	19.68	-0.789	-232.2	-1.672	-406	0.374	0.548
A2-C2x-8	66.093	28.02	20.24	-0.782	-219.1	-1.683	-401.5	0.436	0.681
Mean	64.855	27.7	20.2	-0.75	-207.6	-1.698	-397.9	0.377	0.646
St Dev	0.995	2	1.24	0.072	21.9	0.151	20.4	0.037	0.048
COV%	1.534	7.22	6.15	-9.64	-10.6	-8.875	-5.1	9.841	7.494

Compression D695 (Panel Two y-direction)									
Specimen	**Area (mm^2)**	**Inital (GPa)**	**Final(GPa)**	**TP Strain%**	**TP Stress (MPa)**	**U Strain%**	**U Stress (MPa)**	**PR Initial**	**PR Final**
A2-C2y-1	0	0	0	0	0	0	0	0	0
A2-C2y-2	0	0	0	0	0	0	0	0	0
A2-C2y-3	0	0	0	0	0	0	0	0	0
A2-C2y-4	0	0	0	0	0	0	0	0	0
A2-C2y-5	59.492	27.67	22.2	-0.779	-215.5	-1.935	-472.3	0.309	0.485
A2-C2y-6	0	0	0	0	0	0	0	0	0
A2-C2y-7	64.787	28.14	21.32	-0.731	-205.8	-1.708	-414.1	0.32	0.628
A2-C2y-8	65.448	28.07	19.47	-0.698	-196	-1.786	-407.7	0.347	0.656
Mean	63.242	27.96	21	-0.736	-205.8	-1.81	-431.4	0.325	0.59
St Dev	3.265	0.25	1.4	0.041	9.8	0.115	35.6	0.019	0.092
COV%	5.162	0.91	6.65	-5.511	-4.8	-6.375	-8.2	5.935	15.525

Table C.5 continued

Compression D695 (Panel Three x-direction)									
Specimen	**Area (mm^2)**	**Inital (GPa)**	**Final(GPa)**	**TP Strain%**	**TP Stress (MPa)**	**U Strain%**	**U Stress (MPa)**	**PR Initial**	**PR Final**
A3-C2x-1	58.842	20.16	12.2	-0.841	-169.5	-2.033	-315	0.428	0.61
A3-C2x-2	57.824	24.4	19.98	-0.628	-153.2	-1.246	-276.7	0.445	0.889
A3-C2x-3	0	0	0	0	0	0	0	0	0
A3-C2x-4	58.909	22.17	11.32	-0.842	-186.7	-1.585	-270.8	0.321	0.586
A3-C2x-5	59.252	19.24	14.57	-0.69	-132.7	-1.937	-314.5	0.379	0.597
A3-C2x-6	58.258	23.15	13.17	-0.807	-186.7	-1.652	-298.1	0.383	0.635
A3-C2x-7	0	0	0	0	0	0	0	0	0
A3-C2x-8	59.236	22.53	16.76	-0.779	-175.5	-1.648	-321.2	0.422	0.547
Mean	58.72	21.94	14.67	-0.764	-167.4	-1.683	-299.4	0.396	0.644
St Dev	0.569	1.92	3.23	0.087	21.1	0.279	21.4	0.045	0.123
COV%	0.968	8.74	22.01	-11.424	-12.6	-16.593	-7.1	11.345	19.174

Compression D695 (Panel Three y-direction)									
Specimen	**Area (mm^2)**	**Inital (GPa)**	**Final(GPa)**	**TP Strain%**	**TP Stress (MPa)**	**U Strain%**	**U Stress (MPa)**	**PR Initial**	**PR Final**
A3-C2y-1	57.905	18.65	9.62	-0.719	-134.2	-1.978	-255.2	0.481	0.683
A3-C2y-2	0	0	0	0	0	0	0	0	0
A3-C2y-3	58.551	17.42	13.09	-0.652	-113.6	-1.744	-256.6	0.436	0.978
A3-C2y-4	58.487	16.83	10.27	-0.85	-143	-1.99	-260.2	0.437	0.756
A3-C2y-5	0	0	0	0	0	0	0	0	0
A3-C2y-6	0	0	0	0	0	0	0	0	0
A3-C2y-7	59.919	14.12	8.79	-0.803	-113.3	-1.829	-203.5	0.45	0.822
A3-C2y-8	59.167	17.18	11	-0.849	-145.9	-1.629	-231.7	0.373	0.696
Mean	58.806	16.84	10.56	-0.775	-130	-1.834	-241.4	0.435	0.787
St Dev	0.766	1.67	1.64	0.087	15.7	0.154	24	0.039	0.12
COV%	1.303	9.91	15.5	-11.208	-12.1	-8.412	-9.9	9.066	15.282

Table C.5 continued

Compression D695 (Panel Four x-direction)									
Specimen	**Area (mm^2)**	**Inital (GPa)**	**Final(GPa)**	**TP Strain%**	**TP Stress (MPa)**	**U Strain%**	**U Stress (MPa)**	**PR Initial**	**PR Final**
A4-C2x-1	63.796	26.44	22.82	-0.623	-164.7	-1.389	-339.5	0.401	0.557
A4-C2x-2	62.329	32.6	34.06	-0.563	-183.6	-1.111	-370.2	0.362	0.448
A4-C2x-3	66.91	33.65	26.92	-0.503	-169.2	-1.245	-368.9	0.254	0.382
A4-C2x-4	0	0	0	0	0	0	0	0	0
A4-C2x-5	66.704	29.78	27.96	-0.869	-258.8	-1.254	-366.4	0.273	0.342
A4-C2x-6	63.679	29.43	26.19	-0.603	-177.6	-1.162	-324	0.304	0.424
A4-C2x-7	64.357	30.67	25.04	-0.523	-160.4	-1.329	-362.3	0.354	0.536
A4-C2x-8	63.977	33.75	29.97	-0.55	-185.5	-1.259	-398	0.4	0.538
Mean	64.536	30.9	27.57	-0.605	-185.7	-1.25	-361.3	0.335	0.461
St Dev	1.675	2.64	3.64	0.124	33.6	0.094	23.7	0.059	0.084
COV%	2.595	8.55	13.19	-20.468	-18.1	-7.496	-6.6	17.614	18.281

Compression D695 (Panel Four y-direction)									
Specimen	**Area (mm^2)**	**Inital (GPa)**	**Final(GPa)**	**TP Strain%**	**TP Stress (MPa)**	**U Strain%**	**U Stress (MPa)**	**PR Initial**	**PR Final**
A4-C2y-1	64.073	28.01	21.37	-0.584	-163.5	-1.536	-367	0.42	0.611
A4-C2y-2	63.462	27.43	21.36	-0.654	-179.5	-1.031	-259.8	0.333	0.537
A4-C2y-3	63.872	29.42	21.5	-0.718	-211.3	-1.316	-339.8	0.338	0.625
A4-C2y-4	63.618	22.67	18.02	-0.63	-142.9	-1.514	-302.1	0.429	0.587
A4-C2y-5	64.964	28.75	23.55	-0.541	-155.5	-1.379	-352.9	0.371	0.542
A4-C2y-6	64.171	30.57	28.65	-0.173	-52.8	-1.185	-342.8	0.337	0.54
A4-C2y-7	63.963	22.63	19.17	-0.662	-149.9	-2.053	-416.4	0.369	0.458
A4-C2y-8	64.795	24.75	22.05	-0.553	-136.8	-1.612	-370.4	0.351	0.562
Mean	64.115	26.78	21.96	-0.564	-149	-1.453	-343.9	0.368	0.558
St Dev	0.527	3.06	3.2	0.169	45.5	0.309	46.9	0.037	0.052
COV%	0.822	11.42	14.56	-29.961	-30.5	-21.297	-13.6	10.149	9.363

Table C.5 continued

Compression D695 (Panel Five x-direction)									
Specimen	**Area (mm^2)**	**Inital (GPa)**	**Final(GPa)**	**TP Strain%**	**TP Stress (MPa)**	**U Strain%**	**U Stress (MPa)**	**PR Initial**	**PR Final**
A5-C2x-1	0	0	0	0	0	0	0	0	0
A5-C2x-2	65.694	27.32	23.28	-0.594	-162.2	-1.508	-375	0.33	0.521
A5-C2x-3	65.293	28.21	23.94	-0.592	-167	-1.511	-387	0.417	0.6
A5-C2x-4	66.553	25.51	21.83	-0.644	-164.4	-1.799	-416.3	0.332	0.504
A5-C2x-5	65.794	27.27	22.83	-0.642	-175.1	-1.73	-423.3	0.344	0.505
A5-C2x-6	66.13	26.53	26.7	0.53	140.5	-1.251	-334.9	0.323	0.455
A5-C2x-7	67.224	28.65	25.91	-0.402	-115.1	-1.405	-375.1	0.463	0.629
Mean	66.115	27.25	24.08	-0.391	-107.2	-1.534	-385.3	0.368	0.536
St Dev	0.69	1.14	1.87	0.46	123.2	0.203	32.1	0.058	0.065
COV%	1.043	4.17	7.77	-117.672	-114.9	-13.243	-8.3	15.71	12.199

Compression D695 (Panel Five y-direction)									
Specimen	**Area (mm^2)**	**Inital (GPa)**	**Final(GPa)**	**TP Strain%**	**TP Stress (MPa)**	**U Strain%**	**U Stress (MPa)**	**PR Initial**	**PR Final**
A5-C2y-1	66.109	27.18	23.74	-0.579	-157.3	-1.383	-348.3	0.328	0.582
A5-C2y-2	66.012	25.99	22.71	-0.626	-162.6	-1.546	-371.7	0.355	0.53
A5-C2y-3	65.763	25.37	33.39	-0.729	-184.8	-1.201	-342.7	0.47	0.576
A5-C2y-4	0	0	0	0	0	0	0	0	0
A5-C2y-5	66.021	30.21	29.13	-0.789	-238.4	-1.044	-312.5	0.381	0.495
A5-C2y-6	67.249	29.37	26.49	-0.716	-210.3	-1.426	-398.2	0.379	0.536
A5-C2y-7	68.241	24.76	23.95	-0.805	-199.4	-1.558	-379.6	0.396	0.48
A5-C2y-8	68.071	24.3	22.97	-0.361	-87.8	-1.473	-343.2	0.355	0.445
Mean	66.781	26.74	26.05	-0.658	-177.2	-1.376	-356.6	0.381	0.521
St Dev	1.054	2.29	3.96	0.154	48.3	0.189	28.5	0.045	0.05
COV%	1.579	8.56	15.19	-23.438	-27.2	-13.756	-8	11.835	9.638

Table C.5 continued

Compression D695 (Panel Six x-direction)									
Specimen	**Area (mm^2)**	**Inital (GPa)**	**Final(GPa)**	**TP Strain%**	**TP Stress (MPa)**	**U Strain%**	**U Stress (MPa)**	**PR Initial**	**PR Final**
A6-C2x-1	0	0	0	0	0	0	0	0	0
A6-C2x-2	0	0	0	0	0	0	0	0	0
A6-C2x-3	58.572	21.02	17.66	-0.58	-121.9	-1.62	-305.6	0.367	0.449
A6-C2x-4	59.477	21.65	17.22	-0.587	-127.1	-1.621	-305.1	0.494	0.669
A6-C2x-5	60.493	24.71	17.77	-0.629	-155.4	-1.388	-290.3	0.466	0.695
A6-C2x-6	60.144	23.04	19.26	-0.472	-108.7	-1.402	-287.9	0.506	0.731
A6-C2x-7	0	0	0	0	0	0	0	0	0
A6-C2x-8	59.693	22.72	18.69	-0.605	-137.5	-1.374	-281.1	0.402	0.525
Mean	59.676	22.63	18.12	-0.575	-130.1	-1.481	-294	0.447	0.614
St Dev	0.732	1.42	0.83	0.06	17.5	0.128	10.9	0.06	0.121
COV%	1.227	6.26	4.59	-10.51	-13.4	-8.629	-3.7	13.482	19.689

Compression D695 (Panel Six y-direction)									
Specimen	**Area (mm^2)**	**Inital (GPa)**	**Final(GPa)**	**TP Strain%**	**TP Stress (MPa)**	**U Strain%**	**U Stress (MPa)**	**PR Initial**	**PR Final**
A6-C2y-1	60.467	23.93	17.83	-0.486	-116.2	-1.381	-275.9	0.467	0.635
A6-C2y-2	61.529	20.59	17.8	-0.713	-146.7	-1.425	-273.5	0.456	0.638
A6-C2y-3	61.855	21.06	16.21	-0.567	-119.5	-1.509	-272.1	0.391	0.573
A6-C2y-4	60.835	21.17	16.19	-0.556	-117.8	-1.458	-263.8	0.374	0.505
A6-C2y-5	62.321	20.41	17.22	-0.559	-114	-1.469	-270.8	0.422	0.593
A6-C2y-6	0	0	0	0	0	0	0	0	0
A6-C2y-7	61.788	21.68	18.67	-0.484	-104.9	-1.326	-262.1	0.457	0.668
A6-C2y-8	61.636	21.64	16.8	-0.577	-124.9	-1.36	-256.4	0.471	0.655
Mean	61.49	21.5	17.24	-0.563	-120.6	-1.418	-267.8	0.434	0.61
St Dev	0.634	1.18	0.92	0.076	13	0.065	7.1	0.039	0.057
COV%	1.031	5.47	5.32	-13.557	-10.8	-4.613	-2.7	8.899	9.353

Table C.6: Modified Compression D6641 Panel One (x and y directions)

Compression D6641 -modified- (Panel One x-direction)									
Specimen	**Area (mm^2)**	**Inital (GPa)**	**Final(GPa)**	**TP Strain%**	**TP Stress (MPa)**	**U Strain%**	**U Stress (MPa)**	**PR Initial**	**PR Final**
A1-mC1x-2	124.33	26.73	23.92	-0.59	-157.8	-1.274	-321.3	0.153	0.146
A1-mC1x-3	121.645	28.02	24.84	-0.575	-161.1	-1.11	-293.9	0.146	0.135
A1-mC1x-4	121.55	29.96	26.83	-0.553	-165.8	-1.267	-357.2	0.153	0.129
A1-mC1x-5	124.022	29.24	27.36	-0.712	-208.3	-1.215	-345.7	0.153	0.132
A1-mC1x-6	126.203	29.08	25.13	-0.614	-178.6	-1.298	-350.6	0.144	0.124
A1-mC1x-7	123.919	29.58	28.15	-0.695	-205.5	-1.174	-340.5	0.164	0.129
A1-mC1x-8	0	0	0	0	0	0	0	0	0
A1-mC1x-9	121.834	31.01	28.58	-0.854	-264.7	-1.208	-365.9	0.135	0.131
Mean	123.358	29.09	26.4	-0.656	-191.7	-1.221	-339.3	0.15	0.132
St Dev	1.747	1.38	1.78	0.106	38.1	0.065	24.4	0.009	0.007
COV%	1.417	4.74	6.76	-16.089	-19.9	-5.358	-7.2	6.031	5.25

Compression D6641 -modified- (Panel One y-direction)									
Specimen	**Area (mm^2)**	**Inital (GPa)**	**Final(GPa)**	**TP Strain%**	**TP Stress (MPa)**	**U Strain%**	**U Stress (MPa)**	**PR Initial**	**PR Final**
A1-mC1y-1	127.525	25.69	22.73	-0.519	-133.2	-1.433	-341.2	0.141	0.115
A1-mC1y-2	124.615	24.76	22.58	-0.589	-145.9	-1.249	-294.8	0.128	0.093
A1-mC1y-3	123.757	27.53	24.22	-0.607	-167.1	-1.283	-330.7	0.153	0.11
A1-mC1y-5	124.368	26.53	23.17	-0.566	-150.1	-1.363	-335	0.132	0.117
A1-mC1y-6	126.05	24.6	21.75	-0.597	-147	-1.345	-309.6	0.14	0.103
A1-mC1y-7	124.194	26.11	22.86	-0.634	-165.6	-1.071	-265.5	0.13	0.088
A1-mC1y-8	127.196	22.34	20.06	-0.62	-138.5	-1.482	-311.4	0.148	0.115
A1-mC1y-9	125.974	22.92	20.33	-0.601	-137.7	-1.51	-322.6	0.134	0.105
Mean	125.46	25.06	22.21	-0.592	-148.1	-1.342	-313.8	0.138	0.106
St Dev	1.429	1.77	1.42	0.036	12.5	0.142	24.7	0.009	0.011
COV%	1.139	7.08	6.4	-6.054	-8.5	-10.616	-7.9	6.412	10.312

Table C.7: Shear D4255 Panel One through Panel Six (x and y Directions)

Shear D4255 (Panel One x-direction)			
Specimen	**Area (mm^2)**	**G12 H_fit (GPa)**	**F6 (MPa)**
A1-S1x-1	749.901	4.748	34.36
A1-S1x-2	743.973	4.918	35.68
A1-S1x-3	728.384	4.939	35.48
A1-S1x-4	735.543	4.617	34.13
A1-S1x-5	728.338	5.05	34.96
A1-S1x-6	724.568	5.074	35.42
A1-S1x-7	746.374	4.85	35.28
A1-S1x-8	731.699	4.662	35.15
Mean	736.097	4.857	35.06
St Dev	9.49	0.17	0.55
COV%	1.289	3.502	1.57

Shear D4255 (Panel One y-direction)			
Specimen	**Area (mm^2)**	**G12 H_fit (GPa)**	**F6 (MPa)**
A1-S1y-1	751.384	4.658	35.12
A1-S1y-2	754.124	4.586	36.25
A1-S1y-3	748.633	4.184	34.68
A1-S1y-4	743.632	4.308	34.77
A1-S1y-5	714.819	4.628	37.56
A1-S1y-6	756.936	4.665	35.94
A1-S1y-7	726	4.898	37.57
A1-S1y-8	745.656	4.652	36.03
Mean	742.648	4.572	35.99
St Dev	14.685	0.224	1.13
COV%	1.977	4.907	3.15

Table C.7 continued

Shear D4255 (Panel Two x-direction)				
Specimen	**Area (mm^2)**	**G12 H_fit (GPa)**	**F6 (MPa)**	**U_Strain (rad)**
A2-S1x-1	794.21	4.247	32.21	0.0126
A2-S1x-2	772.185	4.515	29.18	0.0094
A2-S1x-3	782.416	4.269	32.42	0.0123
A2-S1x-4	774.629	4.571	32.75	0.012
A2-S1x-5	761.507	4.278	33.31	0.0127
A2-S1x-6	790.28	4.426	32.16	0.0124
A2-S1x-7	779.736	4.461	32.59	0.0128
A2-S1x-8	772.394	4.744	32.81	0.0116
Mean	778.42	4.439	32.18	0.012
St Dev	10.578	0.173	1.26	0.0011
COV%	1.359	3.886	3.93	9.3365

Shear D4255 (Panel Two y-direction)				
Specimen	**Area (mm^2)**	**G12 H_fit (GPa)**	**F6 (MPa)**	**U_Strain (rad)**
A2-S1y-1	750.332	4.838	33.84	0.012
A2-S1y-2	732.855	4.777	34.84	0.0125
A2-S1y-3	738.072	4.808	34.6	0.013
A2-S1y-4	767.189	4.866	33.29	0.0117
A2-S1y-5	771.119	4.914	32.8	0.0114
A2-S1y-6	768.373	4.151	32.85	0.0133
A2-S1y-7	770.465	4.262	32.8	0.0129
A2-S1y-8	772.23	4.363	32.53	0.0123
Mean	758.829	4.623	33.44	0.0124
St Dev	16.057	0.309	0.89	0.0007
COV%	2.116	6.69	2.65	5.3836

Table C.7 continued

Shear D4255 (Panel Three x-direction)				
Specimen	**Area (mm^2)**	**G12 H_fit (GPa)**	**F6 (MPa)**	**U_Strain (rad)**
A3-S1x-1	0	0	0	0
A3-S1x-2	0	0	0	0
A3-S1x-3	0	0	0	0
A3-S1x-4	765.395	7.251	32.79	0.0051
A3-S1x-5	767.065	6.914	32.81	0.0051
A3-S1x-6	765.131	7.54	32.86	0.0049
A3-S1x-7	762.329	7.385	32.95	0.005
A3-S1x-8	774.893	7.218	32.48	0.005
Mean	766.963	7.262	32.78	0.005
St Dev	4.748	0.232	0.18	0.0001
COV%	0.619	3.196	0.54	1.4453

Shear D4255 (Panel Three y-direction)				
Specimen	**Area (mm^2)**	**G12 H_fit (GPa)**	**F6 (MPa)**	**U_Strain (rad)**
A3-S1y-1	744.346	7.445	34.08	0.005
A3-S1y-2	751.762	7.637	33.42	0.005
A3-S1y-3	757.405	9.448	33.39	0.0039
A3-S1y-4	745.363	7.333	33.67	0.0051
A3-S1y-5	756.424	8.973	33.21	0.0047
A3-S1y-6	757.541	7.289	33.23	0.0051
A3-S1y-7	742.98	8.068	33.91	0.0049
A3-S1y-8	754.404	9.252	33.66	0.0039
A3-S1y-9	732.302	8.196	34.27	0.0049
A3-S1y-10	741.009	8.103	33.93	0.0049
A3-S1y-11	733.089	8.295	34.33	0.0049
Mean	746.966	8.185	33.74	0.0047
St Dev	9.257	0.759	0.4	0.0005
COV%	1.239	9.273	1.18	9.5071

Table C.7 continued

Shear D4255 (Panel Four x-direction)				
Specimen	**Area (mm^2)**	**G12 H_fit (GPa)**	**F6 (MPa)**	**U_Strain (rad)**
A4-S1x-1	754.433	5.705	22.47	0.0056
A4-S1x-2	735.207	5.876	23.16	0.0057
A4-S1x-3	752.47	5.68	22.4	0.0056
A4-S1x-4	752.567	5.457	18.18	0.0042
A4-S1x-5	0	0	0	0
A4-S1x-6	744.01	5.198	18.29	0.0046
A4-S1x-7	777.106	4.792	17.42	0.0046
A4-S1x-8	762.946	4.936	16.91	0.004
Mean	754.106	5.378	19.83	0.0049
St Dev	13.363	0.413	2.71	0.0007
COV%	1.772	7.677	13.66	14.5617

Shear D4255 (Panel Four y-direction)				
Specimen	**Area (mm^2)**	**G12 H_fit (GPa)**	**F6 (MPa)**	**U_Strain (rad)**
A4-S1y-1	752.303	4.645	18.19	0.005
A4-S1y-2	758.909	4.903	17.93	0.0047
A4-S1y-3	728.263	5.28	18.52	0.0043
A4-S1y-4	756.608	5.395	18.37	0.0044
A4-S1y-5	772.141	4.985	17.72	0.0045
A4-S1y-6	730.322	5.183	18.43	0.0045
A4-S1y-7	728.31	5.485	18.65	0.0043
A4-S1y-8	750.455	5.139	17.97	0.0044
Mean	747.164	5.127	18.22	0.0045
St Dev	16.408	0.275	0.33	0.0002
COV%	2.196	5.366	1.79	4.9699

Table C.7 continued

Shear D4255 (Panel Five x-direction)				
Specimen	**Area (mm^2)**	**G12 H_fit (GPa)**	**F6 (MPa)**	**U_Strain (rad)**
A5-S1x-1	780.577	5.19	17.28	0.0043
A5-S1x-2	788.463	5.311	17.01	0.0042
A5-S1x-3	0	0	0	0
A5-S1x-4	760.271	5.237	18.41	0.0045
A5-S1x-5	773.098	4.719	17.45	0.0045
A5-S1x-6	767.023	4.867	17.46	0.0042
A5-S1x-7	754.459	5.247	17.65	0.0043
A5-S1x-8	724.622	5.3	18.75	0.0047
Mean	764.073	5.124	17.72	0.0044
St Dev	20.899	0.234	0.63	0.0002
COV%	2.735	4.568	3.56	4.7721

Shear D4255 (Panel Five y-direction)				
Specimen	**Area (mm^2)**	**G12 H_fit (GPa)**	**F6 (MPa)**	**U_Strain (rad)**
A5-S1y-1	749.238	5.032	18	0.0045
A5-S1y-2	739.657	5.093	18.04	0.0044
A5-S1y-3	748.871	5.139	17.88	0.0043
A5-S1y-4	751.721	4.959	17.91	0.0045
A5-S1y-5	768.273	4.925	17.59	0.0043
A5-S1y-6	752.618	5.061	18.05	0.0047
A5-S1y-7	762.316	5.047	17.82	0.0046
Mean	753.242	5.037	17.9	0.0044
St Dev	9.404	0.074	0.16	0.0002
COV%	1.249	1.471	0.9	3.7966

Table C.7 continued

Shear D4255 (Panel Six x-direction)				
Specimen	**Area (mm^2)**	**G12 H_fit (GPa)**	**F6 (MPa)**	**U_Strain (rad)**
A6-S1x-1	774.918	9.14	39.85	0.0047
A6-S1x-2	766.173	7.342	39.38	0.0059
A6-S1x-3	770.574	8.167	38.01	0.0053
A6-S1x-4	754.589	9.471	39.34	0.0045
A6-S1x-5	763.258	8.737	33.74	0.0043
A6-S1x-6	767.091	7.751	46.52	0.0068
A6-S1x-7	774.956	7.693	45.82	0.0067
Mean	767.366	8.329	40.38	0.0055
St Dev	7.148	0.803	4.46	0.001
COV%	0.931	9.638	11.04	19.1751

Shear D4255 (Panel Six y-direction)				
Specimen	**Area (mm^2)**	**G12 H_fit (GPa)**	**F6 (MPa)**	**U_Strain (rad)**
A6-S1y-1	761.486	7.299	46.44	0.0071
A6-S1y-2	751.65	8.415	46.5	0.0064
A6-S1y-3	759.44	8.776	45.76	0.0062
A6-S1y-4	762.341	7.51	45.97	0.0069
A6-S1y-5	759.427	8.583	47.11	0.006
A6-S1y-6	746.63	8.747	47.56	0.006
A6-S1y-7	761.237	9.239	46.04	0.0055
A6-S1y-8	753.883	8.04	47.36	0.0062
Mean	757.012	8.326	46.59	0.0063
St Dev	5.661	0.664	0.68	0.0005
COV%	0.748	7.98	1.45	8.3728

Table C.8: Shear D5379 Panel One through Panel Six (x and y Directions)

Shear D5379 (Panel One x-direction)			
Specimen	**Area (mm^2)**	**G12 H_fit (GPa)**	**F6 (MPa)**
A1-S2x-1	51.415	2.199	58.43
A1-S2x-2	52.062	3.85	64.99
A1-S2x-3	52.048	1.912	59.56
A1-S2x-4	51.624	2.093	59.02
A1-S2x-5	55.012	2.699	60.41
A1-S2x-6	53.393	4.259	67.45
A1-S2x-7	53.593	3.017	56.84
A1-S2x-8	53.527	2.691	56.81
Mean	52.834	2.84	60.44
St Dev	1.242	0.84	3.83
COV%	2.351	29.567	6.34

Shear D5379 (Panel One y-direction)			
Specimen	**Area (mm^2)**	**G12 H_fit (GPa)**	**F6 (MPa)**
A1-S2y-1	52.208	2.682	60.8
A1-S2y-2	53.518	3.149	59.67
A1-S2y-3	52.358	2.564	58.93
A1-S2y-4	53.422	2.843	60.08
A1-S2y-5	51.24	3.093	59.47
A1-S2y-6	52.543	2.965	61.68
A1-S2y-7	52.376	2.925	61.87
A1-S2y-8	52.617	2.663	62.44
Mean	52.535	2.861	60.62
St Dev	0.717	0.211	1.28
COV%	1.365	7.375	2.11

Table C.8 continued

Shear D5379 (Panel Two x-direction)			
Specimen	**Area (mm^2)**	**G12 H_fit (GPa)**	**F6 (MPa)**
A2-S2x-1	0	0	0
A2-S2x-2	58.375	2.359	59.72
A2-S2x-3	57.429	2.21	64.29
A2-S2x-4	56.799	2.518	62.15
A2-S2x-5	57.057	2.399	61.91
A2-S2x-6	56.567	2.529	61.14
A2-S2x-7	57.002	2.188	60.57
A2-S2x-8	57.067	2.02	60.31
Mean	57.185	2.317	61.44
St Dev	0.587	0.187	1.52
COV%	1.027	8.075	2.48

Shear D5379 (Panel Two y-direction)			
Specimen	**Area (mm^2)**	**G12 H_fit (GPa)**	**F6 (MPa)**
A2-S2y-1	57.595	2.16	60.53
A2-S2y-2	58.05	1.965	59.86
A2-S2y-3	0	0	0
A2-S2y-4	0	0	0
A2-S2y-5	57.015	2.164	65.52
A2-S2y-6	56.851	2.419	66.48
A2-S2y-7	57.76	2.331	64.57
A2-S2y-8	58.304	2.301	63.55
Mean	57.596	2.223	63.42
St Dev	0.57	0.161	2.69
COV%	0.99	7.253	4.24

Table C.8 continued

Shear D5379 (Panel Three x-direction)			
Specimen	**Area (mm^2)**	**G12 H_fit (GPa)**	**F6 (MPa)**
A3-S2x-1	52.298	15.57	122.25
A3-S2x-2	52.444	12.254	128.79
A3-S2x-3	51.439	12.427	133.29
A3-S2x-4	51.433	12.813	124.2
A3-S2x-5	50.497	17.175	126.47
A3-S2x-6	50.659	14.47	114.72
A3-S2x-7	51.579	12.54	135.68
A3-S2x-8	51.109	14.032	122.25
Mean	51.432	13.91	125.96
St Dev	0.694	1.763	6.69
COV%	1.349	12.677	5.31

Shear D5379 (Panel Three y-direction)			
Specimen	**Area (mm^2)**	**G12 H_fit (GPa)**	**F6 (MPa)**
A3-S2y-1	52.9	14.751	111.87
A3-S2y-2	52.147	13.741	131.49
A3-S2y-3	52.312	16.081	130.2
A3-S2y-4	52.517	15.034	123.24
A3-S2y-5	52.25	16.253	117.37
A3-S2y-6	52.32	12.336	128.5
A3-S2y-7	52.723	11.918	129.84
A3-S2y-8	52.329	11.628	132.39
Mean	52.437	13.968	125.61
St Dev	0.257	1.845	7.46
COV%	0.49	13.208	5.94

Table C.8 continued

Shear D5379 (Panel Four x-direction)			
Specimen	**Area (mm^2)**	**G12 H_fit (GPa)**	**F6 (MPa)**
A4-S2x-1	58.019	0.325	5.98
A4-S2x-2	58.354	0.42	5.87
A4-S2x-3	59.806	0.561	5.92
A4-S2x-4	58.886	0.379	6.12
A4-S2x-5	58.828	0.447	5.75
A4-S2x-6	57.469	0.34	6.04
A4-S2x-7	58.69	0.304	6.01
A4-S2x-8	58.47	0.303	5.73
Mean	58.565	0.385	5.92
St Dev	0.685	0.089	0.14
COV%	1.169	22.996	2.34

Shear D5379 (Panel Four y-direction)			
Specimen	**Area (mm^2)**	**G12 H_fit (GPa)**	**F6 (MPa)**
A4-S2y-1	56.651	0.333	5.92
A4-S2y-2	57.017	0.343	5.62
A4-S2y-3	56.345	0.367	5.88
A4-S2y-4	56.079	0.343	5.9
A4-S2y-5	55.691	0.339	5.78
A4-S2y-6	56.867	0.336	5.6
A4-S2y-7	55.683	0.299	5.86
A4-S2y-8	56.469	0.302	5.53
Mean	56.35	0.333	5.76
St Dev	0.503	0.022	0.16
COV%	0.892	6.733	2.72

Table C.8 continued

Shear D5379 (Panel Five x-direction)			
Specimen	**Area (mm^2)**	**G12 H_fit (GPa)**	**F6 (MPa)**
A5-S2x-1	60.391	0.249	5.88
A5-S2x-2	59.532	0.27	5.83
A5-S2x-3	57.945	0.379	6.18
A5-S2x-4	58.733	0.343	6.02
A5-S2x-5	58.278	0.313	6.42
A5-S2x-6	57.619	0.369	6.27
A5-S2x-7	58.376	0.352	6.01
A5-S2x-8	57.936	0.354	6.38
Mean	58.601	0.329	6.12
St Dev	0.932	0.047	0.22
COV%	1.59	14.331	3.64

Shear D5379 (Panel Five y-direction)			
Specimen	**Area (mm^2)**	**G12 H_fit (GPa)**	**F6 (MPa)**
A5-S2y-1	56.543	0.453	5.49
A5-S2y-2	57.247	0.427	5.56
A5-S2y-3	55.785	0.508	5.98
A5-S2y-4	56.428	0.388	5.68
A5-S2y-5	56.513	0.498	5.71
A5-S2y-6	55.812	0.414	5.71
A5-S2y-7	55.756	0.435	5.3
A5-S2y-8	54.944	0.41	5.61
Mean	56.128	0.442	5.63
St Dev	0.699	0.042	0.2
COV%	1.245	9.589	3.49

Table C.8 continued

Shear D5379 (Panel Six x-direction)			
Specimen	**Area (mm^2)**	**G12 H_fit (GPa)**	**F6 (MPa)**
A6-S2x-1	53.929	0.87	12.9
A6-S2x-2	54.6	1.048	13.4
A6-S2x-3	55.357	0.856	15.09
A6-S2x-4	54.681	0.7	19.2
A6-S2x-5	54.973	0.937	13.01
A6-S2x-6	55.014	0.939	12.25
A6-S2x-7	54.116	0.812	13.35
A6-S2x-8	54.281	0.85	12.34
Mean	54.619	0.877	13.94
St Dev	0.489	0.103	2.3
COV%	0.895	11.708	16.49

Shear D5379 (Panel Six y-direction)			
Specimen	**Area (mm^2)**	**G12 H_fit (GPa)**	**F6 (MPa)**
A6-S2y-1	55.094	1.017	13.01
A6-S2y-2	54.586	1.202	13.51
A6-S2y-3	55.013	1.289	12.49
A6-S2y-4	54.524	1.148	12.82
A6-S2y-5	54.726	0.87	13.72
A6-S2y-6	54.402	0.808	13.95
A6-S2y-7	54.172	0.996	11.83
A6-S2y-8	54.285	0.742	13.75
Mean	54.6	1.009	13.13
St Dev	0.329	0.195	0.73
COV%	0.603	19.321	5.57

BIOGRAPHY OF THE AUTHOR

Fadi El-Chiti was born in Kuwait, on January 14, 1979, with a Lebanese nationality. He was raised in Beirut, Lebanon and graduated from Beirut Evangelical School in 1997. He attended the Notre Dame University in Lebanon and graduated with a Bachelor of Engineering in Mechanical Engineering in 2002.

He plans to return to his home country, Lebanon, to begin a career as an engineer. Fadi is a candidate for The Master of Science degree in Mechanical Engineering from The University of Maine in August, 2005.

REPORT DOCUMENTATION PAGE

Form Approved
OMB No. 0704-0188

1. REPORT DATE *(DD-MM-YYYY)*	2. REPORT TYPE	3. DATES COVERED *(From - To)*
04-09-2007	Master's Thesis	March 2003 - December 2006

4. TITLE AND SUBTITLE
Experimental Variability of E-Glass Reinforced Vinyl Ester Composites Fabricated by VARTM/SCRIMP

5a. CONTRACT NUMBER
n/a

5b. GRANT NUMBER
N0014-03-1-0542

5c. PROGRAM ELEMENT NUMBER
n/a

6. AUTHOR(S)
Fadi El-Chiti

5d. PROJECT NUMBER
n/a

5e. TASK NUMBER
n/a

5f. WORK UNIT NUMBER
n/a

7. PERFORMING ORGANIZATION NAME(S) AND ADDRESS(ES)
The AEWC Center
University of Maine
Orono, ME 04469

8. PERFORMING ORGANIZATION REPORT NUMBER
Report 08-01 Project 206

9. SPONSORING/MONITORING AGENCY NAME(S) AND ADDRESS(ES)
Dr. Roshdy Barsoum
Office of Naval Research
Ballston Center Tower ONE
800 North Quincy Street
Arlington, Virginia 22217-5560

10. SPONSOR/MONITOR'S ACRONYM(S)
n/a

11. SPONSOR/MONITOR'S REPORT NUMBER(S)
n/a

12. DISTRIBUTION/AVAILABILITY STATEMENT
APPROVED FOR PUBLIC RELEASE

13. SUPPLEMENTARY NOTES
n/a

14. ABSTRACT

It was found that there is significant variability in physical and mechanical properties of marine composites among different manufacturers resulting in inconsistent parameters for structural analysis and design. Experimental variability can be classified in two main groups: 1) variability from experimental preparation and testing techniques and 2) variability from the material constituents and manufacturing process. The objective of the thesis is to resolve the uncertainty surrounding mechanical properties obtained from conventional standard testing by optimizing the testing procedure used in obtaining the material properties of marine FRP composites. A series of ASTM standard test procedures for each material property (tensile, compressive, and shear) are conducted using a 3D digital image correlation system for measuring full-field strains. Glass transition temperature, fiber volume fraction, and density will be measured using ASTM standard tests. The study will lead to drafting material testing specifications to be used in obtaining reliable mechanical and physical properties for FRP composites used in structural applications. Finally, the testing program will be accompanied with a micromechanics analysis that will be used to characterize the FRP properties using an array of techniques. The micromechanics analysis will be used to explain the results of the material coupon tests and characterize the variability in the tests.

15. SUBJECT TERMS
experimental variability, composites, material testing, fiberglass reinforced plastics

16. SECURITY CLASSIFICATION OF:			17. LIMITATION OF ABSTRACT	18. NUMBER OF PAGES	19a. NAME OF RESPONSIBLE PERSON
a. REPORT	b. ABSTRACT	c. THIS PAGE			Dr. Habib Dagher
U	U	U	UU	266	19b. TELEPHONE NUMBER *(Include area code)* 207-581-2138